Thèse de doctorat

Advanced integrability techniques and analysis for quantum spin chains

Thèse de doctorat de l'Université Paris-Saclay
préparée à l'Université Paris-Sud
dans les locaux de l'Institut de Physique Théorique et de l'Ecole Normale Supérieure

Ecole doctorale n°564 Ecole Doctorale Physique en Ile-de-France (EDPIF)
Spécialité de doctorat : Physique

Thèse présentée et soutenue à Saclay, le 3 Septembre 2019, par

ETIENNE GRANET

Composition du Jury :

Jean-Michel Maillet
Directeur de recherche, ENS Lyon   Président du jury

Fabian Essler
Professor, Oxford University   Rapporteur

Andreas Klümper
Professor, Wuppertal University   Rapporteur

Véronique Terras
Directrice de recherche, Université Paris-Sud   Examinateur

Jean-Sébastien Caux
Professor, University of Amsterdam   Examinateur

Hubert Saleur
Directeur de recherche, IPhT Saclay   Directeur de thèse

Jesper Jacobsen
Professeur, ENS Paris   Co-directeur de thèse

Abstract

This thesis mainly deals with integrable quantum critical systems that exhibit peculiar features such as non-unitarity or non-compactness, through the technology of Bethe ansatz. These features arise in non-local statistical physics models such as percolation, but also in for example disordered systems. The manuscript both presents detailed studies of the continuum limit of finite-size lattice integrable models, and develops new techniques to study this correspondance.

In a first part we study in great detail the continuum limit of non-unitary (and sometimes non-compact) super spin chains with orthosymplectic symmetry which is shown to be super-sphere sigma models, by computing their spectrum from field theory, from the Bethe ansatz, and numerically. The non-unitarity allows for a spontenous symmetry breaking usually forbidden by the Mermin-Wagner theorem. The fact that they are marginal perturbations of a Logarithmic Conformal Field Theory is particularly investigated. We also establish a precise correspondance between the spectrum and intersecting loops configurations, and derive new critical exponents for fully-packed trails, as well as their multiplicative logarithmic corrections. During this study we developed a new method to compute the excitation spectrum of a critical quantum spin chain from the Bethe ansatz, together with their logarithmic corrections, that is also applicable in presence of so-called 'strings', and that avoids Wiener-Hopf and Non-Linear Integral Equations.

In a second part we address the problem of the behaviour of a spin chain in a magnetic field, and show that one can derive convergent series for several physical quantities such as the acquired magnetization or the critical exponents, whose coefficients can be efficiently and explicitely computed recursively using only algebraic manipulations. The structure of the recurrence relations permits to study generically the excitation spectrum content - moreover they are applicable even to some cases where the Bethe roots lie on a curve in the complex plane. It is our hope that the analytic continuation of such series might be helpful the study non-compact spin chains, for which we give some flavour. Besides, we show that the fluctuations within the arctic curve of the six-vertex model with domain-wall boundary conditions are captured by a Gaussian free field with space-dependent coupling constant that can be computed from the free energy of the periodic XXZ spin chain with an imaginary twist and in a magnetic field.

Remerciements

Mes premiers remerciements vont à mes directeurs de thèse, Hubert Saleur et Jesper Jacobsen, pour le temps inestimable qu'ils ont consacré à m'apprendre leur métier. Leur soutien a été sûr, leurs conseils toujours utiles et leurs encouragements indispensables. Je garderai un très bon souvenir de leurs discussions et de leurs enseignements.

Je suis ensuite très honoré et reconnaissant envers Fabian Essler et Andreas Klümper, d'avoir bien voulu remplir le lourd travail de rapporteurs, ainsi qu'à Jean-Michel Maillet, Jean-Sébastien Caux et Véronique Terras pour avoir accepté de faire partie de mon jury. Il se trouve que les quatre premiers ont organisé ou enseigné à l'excellente Ecole des Houches 2018 sur l'Integrabilité, et je profite de les avoir mentionnés ici pour les en remercier également.

Parmi les autres chercheurs que j'ai eu l'opportunité de rencontrer au cours de ces années, je remercie particulièrement Jérôme Dubail, Philippe Ruelle, Pasquale Calabrese et Fabian Essler encore pour des visites ou des collaborations très intéressantes, Yacine Ikhlef, Kirone Mallick et Gregory Korchemsky pour des discussions ponctuelles utiles, ainsi que Christoph Kopper pour son soutien invariable depuis mon master. Je remercie également Riccardo Guida et Didina Serban pour avoir été mes tuteur et parrain, et enfin Sylvie Zaffanella, Laure Sauboy, Loïc Bervas et Emmanuelle de Laborderie pour l'aide administrative indispensable.

Un grand merci maintenant à Assaf, Toan, Arnaud, Elise, à mes collègues de bureau Romain et Niall, ainsi qu'aux thésards et postdocs que j'ai pu croiser et qui ont rendu les pauses de midi agréables, Bryan, Kemal, Tony, Yifei, Séverin, Corentin, Benoît, Lilian, Thiago, Dinh-Long, Pierre, Linnea, Michal, Jonathan, Dongsheng, Zhihao, Augustin, Thomas, Gwenaël.

Et surtout bien sûr, un grand merci à ma famille, mes parents et mes frères.

Contents

Chapter 1

Introduction

Exactly solvable models are invaluable in physics, since they provide important benchmarks on which new ideas and theories can be tested, or around which perturbations can be performed to describe real systems. Sometimes these models even catch an essential feature of a physical mechanism that is similarly observed in other situations. One of such paradigmatic models in quantum and statistical physics is that of the Heisenberg spin chain, introduced to explain magnetism as being a long-range order resulting from the short-range interactions between a multitude of spinful atoms. The breakthrough was done by Bethe [1] who showed that the one-dimensional chain can be diagonalized exactly[1] with a particular ansatz. Because of its adaptability to many other models, this ansatz has ever since been the subject of a considerable amount of research for its applications in quantum, statistical and condensed matter physics, as well as in some areas of high-energy physics.

The original form of the ansatz was a kind of educated Fourier transform, in which the eigenstates are expressed as a superposition of plane waves whose amplitudes and phases must satisfy a particular set of non-linear equations, called Bethe equations. It requires precise assumptions on the model to work, and it was understood only decades later partly by Onsager in his solution of the two-dimensional Ising model [2], Baxter [3] and the Russian school [4, 5, 6] that this exact solvability could be traced back to algebraic relations between certain operators, revisiting the ansatz under the name *algebraic Bethe ansatz*, while the historical approach was renamed *coordinate Bethe ansatz*. In this approach, the Hamiltonian or the transfer matrix is constructed from an R-matrix and the ansatz can be applied as soon as it satisfies the so-called *Yang-Baxter equation* [7] and if there is a pseudo-vacuum or reference state in the Hilbert space. Other more general forms of the ansatz were then found later, such as Baxter's Q-operator [3] that enables to analytically continue certain parameters and thus reach new solutions [8], or Sklyanin's quantum separation of variables recently blossoming under the work of Maillet's group [9, 10] which is not anymore an ansatz so to speak, and should be the right framework to answer questions such as completeness of the set of solutions.

Since the Bethe ansatz yields an explicit expression for all the eigenvalues and eigen-

---

[1]The completeness of the ansatz, namely that it yields all the eigenstates, was however proven much later.

states, admittedly in terms of Bethe roots defined only implicitly as solutions to coupled non-linear equations, one can in principle compute any correlation function; but it turns out that it is only the beginning of the journey, for these exact finite-size formulas are difficult to handle. One of the major steps is Slavnov's determinant formula for scalar products between Bethe states [11], that enabled then Maillet's group after a considerable amount of analytical work to extract from these exact finite-size formulas the asymptotic behaviours predicted by field theory [12, 13]. But Slavnov's formula also permitted to compute numerically – evaluational numerics, not simulations – dynamical structure factors for very large systems with e.g. Caux's algorithm [14], with a striking agreement with neutron scattering experiments performed on real materials [15, 16], hence showing that integrability is not a mere mathematical curiosity but can also prove to be a relevant and very powerful way to understand experiments.

However, an important idea that often goes together with integrability is that of *universality*, namely that the details of the short-range interactions of a quantum or statistical physics system – be it defined on a square or hexagonal lattice, with next-nearest neighbours interactions or not – do not influence the critical long-range correlations, that depend then only on a few essential features of the defining interactions such as their symmetries. A famous historical example is that of a large assembly of particles interacting all together in a complex enough way so that their Hamiltonian is effectively a random matrix; then depending on the symmetries of the matrix, be it e.g. hermitian or unitary, the limit of the spectrum is fixed to be for instance Wigner's semi-circle law. Hence one of the cornerstones of modern quantum and statistical physics is to draw a correspondence between the symmetries of the defining Boltzmann weights and the continuum limit of the model. Under this perspective, an integrable system is seen as a mere representative of a universality class possibly containing physically interesting but non-integrable systems, on which exact analytical calculations can be exceptionally performed.

This general but deep idea is backed by the existence of R-matrices solutions to the Yang-Baxter equation – and thus integrable spin chains – that are representations of any of the existing Lie algebras. The construction of these solutions has been the object of important developments in algebra culminating with quantum groups [17], and their q-deformations led to the discovery of whole new classes of integrable spin chains, whose number now largely exceeds that of their physical studies. Because of their exact solvability, these models were indeed particularly well-suited for extensive analytical and numerical studies, hence stimulating the formidable task of classifying the different possible continuum limits. For example it is now understood that the spin chains built on a representation of a simply laced Lie algebra of a compact group G converge to a Wess-Zumino-Witten (WZW) model on the same group G in the thermodynamic limit [18].

A crucial property that makes easier these identifications is the conformal invariance of their continuum limit, that must be then a Conformal Field Theory (CFT) [19]. Under

this assumption the continuum limit is characterized by a set of numbers termed CFT data, such as the central charge, the scaling dimensions of the fields and the structure constants; and conformal invariance actually implies that a good part of them is present and visible in the asymptotic behaviour of the low-lying spectrum of the spin chain in the large system size limit [20, 21, 22]. This is a remarkable property – among one of the most important in the study of two-dimensional criticality – that permits to infer a lot on the field theory and thus on the correlation functions, from the sole knowledge of the eigenvalues of the Hamiltonian, without knowing anything on the eigenstates that are more difficult to grasp. However big the simplification is, these asymptotic expansions are still technically demanding and have been carried out with Wiener-Hopf equations and Non-Linear Integral Equations [23, 24, 25, 26], with sometimes significant analytical difficulties, e.g. to identify the central charge of the higher-level WZW models. A chapter of this manuscript is devoted to this step of the identification, where we present a new method to calculate the leading corrections.

Although the continuum limit of the spin chains built from classical Lie algebras are well understood, those based on representations of Lie *superalgebras* turned out to be more involved [27], and some of their continuum limits are not known up to this day. Supersymmetry[2], i.e. the mixing of bosonic (commuting) and fermionic (Grassmanian, anti-commuting) variables occurs in some models as their defining features such as the Hubbard or $t - J$ model [28, 29, 30], but is also a way to extend the range of some parameters to zero or negative integers, by making fermionic variables play the role of negative degrees of freedom. Hence it is an alternative to the $n \to 0$ replica approach in disordered systems for averaging over the disorder [31, 32, 33], revealing e.g. an $osp(2n|2n)$ symmetry in the disordered Ising model, where the *orthosymplectic* symmetry osp is the graded analog of the orthogonal $o(n)$ symmetry for spaces with both bosonic and fermionic variables. Several geometrical and paradigmatic models are described by supersymmetric field theories as well, such as polymers whose continuum limit is a so-called $\eta\xi$ system [34], spanning trees and forests which have an $osp(1|2)$ symmetry rather directly visible in finite-size [35, 36, 37], or percolation possibly described by an $osp(3|2)$ symmetric spin chain. A chapter of this manuscript is devoted to the thorough study of these spin chains with orthosymplectic symmetry, for which we derive several new results explained further on their continuum limit and their 2D statistical physics realizations as *fully packed trails*.

The poor understanding of the continuum limit of supersymmetric spin chains comes from a certain number of oddities. Firstly, the cancellation of degrees of freedom implies that a same model such as disordered Ising may be viewed as having different symmetries $osp(2n|2n)$, whereas the natural candidates that are the WZW models on the corresponding groups depend on n. Secondly, these models often exhibit *non-compact* degrees of freedom

---

in their continuum limit, namely there are fields with arbitrary real conformal dimension, whereas the representations of the Lie superalgebras over which the spin chains are built are finite dimensional. Lastly, these models often happen to be marginal perturbations of Logarithmic Conformal Field Theories (LCFT) – a variation of CFT's where the linearized Renormalization Group (RG) flow is assumed to be non-diagonalizable at a fixed point, resulting in correlation functions with integral powers of logarithms even at the RG fixed point [38].

These singular behaviours are in a sense brought together in the celebrated Integer Quantum Hall Effect (IQHE), a physical phenomenon that has attracted a lot of attention from theoreticians in the past decades for its striking universal nature. It occurs in a cold 2D electron gas placed in a high magnetic field and subjected to an electric current, in which the perpendicular voltage difference divided by the longitudinal current is extremely accurate and is measured to be an integer multiple of $\frac{e}{h^2}$, thereby remarkably involving two fundamental physical constants [39] – and the result is astonishingly independent of the disorder in the sample or of its geometry[3]. Although the plateaux themselves are well understood, the question of the *transition* between them and their associated critical exponents is a famous still unsolved problem. It is a *localization-delocalization* transition of electrons in a disordered potential moving from one Landau level to another, that is both a geometrical percolation-like and disordered problem. One of the major attempts to solve it is the Chalker-Coddington model [40], that describes the evolution of an electron in a disordered potential landscape with possible tunnel effect and whose numerical simulation has yielded exponents in good agreement with experiment [41]; however, there are still unresolved problems in a purely numerical approach, which would require analytical work to fill the gaps; but it is of considerable difficulty to tackle analytically, because of its supersymmetric formulation, of its *non-unitarity*, namely the non-hermiticity of its Hamiltonian, and of its non-compactness, true even in finite-size since each site of the lattice is described by an infinite-dimensional vector space. On the field theory side, it is expected to be described by a sigma model with target space $\frac{U(1,1|2)}{U(1,1)\times U(1,1)}$ [42, 43], but out of reach of analytical study. All these particularities call for the development of new concepts and techniques, and this manuscript takes place among this wider project.

The first peculiarity to elaborate on is non-unitarity. Although unitarity is an essential feature of quantum mechanics on which the probabilistic interpretation of the wave function amplitude rests, the spin chains involved are effective quantum systems obtained from discretization of some field theories built from unitary ones after e.g. averaging over the disorder, at the cost of introducing new fermionic variables that need not necessarily conserve unitarity. On the 2D statistical physics side, the notion of non-unitarity often refers

---

[3]Note that this particular resistance is the only quantity that has a chance of being universal, since any rescaling of the length has no effect on neither the perpendicular voltage difference nor the longitudinal current, and any rescaling of the width changes both equally, whereas the imprecision of these lengths would otherwise spoil any measure of a universal quantity.

to the non-positivity of local Boltzmann weights, that permits after summing over intermediate configurations to effectively describe *non-local* systems such as percolation, or some non-local observables in still local models such as the Ising model. On the CFT side, non-unitarity bears still another meaning, referring to theories in which some states may have zero or negative norm, implying e.g. that some states may have lower energy than the CFT vacuum state. These three notions do not necessarily exactly overlap and their connections are not fully established to this day, but correspond anyway to the loss of several common properties – for example the existence of negative conformal dimensions implies that some states must have lower energy than the CFT vacuum state.

An important class of non-unitary field theories are the LCFT's alluded to above, whose classification happens to be of considerable difficulty and should be of central interest for these topics – for instance, on general grounds disordered systems are described by CFT's with vanishing central charge, and to be non trivial they must be logarithmic. Several aspects of ordinary CFT's are lost, such as the general structure of the three point function, which complicates their perturbation in particular. We note that in case of a perturbation by a marginal operator, there may be supplementary multiplicative logarithmic corrections to their correlation functions, whose identification in the spectrum as finite-size corrections comes with technical difficulties.

Lastly, non-compactness affects and questions the mere identification of the spectrum from the asymptotics of the energy levels. When the spin chain is built on finite-dimensional representations, in the asymptotics this non-compactness translates into an infinite number of states that have the same conformal dimensions, corrected in finite-size by a sub-leading marginal term [44], problematic to handle both analytically and numerically. When the spin chain is itself built on infinite-dimensional vector spaces [8], as should be the case of the Chalker-Coddington model, the usual Bethe ansatz fails and one has to rely on more advanced techniques, that permitted at this day to handle only chains with a few sites [45]. It is our hope that this manuscript sheds light on some of these aspects, makes some steps and proposes new ideas towards the understanding of these exotic quantum systems.

The manuscript is organized as follows:

1. The first chapter introduces notations and classical results on the Bethe ansatz and the correspondence between lattice models and CFT, that we will use throughout the manuscript. It comprises a new criterion to distinguish admissible from non-admissible solutions to the Bethe equations – this work should be part of a forthcoming preprint.

2. The second chapter is a thorough study of non-unitary spin chains with orthosymplectic *osp* symmetry, their continuum limit that are marginally perturbed LCFT's, their 2D statistical physics realizations as fully packed trails and the logarithmic corrections it implies on their correlation functions. This has been the object of a publication in a peer-reviewed journal [46].

3. The third chapter presents a different approach to the calculation of the excitation

13

spectrum of critical spin chains, that avoids the use of Wiener-Hopf or Non-Linear Integral Equations. It comprises a detailed study of the dependence of the spectrum and its logarithmic corrections on the Bethe ansatz functions. Part of this work has been the object of a publication in a peer-reviewed journal [47], that does not comprise the part on strings and logarithmic corrections.

4. The fourth chapter is a study of magnetic field influence, motivated by the regularization effect it may have on these exotic spin chains. It is shown how to derive series expansions for spin chains in an external field through recurrence relations, and explained how this could be used to study non-compact models, which is still an ongoing project. Section 5.2 has been published in a peer-reviewed journal [48]. We also study the field theory that describes the fluctuations inside the arctic curve of the six-vertex model with domain-wall boundary conditions, which has been the object of another peer-reviewed publication [49].

Chapter 2

Bethe ansatz and related aspects

The goal of this chapter is mainly to expose the ideas and techniques that we are going to make use of throughout this thesis. We start by a presentation of the Bethe ansatz in the context of the XXZ spin chain and its relation with geometrical models such as loops, Potts model and percolation. We explain then how conformal invariance permits to infer crucial information on the field theory that describes its continuum limit, from the asymptotic expansion of the low-lying spectrum of the lattice model.

Most of the content of this chapter is thus a summary of several techniques honed through the past decades, with the exception however of section 2.2 which is a personal contribution. There, we study the technical question of admissible solutions to the Bethe ansatz equations, and show that it requires to supplement the usual TQ relation with an additional TQ-like relation. It bridges the gap between different methods and algorithms that seemed to be unrelated to each other, and its precise position within the existing literature is detailed in subsection 2.1.4.

2.1 Bethe ansatz

2.1.1 Notations and definitions

The Hilbert spaces of the quantum systems we study are all expressed in terms of a tensor product of L individual vector spaces V of finite dimension D, each representing a particle. Given an operator σ on V, we denote by $\sigma_a = \underset{1}{I} \otimes ... \otimes \underset{a}{\sigma} \otimes ... \otimes \underset{L}{I}$ the corresponding operator on $V^{\otimes L}$ that acts non-trivially only on the a-th vector space where it acts as σ. Similarly, given an operator R on $V \otimes V$, we denote by R_{ab} the operator on $V^{\otimes L}$ that acts non-trivially only on the a-th and b-th vector spaces, where it acts as R. The entry $((i-1)D+k, (j-1)D+l)$ of the matrix R (where $i, j, k, l = 1, ..., D$), i.e. the component along $e_k \otimes e_l$ of the action of R on $e_i \otimes e_j$ where the e_i's denote the canonical vector basis, will be denoted by R_{ik}^{lj}. [1] We

---

[1] In absence of a widespread convention in the literature, the position of the indices in R_{ik}^{lj} is merely chosen to facilitate the vertex interpretation in Figure 2.1.

will finally denote by tr_a the trace over the a-th vector space.

The elementary components of the system, be they quantum objects or classical vertices, are considered to interact locally with their nearest neighbours through a matrix(-valued function) $\lambda \mapsto R(\lambda)$ acting on $V \otimes V$, called *R-matrix*, that satisfies the *Yang-Baxter equation*

$$R_{12}(\lambda - \mu)R_{13}(\lambda)R_{23}(\mu) = R_{23}(\mu)R_{13}(\lambda)R_{12}(\lambda - \mu) \tag{2.1}$$

An important solution to this equation is given by the R-matrix of the *XXZ spin chain*, a model first introduced and solved in [50]. This is the example that we will consider for concreteness in the following, where $D = 2$ and γ is a complex parameter:

$$R(\lambda) = \begin{pmatrix} \sinh(\lambda + i\gamma) & 0 & 0 & 0 \\ 0 & \sinh\lambda & \sinh i\gamma & 0 \\ 0 & \sinh i\gamma & \sinh\lambda & 0 \\ 0 & 0 & 0 & \sinh(\lambda + i\gamma) \end{pmatrix} \tag{2.2}$$

We note that $R(0) = (\sinh i\gamma)P$ where P is the permutation matrix defined by $Px \otimes y = y \otimes x$ for $x, y \in V$. We define $M_a(\lambda)$ the *monodromy matrix* by

$$M_a(\lambda) = R_{a,L}(\lambda)R_{a,L-1}(\lambda)...R_{a,1}(\lambda) \tag{2.3}$$

that acts on $V \otimes V^{\otimes L}$, and is usually represented under the form

$$M_a(\lambda) = \begin{pmatrix} A(\lambda) & B(\lambda) \\ C(\lambda) & D(\lambda) \end{pmatrix} \tag{2.4}$$

where A, B, C, D are operators on $V^{\otimes L}$. The *transfer matrix* $t(\lambda)$ of the system with periodic boundary conditions is then defined by

$$t(\lambda) = \text{tr}_a M_a(\lambda) = A(\lambda) + D(\lambda) \tag{2.5}$$

We note that the coefficients of the R-matrix have then a natural interpretation in terms of Boltzmann weights of a $2D$-statistical system. Indeed, if we consider an $L \times M$ square lattice with periodic boundary conditions, whose edges carry an index $i = 1, ..., D$, and impose a Boltzmann weight R_{ik}^{lj} at each vertex where edges with indices i, j, k, l meet according to Figure 2.1, then the partition function Z_{LM} of the system is, with $\alpha_i^{M+1} \equiv \alpha_i^1$

$$Z_{LM} = \sum_{c_\cdot, \alpha_\cdot = 1}^{D} \prod_{m=1}^{M} R_{c_1^m \alpha_L^m}^{\alpha_L^{m+1} c_L^m} R_{c_L^m \alpha_{L-1}^m}^{\alpha_{L-1}^{m+1} c_{L-1}^m} ... R_{c_2^m \alpha_1^m}^{\alpha_1^{m+1} c_1^m} = \text{tr}_{1,...,L}(t(\lambda)^M) \tag{2.6}$$

The transfer matrix can be used to define a *Hamiltonian* with nearest-neighbour interactions if there is a point λ (that shall be assumed to be 0, without loss of generality) such that $R(0) = \alpha P$ is proportional to the permutation operator. Indeed, if the Hamiltonian H is defined as

$$H = \alpha t'(0) \cdot t(0)^{-1} \tag{2.7}$$

16
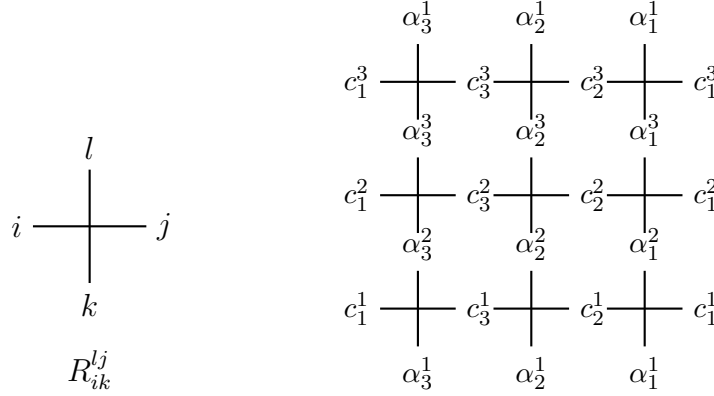
Figure 2.1: Illustration of the vertex model interpretation of the R-matrix and of the partition function.

where $'$ denotes the derivative with respect to λ, then in terms of R it reads

$$H = \sum_{i=1}^{L} R'_{i,i+1}(0) \tag{2.8}$$

with the periodic boundary condition $L+1 \equiv 1$, which is naturally interpreted as a quantum mechanical Hamiltonian for a spin chain of L spins $\sigma \in V$ interacting via $R'(0)$.

2.1.2 The ansatz

The fundamental relation that comes from the successive use of Yang-Baxter equation (2.1) and that permits to diagonalize $t(\lambda)$ is a set of commutation relations between A, B, C, D encapsulated in

$$R_{ab}(\lambda - \mu) M_a(\lambda) M_b(\mu) = M_b(\mu) M_a(\lambda) R_{ab}(\lambda - \mu) \tag{2.9}$$

For example, specializing this 4×4 matrix equation to the entries $(i, j) = (1, 3)$, $(3, 4)$ and $(1, 4)$ yields

$$\sinh(\lambda - \mu + i\gamma) B(\lambda) A(\mu) = \sinh(i\gamma) B(\mu) A(\lambda) + \sinh(\lambda - \mu) A(\mu) B(\lambda)$$
$$\sinh(i\gamma) B(\lambda) D(\mu) + \sinh(\lambda - \mu) D(\lambda) B(\mu) = \sinh(\lambda - \mu + i\gamma) B(\mu) D(\lambda)$$
$$B(\lambda) B(\mu) = B(\mu) B(\lambda)$$

$$\tag{2.10}$$

The algebraic Bethe ansatz relies on the existence of a vacuum vector $|0\rangle \in V^{\otimes L}$ such that

$$A(\lambda)|0\rangle = a(\lambda)^L |0\rangle \,, \qquad D(\lambda)|0\rangle = d(\lambda)^L |0\rangle \,, \qquad C(\lambda)|0\rangle = 0 \tag{2.11}$$

for $a(\lambda), d(\lambda)$ some functions of λ. In our case of the R-matrix (2.2) we can choose

$$|0\rangle = \begin{pmatrix} 1 \\ 0 \end{pmatrix}^{\otimes L}, \qquad a(\lambda) = \sinh(\lambda + i\gamma) \,, \qquad d(\lambda) = \sinh \lambda \tag{2.12}$$

The ansatz consists in searching for eigenvectors of $t(\lambda)$ under the form

$$X = B(\mu_1)...B(\mu_K)|0\rangle \tag{2.13}$$

where K is a priori an arbitrary integer. Using the commutation relations (2.10), it is shown by recurrence on K (acting separately with A and D) that

$$t(\lambda)B(\mu_1)...B(\mu_K)|0\rangle = T(\lambda)B(\mu_1)...B(\mu_K)|0\rangle + \sum_{i=1}^{K} F_i(\lambda)B(\lambda)B(\mu_1)...\widehat{B}(\mu_i)...B(\mu_K)|0\rangle \tag{2.14}$$

where the hat $\widehat{B}(\mu_i)$ indicates that the term is omitted in the product, and where

$$T(\lambda) = a(\lambda)^L \prod_{j=1}^{K} \frac{\sinh(\lambda - \mu_j - i\gamma)}{\sinh(\lambda - \mu_j)} + d(\lambda)^L \prod_{j=1}^{K} \frac{\sinh(\lambda - \mu_j + i\gamma)}{\sinh(\lambda - \mu_j)}$$

$$F_i(\lambda) = a(\mu_i)^L \frac{\sinh i\gamma}{\sinh(\lambda - \mu_i)} \prod_{j=1,\neq i}^{K} \frac{\sinh(\mu_i - \mu_j - i\gamma)}{\sinh(\mu_i - \mu_j)} - d(\mu_i)^L \frac{\sinh i\gamma}{\sinh(\lambda - \mu_i)} \prod_{j=1,\neq i}^{K} \frac{\sinh(\mu_i - \mu_j + i\gamma)}{\sinh(\mu_i - \mu_j)} \tag{2.15}$$

A sufficient condition for $B(\mu_1)...B(\mu_K)|0\rangle$ to be an eigenvector[2] of the transfer matrix is the vanishing of the rightmost terms in (2.14) since they are not proportional to $B(\mu_1)...B(\mu_K)|0\rangle$. With the expression of $F_i(\lambda)$, and shifting $\lambda_i = \mu_i + i\gamma/2$, it gives a set of conditions on $\lambda_1, ..., \lambda_K$, called the *Bethe ansatz equations*

$$\left(\frac{\sinh(\lambda_i + i\gamma/2)}{\sinh(\lambda_i - i\gamma/2)}\right)^L = \prod_{j\neq i} \frac{\sinh(\lambda_i - \lambda_j + i\gamma)}{\sinh(\lambda_i - \lambda_j - i\gamma)} \tag{2.16}$$

Some important comments have to be made on these equations, that we report to section 2.1.4. Letting them aside for the moment, if these equations are satisfied, then the eigenvalue $T(\lambda)$ of the transfer matrix is

$$T(\lambda) = \sinh(\lambda + i\gamma)^L \prod_{j=1}^{K} \frac{\sinh(\lambda - \lambda_j - i\gamma/2)}{\sinh(\lambda - \lambda_j + i\gamma/2)} + \sinh(\lambda)^L \prod_{j=1}^{K} \frac{\sinh(\lambda - \lambda_j + 3i\gamma/2)}{\sinh(\lambda - \lambda_j + i\gamma/2)} \tag{2.17}$$

We remark that the Bethe vector (2.13) does not depend on λ. Indeed, it is obtained from (2.9) that the transfer matrices at different spectral parameters commute

$$[t(\lambda), t(\mu)] = 0 \tag{2.18}$$

so that they can be diagonalized simultaneously. Then all the derivatives $t^{(k)}(0)$ for $k = 1, .., L$ give commuting charges that are conserved during the evolution by the Hamiltonian H.

---

[2]We should rather say a *candidate* eigenvector, in absence of further indication that this vector is non-zero.

The number of Bethe roots K is related to the total *magnetization* of the system. Indeed, denoting the spin matrices $S^z = \begin{pmatrix} 1/2 & 0 \\ 0 & -1/2 \end{pmatrix}$, $S^+ = \begin{pmatrix} 0 & 1 \\ 0 & 0 \end{pmatrix}$ and $S^- = \begin{pmatrix} 0 & 0 \\ 1 & 0 \end{pmatrix}$ and $S_{\text{tot}}^X = \sum_{i=1}^{L} S_i^X$ the total spin matrices, we have

$$[S_{\text{tot}}^z, B(\lambda)] = -B(\lambda) \tag{2.19}$$

and since $S_{\text{tot}}^z |0\rangle = \frac{L}{2}|0\rangle$, we conclude that the Bethe vectors with K Bethe roots are eigenstates of S_{tot}^z with eigenvalue $\frac{L}{2} - K$.

Let us come back to (2.18), where by differentiating the transfer matrix multiple times we get L conserved charges. This fact is often said to make the system *integrable*, in analogy to the classical case where integrability is defined as the existence of a maximal set of independent and Poisson-commuting charges. However, there are two objections to make: the first is that it gives only L charges in a space of dimension D^L; and the second is that any diagonalizable Hamiltonian has actually a maximal set of independent and commuting charges, that is given by the set of projectors onto their eigenstates. Consequently, even the definition of integrability in the quantum case is subject to discussion. The actual important property of 'what we usually call' integrable systems in the quantum case, is that it has a large number of *local* charges, i.e. charges whose matrix representation has only a number $O(L)$ of non-vanishing terms, contrarily to a generic system whose charges are typically delocalized on the whole spin chain. In fact, some authors suggest that quantum integrability should not be a binary property, but rather a property classifying the degree of locality of the charges [51]. It is also argued by other authors that the method of separation of variables could provide the right framework to define the notion of quantum integrability [10].

Anyway, the property that we use in the models that we study in this thesis is especially their *exactly solvable* nature rather than the actual presence of local conserved charges.

2.1.3   A word on numerically solving the Bethe equations

Apart from some very special cases, the Bethe equations (2.16) cannot be solved analytically in finite size, and numerics is often used to conjecture the pattern of roots. To that purpose the equations (2.16) are transformed into *logarithmic form* by taking the logarithm of them. Transforming the product into sums, using $\log(zz') = \log z + \log z' + 2i\pi p$ with $p \in \{-1, 0, 1\}$ we accumulate an integer and get

$$s(\lambda_i) = \frac{I_i}{L} + \frac{1}{L}\sum_{j=1}^{K} r(\lambda_i - \lambda_j) \tag{2.20}$$

with

$$\begin{aligned} s(\lambda) &= \frac{i}{2\pi}\log-\frac{\sinh(\lambda + i\gamma/2)}{\sinh(\lambda - i\gamma/2)} = \frac{1}{\pi}\arctan\frac{\tanh\lambda}{\tan\gamma/2} \\ r(\lambda) &= \frac{i}{2\pi}\log-\frac{\sinh(\lambda + i\gamma)}{\sinh(\lambda - i\gamma)} = \frac{1}{\pi}\arctan\frac{\tanh\lambda}{\tan\gamma} \end{aligned} \tag{2.21}$$

The logarithm is defined such that $\log e^{i\theta} = i\theta$ for $-\pi < \theta \leq \pi$. I_i are integers (if K is odd) or half-integers (if K is even, because of the $-$ sign in the definition of r) and are called *Bethe numbers*. These numbers clearly depend on the position of the branch cut of the logarithm, and on the way we 'slice' the product. With these conventions, they are typically all distinct and range from $-L/4$ to $L/4$. We should however mention that exceptions to the rules are unfortunately rather common in the Bethe ansatz, see e.g. [52].

The method usually used to solve these equations depends on the goal:

- If the objective is to find all the solutions at a given (small) size L, then it is actually more efficient to solve the zero-remainder conditions of the TQ relations mentioned further below (2.23) or of the set of two TQ relations in (2.66) to discard the inadmissible solutions. If one searches for a particular solution that corresponds to a given eigenvalue for which we know the λ dependence, then the so-called Mac-Coy method [53] can be used, that consists in solving for the coefficients of $Q(\lambda)$ in (2.23) from the known expression of the eigenvalue $T(\lambda)$.

- If the objective is to determine one given eigenvalue at a large system size L, then one can use a Newton method to solve numerically (2.20) with the corresponding Bethe numbers and an appropriate initial guess. If the Bethe roots are real, then the initial guess need not be particularly close to the solution, and the algorithm converges fast. However, if there are *approximate strings* in the solution (i.e., solutions where a Bethe root or the difference between two Bethe roots are close to a singularity of the logarithms in (2.20)) then the initial guess has to be close, and sometimes even *very* close to the solution to converge. To that end, one can start from a small size L where the root pattern has been found by other methods, and use it to build an initial guess in size $L + 2$. Iterating the procedure often permits to reach hundreds or even thousands of sites. In case of additional parameters such as a twist, if the solution is easier to find in the limit of vanishing parameter, one can increase it gradually while updating the solution to the equations.

2.1.4 Admissible and non-admissible solutions

There are some subtleties in the derivation and in the resolution of (2.16).

Firstly, from the expression of $F_i(\lambda)$, it was implicitly assumed that there are no coinciding $\lambda_i = \lambda_j$ with $i \neq j$, whereas this case has no reason to be excluded solely from (2.16). Secondly, since $[B(\lambda), B(\mu)] = 0$, the ordering of the λ_i is irrelevant and two solutions of (2.16) differing only by a permutation of the Bethe roots λ_i should be considered identical. Thirdly, the Bethe equations (2.16) are singular (zero or divergent, depending on their writing) in presence of *exact strings*, i.e. whenever there are two roots whose difference is exactly equal to $\pm i\gamma$.

The first point can be understood with the following observation. Since the coefficients of $R(\lambda)$ do not have any singularity, and since the eigenvectors of $t(\lambda)$ that is constructed from $R(\lambda)$ do not depend on λ, the eigenvalues must have no singularity in λ. However, the

expression of the eigenvalue (2.17) has a priori poles at each $\lambda_i - i\gamma/2$. In fact, it is readily checked that the condition under which the residue of $T(\lambda)$ at $\lambda_i - i\gamma/2$ vanishes is exactly the Bethe equation (2.16). Moreover, if there are two coinciding Bethe roots $\lambda_i = \lambda_j$, then there is a priori an additional pole of order 2 at $\lambda_i - i\gamma/2$ in $T(\lambda)$, and the vanishing of this pole of order 2 imposes two conditions, whereas there is only one variable associated to it. Thus, globally there is one equation more than unknowns, so that the mere verification of (2.16) is not enough to cancel the poles. A solution with coinciding Bethe roots thus does not generically yield an eigenvector.

The second point can be solved if one defines

$$Q(\lambda) = \prod_{j=1}^{K} \sinh(\lambda - \lambda_j) \tag{2.22}$$

and searches directly for $Q(\lambda)$ rather than its roots λ_i. The eigenvalue (2.17) can be rewritten in terms of Q to give the so-called TQ-relation

$$\tilde{T}(\lambda)Q(\lambda) = \sinh(\lambda + i\gamma/2)^L Q(\lambda - i\gamma) + \sinh(\lambda - i\gamma/2)^L Q(\lambda + i\gamma) \tag{2.23}$$

with $\tilde{T}(\lambda) = T(\lambda - i\gamma/2)$. The condition under which $T(\lambda)$ is a trigonometric polynomial in λ is actually stronger than the Bethe equations (2.16) since coinciding roots that do not cancel both poles are discarded. Hence, solving for $Q(\lambda)$ in (2.23) rather than for λ_i's in (2.16) solves the two first points in one shot.

However, it does not answer the third point. Indeed, any solution $(i\gamma/2, -i\gamma/2, \lambda_3, ..., \lambda_K)$ where $\lambda_3, ..., \lambda_K$ satisfy the Bethe equations (2.16) (for $\pm i\gamma/2$, they are automatically satisfied if both sides are multiplied by the denominators beforehand) gives a trigonometric polynomial $T(\lambda)$. However, it turns out that the Bethe vector satisfies $B(0)B(-i\gamma)B(\mu_3)...B(\mu_K)|0\rangle = 0$. It could be normalized beforehand so that it is never zero, and take the case of exact strings as a limiting case; but then the limit would depend on the way the roots λ_i of the strings converge to $\pm i\gamma/2$, which does not permit to conclude whether (2.17) is indeed an eigenvalue or not. In fact, the solutions to the Bethe equations with exact strings sometimes do yield eigenvalues and eigenvectors of the transfer matrix, and sometimes not. The problem is to be able to find a way of taking the limits so that the 'unwanted' terms in (2.14), i.e. the right-most terms that are not proportional to the left-hand side, actually vanish faster than the 'wanted' term that is the first term in the right-hand side. In [54, 55] a sufficient condition was found under which such a limit can be taken, and thus for which the Bethe vector is indeed an eigenvector, consisting in taking a particular ansatz for the limit. How adding a twist to the Bethe equations permits to distinguish admissible from inadmissible solutions was studied in [56]. Besides, very recently an efficient algorithm [57] was found to solve the TQ relation (2.23) while discarding automatically the inadmissible solutions among those with an exact string, with only algebraic manipulations and zero-remainder conditions. However, the reason why the algorithm works is arguably mysterious, and in particular is very far from the reasoning done in [54, 56, 55].

In the next section, we present a personal contribution to this question, that both explains why the algorithm of [57] works, i.e. why it imposes the condition derived in [54, 55], and

shows that the TQ relation (2.23) has to be supplemented with another TQ-like relation to yield only admissible solutions. It bridges the gap between different approaches and yield an elegant criterion to distinguish between admissible and non-admissible solutions.

2.2 An additional TQ relation

The goal of this section is to establish that the TQ relation (2.23) in the limit $\gamma \to 0$ has to be supplemented with another TQ relation to discard the inadmissible solutions that do not yield eigenvalues of the transfer matrix. For $e^{i\gamma}$ not root of unity, an analogous result to Theorem 1 can be established with the same arguments[3].

We thus consider Bethe roots $\Lambda = \{\lambda_1, ..., \lambda_K\}$ solution to the equations

$$\left(\frac{\lambda_i + i/2}{\lambda_i - i/2}\right)^L = \prod_{j=1, \neq i}^{K} \frac{\lambda_i - \lambda_j + i}{\lambda_i - \lambda_j - i} \tag{2.24}$$

and denote $Q(\lambda) = \prod_k (\lambda - \lambda_k)$. We denote $\bar{\Lambda}$ the set of λ_i's such that there does not exist another λ_j with $\lambda_i - \lambda_j = \pm i$, and S the set of complex numbers s (the 'center of strings') such that $s + i/2 \in \Lambda$ and $s - i/2 \in \Lambda$. We denote $\bar{Q}(\lambda) = \prod_{\lambda_k \in \bar{\Lambda}} (\lambda - \lambda_k)$. We will finally use the slightly abusive notation $Q^*(\lambda) = \prod_k (\lambda - \lambda_k)$ if $\lambda \notin \Lambda$ and $Q^*(\lambda_p) = \prod_{k \neq p} (\lambda_p - \lambda_k)$ for $\lambda_p \in \Lambda$. Here, the TQ relation (2.23) reads[4]

$$T(\lambda)Q(\lambda) = (\lambda + i/2)^L Q(\lambda - i) + (\lambda - i/2)^L Q(\lambda + i) \tag{2.25}$$

Before addressing the main results, for sake of completeness we recall here the following

Lemma 1. *We have $S = \varnothing$ or $S = \{0\}$.*

Proof. Assume that there are two roots such that $\lambda_{i_1} - \lambda_{i_2} = i$. Denote $s = \lambda_{i_1} - i/2$. Then from (2.24) with $i = i_1$, either $\lambda_{i_1} = i/2$, in which case $s = 0$, or there exists another λ_{i_3} such that $\lambda_{i_1} - \lambda_{i_3} = -i$. The same argument can be then repeated with $i = i_3$, so that $s = ni$ with n a negative or null integer, since there is a finite number of roots. Now, (2.24) for $i = i_2$ implies that either $\lambda_{i_2} = -i/2$, in which case $s = 0$, or there exists another λ_{i_4} such that $\lambda_{i_2} - \lambda_{i_4} = i$. The same argument can be then repeated with $i = i_4$, implying that $s = ni$ with n a positive or null integer. Thus $s = 0$. □

2.2.1 Polynomiality of the other solution to the TQ relation

Let us start with the following property, that generalizes [58] to the exact strings case.

---

[3]For $e^{i\gamma}$ root of unity, there are more possible strings than what is written in Lemma 1, so that the arguments and the result could change significantly.

[4]We dropped the tilde in $\tilde{T}$ in (2.23) for convenience.

Lemma 2. *There exist a polynomial $P_0(\lambda)$ and complex numbers α_s for $s \in S$ such that*

$$P(\lambda + i/2)Q(\lambda - i/2) - P(\lambda - i/2)Q(\lambda + i/2) = \lambda^L \tag{2.26}$$

with

$$P(\lambda) = P_0(\lambda) + Q(\lambda)\sum_{s \in S}\alpha_s\psi(-i(\lambda - s) + 1/2) \tag{2.27}$$

where $\psi(x)$ is the digamma function. Moreover, $\alpha_0 = 0$ if and only if the following additional Bethe equation is satisfied

$$(-1)^L = \prod_{\lambda_j \neq \pm i/2} \frac{\lambda_j + i/2}{\lambda_j - i/2} \cdot \frac{\lambda_j + 3i/2}{\lambda_j - 3i/2} \tag{2.28}$$

Proof. It is directly inspired by [58], where they (implictly) treated the case $S = \varnothing$.
Denote

$$R(\lambda) = \frac{\lambda^L}{Q(\lambda + i/2)Q(\lambda - i/2)} \tag{2.29}$$

We have

$$\frac{T(\lambda)}{Q(\lambda + i)Q(\lambda - i)} = R(\lambda + i/2) + R(\lambda - i/2) \tag{2.30}$$

Since each $s \in S$ appears twice in the denominator in $R(\lambda)$, we can decompose

$$R(\lambda) = \pi(\lambda) + \frac{q_-(\lambda)}{Q(\lambda - i/2)} + \frac{q_+(\lambda)}{Q(\lambda + i/2)} + \sum_{s \in S}\frac{c_s}{(\lambda - s)^2} \tag{2.31}$$

with $\pi(\lambda), q_\pm(\lambda)$ polynomials of degree less than or equal to $L - 2n$ and $n - 1$ respectively (since a term of order n in the numerator could be reabsorbed in the $\pi(\lambda)$ term), and c_s complex numbers. From this one gets

$$\begin{aligned}\frac{T(\lambda)}{Q(\lambda + i)Q(\lambda - i)} =& \pi(\lambda - i/2) + \pi(\lambda + i/2) + \frac{q_-(\lambda - i/2)}{Q(\lambda - i)} + \frac{q_+(\lambda + i/2)}{Q(\lambda + i)}\\ & + \frac{q_+(\lambda - i/2) + q_-(\lambda + i/2)}{Q(\lambda)} + \sum_{s \in S}\frac{c_s}{(\lambda - s + i/2)^2} + \frac{c_s}{(\lambda - s - i/2)^2}\end{aligned} \tag{2.32}$$

Multiplying by $(\lambda - s + i/2)^2$ and sending $\lambda \to s - i/2$, since there is no double pole in $s - i/2$ in the left-hand side, one gets $c_s = 0$. For $\lambda_j \in \bar{\Lambda}$, multiplying by $(\lambda - \lambda_j)$ and taking $\lambda \to \lambda_j$ yields

$$q_+(\lambda_j - i/2) + q_-(\lambda_j + i/2) = 0 \tag{2.33}$$

meaning that there exists a polynomial σ such that

$$q_+(\lambda - i/2) + q_-(\lambda + i/2) = \bar{Q}(\lambda)\sigma(\lambda) \tag{2.34}$$

23

and thus a polynomial $q(\lambda)$ such that

$$q_{\pm}(\lambda) = \pm q(\lambda \pm i/2) + \frac{1}{2}\bar{Q}(\lambda \pm i/2)\sigma(\lambda \pm i/2) \qquad (2.35)$$

(for example, take $q(\lambda) = q_+(\lambda - i/2) - \frac{1}{2}\bar{Q}(\lambda)\sigma(\lambda)$). Thus

$$R(\lambda) = \pi(\lambda) - \frac{q(\lambda - i/2)}{Q(\lambda - i/2)} + \frac{q(\lambda + i/2)}{Q(\lambda + i/2)} + \frac{1}{2}\left(\frac{\sigma(\lambda - i/2)}{\prod_{s\in S}(\lambda - s)(\lambda - i - s)} + \frac{\sigma(\lambda + i/2)}{\prod_{s\in S}(\lambda + i - s)(\lambda - s)}\right) \qquad (2.36)$$

$\pi(\lambda)$ can be decomposed as any polynomial into

$$\pi(\lambda) = \rho(\lambda + i/2) - \rho(\lambda - i/2) \qquad (2.37)$$

with $\rho(\lambda)$ a polynomial, unique up to an additive constant. Denote now

$$U(\lambda) = \frac{1}{2}\left(\frac{\sigma(\lambda - i/2)}{\prod_{s\in S}(\lambda - s)(\lambda - i - s)} + \frac{\sigma(\lambda + i/2)}{\prod_{s\in S}(\lambda + i - s)(\lambda - s)}\right) \qquad (2.38)$$

It can be decomposed as

$$U(\lambda) = \sum_{s\in S}\frac{a_s}{\lambda - s} + \frac{b_s^+}{\lambda - (s + i)} + \frac{b_s^-}{\lambda - (s - i)} \qquad (2.39)$$

with a_s, b_s^+, b_s^- constants. Using the property of the digamma function $\psi(x)$

$$\psi(x + 1) - \psi(x) = \frac{1}{x} \qquad (2.40)$$

one can rewrite it as

$$U(\lambda) = V(\lambda + i/2) - V(\lambda - i/2) \qquad (2.41)$$

where

$$V(\lambda) = \sum_{s\in S_0} -i(a_s + b_s^+ + b_s^-)\psi(-i(\lambda - s) + 1/2) + \frac{b_s^-}{\lambda - (s - i/2)} - \frac{b_s^+}{\lambda - (s + i/2)} \qquad (2.42)$$

Therefore

$$R(\lambda) = \frac{P(\lambda + i/2)}{Q(\lambda + i/2)} - \frac{P(\lambda - i/2)}{Q(\lambda - i/2)} \qquad (2.43)$$

with

$$P(\lambda) = \rho(\lambda)Q(\lambda) + q(\lambda) + Q(\lambda)V(\lambda) \qquad (2.44)$$

Note that since $s \pm i/2$ is a root of $Q(\lambda)$, P is a polynomial if and only if $a_s + b_s^+ + b_s^- = 0$ for all $s \in S$. Recalling (2.29), one gets

$$P(\lambda + i/2)Q(\lambda - i/2) - P(\lambda - i/2)Q(\lambda + i/2) = \lambda^L \qquad (2.45)$$

24

as stated in the Lemma. Replacing the $(\lambda \pm i/2)^L$ in the TQ relation (2.25) with this equation, one gets

$$T(\lambda) = P(\lambda + i)Q(\lambda - i) - P(\lambda - i)Q(\lambda + i) \tag{2.46}$$

Evaluating this relation at $s - i/2$ yields

$$T(s - i/2) = P(s + i/2)Q(s - 3i/2) + (a_s + b_s^+ + b_s^-)Q^*(s + i/2)Q(s - 3i/2) \tag{2.47}$$

Using now the TQ relation:

$$T(s - i/2) = \frac{Q^*(s + i/2)}{Q^*(s - i/2)}(s - i)^L + \frac{Q(s - 3i/2)}{Q^*(s - i/2)}s^L \tag{2.48}$$

and relation (2.45) for $\lambda = s + i$

$$P(s + i/2) = -\frac{(s + i)^L}{Q(s + 3i/2)} \tag{2.49}$$

together with the fact that $s = 0$ is the only possible string, one gets from (2.47) and (2.48) that $a_s + b_s^+ + b_s^- = 0$ if and only if

$$(-1)^L = \prod_{\lambda_j \neq \pm i/2} \frac{\lambda_j + i/2}{\lambda_j - i/2} \cdot \frac{\lambda_j + 3i/2}{\lambda_j - 3i/2} \tag{2.50}$$

which concludes the proof. $\qquad\square$

2.2.2 Polynomiality of $P(\lambda)$ and constructability of the Bethe state

We remark that (2.50) is exactly the condition found in [54, 55] to have an admissible solution of the Bethe equations. In fact, we have the following

Lemma 3. *Let $\{\lambda_1, ..., \lambda_K\}$ a solution to the Bethe equations. There exists a function $\epsilon \mapsto \{\lambda_1^\epsilon, ..., \lambda_K^\epsilon\}$ with $\lim_{\epsilon \to 0} \lambda_i^\epsilon = \lambda_i$ and $\lambda_k^\epsilon - \lambda_p^\epsilon \neq \pm i$ such that*

$$\lim_{\epsilon \to 0} B(\lambda_1^\epsilon - i/2)...B(\lambda_K^\epsilon - i/2)|0\rangle \tag{2.51}$$

exists and is an eigenvector of the transfer matrix, if and only if the function $P(\lambda)$ of Lemma 2 is a polynomial.

Proof. Let us denote

$$F(\lambda) = \frac{T(\lambda)}{(\lambda + i/2)^L(\lambda - i/2)^L} \tag{2.52}$$

with $F_\epsilon(\lambda)$ its perturbed version, involving $T_\epsilon(\lambda)$ defined in terms of Q_ϵ:

$$T_\epsilon(\lambda) = \frac{Q_\epsilon(\lambda + i)(\lambda - i/2)^L + Q_\epsilon(\lambda - i)(\lambda + i/2)^L}{Q_\epsilon(\lambda)} \tag{2.53}$$

that is not anymore a polynomial when $\epsilon \neq 0$.

The condition for $B(\lambda_1^\epsilon - i/2)...B(\lambda_K^\epsilon - i/2)|0\rangle$ to be an eigenvector of the transfer matrix in the limit $\epsilon \to 0$ is

$$\lim_{\epsilon \to 0} \text{Res}\,(F_\epsilon(\lambda), \lambda_i^\epsilon) = 0 \tag{2.54}$$

for all i, as shown in [54] (although written in a different form).

Let us first build a P_ϵ corresponding to the Q_ϵ. Decomposing

$$\frac{\lambda^L}{Q_\epsilon(\lambda + i/2)Q_\epsilon(\lambda - i/2)} = \sum_k \frac{a_k^+(\epsilon)}{\lambda - (\lambda_k^\epsilon + i/2)} + \frac{a_k^-(\epsilon)}{\lambda - (\lambda_k^\epsilon - i/2)} \tag{2.55}$$

one can write

$$\frac{\lambda^L}{Q_\epsilon(\lambda + i/2)Q_\epsilon(\lambda - i/2)} = U_\epsilon(\lambda + i/2) - U_\epsilon(\lambda - i/2) \tag{2.56}$$

with

$$U_\epsilon(\lambda) = \sum_k -ia_k^+(\epsilon)\psi(-i(\lambda - (\lambda_k^\epsilon + i/2)) + 1/2) - ia_k^-(\epsilon)\psi(-i(\lambda - (\lambda_k^\epsilon - i/2)) + 1/2) \tag{2.57}$$

and so

$$P_\epsilon(\lambda + i/2)Q_\epsilon(\lambda - i/2) - P_\epsilon(\lambda - i/2)Q_\epsilon(\lambda + i/2) = \lambda^L \tag{2.58}$$

with

$$P_\epsilon(\lambda) = Q_\epsilon(\lambda)U_\epsilon(\lambda) \tag{2.59}$$

which has poles at $\lambda_k^\epsilon - ni$ with n a strictly positive integer, with residue $-(a_k^+(\epsilon) + a_k^-(\epsilon))Q_\epsilon(\lambda_k^\epsilon - ni)$. With relation (2.58), one has

$$F_\epsilon(\lambda) = \frac{P_\epsilon(\lambda + i)Q_\epsilon(\lambda - i) - P_\epsilon(\lambda - i)Q_\epsilon(\lambda + i)}{(\lambda + i/2)^L(\lambda - i/2)^L} \tag{2.60}$$

which has a pole at every λ_k^ϵ with residue

$$r_k(\epsilon) = \frac{(a_k^+(\epsilon) + a_k^-(\epsilon))Q_\epsilon(\lambda_k^\epsilon - i)Q_\epsilon(\lambda_k^\epsilon + i)}{(\lambda_k^\epsilon + i/2)^L(\lambda_k^\epsilon - i/2)^L} \tag{2.61}$$

We now pick a k that corresponds to $i/2$ or $-i/2$, for example without loss of generality $\lambda_k = i/2$. The quantity $(a_k^+(\epsilon) + a_k^-(\epsilon))Q_\epsilon(\lambda_k^\epsilon - i)/(\lambda_k^\epsilon - i/2)^L$ is undetermined when $\epsilon \to 0$. With relation (2.58) at $\lambda_k^\epsilon - i/2$, one gets

$$P_\epsilon(\lambda_k^\epsilon)Q_\epsilon(\lambda_k^\epsilon - i) + (a_k^+(\epsilon) + a_k^-(\epsilon))Q_\epsilon(\lambda_k^\epsilon - i)Q_\epsilon^*(\lambda_k^\epsilon) = (\lambda_k^\epsilon - i/2)^L \tag{2.62}$$

thus

$$\frac{(a_k^+(\epsilon) + a_k^-(\epsilon))Q_\epsilon(\lambda_k^\epsilon - i)}{(\lambda_k^\epsilon - i/2)^L} = \frac{1}{Q_\epsilon^*(\lambda_k^\epsilon)}\left(1 - \frac{P_\epsilon(\lambda_k^\epsilon)Q_\epsilon(\lambda_k^\epsilon - i)}{(\lambda_k^\epsilon - i/2)^L}\right) \tag{2.63}$$

The left-hand side vanishes if and only if $a_k^+(\epsilon) + a_k^-(\epsilon)$ vanishes. Indeed, if the left-hand side vanishes, then $\frac{Q_\epsilon(\lambda_k^\epsilon - i)}{(\lambda_k^\epsilon - i/2)^L}$ cannot vanish in the right hand-side. If $a_k^+(\epsilon) + a_k^-(\epsilon)$ vanishes,

then $\frac{Q_\epsilon(\lambda_k^\epsilon - i)}{(\lambda_k^\epsilon - i/2)^L}$ cannot diverge when $\epsilon \to 0$, otherwise the right-hand side would diverge faster since $P(i/2) \neq 0$, see (2.49); and so the whole left-hand side must vanish.

If P is not a polynomial, according to Lemma 2 it must have a pole at $-3i/2$, so that $a_k^+(\epsilon) + a_k^-(\epsilon)$ does not vanish when $\epsilon \to 0$, at least for one k such that $\lambda_k = i/2$ or $\lambda_k = -i/2$ (we can assume that it is true for $i/2$; otherwise we could have chosen $-i/2$ before). Hence the left-hand side of (2.63) does not vanish and we cannot have $r_k(\epsilon) \to 0$ when $\epsilon \to 0$.

If P is a polynomial, for an arbitrary function $\epsilon \mapsto \lambda_k^\epsilon$, the different poles $a_k^+(\epsilon) + a_k^-(\epsilon)$ do not necessarily vanish individually in the limit $\epsilon \to 0$, since they can compensate each other (for example, $1/(\lambda - \epsilon) - 1/(\lambda + \epsilon)$ does not have any poles in the limit $\epsilon \to 0$, even if the residues at $\epsilon \neq 0$ do not vanish in the limit $\epsilon \to 0$). Coming back to (2.58) evaluated at $\lambda = \lambda_k^\epsilon - i/2$ for $\lambda_k = -i/2$ and for $\lambda_k = i/2$, one sees that the vanishing of the residues is equivalent to

$$Q(-3i/2) = \frac{(-i)^L}{P(-i/2)}, \qquad Q_\epsilon(\lambda_k^\epsilon - i) \sim \frac{(\lambda_k^\epsilon - i/2)^L}{P(i/2)} \quad \text{for } \lambda_k = i/2 \qquad (2.64)$$

The first condition is always satisfied when P is a polynomial, and the second one is an additional one that has to be satisfied for the Bethe vector to be an eigenvector in the limit $\epsilon \to 0$. This shows that if P is a polynomial, then the poles $r_k(\epsilon)$ can vanish in the limit $\epsilon \to 0$ with an appropriate choice of roots λ_k^ϵ.

$\square$

We remark that the second condition in (2.64), writing $i/2 + \epsilon$ and $-i/2 + \eta(\epsilon)$ the perturbed roots, can be translated into

$$\eta(\epsilon) = \epsilon + \frac{\epsilon^L Q(3i/2)}{i^L Q^*(-i/2)} + o(\epsilon^L) \qquad (2.65)$$

which was the regularization found in [54].

2.2.3 An additional TQ relation

We can now prove the

Theorem 1. $Q(\lambda) = \prod_{i=1}^K (\lambda - \lambda_i)$ *is an admissible solution to the Bethe equations if and only if in the two TQ relations*

$$\begin{aligned} T_0(\lambda)Q(\lambda) &= W_0(\lambda - i/2)Q(\lambda + i) + W_0(\lambda + i/2)Q(\lambda - i) \\ T_1(\lambda)Q'(\lambda) &= W_1(\lambda - i/2)Q'(\lambda + i) + W_1(\lambda + i/2)Q'(\lambda - i) \end{aligned} \qquad (2.66)$$

where
$$\begin{aligned} Q'(\lambda) &= Q(\lambda + i/2) - Q(\lambda - i/2) \\ W_0(\lambda) &= \lambda^L \\ W_1(\lambda) &= W_0(\lambda + i/2) + W_0(\lambda - i/2) - T_0(\lambda) \end{aligned} \qquad (2.67)$$

the functions $T_0(\lambda)$ and $T_1(\lambda)$ are polynomials.

Proof. It is straightforward to show that

$$W_1(\lambda) = Q'(\lambda - i/2)P'(\lambda + i/2) - Q'(\lambda + i/2)P'(\lambda - i/2) \tag{2.68}$$

where $P'(\lambda) = P(\lambda + i/2) - P(\lambda - i/2)$ with $P(\lambda)$ the function introduced in Lemma 2, using equation (2.26). Then

$$T_1(\lambda) = P'(\lambda + i)Q'(\lambda - i) - P'(\lambda - i)Q'(\lambda + i) \tag{2.69}$$

Now, from the general form of P in Lemma 2, one has

$$P'(\lambda) = A(\lambda) + Q'(\lambda)\alpha_0\psi(-i\lambda) \tag{2.70}$$

with $A(\lambda)$ a rational function with a sole pole at 0 with residue proportional to α_0, using $\psi(x+1) - \psi(x) = 1/x$. Since ψ has a pole at -1, T_1 has a priori a pole at 0 with residue $i\alpha_0 Q'(-i)Q'(i)$. From Lemma 1, $\pm i$ are never center of strings and so $Q'(\pm i) \neq 0$ if $\alpha_0 \neq 0$. It follows that T_1 is a polynomial if and only if P is. Then Lemma 3 concludes the proof. $\square$

Let us now come back to the algorithm of Marboe and Volin [57]. It consists in introducing functions $Q_{a,s}$ with $s = 0, ..., L$ and $a = 0, 1, 2$ if $s \leq K$ and $a = 0, 1$ if $s > K$, satisfying the following QQ relations

$$Q_{a+1,s}(\lambda)Q_{a,s+1}(\lambda) \propto Q_{a+1,s+1}(\lambda + i/2)Q_{a,s}(\lambda - i/2) - Q_{a+1,s+1}(\lambda - i/2)Q_{a,s}(\lambda + i/2) \tag{2.71}$$

with the boundary conditions $Q_{0,0}(\lambda) = \lambda^L$, $Q_{2,s} = 1$ for $s \leq K$, $Q_{1,s} = 1$ for $s > K$, and imposing that all the $Q_{a,s}$ are polynomials. The $Q(\lambda)$ is then given by $Q_{1,0}(\lambda)$. Actually, it is readily checked that the two TQ relations (2.66) are exactly the relations obtained when $Q_{a,s}$ are imposed to be polynomials for $a = 0, 1, 2$ and $s = 0, 1$ (in the special case $K = 1$ there cannot be strings and the second equation of (2.66) is trivially satisfied). Thus, according to Theorem 1, all the other polynomials $Q_{a,s}$ for $s > 1$ are actually superfluous.

We also remark that the fact that only one additional TQ relation is needed to discard the inadmissible solutions is linked to the fact that there is only one possible exact string (otherwise this TQ relation would only give one equation relating the α_s's).

Let us illustrate Theorem 1 with sizes $L = 4$ and $L = 5$. In both cases the polynomial $Q(\lambda) = (\lambda + i/2)(\lambda - i/2) = \lambda^2 + \frac{1}{4}$ is a solution to the first TQ relation with

$$\begin{aligned} T_0(\lambda) &= -\tfrac{3}{8} + 3\lambda^2 + 2\lambda^4 , && \text{if } L = 4 \\ T_0(\lambda) &= -\tfrac{11}{8}\lambda + 3\lambda^3 + 2\lambda^5 , && \text{if } L = 5 \end{aligned} \tag{2.72}$$

However, the corresponding $T_1(\lambda)$ reads

$$\begin{aligned} T_1(\lambda) &= -4(2 + 3\lambda^2) , && \text{if } L = 4 \\ T_1(\lambda) &= \frac{4}{\lambda} - 8\lambda - 16\lambda^3 , && \text{if } L = 5 \end{aligned} \tag{2.73}$$

indicating that the second TQ relation is satisfied for $L = 4$ but not for $L = 5$. Besides, the function $P(\lambda)$ of Lemma 2 reads

$$P(\lambda) = -i\lambda \left(\lambda^2 + \tfrac{5}{4}\right), \qquad \text{if } L = 4$$

$$P(\lambda) = \frac{1}{2i}\lambda^2 \left(\lambda^2 + \tfrac{1}{4}\right) + \tfrac{i}{2} + \left(\lambda^2 + \tfrac{1}{4}\right) i\psi(-i\lambda + 1/2), \qquad \text{if } L = 5 \tag{2.74}$$

and is a polynomial if and only if $T_1(\lambda)$ is a polynomial. It turns out that $T_0(\lambda)$ is indeed an eigenvalue of the transfer matrix for $L = 4$, but not for $L = 5$, in agreement with the Theorem.

In Figure 2.2 we plot the roots of all the polynomials $Q(\lambda)$ solution to the TQ relation (2.25) in size $L = 6$, showing in blue those that solve the two TQ relations (2.66) and in red those that only solve the first one. Only the solutions $(-i/2, i/2)$ $(-i/2, 0, i/2)$ among the blue ones involve exact strings in Figure 2.2 (all the red inadmissible solutions must exhibit exact strings). We see that the number of admissible solutions with K roots is $\binom{L}{K} - \binom{L}{K-1}$. We recall that in the Heisenberg spin chain case the Bethe states are necessarily highest-weight states with respect to the underlying $su(2)$ algebra. Taking into account that the eigenvalue corresponding to a solution with K Bethe roots is $(L - 2K + 1)$-fold degenerate, one obtains 2^6 eigenstates indeed.
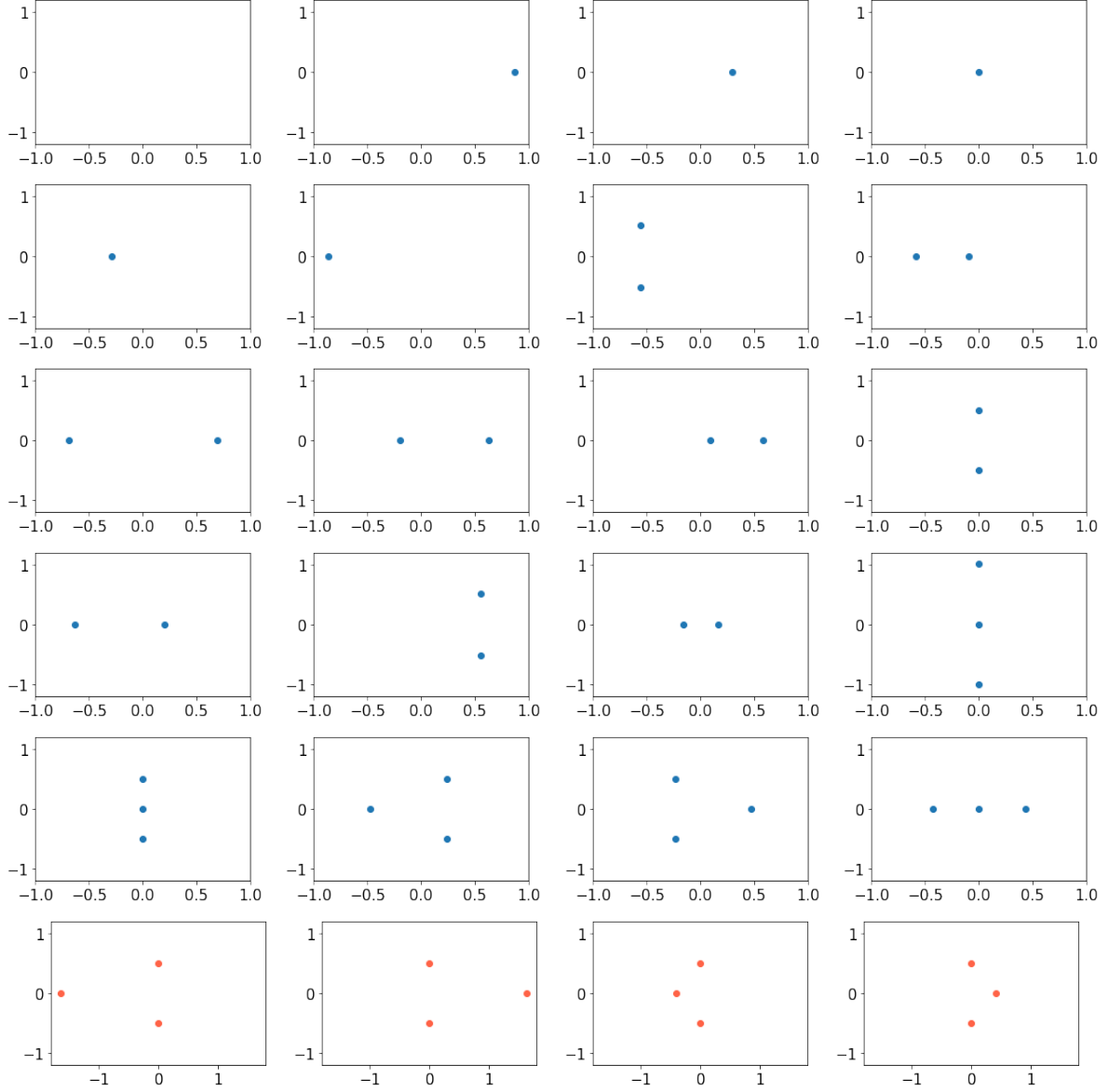
Figure 2.2: In blue: the roots of all the solutions $Q(\lambda)$ to the TQ relations (2.66) in size $L = 6$. In red: the roots of the solutions to the first TQ relation in (2.66) that are not solution to the second one, and thus that do not contribute to the spectrum.

2.3 Geometrical models

As it is often the case in statistical mechanics, a single model can be interpreted as describing several different physical systems, sometimes through an exact mapping and sometimes through partial summation of degrees of freedom and rearrangement. In this section we

explain how the XXZ spin chain presented above is related to geometrical models such as the $O(N)$ loop model or the Q-state Potts model and percolation.

2.3.1 Loop models

Mapping

In section 2.1.1 we saw that the integrable model built from an R-matrix has a direct interpretation in terms of both a 2D vertex model and of a quantum spin chain. There is another interesting interpretation in terms of *loop models*. Let us first write the R-matrix of the XXZ spin chain as

$$R(\lambda) = \sinh(\lambda + i\gamma) \, \overset{\displaystyle \frown}{} \, + \sinh\lambda \, \overset{\displaystyle \frown}{} \tag{2.75}$$

with

$$\overset{\displaystyle \frown}{} = \begin{pmatrix} 1 & 0 & 0 & 0 \\ 0 & 0 & x^{-1}\omega^{-2} & 0 \\ 0 & x\omega^2 & 0 & 0 \\ 0 & 0 & 0 & 1 \end{pmatrix}, \qquad \overset{\displaystyle \frown}{} = \begin{pmatrix} 0 & 0 & 0 & 0 \\ 0 & 1 & x^{-1}\omega^2 & 0 \\ 0 & x\omega^{-2} & 1 & 0 \\ 0 & 0 & 0 & 0 \end{pmatrix} \tag{2.76}$$

with x and ω parameters that must satisfy

$$\sinh(\lambda + i\gamma)\omega^{-2} + \sinh(\lambda)\omega^2 = x\sinh(i\gamma)$$
$$\sinh(\lambda + i\gamma)\omega^2 + \sinh(\lambda)\omega^{-2} = x^{-1}\sinh(i\gamma) \tag{2.77}$$

which requires $x^2 = \frac{\sinh(\lambda+i\gamma)-e^{i\gamma}\sinh\lambda}{-e^{i\gamma}\sinh(\lambda+i\gamma)+\sinh\lambda}$ and $\omega^4 = -e^{i\gamma}$. The important point to notice is that in the partition function (2.6), because of the periodic boundary conditions, on a given line a change of indices from 1 to 2 must occur the same number of times than a change of indices from 2 to 1. Hence x and x^{-1} in $\overset{\displaystyle \frown}{}$ and $\overset{\displaystyle \frown}{}$ appear the same number of times in the total weight of a configuration. It follows that after changing the value of x in (2.76), although it modifies the R-matrix that would no longer satisfy the Yang-Baxter equation, each term in the partition function (2.6) takes exactly the same value. Effectively, the value of x in (2.76) can be changed at will, and be set for convenience to 1.

The position of the non-zero terms in the matrices $\overset{\displaystyle \frown}{}$ and $\overset{\displaystyle \frown}{}$ constrains the indices to follow a certain pattern in each non-vanishing term in the partition function (2.6). Indeed, the action of R on a basis vector $e_i \otimes e_j$ has a non-zero component over $e_k \otimes e_l$ only if $i = l$ and $j = k$, or if $i = k'$ and $j = l'$ with by definition $x' = D - x + 1$ for an index $x = 1, ..., D$. If imposing an equality between indices is depicted by a line in Figure 2.1, then the two matrices correspond to inserting portions of loops depicted by their notation, see Figure 2.3.

Each configuration is thus a loop configuration, but with purely local weights for each tile, i.e. there is no weight given to a whole loop, but only to portions of loops. Moreover, the loops *carry an index* 1 or 2, that is changed at each SW or NE corner[5]. A SE corner

---

[5]Speaking of oriented loops and materializing each index with an arrow on each loop is much more convenient in this particular case, but this terminology is then less adapted to the super spin chains we will study in the next chapter.
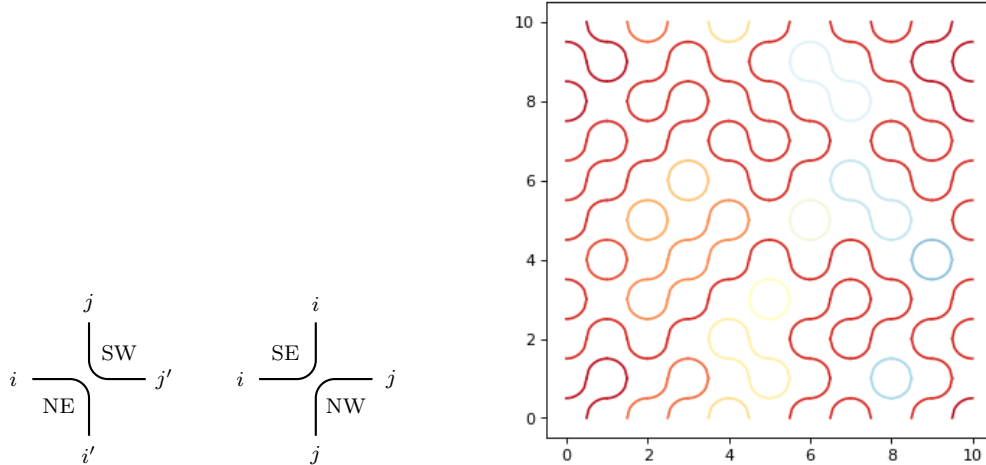
Figure 2.3: Left: the two elementary portions of loops and their indices, with the notation $i' = D + 1 - i$. Right: an example of a loop configuration (each loop has been given a different colour, but it is not part of the model).

with index 1 (resp. 2) or a NW corner with index 2 (resp. 1) gets a weight ω^{-1} (resp. ω). A SW corner with index 1 at the top (resp. 2) or a NE corner with index 1 at the left (resp. 2) gets a weight ω (resp. ω^{-1}). It is then seen with the help of a little picture that a closed loop that *does not cross the periodic boundaries* gets a total weight ω^4 if its NW corners have index 1, and ω^{-4} if its NW corners have index 2. The indexed loops that cross the periodic boundaries (horizontal or vertical) an even number of times also get the same weight (because they are *contractible*, i.e. they can be transformed into a point by modifying it locally, so that along a loop there is globally a rotation by an odd multiple of 2π). However, the indexed loops that cross the periodic boundaries an odd number of times get the weight 1 (because they are not contractible, and along a loop there is globally a rotation by an even multiple of 2π).

Loop models are usually defined in terms of unspecified loops that do not carry any indices. After summing over the indices of the loops, one obtains that Z_{LM} in (2.6) can be rewritten as

$$Z_{LM} = \sum_{\mathcal{L}} a^{x_1} b^{x_2} N^{l(\mathcal{L})} 2^{l_{\mathrm{nc}}(\mathcal{L})} \tag{2.78}$$

where the sum runs over (unspecified) loop configurations $\mathcal{L}$, x_1 and x_2 are the number of tiles ⌒ and ⌒, $l(\mathcal{L})$ is the number of contractible loops in $\mathcal{L}$, and $l_{\mathrm{nc}}(\mathcal{L})$ the number of non-contractible loops. The parameters N, a and b are

$$N = -2\cos\gamma\,, \qquad a = \sinh(\lambda + i\gamma)\,, \qquad b = \sinh\lambda \tag{2.79}$$

Boundary conditions and modified trace

To impose a common weight N to every loop, contractible or not, one has to modify the boundary conditions in both directions. In the L direction (that is, in the direction in which the trace of the monodromy matrix is taken), one needs to define a *twisted* transfer matrix $\tilde{t}(\lambda)$ by

$$\tilde{t}(\lambda) = \mathrm{tr}_a \begin{pmatrix} -e^{-i\pi\varphi} & 0 \\ 0 & -e^{i\pi\varphi} \end{pmatrix} M_a(\lambda) \tag{2.80}$$

with $\varphi = \gamma/\pi$ so that to compensate an odd number of crossings in the horizontal boundary condition. This transfer matrix is still integrable and can be solved with the Bethe ansatz; the Bethe equations (2.16) are modified with a multiplicative factor $e^{2i\pi\varphi}$ on the right-hand side.

However, the M-direction cannot be taken into account in such a way, and one has to generically introduce a matrix K_L that gives the desired weight to a given set of index values in the first and last row of the configuration (those separated by the periodic boundary condition in the M direction), so that the partition function

$$\tilde{Z}_{LM} = \mathrm{tr}(K_L \tilde{t}(\lambda)^M) \tag{2.81}$$

is the partition function for loops with weights $-2\cos\gamma$, contractible or not, with periodic boundary conditions in both directions:

$$\tilde{Z}_{LM} = \sum_{\mathcal{L}} a^{x_1} b^{x_2} N^{l(\mathcal{L})+l_{\mathrm{nc}}(\mathcal{L})} \tag{2.82}$$

This modified version of the trace is called the *Markov trace*.

Sectors of fixed magnetization

We saw in section 2.1.2 that the transfer matrix conserves the total magnetization S^z_{tot}, and that imposing a certain number K of Bethe roots fixes it to $\frac{L}{2} - K$. Because of this conservation, one can define a partition function Z^K_{LM} with a trace $\mathrm{tr}^{(K)}$ only over the sector of such magnetization:

$$Z_{LM} = \mathrm{tr}^{(K)}(t(\lambda)^M) \tag{2.83}$$

which corresponds in the loop model language to sum over a subset of loop configurations with a certain constraint.

This constraint can be understood as follows. Imposing a magnetization $m = \frac{L}{2} - K$ means that at the bottom of the lattice, there are $2m$ more strands with index 1 than with index 2, since each index $1, 2$ contributes to $\pm 1/2$ to m. Because the index of a loop is changed along a loop whenever a half-turn is made, these m extra strands with index 1 cannot go in the bulk of the lattice for a while and come back down to the bottom of the lattice connecting with another extra strand with index 1. Hence they must go through the lattice and cross the vertical periodic boundary (the one in the M-direction) to connect with another extra strand with index 1. Clearly, it can also cross the vertical periodic

boundary an additional number of times. Thus imposing a magnetization m constrains the loop configurations $\mathcal{L}$ in (2.78) to have m *non-contractible* strands in the vertical direction, i.e. strands that can be followed from the bottom of the lattice to the top without crossing the vertical periodic boundary condition (these strands might form only one loop though).

An important comment has to be made on the twist discussed in the previous subsection, that gave the correct weight to the non-contractible loops in the horizontal direction. If some strands are propagating freely along the lattice without forming any loops, then clearly there cannot be non-contractible loops in the horizontal direction, so that the twist is unnecessary in that respect. Besides, this twist will give a special weight to the cases where all the freely propagating strands wind around the lattice in the horizontal periodic boundary condition, which will favour certain configurations. For these reasons, in presence of freely propagating strands the twist $\varphi = 0$ should be set.

Another representation of the transfer matrix

We saw that the partition function of the completely packed loop model can be obtained from the transfer matrix of the XXZ spin chain. In this language, the non-local weight for a loop comes from the sum of different configurations of indexed loops described locally (since each site of the chain knows only about the index of the loop that visits it) and with local and complex weights. It is naturally possible to write a transfer matrix directly for the model with unspecified loops, if the Hilbert space encodes the connection between the strands that visit each site. We briefly describe this representation and will restrict to L even for simplicity. In particular we will not detail the treatment of boundary conditions, that are especially relevant for the numerics.

In the right panel of Figure 2.3, a horizontal slice will cross L strands, each of them being either connected to another strand or not connected to any other strands (if we forget about the vertical periodic boundary condition), that we will call a free strand. Hence the transfer matrix on unspecified loops acts on a vector space that is a direct sum $E = \oplus_k E_{2k}$ of vector spaces E_{2k}, each describing a state with L strands among which $2k$ are free, the other ones being paired between themselves and without crossings, see Figure 2.4. States with an apparent crossing in their graphical notation might be obtainable without crossings on a lattice because of the horizontal periodic boundary condition. The dimension of E_{2k} is $\binom{L}{2k}\left(\binom{L-2k}{L/2-k} - \binom{L-2k}{L/2-k+1}\right)$. At each transfer matrix step, each of these states is mapped onto all the possible states that can be obtained from it after one row. The loop weight N can be then directly written in the transfer matrix whenever a loop is formed.

$$
\begin{array}{c}
| \; | \; | \; | \; , \\[4pt]
\cup | \; | \; , \quad | \cup | \; , \quad | \; | \cup , \quad \Psi | \; , \quad | \; \Psi , \quad \cup | \; | \; \cup , \\[4pt]
\cup \cup , \quad \underset{\cup}{\cup}
\end{array}
\tag{2.84}
$$

Figure 2.4: The 9 states in $E = E_4 \oplus E_2 \oplus E_0$ in size $L = 4$.

34

Crossings

Let us anticipate a bit on the next chapter, and modify the previous loop models by authorizing the indexed loops to cross each other, see Figure 2.5. This corresponds to considering an additional possible tile $+$ whose matrix representation is nothing but the identity matrix

$$+ = \begin{pmatrix} 1 & 0 & 0 & 0 \\ 0 & 1 & 0 & 0 \\ 0 & 0 & 1 & 0 \\ 0 & 0 & 0 & 1 \end{pmatrix} \tag{2.85}$$

and define the R matrix R_{cross} as

$$R_{\text{cross}}(\lambda) = \sinh(\lambda + i\gamma)\, \diagup\!\diagdown + \sinh\lambda\, \diagdown\!\diagup + w + \tag{2.86}$$

with w the weight for a crossing. Using the matrix representation for the other tiles $\diagup\!\diagdown$ and $\diagdown\!\diagup$, one actually has

$$R_{\text{cross}}(\lambda) = (\sinh(\lambda + i\gamma) + w)\, \diagup\!\diagdown + (\sinh\lambda + w)\, \diagdown\!\diagup \tag{2.87}$$

if the free parameter x in (2.76) is chosen so that the following equations are satisfied

$$
\begin{aligned}
(\sinh(\lambda + i\gamma) + w)\omega^{-2} + (\sinh\lambda + w)\omega^2 &= x\sinh(i\gamma) \\
(\sinh(\lambda + i\gamma) + w)\omega^2 + (\sinh\lambda + w)\omega^{-2} &= x^{-1}\sinh(i\gamma)
\end{aligned}
\tag{2.88}
$$

We remark that it modifies the weight ω and the weights for the tiles. Thus the model with a crossing weight w *for the indexed loops* is actually equivalent to a model without crossings *for the unspecified loops*, but with an effective weight for a loop N':

$$N' = \frac{(\sinh(\lambda + i\gamma) + w)^2 + (\sinh\lambda + w)^2 - \sinh^2 i\gamma}{(\sinh\lambda + w)(\sinh(\lambda + i\gamma) + w)} \tag{2.89}$$

However, this is different from a model where the intersections occur between the unspecified loops. The definition of such a model requires more degrees of freedom for the indexed loops, and will be studied in the next chapter.

2.3.2 The Potts model

The previous loop model formulation can be mapped onto the so-called *Potts model*. To that end, let us represent a loop configuration on the $[0, L] \times [0, M]$ portion of the plane (as in Figure 2.3 for $L = M = 10$), and consider V the set of vertices of coordinates (i, j) with $i + j$ even, $0 \leq i < L, 0 \leq j < M$, together with E the set of all the edges $((i, j), (i \pm 1, j \pm 1))$ for $i + j$ even.

To each loop configuration $\mathcal{L}$ we associate the subset of edges $E' \subset E$ that do not intersect the loops, see Figure 2.6. Reciprocally, to each subset of edges $E' \subset E$ one can associate a
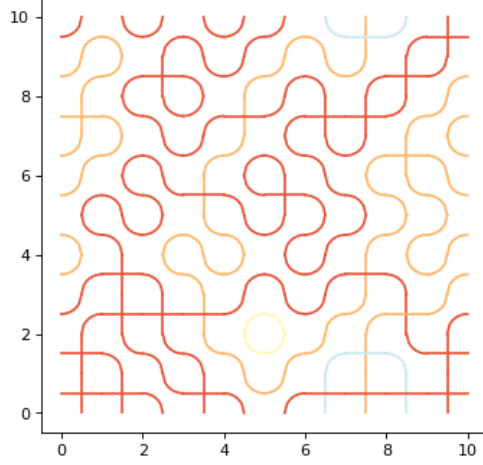
Figure 2.5: An example of a loop configuration with crossings (each loop has been given a different colour, but it is not part of the model).

unique loop configuration with the following procedure: at position (i, j) with $i + j$ even is placed ⌐ if $((i, j), (i + 1, j + 1)) \in E'$, and ⌐ otherwise; at position (i, j) with $i + j$ odd is placed ⌐ if $((i + 1, j), (i, j + 1)) \in E'$, and ⌐ otherwise.

One can translate the partition function (2.82) in this language. Given $E' \subset E$, we denote $l_{\text{tot}}(E')$ the number of loops (contractible or not) in a loop configuration built from E', $k(E')$ the number of connected components of E', and $c(E')$ the number of *independent cycles* of E' (i.e., the smallest number of edges that must be removed from E' so that no cycles remain). We have the following relations

$$l_{\text{tot}}(E') = k(E') + c(E'), \qquad c(E') = k(E') - |V| - |E'| \tag{2.90}$$

so that the partition function (2.82) with $a = b$ (and only in this case) becomes

$$\tilde{Z}_{LM} = \left(\frac{a^2}{N}\right)^{|V|} \sum_{E' \subset E} N^{2k(E') - |E'|} \tag{2.91}$$

which is (proportional to) the partition function of the Potts model with $Q = N^2$ states and weight $x = 1/N$ for each edge, defined as

$$Z_{LM}^{(Q)} = \sum_{E' \subset E} x^{|E'|} Q^{k(E')} \tag{2.92}$$

When Q is a positive integer, it is not difficult to see that this latter partition function is actually

$$Z_{LM}^{(Q)} = \sum_{\sigma} e^{-H}, \qquad \text{with} \quad H = -\log(1 + x) \sum_{(i,j) \in E} \delta(\sigma_i, \sigma_j) \tag{2.93}$$

36
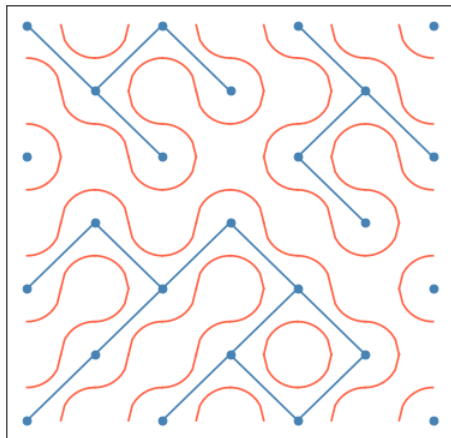
Figure 2.6: An example of a loop configuration (in red), together with its corresponding subset of edges E' (in blue). The blue dots are the vertices in V.

where σ denotes a configuration of classical spins σ_i that live on the set of vertices V and that can take values $1, ..., Q$.

Thus, at $Q = 2$, or equivalently $N = \sqrt{2}$, this partition function is that of the Ising model. The (limiting) case $Q = 1$ corresponds to critical percolation, i.e. opening a bond between two sites with probability $1/2$, irrespective of the size of the clusters formed. As for the (limiting) case $Q = 0$, because of the Q-dependence of the weight x for an edge, it corresponds to having only one big cluster without cycles hence is a model for spanning trees.

2.4 Identifying the continuum limit

2.4.1 Conformal field theory

The ultimate goal of statistical mechanics is to identify the *continuum limit* of a model; that is, obtaining a description of the long-range, *macroscopic* correlations that exist in a large system from the *microscopic* interactions that define the model.

The simplest example of a continuum limit is given by a *Gaussian Free Field*, in which the macroscopic observables are described by a field $\phi(x, y)$ whose all correlations can be computed by Wick's theorem. This is for example the case of the uniform random planar domino tilings [59]. In the continuum limit, a configuration of the system can be thought of as a 'Brownian surface' generalizing a Brownian motion.

The models described by a Gaussian Free Field in the continuum limit have the important property of being *conformally invariant*, that is, if Ω and Ω' are two bounded simply connected domains related by a conformal transformation $w(\Omega) = \Omega'$ depicted in Figure 2.7, then the correlation functions $G_{i_1...i_n}(z_1, \bar{z}_1, ..., z_n, \bar{z}_n)$ of n fields at positions $z_i, \bar{z}_i$ in Ω are

related to those in Ω' by

$$G_{i_1\dots i_n}(z_1, \bar{z}_1, \dots, z_n, \bar{z}_n) = \prod_{j=1}^n \left(\frac{dw}{dz}(z_j)\right)^{h_j} \left(\overline{\frac{dw}{dz}(z_j)}\right)^{\bar{h}_j} G_{i_1\dots i_n}(w(z_1), \overline{w(z_1)}, \dots, w(z_n), \overline{w(z_n)}))$$

(2.94)

where h_j are the *conformal dimensions* (or conformal weights) of the fields.
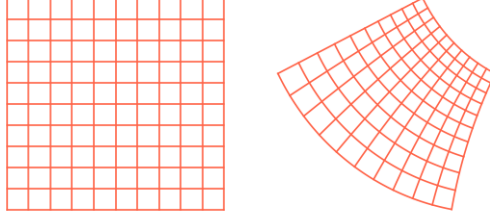
Figure 2.7: A grid and its image by the two-dimensional conformal map $x \mapsto \frac{x+2i}{x+2}$.

Although many statistical mechanics models are not described by a Gaussian Free Field in the continuum limit, they are still very often assumed (and observed) to be conformally invariant; it has also been proved for certain cases such as critical percolation [60]. This assumption directly imposes a general form to the 2 and 3-point functions of the fields: denoting Δ_i the conformal dimension of the field ϕ_i, one has

$$\langle \phi_1(z_1)\phi_2(z_2)\rangle = C_{12}\frac{\delta_{\Delta_1,\Delta_2}}{|z_1 - z_2|^{2\Delta_1}}$$

(2.95)

$$\langle \phi_1(z_1)\phi_2(z_2)\phi_3(z_3)\rangle = \frac{b_{123}}{|z_1 - z_2|^{\Delta_1+\Delta_2-\Delta_3}|z_1 - z_3|^{\Delta_1+\Delta_3-\Delta_2}|z_2 - z_3|^{\Delta_2+\Delta_3-\Delta_1}}$$

with C_{12} a constant that can be set to 1 upon a rescaling of the fields, and b_{123} a constant called structure constant.

In two dimensions, the assumption of conformal invariance is particularly powerful and has stimulated a very large amount of research under the name of *conformal field theory* (CFT) [19], impacting statistical mechanics, condensed matter physics, string theory and mathematical physics. Indeed, in two dimensions the (locally) conformal maps are the analytic functions, so that the corresponding Lie algebra has infinite dimension. It is given by the *Witt algebra* with generators $W_n = z^{1-n}\partial_z$ that satisfy

$$[W_n, W_m] = (n - m)W_{n+m}$$

(2.96)

At the quantum level, a symmetry is a weaker assumption since the states of the Hilbert space are defined up to a global phase, and turns out to be described by a Lie algebra that is a central extension of its classical counterpart. The only central extension of the Witt

38

algebra is the *Virasoro algebra*, that depends on an additional number, termed *central charge* and denoted by c, and whose generators L_n satisfy

$$[L_n, L_m] = (n - m)L_{n+m} + \delta_{n+m,0} \frac{n(n^2 - 1)}{12} c \tag{2.97}$$

The central charge, the conformal weights and the structure constant alluded to above are part of the so-called *CFT data*, that is the information necessary to characterize a CFT. For example, if there are only a finite number of primary fields with strictly positive $h > 0$, then the sole value of the central charge c is enough to characterize entirely the model, that is then called (unitary) *minimal model*. It must read

$$c = 1 - \frac{6}{m(m+1)} \tag{2.98}$$

with $m \geq 2$ an integer, and the conformal weights h must belong to the so-called *Kac table*

$$h_{r,s} = \frac{m+1}{4m}r^2 + \frac{m}{4(m+1)}s^2 - \frac{1}{4m(m+1)} - \frac{rs}{2}, \qquad 1 \leq r < m, \quad 1 \leq s \leq r \tag{2.99}$$

2.4.2   From the cylinder to the plane

A significant part of this thesis consists in determining the characteristics of the continuum limit of a model from the hints it leaves in finite size. In particular, upon the hypothesis of conformal invariance, part of the CFT data can be read off from the asymptotic expansion in L of the spectrum of the Hamiltonian or the transfer matrix in size L. In this subsection we remind the reader of the origin of this important link between the discrete quantum or statistical system and its continuum limit, emphasizing the role of the different limits.

To that end, we consider a transfer matrix T_L on L sites with D degrees of freedom per site that we assume for simplicity to be diagonalizable with orthogonal eigenvectors $|i\rangle$ with eigenvalues $\lambda_{i,L}$, and σ_L a given observable in size L. These objects are thus $D^L \times D^L$ matrices. On an $L \times M$ lattice with periodic boundary conditions, the correlation function of σ_L separated by Y rows is denoted $G^\sigma_{L,M}(Y)$ and is

$$G^\sigma_{L,M}(Y) = \frac{\text{tr}(T_L^{M-Y}\sigma_L T_L^Y \sigma_L)}{\text{tr}(T_L^M)} \tag{2.100}$$

After inserting the eigenvectors of T_L, one has

$$G^\sigma_{L,M}(Y) = \frac{\sum_i \lambda_{i,L}^{M-Y} \langle i|\sigma_L|k\rangle \lambda_{k,L}^Y \langle k|\sigma_L|i\rangle}{\sum_i \lambda_{i,L}^M} \tag{2.101}$$

The correlation of σ on a lattice of size L in one direction and infinite in the other is then obtained with the limit $M \to \infty$. Denoting $\lambda_{0,L}$ the dominant eigenvalue of T_L, one has when $M \to \infty$:

$$G^\sigma_{L,\infty}(Y) = \sum_k \langle 0|\sigma_L|k\rangle^2 \left(\frac{\lambda_{k,L}}{\lambda_{0,L}}\right)^Y \tag{2.102}$$

One would now like to have a field theory description of these correlations when $L \to \infty$. To that end, we associate each vertex of the lattice (i,j) where $i = 1, ..., L$ and j is an integer, to a point $(x, y) = (2\pi di/L, j/L)$ on a cylinder of radius d. The parameter d is a free parameter that simply permits to rescale arbitrarily one of the axes in the continuum limit $L \to \infty$, and that corresponds to the additional information that is encoded in this description, namely the distance between the sites. In this limit, the local observable σ_L is represented by a field $\phi(x, y)$ (the coordinate x on the compact direction of the cylinder depends on σ_L in finite size, but not the coordinate y).

Let us assume that $\langle 0|\sigma_L|k\rangle$ converges to a finite non-zero value when $L \to \infty$ for a k-th excited state at finite distance from the ground state, denoted C_k. Rescaling $Y = yL$, one sees from (2.102) that this field theory description is non-trivial only if $L \log(\lambda_{k,L}/\lambda_{0,L})$ has a non-zero finite value when $L \to \infty$. Let us denote this limit by $-\alpha_k$. Then, (2.102) gives

$$\langle \phi(x, 0)\phi(x, y)\rangle = \sum_k C_k e^{-\alpha_k y} \tag{2.103}$$

Let us now assume that the continuum limit is conformally invariant, and consider ψ a primary field with conformal dimensions $h = \bar{h} = \Delta/2$. Using (2.94) with the local conformal transformation $w(z) = d \cdot \log z$ that maps the plane onto the cylinder of radius d, one finds the dominant behaviour on the cylinder:

$$\langle \psi(x, 0)\psi(x, y)\rangle \sim \frac{e^{-\frac{\Delta}{d}y}}{d^{2\Delta}} \tag{2.104}$$

Note that there are no system size L here: these are the correlations on a cylinder of radius d in the continuum limit. We also note that this exponential decay is not the exponential decay that characterizes non-critical systems: the former one occurs in the continuum limit where there is an infinite number of sites between two distinct points, whereas the latter one occurs in the non-rescaled lattice. It follows that in the CFT describing the system in the continuum limit, considering the first k such that $C_k \neq 0$ in (2.103), there must be a field with conformal dimension

$$\Delta = \alpha_k d \tag{2.105}$$

Stated differently, there must be an excited state of the transfer matrix with eigenvalue $\lambda_{k,L}$ and a multiplicative constant d such that

$$-\log \frac{\lambda_{k,L}}{\lambda_{0,L}} = \frac{1}{Ld}(h + \bar{h}) + o(L^{-1}) \tag{2.106}$$

where the factor d must be the same for all the fields in the CFT. This equation is more usually written for the eigenvalues Le_L of the Hamiltonian that correspond to a very anisotropic limit in one direction, and with the rewriting $d = (2\pi v_F)^{-1}$ where v_F is called Fermi velocity. Then it reads, with Le_L^{gs} the ground state energy

$$e_L - e_L^{\text{gs}} = \frac{2\pi v_F}{L^2}\left(h + \bar{h}\right) + o(L^{-2}) \tag{2.107}$$

40

This equation relates differences between energy levels on the cylinder to the critical exponents on the lattice, and is among the most useful relations in the study of two-dimensional critical phenomena. As for the finite-size correction to the ground state, it can be shown to be related to the central charge c of the system through [21, 20]

$$e_L^{\text{gs}} - e_\infty = -\frac{\pi c}{6L^2} + o(L^{-2}) \tag{2.108}$$

Hence a good part of the CFT data can be read off from the finite-size corrections to the low-lying spectrum of the Hamiltonian on the cylinder.

As mentioned in [61], equation (2.107) is actually more general than what its derivation suggests. Indeed, the use of (2.94) is legitimate only for primary fields ψ, whether it is routinely observed in lattice models that the result (2.107) also applies to secondary fields. Moreover this correspondence between the spectrum on the cylinder and the critical exponents on the plane has been observed in some cases where the above derivation does not apply [61].

2.4.3   Perturbation by irrelevant operators

In a finite size system, there are clearly always higher-order corrections to equation (2.106). These corrections can be described in an *effective* way by perturbing the Hamiltonian in the continuum limit by irrelevant operators with a coupling constant g, that depends thus on L. The model *in finite size* is described in a continuous way by perturbing the limit theory in infinite size. Let us consider a Hamiltonian H_0 that describes the system in the continuum limit, and we perturb it by a field $\mathcal{V}$:

$$H = H_0 + \frac{g}{2\pi d} \int_0^{2\pi d} \mathcal{V}(x,t)dx \tag{2.109}$$

with g a coupling that satisfies

$$\frac{dg}{d\log L} = \beta(g), \qquad \beta(g) = (2 - \Delta_{\mathcal{V}})g - \pi b g^2 + O(g^3) \tag{2.110}$$

where $\Delta_{\mathcal{V}} = h + \bar{h}$ is the scaling dimension of $\mathcal{V}$ with the assumption $h = \bar{h}$, and b a parameter. At leading order in L, this is solved into

$$g(L) = \frac{a}{L^{\Delta_{\mathcal{V}}-2}} \tag{2.111}$$

with a constant a if $\Delta_{\mathcal{V}} > 2$, i.e. if the perturbation is (truly) irrelevant, and

$$g(L) = \frac{1}{\pi b \log L} \tag{2.112}$$

if $\Delta_{\mathcal{V}} = 2$, i.e. if the perturbation is only marginally irrelevant.

Correction to the energy levels

Take now E_n an energy level and $|\phi_n\rangle$ the corresponding eigenstate, $\phi_n(z, \bar{z})$ the corresponding operator. At leading order in g, the perturbed energy level δE_n is

$$\delta E_n = \frac{g}{2\pi d} \int_0^{2\pi d} \langle \phi_n | \mathcal{V}(x, t) | \phi_n \rangle dx \tag{2.113}$$

By definition of $|\phi_n\rangle$ and $\langle\phi_n|$ in terms of $\phi_n(z)$, we have

$$\langle \phi_n | \mathcal{V}(x) | \phi_n \rangle = \lim_{z, w \to 0} \langle 0 | z^{-2h} \bar{z}^{-2\bar{h}} \phi_n(1/z, 1/\bar{z}) \mathcal{V}(x, t) \phi_n(w, \bar{w}) | 0 \rangle \tag{2.114}$$

In CFT, this three point function is constrained to be

$$\langle 0 | \phi_n(z) \mathcal{V}(y) \phi_n(w) | 0 \rangle = \frac{b_n}{|z - y|^{2\Delta_\mathcal{V}} |y - w|^{2\Delta_\mathcal{V}} |z - w|^{4h - 2\Delta_\mathcal{V}}} \tag{2.115}$$

with b_n a structure constant. Expanding in $z, y = e^{-ix+it}, w$ one finds

$$\delta E_n = g b_n \tag{2.116}$$

Hence in the spectrum of the spin chain, the energy levels are perturbed at order $L^{-\Delta_\mathcal{V}}$ if the perturbation is irrelevant, and $L^{-2}(\log L)^{-1}$ if the perturbation is marginally irrelevant, and the amplitude is related to the three-point function amplitudes, showing that the finite-size corrections contain another part of the CFT data.

Correction to the correlation functions

From the energy displacement it follows that the scaling dimension γ_n of the field ϕ_n is perturbed by g as

$$\gamma_n = \Delta_n + g \frac{b_n}{2\pi v_F} \tag{2.117}$$

with Δ_n the unperturbed value of the conformal dimension. The correlation function

$$G_n(x) = \langle \phi_n(0) \phi_n(x) \rangle \tag{2.118}$$

satisfies the Callan-Symanzik renormalization equation

$$\left(\frac{\partial}{\partial \log x} + \beta(g) \frac{\partial}{\partial g} + 2\gamma_n(g) \right) G_n(x, g) = 0 \tag{2.119}$$

At first order in g it gives

$$G_n(x) = G_n(x_0) \left(\frac{x_0}{x} \right)^{2\Delta_n} \exp\left(-\frac{b_n}{\pi v_F} \int_{x_0}^x d(\log y) g(y) \right) \tag{2.120}$$

Whenever $g(y) = O((\log y)^{-2})$, that includes the case of 'truly' irrelevant operators, but also some marginally irrelevant operators, the integral inside the exponential is convergent when $x \to \infty$ and thus the corrections induced by this term are *additive* corrections to the dominant scaling of $G_n(x)$. However, in the case of a beta function $\beta \propto -g^2$, the integral is divergent, which gives a *multiplicative* correction to the dominant behaviour [62, 63]

$$G_n(x) \propto \frac{1}{x^{2\Delta_n}(\log x)^{b_n/(\pi^2 v_F b)}} \tag{2.121}$$

Summary

We can summarize these different relations by writing that if one has the following finite-size corrections to an energy level e_L on the cylinder

$$e_L = e_\infty + \frac{2\pi v_F}{L^2}\left(-\frac{c}{12} + h + \bar{h} + \frac{\beta}{\log L}\right) + o(L^{-2}(\log L)^{-1}) \tag{2.122}$$

then the correlation function of the field ϕ corresponding to this energy level has the following large distance decay

$$\langle \phi(0)\phi(x)\rangle \sim \frac{1}{x^{2(h+\bar{h})}(\log x)^{2\beta}} \tag{2.123}$$

We emphasize that this logarithmic correction to the power-law comes from the presence of a marginally irrelevant operator, and is in particular not related to LCFT.

2.4.4 A basic application of conformal invariance

For sake of completeness, in this subsection we give a basic example of application of conformal invariance, whose explanation will be useful in the next chapter.

We consider the completely packed $O(N)$ loop model on a square lattice of size $(LK) \times (LK)$, and ask what is the large-x behaviour of the probability $G_p(0, x)$ that two points separated by $X = xL$ are visited by the same loop in the limit $L \to \infty, K \to \infty$ [6].

To that end, we use the hypothesis of conformal invariance to map the problem on the geometry of the cylinder, better suited for a transfer matrix approach. On the cylinder, the probability that two strands are propagating without forming a loop on a certain distance Y can be written with a similar equation to (2.100)

$$G^\sigma_{L,M}(Y) = \frac{\text{tr}(\tilde{T}_L^{M-Y}\sigma_L^1\tilde{T}_L^Y\sigma_L^2)}{\text{tr}(\tilde{T}_L^M)} \tag{2.124}$$

where σ_L^1 and σ_L^2 create and contract a particular marked loop, than cannot be contracted nor created by $\tilde{T}_L$, the transfer matrix $\tilde{T}_L$ now acting on states consisting on regular loops

---

[6]The two limits are required to be on the geometry of the plane, rather than on a bounded region. Boundary CFT should otherwise be used to solve the problem on this latter geometry.

and possible marked loops. The action of the $\tilde{T}_L^Y$ in between is then identical to the action of the transfer matrix without marked loop, but imposing that there are 2 free strands propagating. Thus in the continuum limit on the cylinder the probability that two points separated by y are visited by the same loop is given by

$$\langle \phi(0)\phi(x) \rangle = C_k e^{-\alpha_2 y} \tag{2.125}$$

where $-\alpha_2 = \lim_{L\to\infty} L \log \frac{\lambda_{2,L}}{\lambda_{0,L}}$ with $\lambda_{0,L}$ the largest eigenvalue of the normal transfer matrix T_L, and $\lambda_{2,L}$ the largest eigenvalue of the normal transfer matrix T_L in the sector with 2 free strands propagating. Now, we saw in section 2.3.1 that the ground state corresponds to the $S_z = 0$ sector in the XXZ spin chain with $N = -2\cos\gamma$ and a twist $\varphi = -\gamma/\pi$, while the configurations with 2 free strands correspond to the $S_z = 1$ magnetization sector and a twist $\varphi = 0$. Besides, the finite-size corrections to a state with $n_\pm$ vacancies in the positive/negative Bethe numbers is

$$e_L - e_\infty = \frac{2\pi v_F}{L^2}\left(-\frac{1}{12} + \frac{1-\gamma/\pi}{2}(n_+ + n_-)^2 + \frac{(n_+ - n_- + 2\varphi)^2}{8(1-\gamma/\pi)}\right) \tag{2.126}$$

see (4.75). The minimal energy in the $S_z = 0$ sector is obtained with $n_+ = n_- = 0$, and in the $S_z = 1$ sector at $\varphi = 0$ with $n_+ + n_- = 1$, $n_+ - n_- = 0$. Hence the following decay [64, 65]

$$G_p(0,x) \sim \frac{1}{x^{(1-\gamma/\pi)-\frac{(\gamma/\pi)^2}{1-\gamma/\pi}}} \tag{2.127}$$

44

Chapter 3

Logarithms in a non-unitary spin chain

3.1 Introduction

3.1.1 Overview

A system with a large number of components interacting at short distance is generically non-critical: the correlations decay exponentially with the distance $\propto e^{-x/\xi}$ with ξ a certain correlation length. At the particular points in the parameter space where this correlation length diverges $\xi \to \infty$, i.e. when the system is critical, the correlations decay much more slowly and take another form, typically that of a power-law $x^{-\alpha}$ with α a critical exponent. However, it may happen – and it actually happens quite often – that this power-law is corrected with a multiplicative logarithm.

The simplest examples of models with such a behaviour are probably disordered magnets like the random bond Ising model in two dimensions. Whereas the pure Ising model magnetization correlation functions at critical temperature famously exhibit power-law decay [66, 67]

$$\langle \sigma(0)\sigma(x) \rangle \sim \frac{1}{x^{1/4}} \tag{3.1}$$

it was shown by Ludwig that the disorder acts as a (marginally) relevant perturbation that corrects this behaviour with a logarithm after averaging over different realizations [68, 69, 32, 70, 71]

$$\overline{\langle \sigma(0)\sigma(x) \rangle^N} \sim \frac{(\log x)^{N(N-1)/8}}{x^{N/4}} \tag{3.2}$$

However, this is not a specificity of disordered systems and a logarithmic behaviour is also present in other pure paradigmatic models such as polymers as first shown by Saleur [34, 72, 73] or in percolation [74, 75], and even in the pure Ising model itself for more involved correlation functions [76, 77, 78]. These latter models share the property of involving *non-local* degrees of freedom or observables that can be made local at the price of non positive

Boltzmann weights, often referred to as non-unitarity, albeit through a specific transformation rather than a canonical procedure – the non-locality is apparent for percolation and polymers since the elements of a configuration are clusters or loops which are extended objects, but some observables in the Ising model can be non-local as well, such as the belonging of two sites to the same cluster of aligned spins. On the other hand, the disorder clearly does not spoil the locality of a pure system, but it is expected from supersymmetric averaging over the disorder [79, 32] that they are described by non-trivial $c = 0$ CFT's, thus necessarily non-unitary. Hence it suggests that the true commonality of these particular models with logarithmic correlations are their *non-unitary* nature.

We should however qualify this conclusion with the following remarks. Firstly, it is not clear to which extent the meaning of non-unitarity for lattice models (non positive Boltzmann weights) and for CFT's (negative norms) coincide. Secondly, the convertibility of the non-locality into non-unitary locality is difficult to characterize since it somehow relies on a trick, such as summing over intermediate configurations, or using supersymmetry, that cannot always be generalized to related models: for example the weight $N = -2\cos\gamma$ assigned to a closed loop in the $O(N)$ model is obtained with a weight $e^{\pm i(\gamma+\pi)/4}$ for each corner in the oriented loops before summing over the orientation; but as soon as one allows intersections between the loops the number of corners is less constrained and the trick fails for N non-integer, although there may still be well logarithms for these values of N. Thirdly, some models such as the Heisenberg XXX spin chain also exhibit logarithms in e.g. their magnetic susceptibility [80], or the famous XY model studied by Kosterlitz and Thouless [81], although unitary and local.

The explanation is that not all the logarithms in the correlation functions have the same origin from a theoretical point of view. There are two distinct mechanisms to allow their appearance. The first one is the perturbation of the Hamiltonian by a marginal operator as explained in Section 2.4.3 [62], and the power of the logarithm that can be any real number is related to the amplitude of this perturbation. If this perturbation is induced by the finite size of the system, since a physical realization of a model cannot be but finite, for all practical purposes this perturbation and thus the logarithm will always be present and observed. However, by definition the perturbation and the logarithmic corrections are absent exactly at the RG fixed point where the coupling constant g vanishes, which implies an unpleasant non-commutativity of two limits.

The second mechanism is more intrinsic and has been termed Logarithmic Conformal Field Theory [82, 38, 83] (LCFT). It relies on the relaxation of a common hypothesis in renormalization group lectures, that is the diagonalizability of the linearized RG flow close to a fixed point. Under this latter hypothesis, the correlation functions are constrained to be power-laws whose exponents are related to the eigenvalues of this linearized flow. However, if it is not diagonalizable, the correlation functions can exhibit multiplicative integral powers of logarithms that corrects the usual power-law. This is conceptually very different from the marginal operator perturbation, since the logarithms are still present at the fixed point and are thus a property of the RG fixed point itself rather than that of a perturbation around it. For this reason the framework of LCFT is more fundamental, and should be the right one

to study e.g. percolation.

This chapter is devoted to the study in full detail of particular examples of discretization of non-unitary models that turn out to mix the two mechanisms described above, i.e. LCFT's perturbed by marginally irrelevant operators. These are the *orthosymplectic* integrable spin chains, i.e. spin chains built from a solution to the (graded) Yang-Baxter equation that has the symmetry of the Lie superalgebra $osp(r|2s)$, which is the analog of the $o(n)$ Lie algebra for graded vector spaces. The cancellation of bosonic/fermionic degrees of freedom actually makes the model a generalization of the $O(N)$ model to $N = r - 2s$ any positive or negative integer. The interest of these spin chains lies in several factors. The first one is their non-unitarity, which forbids the Mermin-Wagner theorem to apply and allows a stable massless Goldstone phase to appear, also called spontaneous symmetry breaking. The second one is the fact that they regularize the *supersphere sigma models*, that are field theories for 'free' fields with bosonic and fermionic degrees of freedom constrained to lie on a supersphere. These models involve free bosons and symplectic fermions, which is the simplest and well-known LCFT [84, 73], and are perturbed in a marginal way as already stated, which makes them interesting ground for understanding aspects of perturbed LCFT's and supersymmetric field theories. Finally, their spin chain discretization is directly related to intersecting loop models, i.e. the completely packed $O(N)$ loop model where intersections between loops are allowed [85]. It was understood by Jacobsen, Read and Saleur [86] that this loop model is somehow the true loop model associated to the $O(N)$ spin model for $N < 2$, in the sense that any weak perturbation around the usual $O(N)$ loop model flows to this intersecting loop model. Moreover these models are directly related to 'trail' models, that is bond-avoiding walks that are alternatives to the self-avoiding walks for polymer universality class [87, 88, 89].

In section 3.2 we study thoroughly the $osp(1|2)$ spin chain and show that in the thermodynamic limit, the low-lying spectrum of the spin chain is that of the $osp(1|2)$ supersphere sigma model. To achieve this, we compute directly from the Hamiltonian derived from the action of the field theory the energy levels at order g and compare them to analytic calculations from the Bethe ansatz of energy levels at order $\frac{1}{L^2 \log L}$, together with numerical calculations with the Bethe ansatz for large spin chains. Even though some energy levels of these super spin chains were studied numerically in [90, 91], no such an explicit calculation and correspondence to the sigma model has been carried out before. Besides, we study for the first time how Cardy's relation [92, 22] between logarithmic corrections and 3-point function amplitudes for classical CFT's generalizes to the logarithmic case; we find that the correspondence is much more involved because the structure of the 3-point function is not as constrained as for the CFT case. These discussions are then partially extended to the $osp(2|2)$ and $osp(3|2)$ cases in Sections 3.3 and 3.4.

In section 3.5 we apply our results to the so-called watermelon correlation functions in the intersecting loop models, with the formalism of the transfer matrix. This model was introduced in [85], and a family of watermelon two-point function with logarithmic decay was calculated and observed numerically with Monte Carlo simulations in [93]; however, there are in the supersphere sigma model other whole families of exponents for which no

observable was known. We establish the precise correspondence between the super spin chains and this model, and explain and prove some facts that were numerically observed to hold, like the inclusion of spectra between different models. But we especially establish a precise correspondence between all the highest-weight state energy levels – including the families that were not studied so far – and constraints on the loop configuration, that enables to relate the finite-size corrections to the energy levels to the long-distance behaviour of more involved weighted sums of watermelon correlation functions, which is a new result.

3.1.2 Definitions

The orthosymplectic symmetry

We give here a brief description of the orthosymplectic symmetry.

We first remind that the superspace $\mathbb{R}^{r|2s}$ is parametrized by r 'bosonic' variables $\phi_1, ..., \phi_r$ and $2s$ 'fermionic' variables $\eta_1^1, \eta_1^2, ..., \eta_s^1 \eta_s^2$ that satisfy $[\phi_i, \phi_j] = 0$, $[\phi_i, \eta_l^k] = 0$, $\{\eta_j^i, \eta_l^k\} = 0$. The scalar product between two vectors $x, y \in \mathbb{R}^{r|2s}$ is defined by

$$\langle x, y \rangle = x^t \cdot J_{r|2s} \cdot y \tag{3.3}$$

where

$$J_{r|2s} = \begin{pmatrix} I_r & O_{r \times 2s} \\ O_{2s \times r} & I_s \otimes J_{0|2} \end{pmatrix}, \quad J_{0|2} = \begin{pmatrix} 0 & 1 \\ -1 & 0 \end{pmatrix} \tag{3.4}$$

with I_r the identity matrix of size $r \times r$, and $O_{a \times b}$ the zero matrix of size $a \times b$.

The group $OSp(r|2s)$ is the set of linear transformations on $\mathbb{R}^{r|2s}$ that leave the norm invariant:

$$OSp(r|2s) = \{M \in \mathcal{M}_{r+2s, r+2s}, \quad \forall x \in \mathbb{R}^{r|2s}, \langle x, Mx \rangle = \langle x, x \rangle\} \tag{3.5}$$

The Lie superalgebra $osp(r|2s)$ of such a group can be represented as [94]

$$osp(r|2s) = \left\{ \begin{pmatrix} A & X & B \\ -Y & E & X^t \\ C & Y^t & -A^t \end{pmatrix}; A, B, C \in \mathcal{M}_{s,s}; X \in \mathcal{M}_{s,r}; Y \in \mathcal{M}_{r,s}; E \in \mathcal{M}_{r,r}; E^t = -E \right\} \tag{3.6}$$

In this representation the generators for $osp(r|2)$ will be denoted $J_z, J_+, J_-, F_1, ..., F_r, G_1, ..., G_r$, Q_{ij}, $i, j = 1, ..., r$, $i > j$ and are such that

$$j_z J_z + j_+ J_+ + j_- J_- + \sum_{k=1}^{r} (f_k F_k + g_k G_k) + \sum_{i>j} q_{ij} Q_{ij} = \begin{pmatrix} j_z/2 & f_1 & ... & f_n & j_+ \\ g_1 & 0 & ... & q_{n1} & f_1 \\ ... & ... & ... & ... & .. \\ g_n & -q_{n1} & ... & 0 & f_n \\ j_- & -g_1 & ... & -g_n & -j_z/2 \end{pmatrix} \tag{3.7}$$

The commutation relations of the generators can be deduced directly from this matrix representation. For example, for $osp(1|2)$ one has 5 generators J_z, J_+, J_-, F_+, F_- that satisfy

the following relations

$$[J_z, J_\pm] = \pm J_\pm\,, \quad [J_+, J_-] = 2J_z$$

$$[J_z, F_1] = \frac{1}{2}F_1\,, \quad [J_z, G_1] = -\frac{1}{2}G_1\,, \quad [J_+, G_1] = -F_1\,, \quad [J_-, F_1] = -G_1 \qquad (3.8)$$

$$\{F_1, F_1\} = 2J_+\,, \quad \{G_1, G_1\} = -2J_-\,, \quad \{F_1, G_1\} = 2J_z$$

As for the Casimir, we normalize it in such a way that it is the inverse of the Killing form of the generators (3.7) (then, the quadratic term in the eigenvalue j of J_z is $2j^2$). For example for $osp(1|2)$ it reads

$$\mathcal{C} = 2J_z^2 + (J_+J_- + J_-J_+) + \frac{1}{2}(G_1F_1 - F_1G_1) \qquad (3.9)$$

The representation theory of the $osp(r|2s)$ algebras is a bit complicated, and involves (except when $r = 1$) issues of typicality. Rather than give generalities at this stage, we will recall necessary features in our case by case analysis below.

The supersphere σ-model

A simple but non-trivial field theory with $OSp(r|2s)$ symmetry is the theory of 'free' fields constrained to lie on the supersphere of dimensions $(r - 1|2s)$, i.e. the subset $S^{r-1|2s} \subset \mathbb{R}^{r|2s}$ such that $\forall x \in S^{r-1|2s}, \langle x, x \rangle = 1$. This is the non-linear σ-model with target space the supersphere $S^{r-1|2s}$. We will restrict in the following to the case $s = 1$, and thus symmetries $OSp(r|2)$. The action is

$$S(\phi_1, ..., \phi_r, \eta^1, \eta^2) = \frac{\kappa}{4\pi g_\sigma} \int dxdt \left(\sum_{i=1}^{r} \partial_\mu \phi_i \partial_\mu \phi_i + 2\partial_\mu \eta^2 \partial_\mu \eta^1 \right) \qquad (3.10)$$

with $\partial_\mu X \partial_\mu X \equiv -(\partial_x X)^2 + (\partial_t X)^2$, and κ a normalization factor to make matching with existing literature easier.

The constraint then translates into

$$\sum_{i=1}^{r} \phi_i^2 + 2\eta^2\eta^1 = 1 \qquad (3.11)$$

The model for $r < 4$ is known to flow to a Goldstone free theory. From integration of the leading order in the β function $\frac{dg_\sigma}{d\log L} \propto (r - 2s - 2)g_\sigma^2$ we find, after properly adjusting normalizations, replacing the RG scale by the size of the system, and setting $g \equiv g_\sigma$ for simplicity [95, 96]

$$g \approx \frac{\kappa}{(4 - r)\log L/L_0}\,, \quad \text{for } L \to \infty \qquad (3.12)$$

where L_0 is, at the order we are working, an irrelevant length scale we shall take equal to unity in the following.

The orthosymplectic spin chain

We will study spin chains built from an R-matrix that satisfies the Yang-Baxter equation and that belongs to the fundamental representation of the $osp(r|2s)$ superalgebra. Periodic boundary conditions will be considered.

The vector space V_i that describes each site is a $\mathbb{Z}_2$-*graded* vector space with dimension $D = r + 2s$. The Grassman parity p_α of the α-th degree of freedom is defined as

$$
\begin{aligned}
p_\alpha &= 1 \quad \text{if } \alpha = 1, ..., s \quad \text{ or } \quad \alpha = r + s + 1, ..., r + 2s \\
&= 0 \quad \text{if } \alpha = s + 1, ..., r + s
\end{aligned}
\tag{3.13}
$$

The transfer matrix $t(\lambda)$ of the model at spectral parameter λ is given by the supertrace of the monodromy matrix

$$
t(\lambda) = \sum_{i=1}^{D} (-1)^{p_i} M_{ii}(\lambda)
\tag{3.14}
$$

$$
\text{with} \quad M(\lambda) = R_{a,L}(\lambda) R_{a,L-1}(\lambda)...R_{a,1}(\lambda)
$$

$M_{ij}(\lambda)$ denotes the (i, j) component of M in the auxiliary vector space V_a. However, the graded tensor product introduces signs in the tensor products, and for clarity we give the explicit expression of the components of the transfer matrix

$$
t(\lambda)^{\alpha_1...\alpha_L}_{\beta_1...\beta_L} = \sum_{c_1,...,c_L=1}^{D} R(\lambda)^{\alpha_L c_L}_{c_1 \beta_L} R(\lambda)^{\alpha_{L-1} c_{L-1}}_{c_L \beta_{L-1}} ... R(\lambda)^{\alpha_1 c_1}_{c_2 \beta_1} (-1)^{p_{c_1}} (-1)^{\sum_{j=2}^{L}(p_{\alpha_j} + p_{\beta_j}) \sum_{i=1}^{j-1} p_{\alpha_i}}
\tag{3.15}
$$

Such an explicit expression can be found e.g. in [97].

The R-matrix we will use have the following properties

1. It satisfies the (graded) Yang-Baxter equation

$$
R_{12}(\lambda) R_{13}(\lambda + \mu) R_{23}(\mu) = R_{23}(\mu) R_{13}(\lambda + \mu) R_{12}(\lambda)
\tag{3.16}
$$

2. It has an $osp(r|2s)$ symmetry: that is, for each generator A of $osp(r|2s)$ (in a certain representation, not necessarily (3.7)), $t(\lambda)$ commutes with $A_{\text{tot}} = \sum_{i=1}^{L} A_i$ where A_i acts on the vector space V_i.

and it reads [98]

$$
R_{ab}(\lambda) = \lambda I_{ab} + P_{ab} + \frac{2\lambda}{2 - r + 2s - 2\lambda} E_{ab}
\tag{3.17}
$$

where I_{ab} is the $D^2 \times D^2$ identity matrix, P_{ab} is the graded permutation operator

$$
(I)^{lj}_{ik} = \delta_{ij}\delta_{kl}, \qquad (P)^{lj}_{ik} = (-1)^{p_i p_j}\delta_{il}\delta_{jk}
\tag{3.18}
$$

and E_{ab} the matrix given by

$$
(E)^{lj}_{ik} = (-1)^{i>r+s}(-1)^{j\leq s}\delta_{ki'}\delta_{lj'}
\tag{3.19}
$$

with $i' = D + 1 - i$, and $(-1)^{x>y}$ is -1 if $x > y$, 1 if $x \leq y$. The Hamiltonian of the chain is then defined as

$$H = \frac{d}{d\lambda} \log t(\lambda)|_{\lambda=0} \tag{3.20}$$

The Yang-Baxter equation ensures that the transfer matrices $t(\lambda)$ and $t(\mu)$ at different spectral parameters commute, and it has been shown[1] that the eigenvalues of t can be determined with the Bethe ansatz [99, 100].

We will finally denote $\Delta e_L = e_L - e_L^{\text{gs}}$ the energy difference between an excited state e_L and the ground state e_L^{gs}, as in (2.107).

3.2 $OSp(1|2)$

3.2.1 The spectrum from field theory

We start by deriving the expected low-lying spectrum of the non-linear σ-model with $OSp(1|2)$ symmetry at first order in $(\log L)^{-1}$.

General strategy

There is a common strategy for studying the different models. The first step is to derive the Hamiltonian in terms of the modes of the fields from the lagrangian. The expectation values of the Hamiltonian within modes are naively divergent: to regularize them, we express them in terms of their normal-ordered versions and isolate infinite sums. Every regularized value for these gives a Hamiltonian with the desired *osp* symmetry, and they have to be fixed by an additional condition. Once the expression of the states in term of the modes are derived, the eigenvalues of the Hamiltonian at order g can then be obtained. This gives access to the logarithmic corrections by using (3.12).

The action

In the $osp(1|2)$ case the constraint (3.11) can be satisfied by imposing

$$\phi_1 = 1 - \eta^2 \eta^1 \tag{3.21}$$

The action becomes then

$$S(\eta^1, \eta^2) = \frac{\kappa}{2\pi g} \int dx dt (\partial_\mu \eta^2 \partial_\mu \eta^1 - \eta^1 \eta^2 \partial_\mu \eta^1 \partial_\mu \eta^2) \tag{3.22}$$

---

[1]Completeness is not proven; moreover some eigenvalues may be a bit singular, like the ground state of the $osp(3|2)$ spin chain for example that is obtained with coinciding Bethe roots that should be normally excluded.

Upon the change of variable $\eta^{1,2} \to \sqrt{g}\eta^{1,2}$ it reads

$$S(\eta^1, \eta^2) = \frac{\kappa}{2\pi} \int dxdt(\partial_\mu\eta^2\partial_\mu\eta^1 - g\eta^1\eta^2\partial_\mu\eta^1\partial_\mu\eta^2) \tag{3.23}$$

Here g shall be treated at order 1. Recall that for large L we have from (3.12)

$$g = \frac{\kappa}{3\log L} \tag{3.24}$$

The Hamiltonian

The first task is to derive the Hamiltonian corresponding to the action (3.23). For calculation convenience we write (3.23) as

$$S = \frac{\kappa}{2\pi} \int dxdt(-\partial_x\eta^2\partial_x\eta^1 + \dot\eta^2\dot\eta^1 + g\mathcal{V}(\eta^1, \eta^2)) \tag{3.25}$$

with $\mathcal{V}(\eta^1, \eta^2)$ a generic potential. We take the system to be defined on a cylinder of unit radius, so that x is integrated between 0 and 2π, and t between 0 and an arbitrary final time T. The derivatives with respect to fermions are always considered from the right (this means for example that $(d/d\dot\eta^2)(\dot\eta^2\dot\eta^1) = -\dot\eta^1$). In terms of modes

$$\eta^{1,2}(x,t) = \sum_k \eta_k^{1,2}(t)e^{ikx} \tag{3.26}$$

the action reads

$$S = \kappa \int dt \left(\sum_k -k^2\eta_k^2\eta_{-k}^1 + \dot\eta_k^2\dot\eta_{-k}^1 + gV \right) = \int dt\mathcal{L} \tag{3.27}$$

with $\mathcal{L}$ the lagrangian density, and

$$V(t) = \frac{1}{2\pi} \int dx\mathcal{V}(x,t) \tag{3.28}$$

The conjugate momenta to η_k^1 and η_k^2 are

$$\pi_k^1 = \kappa\dot\eta_{-k}^2 + \kappa g\frac{dV}{d\dot\eta_k^1}, \quad \pi_k^2 = -\kappa\dot\eta_{-k}^1 + \kappa g\frac{dV}{d\dot\eta_k^2} \tag{3.29}$$

The quantization procedure imposes the following anticommutators at equal times at all orders in g:

$$\{\eta_k^{1,2}, \pi_p^{1,2}\} = i\delta_{k,p} \tag{3.30}$$

The corresponding Hamiltonian is then defined as

$$H = \sum_k (\pi_k^1\dot\eta_k^1 - \dot\eta_k^2\pi_k^2) - \mathcal{L} \tag{3.31}$$

It gives, neglecting terms of order $O(g^2)$:

$$H = \sum_k (\kappa k^2 \eta_k^2 \eta_{-k}^1 + \kappa^{-1} \pi_k^2 \pi_{-k}^1) - \kappa g V + O(g^2) \tag{3.32}$$

We now use the following expression of the time derivative for a quantity X

$$\dot{X} = i[H, X] \tag{3.33}$$

and the relation valid for all (commuting or anticommuting) quantities a_i and b ($n \geq 2$)

$$[a_n...a_1, b] = \sum_{i=1}^{n} (-1)^{i-1} a_n...a_{i+1}\{a_i, b\}a_{i-1}...a_1 \tag{3.34}$$

to compute

$$\dot{\eta}_k^1 = -\kappa^{-1} \pi_{-k}^2 + \kappa g \frac{dV}{d\pi_k^1}, \qquad \dot{\eta}_k^2 = \kappa^{-1} \pi_{-k}^1 + \kappa g \frac{dV}{d\pi_k^2}$$

$$\dot{\pi}_k^1 = -\kappa k^2 \eta_{-k}^2 + \kappa g \frac{dV}{d\eta_k^1}, \qquad \dot{\pi}_k^2 = \kappa k^2 \eta_{-k}^1 + \kappa g \frac{dV}{d\eta_k^2} \tag{3.35}$$

Now let us define the following charges

$$J_z = \sum_k \frac{\eta_k^1 \pi_k^1 - \eta_k^2 \pi_k^2}{2i}, \qquad J_+ = -\sum_k i\eta_k^1 \pi_k^2, \qquad J_- = -\sum_k i\eta_k^2 \pi_k^1$$

$$F_1 = \sum_{k+l+m=0} \pi_{-k}^2 (\delta_{l,0}\delta_{m,0} + g\eta_l^1 \eta_m^2), \qquad G_1 = \sum_{k+l+m=0} \pi_{-k}^1 (\delta_{l,0}\delta_{m,0} - g\eta_l^2 \eta_m^1) \tag{3.36}$$

Using (3.30) one can check that they satisfy the $osp(1|2)$ relations (3.8) at order $O(g)$ – remember that before (3.23) we made the replacement $\eta^{1,2} \to \sqrt{g}\eta^{1,2}$. With the formulas (3.35) one has:

$$\partial_t J_z = \sum_k \frac{\kappa g}{2} \left(\frac{dV}{d\pi_k^1}\pi_k^1 + \eta_k^1 \frac{dV}{d\eta_k^1} - \eta_k^2 \frac{dV}{d\eta_k^2} - \frac{dV}{d\pi_k^2}\pi_k^2 \right)$$

$$\partial_t J_+ = \sum_k \kappa g \left(\frac{dV}{d\pi_k^1}\pi_k^2 + \eta_k^1 \frac{dV}{d\eta_k^2} \right), \qquad \partial_t J_- = \sum_k \kappa g \left(\frac{dV}{d\pi_k^2}\pi_k^1 + \eta_k^2 \frac{dV}{d\eta_k^1} \right)$$

$$\partial_t F_1 = \sum_{k+l+m=0} g \left(\kappa \frac{dV}{d\eta_0^2}\delta_{l,0}\delta_{m,0} - \kappa km\eta_l^1 \eta_m^2 \eta_k^1 + \kappa^{-1}\eta_k^1 \pi_{-l}^1 \pi_{-m}^2 \right)$$

$$\partial_t G_1 = \sum_{k+l+m=0} g \left(\kappa \frac{dV}{d\eta_0^1}\delta_{l,0}\delta_{m,0} + \kappa km\eta_l^2 \eta_m^2 \eta_k^1 - \kappa^{-1}\eta_k^2 \pi_{-l}^1 \pi_{-m}^2 \right) \tag{3.37}$$

where the following relation has been used (it is an integration by part)

$$\sum_{k+l+m=0} k^2 \eta_k^1 \eta_l^1 \eta_m^2 = \sum_{k+l+m=0} k(k-k-l-m)\eta_k^1 \eta_l^1 \eta_m^2 = \sum_{k+l+m=0} -km\eta_k^1 \eta_l^1 \eta_m^2 \tag{3.38}$$

With the equations (3.37) it can be checked that the following potential implies the conservation of all these charges:

$$\mathcal{V}(\eta^1, \eta^2) = \eta^2 \eta^1 \partial_x \eta^2 \partial_x \eta^1 - \eta^2 \eta^1 \partial_t \eta^2 \partial_t \eta^1 \tag{3.39}$$

or in terms of V

$$V = \sum_{k+l+m+n=0} \left(-mn\eta_k^2 \eta_l^1 \eta_m^2 \eta_n^1 + \kappa^{-2} \eta_k^2 \eta_l^1 \pi_{-m}^1 \pi_{-n}^2 \right) \tag{3.40}$$

Define now the following modes for all k

$$\psi_k^1 = \frac{-ik\eta_k^1 \kappa^{1/2} - \pi_{-k}^2 \kappa^{-1/2}}{\sqrt{2}}, \quad \psi_k^2 = \frac{-ik\eta_k^2 \kappa^{1/2} + \pi_{-k}^1 \kappa^{-1/2}}{\sqrt{2}}$$

$$\bar{\psi}_k^1 = \frac{-ik\eta_{-k}^1 \kappa^{1/2} - \pi_k^2 \kappa^{-1/2}}{\sqrt{2}}, \quad \bar{\psi}_k^2 = \frac{-ik\eta_{-k}^2 \kappa^{1/2} + \pi_k^1 \kappa^{-1/2}}{\sqrt{2}} \tag{3.41}$$

They satisfy

$$\{\psi_k^1, \psi_p^2\} = k\delta_{k+p,0}, \qquad \{\bar{\psi}_k^1, \bar{\psi}_p^2\} = k\delta_{k+p,0} \tag{3.42}$$

for $k, p \neq 0$, the other anticommutators being zero. The original modes for $k \neq 0$ read in terms of the ψ's:

$$\eta_k^{1,2} = \frac{i}{k\sqrt{2\kappa}}(\psi_k^{1,2} - \bar{\psi}_{-k}^{1,2})$$

$$\pi_{-k}^{1,2} = \pm\sqrt{\kappa/2}(\psi_k^{2,1} + \bar{\psi}_{-k}^{2,1}) \tag{3.43}$$

The potential then reads

$$V = \sum_{k+l+m+n=0} \frac{1}{2\kappa^2} \left(-i\sqrt{2\kappa}\eta_0^2 + \frac{\psi_k^2 - \bar{\psi}_{-k}^2}{k} \right) \left(-i\sqrt{2\kappa}\eta_0^1 + \frac{\psi_l^1 - \bar{\psi}_{-l}^1}{l} \right) (\psi_m^2 \bar{\psi}_{-n}^1 + \bar{\psi}_{-m}^2 \psi_n^1) \tag{3.44}$$

Normal order

Up to now no normal order has been put on the fields. The elementary annihilation operators are set to be the $\psi_m^{1,2}$, $\bar{\psi}_m^{1,2}$ with $m \geq 0$, and the elementary creation operators the same modes but for $m < 0$, as well as $\eta_0^{1,2}$. The normally ordered version of an operator X is denoted $:X:$ and is defined, for every product of elementary operators that appear in the expression of X, by putting all the annihilation operators to the right of their creation operators, multiplied by the corresponding fermionic sign. Equivalently (this is much more convenient for practical purposes), it amounts to forbidding contractions between modes that compose the Hamiltonian. Indeed, the only difference between the Hamiltonian and its normally-ordered version is the contractions that appear whenever an annhilation operator is moved to the right of a creation operator. For example if one computes the expectation value

$$\langle 0|\psi_1^2 \left(\sum_k :\psi_k^2 \psi_{-k}^1: \right) \psi_{-1}^1 |0\rangle = \langle 0|\psi_1^2 \left(\sum_{k<0} \psi_k^2 \psi_{-k}^1 - \sum_{k>0} \psi_{-k}^1 \psi_k^2 + \psi_0^2 \psi_0^1 \right) \psi_{-1}^1 |0\rangle$$

$$= \langle 0|\psi_1^2 \left(-\psi_{-1}^1 \psi_1^2 \right) \psi_{-1}^1 |0\rangle$$

$$= -1 \tag{3.45}$$

one actually contracts the ψ_1^2 inside the Hamiltonian with the ψ_{-1}^1 outside the Hamiltonian, without touching the ψ_{-1}^1 inside the Hamiltonian (but counting the $-$ sign that comes when going through it).

The normal ordering is known to remove 'infinite quantities' from the expression of the fields. These are actually sums of anticommutators $\{\eta_k^1, \pi_k^1\} = i$. While no expectation value is taken, one may equally consider that $\{\eta_k^1, \pi_k^1\} = i \cdot 1_{|k|}$ where $1_k = 1_{-k}$ is a bosonic variable that commutes with everything, and that could be treated on the same footing as the fermionic variables η's. This way these 'infinite quantities' are of the form $\sum_{k>0} 1_k$ which are regular elements of the algebra we are using. The only point is then to define a vacuum expectation value for this element of the algebra. Let us define thus

$$\xi_0 = \sum_{m>0} 1_m, \quad \xi_{-1} = \sum_{m>0} \frac{1_m}{m} \tag{3.46}$$

The bosonic charges are not altered by the normal order:

$$J_z = :J_z:, \qquad J_+ = :J_+:, \qquad J_- = :J_-: \tag{3.47}$$

However the fermionic charges change. With an implicit sum over $k + l + m = 0$ (that is explicitly written for m in case of constraints), we have

$$
\begin{aligned}
F_1 &= \pi_0^2 + g\pi_{-k}^2 \eta_l^1 \eta_m^2 \\
&= \pi_0^2 + g\pi_{-k}^2 \eta_{-k}^1 \eta_0^2 + \frac{ig}{\sqrt{2\kappa}} \pi_{-k}^2 \eta_l^1 \left(\frac{\psi_m^2}{m} - \frac{\bar{\psi}_{-m}^2}{m} \right) \\
&= :F_1: -ig\eta_0^1 + \frac{ig}{\sqrt{2\kappa}} \left(\sum_{m<0} [\pi_{-k}^2 \eta_l^1, \frac{\psi_m^2}{m}] - \sum_{m>0} [\pi_{-k}^2 \eta_l^1, \frac{\bar{\psi}_{-m}^2}{m}] \right) \\
&= :F_1: -ig\eta_0^1 - \frac{2ig}{\sqrt{2\kappa}} \sum_{m>0} \left(\frac{i}{m\sqrt{2\kappa}} \pi_0^2 + \sqrt{\kappa/2}\eta_0^1 \right) 1_m \\
&= :F_1: -ig\eta_0^1 - ig\eta_0^1 \xi_0 + g\kappa^{-1}\pi_0^2 \xi_{-1}
\end{aligned}
\tag{3.48}
$$

To go from the second line to the third line, we noticed that $\pi_{-k}^2 \eta_l^1$ only involves $\psi^1, \bar{\psi}^1$ that anticommute, so that the only 'ill-ordered' case that can occur is when a creation operator $\psi_m^2, \bar{\psi}_m^2$ with $m < 0$ is at the right. Similarly:

$$G_1 = :G_1: +ig\eta_0^2 + ig\eta_0^2 \xi_0 + g\kappa^{-1}\pi_0^1 \xi_{-1} \tag{3.49}$$

As for the potential, it reads with an implicit summation over $k + l + m + n = 0$

$$V = -\kappa^{-1}\eta_k^2\eta_l^1(\psi_m^2\bar{\psi}_{-n}^1 + \bar{\psi}_{-m}^2\psi_n^1)$$

$$=:V: -\kappa^{-1}\sum_{\substack{m<0\\n\leq 0}}[\eta_k^2\eta_l^1,\psi_m^2]\bar{\psi}_{-n}^1 + \kappa^{-1}\sum_{\substack{m\geq 0\\n>0}}[\eta_k^2\eta_l^1,\bar{\psi}_{-n}^1]\psi_m^2 - \kappa^{-1}\sum_{\substack{m<0\\n>0}}\left([\eta_k^2\eta_l^1,\psi_m^2]\bar{\psi}_{-n}^1 + \psi_m^2[\eta_k^2\eta_l^1,\bar{\psi}_{-n}^1]\right)$$

$$+ \kappa^{-1}\sum_{\substack{n<0\\m\leq 0}}[\eta_k^2\eta_l^1,\psi_n^1]\bar{\psi}_{-m}^2 - \kappa^{-1}\sum_{\substack{n\geq 0\\m>0}}[\eta_k^2\eta_l^1,\bar{\psi}_{-m}^2]\psi_n^1 + \kappa^{-1}\sum_{\substack{n<0\\m>0}}\left([\eta_k^2\eta_l^1,\psi_n^1]\bar{\psi}_{-m}^2 + \psi_n^1[\eta_k^2\eta_l^1,\bar{\psi}_{-m}^2]\right)$$

$$=:V: -\frac{i}{\kappa\sqrt{2\kappa}}\sum_k\sum_{m>0}(\eta_k^2\bar{\psi}_k^1 - \eta_{-k}^1\psi_k^2 - \eta_k^1\bar{\psi}_k^2 + \eta_{-k}^2\psi_k^1)1_m$$

$$=:V: +i\kappa^{-2}\sum_k(\eta_k^2\pi_k^2 + \eta_k^1\pi_k^1)\xi_0$$

(3.50)

Here, to get to the second line we had to treat separately the 6 different cases where at least one of the fields in $(\psi_m^2\bar{\psi}_{-n}^1 + \bar{\psi}_{-m}^2\psi_n^1)$ is a creation operator. The $\eta_k^2\eta_l^1$ part is then already normally ordered, since the only possible ill-ordered case is when $k = -l$, but then the ordering of the ψ part inside $\eta_k^2\eta_l^1$ for $k > 0$ cancels out with the ordering of the $\bar{\psi}$ part for $k < 0$.

The whole Hamiltonian is

$$H = \sum_{k<0}(\psi_k^2\psi_{-k}^1 - \psi_k^1\psi_{-k}^2 + \bar{\psi}_k^2\bar{\psi}_{-k}^1 - \bar{\psi}_k^1\bar{\psi}_{-k}^2) + 2\psi_0^2\psi_0^1 - \frac{c}{12} - \kappa g :V:$$
$$- i\kappa^{-1}g\sum_k(\eta_k^2\pi_k^2 + \eta_k^1\pi_k^1)\xi_0$$

(3.51)

with the central charge $c = -2$ obtained with a usual zeta regularization, namely assigning the value $\zeta(-1) = -1/12$ to the formal sum '$\sum_{k>0}k$' by analytically continuing the zeta function $\zeta(x) = \sum_{n>0}n^{-x}$ to the negative axis. The normally ordered Hamiltonian corresponds to the first line. Although the total Hamiltonian commutes with the $osp(1|2)$ charges, this is not the case anymore when normal order is imposed. One thus has to work with the total Hamiltonian, taking into account the ξ's for which a prescription of expectation value has to be given. Note that any (complex) value of the ξ's preserves the commutation relations.

Building the states

Let us define the states on which we will compute expectation values. We define the conformal variables $z = e^{-ix+\tau}$ and $\bar{z} = e^{ix+\tau}$ with $\tau = it$. A state $|\phi\rangle$ for a field $\phi(x,t)$ is defined by

$$|\phi\rangle = \phi(z = 0)|0\rangle \tag{3.52}$$

For example one has

$$|\eta^1\rangle = \eta_0^1|0\rangle \tag{3.53}$$

The derivatives with respect to z such as $|\partial_z \eta^1\rangle$ deserve some comments. Because of the definition of the modes ψ, we still have at all time

$$\eta^1(x,t) = \sum_k \eta^1_k(t)e^{ikx} = \eta^1_0 + i\sum_{k\neq 0} \frac{\psi^1_k(t) - \bar{\psi}^1_{-k}(t)}{k\sqrt{2\kappa}}e^{ikx} \tag{3.54}$$

Without interaction we simply have $\psi^1_k(\tau) = \psi^1_k(0)e^{-k\tau}$. But with the interaction the time evolution of the ψ's is not trivial anymore, and involves a term of order g with a product of three ψ's. The expression of η in terms of $z, \bar{z}$, and even more for $\partial_z \eta$, is not valid anymore. In particular one cannot build the states as usual:

$$|\partial_z \eta^1\rangle \neq -i\psi^1_{-1}|0\rangle \tag{3.55}$$

contrary to the case $g = 0$. The left-hand side now involves a term of order g. Precisely, using:

$$\partial_z = -\frac{1}{2i}e^{ix-\tau}\partial_x + \frac{1}{2}e^{ix-\tau}\partial_\tau \tag{3.56}$$

we get

$$\partial_z \eta^1(x,\tau) = \frac{-i}{\sqrt{2\kappa}}\sum_k \left(\psi^1_k(\tau) + g\kappa\sqrt{\frac{\kappa}{2}}\frac{dV}{d\pi^1_k}(\tau)\right)e^{ix(k+1)}e^{-\tau} \tag{3.57}$$

Taking $z = 0$ selects $k = -1$ because of the factor $e^{ix(k+1)}$, hence

$$|\partial_z \eta^1\rangle = \frac{-i}{\sqrt{2\kappa}}\psi^1_{-1}|0\rangle - i\frac{\kappa g}{2}\frac{dV}{d\pi^1_{-1}}|0\rangle \tag{3.58}$$

that is

$$|\partial_z \eta^1\rangle = -i(1 + \frac{g}{2}\eta^2_0\eta^1_0)\psi^1_{-1}|0\rangle \tag{3.59}$$

Remark moreover that one has indeed $F_1(1 + \frac{g}{2}\eta^2_0\eta^1_0)\psi^1_{-1}|0\rangle = 0$ and $J_+(1 + \frac{g}{2}\eta^2_0\eta^1_0)\psi^1_{-1}|0\rangle = 0$ and this state is indeed highest-weight.

However, if we look at terms involving a η times a derivative, since we have

$$\eta^1_k \frac{dV}{d\pi^1_{-k}} = 0 \tag{3.60}$$

we do have

$$|\eta^1\partial_z \eta^1\rangle = -i\eta^1_0\psi^1_{-1}|0\rangle \tag{3.61}$$

without any corrections in g.

For terms such as $|\eta^1\partial_z\eta^1...\partial_z^m\eta^1\rangle$ the corresponding calculations happen to be not as easily tractable, but the state $\eta^1_0\psi^1_{-1}...\psi^1_{-m}$ is indeed annihilated by F_1 (and J_+). Similarly, $|\partial_z\eta^1...\partial_z^m\eta^1\rangle$ is not as easily computed, but $(1 + m\frac{g}{2}\eta^2_0\eta^1_0)\psi^1_{-1}...\psi^1_{-m}$ is annihilated by F_1 and J_+.

Regularization

Any complex values for the ξ's give a Hamiltonian that commutes with the charges (that also depend on ξ), and thus that has the $osp(1|2)$ symmetry and the classical non-linear sigma model as classical limit. However, since some of them appear in expectation values, one has to fix their value with an exterior argument. This is the only additional information that we need to quantize the model. Here we choose to fix the zero mode of the Hamiltonian. It reads

$$H_0 = -\kappa^{-1}(1 - g\eta_0^1\eta_0^2)\pi_0^1\pi_0^2 - \kappa^{-1}ig(\eta_0^2\pi_0^2 + \eta_0^1\pi_0^1)\xi_0 \tag{3.62}$$

This zero mode should give the Laplace-Casimir operator of the algebra, see [101], thus be proportional to $(1 - g\eta_0^1\eta_0^2)\pi_0^1\pi_0^2 - ig(\eta_0^2\pi_0^2 + \eta_0^1\pi_0^1)$. Hence we impose the value

$$\langle 0|\xi_0|0\rangle = -1 \tag{3.63}$$

As for the value of $\langle 0|\xi_{-1}|0\rangle$, it does not enter the Hamiltonian nor the construction of the states, and thus has no influence on any expectation values.

Equivalently we could impose that the fermionic charges (and the bosonic ones) are not modified by the normal order. This constrains ξ_0 to take the value -1 and ξ_{-1} the value 0.

Correction to the energy levels

To evaluate the corrections at order g to the energy levels, one has to compute the matrix elements $\langle\phi_1|H|\phi_2\rangle$ where ϕ_1 and ϕ_2 are eigenstates of the unperturbed H with the same energy. In the following we will compute the action of H on some state $|\phi\rangle$. Consider one term in the Hamiltonian (3.51) and denote n and $\bar{n}$ the sum of the indices of the ψ's and $\bar{\psi}'s$ that compose this term. In general we have $n - \bar{n} = 0$, but not necessarily $n = \bar{n} = 0$ separately. Thus a state $|\phi_1\rangle$ with a certain value of $n - \bar{n}$ is mapped by H onto another state with the same value of $n - \bar{n}$. Since $|\phi_1\rangle$ and $|\phi_2\rangle$ have the same energy, they must have the same value of $n + \bar{n}$, hence the same value of n and $\bar{n}$ separately to have a non-zero matrix elements by H. This way one can consider only the 'conservative' part of H, i.e. its terms with $n = \bar{n} = 0$. It corresponds to summing the indices of the ψ's to zero, and to summing the indices of the $\bar{\psi}$'s to zero separately as well. Note that in the term $\eta_k^2\pi_k^2 + \eta_k^1\pi_k^1$, the only 'conservative' term is the zero mode $\eta_0^2\pi_0^2 + \eta_0^1\pi_0^1$.

- $|0\rangle$. We have

$$H|0\rangle = 0 \tag{3.64}$$

  that will be the reference state (in all finite sizes L) for our computations.

- $|\eta^1\rangle \propto \eta_0^1|0\rangle$. We have

$$:V: \eta_0^1|0\rangle = 0 \tag{3.65}$$

  thus

$$H\eta_0^1|0\rangle = -\kappa^{-1}g\eta_0^1|0\rangle \tag{3.66}$$

and a correction $-\kappa^{-1}g = -1/3\log L$. Note that it is below the ground state of the zero magnetization sector.

The other states in the multiplet are $(1 - g\eta_0^2\bar{\eta}_0^1)|0\rangle$ and $\eta_0^2|0\rangle$, i.e. the states obtained from $\eta_0^1|0\rangle$ by applying the lowering operators J_- and F_-. They indeed have the same correction:

$$H(1 - g\eta_0^2\bar{\eta}_0^1)|0\rangle = 0 - gH\eta_0^2\bar{\eta}_0^1|0\rangle$$
$$= -\kappa^{-1}g|0\rangle + O(g^2) \tag{3.67}$$
$$= -\kappa^{-1}g(1 - g\eta_0^2\bar{\eta}_0^1)|0\rangle + O(g^2)$$

and

$$H\eta_0^2|0\rangle = -\kappa^{-1}g\eta_0^2|0\rangle \tag{3.68}$$

hence

$$\frac{L^2\Delta e_L}{2\pi v_F} = -\kappa^{-1}g \tag{3.69}$$

- $|\eta^1\partial\eta^1....\partial^m\bar{\partial}\eta^1....\bar{\partial}^{\bar{m}}\eta^1\rangle \propto \eta_0^1\psi_{-1}^1...\psi_{-m}^1\bar{\psi}_{-1}^1...\bar{\psi}_{-\bar{m}}^1|0\rangle$. We have

$$:V: \eta_0^1\psi_{-1}^1...\psi_{-m}^1\bar{\psi}_{-1}^1...\bar{\psi}_{-\bar{m}}^1|0\rangle$$

$$= \frac{1}{2\kappa^2}\left(\sum_{n=1}^{\bar{m}}:\frac{-\bar{\psi}_n^2}{-n}(-i\eta_0^1)\psi_0^2\bar{\psi}_{-n}^1: + \sum_{n=1}^{\bar{m}}\sum_{k=1}^{m}:\frac{-\bar{\psi}_n^2}{-n}\frac{\psi_{-k}^1}{-k}\psi_k^2\bar{\psi}_{-n}^1:\right)\eta_0^1\psi_{-1}^1...\psi_{-m}^1\bar{\psi}_{-1}^1...\bar{\psi}_{-\bar{m}}^1|0\rangle$$

$$+ \frac{1}{2\kappa^2}\left(\sum_{n=1}^{m}:\frac{\psi_n^2}{n}(-i\eta_0^1)\bar{\psi}_0^2\psi_{-n}^1: + \sum_{n=1}^{m}\sum_{k=1}^{\bar{m}}:\frac{\psi_n^2}{n}\frac{-\bar{\psi}_{-k}^1}{k}\bar{\psi}_k^2\psi_{-n}^1:\right)\eta_0^1\psi_{-1}^1...\psi_{-m}^1\bar{\psi}_{-1}^1...\bar{\psi}_{-\bar{m}}^1|0\rangle$$

$$= \frac{1}{2\kappa^2}\left(-\sum_{n=1}^{\bar{m}}\frac{-n}{n} - \sum_{n=1}^{\bar{m}}\sum_{k=1}^{m}\frac{-n}{n}\frac{k}{k} - \sum_{n=1}^{m}\frac{-n}{n} - \sum_{n=1}^{m}\sum_{k=1}^{\bar{m}}\frac{-n}{n}\frac{k}{k}\right)\eta_0^1\psi_{-1}^1...\psi_{-m}^1\bar{\psi}_{-1}^1...\bar{\psi}_{-\bar{m}}^1|0\rangle$$

$$= \frac{1}{2\kappa^2}(\bar{m}(m+1) + m(\bar{m}+1))\eta_0^1\psi_{-1}^1...\psi_{-m}^1\bar{\psi}_{-1}^1...\bar{\psi}_{-m}^1|0\rangle$$

(3.70)

Indeed in $:V:$, every ψ_k^2 with $k > m$ or $\bar{\psi}_k^2$ with $k > \bar{m}$ anticommutes with all the fields in the state and annihilates $|0\rangle$, hence the restriction over the summations.

Thus

$$H\eta_0^1\psi_{-1}^1...\psi_{-m}^1\bar{\psi}_{-1}^1...\bar{\psi}_{-\bar{m}}^1|0\rangle = (m(m+1)-(2m\bar{m}+m+\bar{m}+2)g)\eta_0^1\psi_{-1}^1...\psi_{-m}^1\bar{\psi}_{-1}^1...\bar{\psi}_{-\bar{m}}^1|0\rangle \tag{3.71}$$

hence

$$\frac{L^2\Delta e_L}{2\pi v_F} = \tfrac{1}{2}m(m+1) + \tfrac{1}{2}\bar{m}(\bar{m}+1) - (m\bar{m} + \tfrac{m+\bar{m}}{2} + 1)\kappa^{-1}g \tag{3.72}$$

Note that the correction is not the sum of left and right contributions, but involves also a cross-term $m\bar{m}$.

For symmetric states $m = \bar{m}$ we find

$$\boxed{\frac{L^2\Delta e_L}{2\pi v_F} = m(m+1) - (m^2 + m + 1)\kappa^{-1}g} \tag{3.73}$$

59

while when $\bar{m} = 0$, the logarithmic correction becomes linear

$$\frac{L^2 \Delta e_L}{2\pi v_F} = \tfrac{1}{2}m(m+1) - (\tfrac{m}{2} + 1)\kappa^{-1}g \qquad (3.74)$$

- $|\partial\eta^1 ... \partial^m\eta^1 \bar{\partial}\eta^1 ... \bar{\partial}^m\eta^1\rangle \propto (1 + mg\eta_0^2\eta_0^1)\psi_{-1}^1 ... \psi_{-m}^1\bar{\psi}_{-1}^1 ... \bar{\psi}_{-m}^1.$

  Here the computation for the part involving the ψ's is similar to the previous case. As for the $\eta_0^2\eta_0^1$ part, only the unperturbed Hamiltonian acts on it. Combining the two parts, one finds

$$\frac{L^2 \Delta e_L}{2\pi v_F} = m(m+1) - m(m-1)\kappa^{-1}g \qquad (3.75)$$

  Note that the other states in the multiplet for $m = 1$ are $(\eta_0^1\psi_{-1}^2 + \psi_{-1}^1\eta_0^2)|0\rangle$ and $(1 + \tfrac{g}{2}\eta_0^2\eta_0^1)\psi_{-1}^2|0\rangle$ and give the same correction as expected, hence the importance of the factor $mg\eta_0^2\eta_0^1$ that comes from the discussion below (3.59).

3.2.2 The spectrum from the spin chain

In the remainder of this section we provide two alternative means of deriving (3.73), or at least special cases thereof. The first of these relies on the Bethe-ansatz diagonalization of the spin chain Hamiltonian, and the other on the computation of three-point functions—either directly, or using a trick reminiscent of Wick's theorem. While both of these methods are of independent relevance, the reader interested mainly in results for other models may chose to skip directly to section 3.3.

Bethe equations

Let us first describe the corresponding $osp(1|2)$ spin chain. Like the sigma model which involves as a basic degree of freedom a field in the vector representation of the algebra, the spin chain involves a tensor product of fundamental representations of $osp(1|2)$. In contrast with the other superalgebras we will encounter in this paper, $osp(1|2)$ has a simple representation theory. Its action on the spin chain is fully reducible, and the Hilbert space decomposes onto a direct sum of 'spin j' representations, with dimension $4j + 1$. Here j is the eigenvalue of the J_z generator on the highest weight state, and $j = 1/2$ corresponds to the fundamental.

The spectrum of the Hamiltonian is described by one family of roots λ_i satisfying the Bethe equations [99, 102]

$$\left(\frac{\lambda_i + i/2}{\lambda_i - i/2}\right)^L = \prod_{j\neq i} \frac{\lambda_i - \lambda_j + i}{\lambda_i - \lambda_j - i} \cdot \frac{\lambda_i - \lambda_j - i/2}{\lambda_i - \lambda_j + i/2} \qquad (3.76)$$

An eigenvalue of the Hamiltonian for one set of solutions $\lambda_1, ..., \lambda_K$ to these equations is then

$$e_L = -\frac{1}{L}\sum_{i=1}^{K} \frac{1}{\lambda_i^2 + 1/4} \qquad (3.77)$$

The spin j (ie, the eigenvalue of J_z) corresponding to a solution with K roots is linked to K through

$$K = L - 2j \tag{3.78}$$

Moreover the $osp(1|2)$ Bethe states are highest-weight states.

This kind of relation, that links the number of Bethe roots to the value of the charges of a state, can be simply deduced from a direct diagonalisation of the Hamiltonian in small sizes. But in some cases it can be obtained analytically from commutation relation between the total charges and the monodromy matrix components.

Bethe root structure

The first task when studying a spin chain with the Bethe ansatz is to find the structure of the roots that correspond to the energies (at least the low-lying ones). There is no generic way of determining this structure from the Bethe equations, implying that a numerical study is an inevitable step.

We observe that on the lattice in size L, the field $\eta^1 \partial \eta^1 ... \partial^m \eta^1 \bar{\partial} \eta^1 ... \bar{\partial}^{\bar{m}} \eta^1$ is obtained with $L - 1 - m - \bar{m}$ real Bethe roots, with m positive vacancies and $\bar{m}$ negative vacancies. The field $\partial \eta^1 ... \partial^m \eta^1 \bar{\partial} \eta^1 ... \bar{\partial}^m \eta^1$ is obtained with $L - 2m$ Bethe roots, among which $L - 2m - 2$ are real and symmetrically distributed, and 2 form an exact 2-string at $\pm i/2$, i.e. a pair of complex conjugate Bethe roots whose values are exactly $\pm i/2$. The field $\partial \eta^1 ... \partial^m \eta^1 \bar{\partial} \eta^1 ... \bar{\partial}^{\bar{m}} \eta^1$ when $m \neq \bar{m}$ is obtained with $L - m - \bar{m}$ Bethe roots, among which $L - m - \bar{m} - 2$ are real with m positive vacancies and $\bar{m}$ negative vacancies, and 2 form an approximate 2-string at $\pm i/2$ with large real part, on the side where there are the most vacancies. See Figure 3.1 for a plot of some root structures.
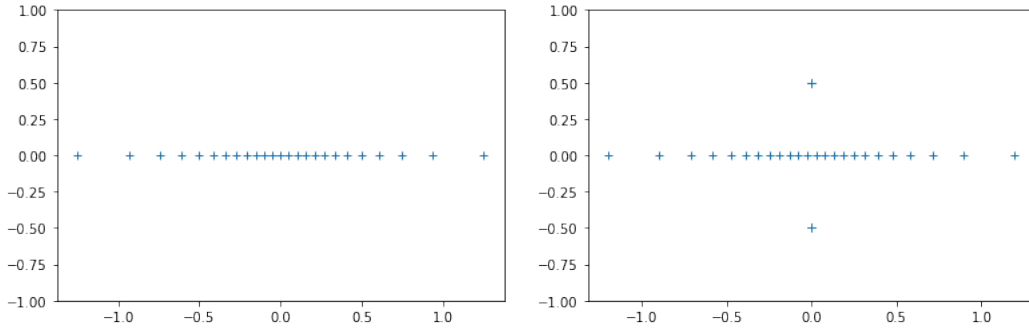
Figure 3.1: Bethe roots in the complex plane for the lowest state of magnetization 1 (left) and 0 (right), for $L = 26$.

The results for the gaps Δe_L of the ground state of the sectors of magnetization j reads then

$$\frac{L^2 \Delta e_L}{2\pi v_F} = \begin{cases} j^2 - \frac{1}{4} - \left(j^2 + \frac{3}{4}\right)\kappa^{-1}g, & \text{if } j \text{ is half-integer}, \\ j(j+1) - j(j-1)\kappa^{-1}g, & \text{if } j \text{ is integer} \end{cases} \tag{3.79}$$

61

in agreement with (3.73) after identifying $j \equiv m + \frac{1}{2}$ for half-integer spins, and with (3.75) where $j \equiv m$ for integer spins, while the value of the Casimir on these states is

$$\mathcal{C} = j(2j+1) \tag{3.80}$$

See below for a discussion of the symmetries at finite and vanishing g.

Note that all these corrections previously derived from field theory can be computed analytically within the Bethe ansatz; see Chapter 4.

Numerical results

We present here the numerical verification of the logarithmic corrections, carried out with the Bethe ansatz. Because of the logarithms, large sizes are needed to get a good precision, but it is still not enough to be in the asymptotic regime where the $(\log L)^{-1}$ can be observed. Thus a fit as a quotient of two polynomials in $(\log L)^{-1}$ is performed. Precisely, we used the function

$$f_n(L) = \frac{a_0 + a_1(\log L)^{-1} + ... + a_{n-1}(\log L)^{-n+1}}{1 + b_1(\log L)^{-1} + ... + b_n(\log L)^{-n}} \tag{3.81}$$

and fitted the parameters $a_0, ..., a_{n-1}, b_1, ..., b_n$ for a value of n depending on the state.

From the Bethe ansatz one computes $Z_L^{m,\bar{m}} = (\frac{L^2}{2\pi v_F}(e_L - e_L^{\text{gs}}) - (h + \bar{h})) \log L$, where e_L^{gs} is the energy of the ground state and e_L the energy of the state studied (here, the one with m positive vacancies and $\bar{m}$ negative vacancies; a $1/2$ vacancy on both sides counts for an odd number of total vacancies), and looks for its limit value, see Figure 3.2.

3.2.3 Relation with 3-point functions

We discuss in this section how the logarithmic corrections can be related to the 3-point functions on the plane. Our calculation parallels the work by Cardy for quasi-primary fields [92], but applies here to the logarithmic case.

Fields with logarithms

The derivation in Section 2.4.3 of the relation between the logarithmic correction and the three point function does not apply to the logarithmic cases discussed above. Indeed, η^1 and η^2 are not quasi-primary: their correlation involves log that is not a scale covariant function, and the three point function is not constrained as before in Section 2.4.3. It thus needs a more detailed study. The purpose of the subsequent sections is to study the link between the correction to the energy levels for the states $|\eta^1 \partial \eta^1 ... \partial^m \eta^1\rangle$ and the three-point function between them and the perturbative potential.

Denote $\phi_m^1(z)$ the field $\eta^1(z)\partial\eta^1(z)...\partial^m\eta^1(z)$ and $\phi_m^2(z)$ the field $\partial^m\eta^2(z)...\partial\eta^2(z)\eta^2(z)$. They have scaling dimensions $m(m+1)/2$. The corresponding state $|\phi_m^1\rangle$ is given by the constant coefficient in $\phi_m^1(z)$, and is $\propto \eta_0^1 \psi_{-1}^1 ... \psi_{-m}^1$. The state $\langle\phi_m^2|$ is defined as the conjugate of $|\phi_m^1\rangle$, thus $\propto \psi_m^2 ... \psi_1^2 \pi_0^1$. It is given by the coefficient $\log|z|^2 z^{-m(m+1)}$ in $\phi_m^2(z)$, denoted
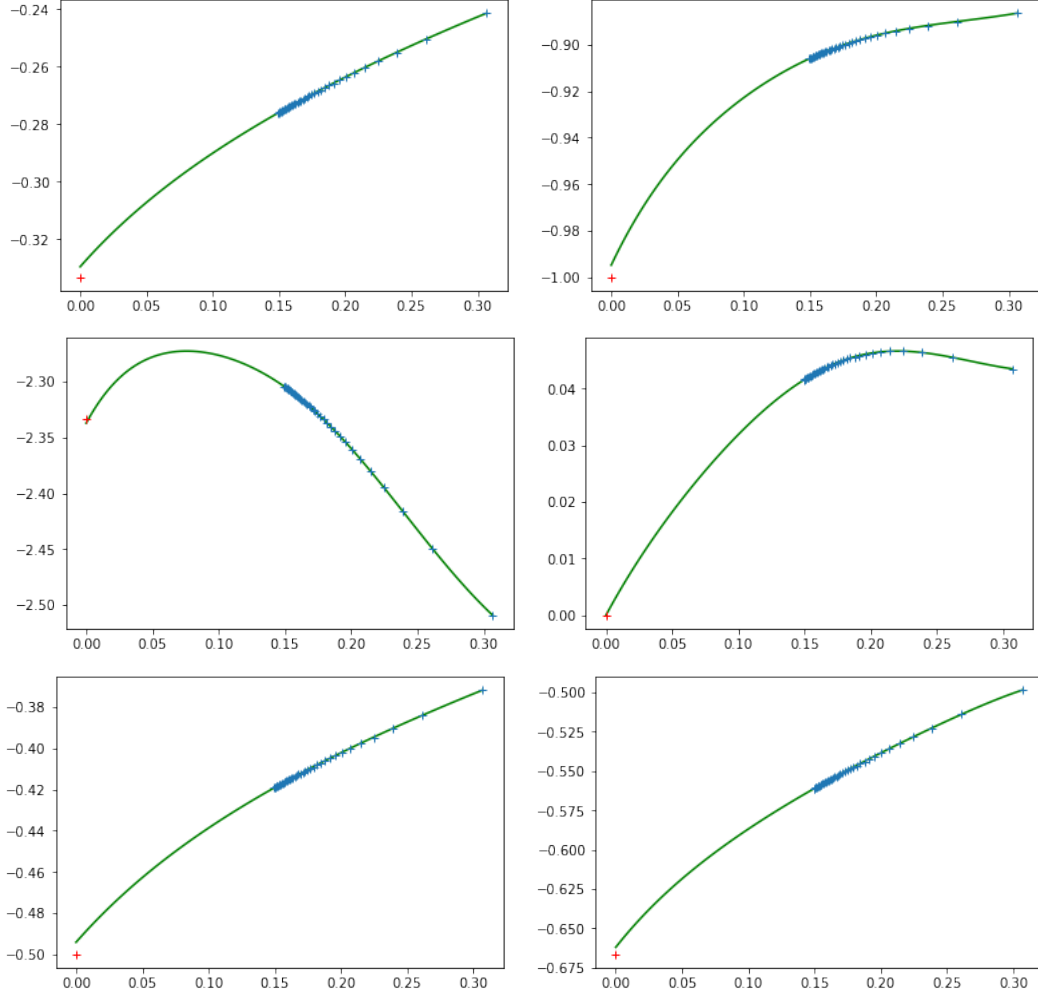
Figure 3.2: In reading direction: plots of $Z_L^{1/2,1/2}$, $Z_L^{1/2+1,1/2+1}$, $Z_L^{1/2+2,1/2+2}$, $Z_L^{1,1}$, $Z_L^{1/2+1,1/2}$, $Z_L^{1/2+2,1/2}$ as a function of $1/\log L$, together with their extrapolated curves f_6, f_7, f_6, f_5, f_8, f_8. The theoretical results are, respectively, $-1/3$, -1, $-7/3$, 0, $-1/2$, $-2/3$.

coeff $_{\log |z|^2 z^{-m(m+1)}}(\langle 0|\phi_m^2(z))$ (one could give an integral formula for this, but it is unnecessary). Note that in absence of log, this matches the usual definitions. One can express these as

$$|\phi_m^1\rangle = \phi_m^1(0,0)|0\rangle, \qquad \langle\phi_m^2| = \text{coeff}_{\log |z|^2 z^{-m(m+1)}}(\langle 0|\phi_m^2(z)) \tag{3.82}$$

The Hamiltonian is perturbed by $-\kappa g/(2\pi)\int \mathcal{V}(x, t = 0)dx$. Since the perturbation $\kappa^{-1}g\delta\hat{e}$ to the energy level of state ϕ_m is given by

$$\delta\hat{e} = -\frac{\kappa^2}{\langle\phi_m^2|\phi_m^1\rangle}\langle\phi_m^2|\frac{1}{2\pi}\int_0^{2\pi}\mathcal{V}(x,t=0)dx|\phi_m^1\rangle \tag{3.83}$$

one sees that it can be expressed in terms of the 3-point function $G_{\phi_m^1}(z_2, z, z_1)$ where

$$G_X(z_2, z, z_1) = \langle 0|X^\dagger(z_2)\mathcal{V}(z)X(z_1)|0\rangle \tag{3.84}$$

for a field $X(z)$. Precisely:

$$\delta\hat{e} = -\frac{\kappa^2}{\langle\phi_m^2|\phi_m^1\rangle}\text{coeff}_{\log |z_2|^2 z_2^{-m(m+1)}\times z^0}(G(z_2, z, 0)) \tag{3.85}$$

An explicit calculation of the 3-point function $\langle\eta^2\mathcal{V}\eta^1\rangle$

The fields are assumed to be radially ordered $|z_1| < |z| < |z_2|$.

Let us first compute explicitly the 3-point function $G_\eta(z_2, z, z_1)$:

$$G_\eta(z_2, z, z_1) = \langle 0|\eta^2(z_2)\mathcal{V}(z)\eta^1(z_1)|0\rangle \tag{3.86}$$

at points $z = e^{-ix+\tau}$. The potential $\mathcal{V}(x, t)$ is

$$\mathcal{V}(x,t) = :\mathcal{V}(x,t): +i\kappa^{-2}\xi_0\sum_{p,k}(\eta_k^2(t)\pi_{k-p}^2(t) + \eta_k^1(t)\pi_{k-p}^1(t))e^{ipx} \tag{3.87}$$

Within the correlator (3.86) the part with the normally ordered potential $:\mathcal{V}(x,t):$ is zero since there are four fields to contract with only two fields at our disposal. Thus we have

$$G_\eta(z_2, z, z_1) = -\langle 0|\eta^2(z_2)\left(i\kappa^{-2}\xi_0\sum_{p,k}(\eta_k^2(t)\pi_{k-p}^2(t) + \eta_k^1(t)\pi_{k-p}^1(t))e^{ipx}\right)\eta^1(z_1)|0\rangle \tag{3.88}$$

We can now use (3.35) to express each of the $\eta_k^{1,2}(t)$ and $\pi_k^{1,2}(t)$ in terms of $z = e^{-ix+\tau} = $

64

e^{-ix+it}. We find

$$G_\eta(z_2, z, z_1) = -\kappa^{-2}i\langle 0|\left(\eta_0^2 - i\frac{\pi_0^1}{2\kappa}\log|z_2|^2 + i\sum_{n\neq 0}\frac{\psi_n^2 z_2^{-n} - \bar\psi_{-n}^2 \bar z_2^n}{n\sqrt{2\kappa}}\right)$$

$$\sum_{k,p}\frac{i}{2k}(\psi_k^1\psi_{-k+p}^2 z^{-p} + \psi_k^1\bar\psi_{k-p}^2 z^{-k}\bar z^{-k+p} - \bar\psi_{-k}^1\psi_{-k+p}^2\bar z^k z^{k-p} - \bar\psi_{-k}^1\bar\psi_{k-p}^2\bar z^p$$

$$- \psi_k^2\psi_{-k+p}^1 z^{-p} - \psi_k^2\bar\psi_{k-p}^1 z^{-k}\bar z^{-k+p} + \bar\psi_{-k}^2\psi_{-k+p}^1 z^{k-p}\bar z^k + \bar\psi_{-k}^2\bar\psi_{k-p}^1\bar z^p)$$

$$\left(\eta_0^1 + i\frac{\pi_0^2}{2\kappa}\log|z_1|^2 + i\sum_{m\neq 0}\frac{\psi_m^1 z_1^{-m} - \bar\psi_{-m}^1 \bar z_1^m}{m\sqrt{2\kappa}}\right)|0\rangle$$

(3.89)

where we use the shortcuts $i\psi_0^{1,2}/(0\sqrt{2\kappa}) = \eta_0^{1,2} \pm i(2\kappa)^{-1}\pi_0^{2,1}\log|z|^2$ and $i\bar\psi_0^{1,2}/0 = 0$ to simplify the notations. One has

$$G_\eta(z_2, z, z_1) =$$

$$-\frac{\kappa^{-3}}{2}\log|z_2|^2\langle 0|\pi_0^1\eta_0^1\psi_0^2\eta_0^1|0\rangle - \frac{\kappa^{-3}}{4}i\log|z_2|^2\sum_{p>0}\langle 0|\pi_0^1\eta_0^1\psi_p^2\frac{\psi_{-p}^1}{-p}|0\rangle z^{-p}z_1^p - \frac{\kappa^{-3}}{4}i\log|z_2|^2\sum_{p<0}\langle 0|\pi_0^1\eta_0^1\bar\psi_{-p}^2\frac{\bar\psi_p^1}{p}|0\rangle\bar z^p$$

$$-\frac{\kappa^{-3}}{4}\sum_{n\neq 0,m}\langle 0|\frac{\psi_n^2}{n}\frac{\psi_{-n}^1}{-n}\psi_{-m}^2\frac{\psi_m^1}{m}|0\rangle z_2^{-n}z^{n+m}z_1^{-m} - \frac{\kappa^{-3}}{4}\sum_{n\neq 0,m}\langle 0|\frac{\psi_n^2}{n}\psi_{-n}^1\frac{\psi_{-m}^2}{-m}\frac{\psi_m^1}{m}|0\rangle z_2^{-n}z^{n+m}z_1^{-m}$$

$$-\frac{\kappa^{-3}}{4}\sum_{n\neq 0,m}\langle 0|\frac{\psi_n^2}{n}\frac{\psi_{-n}^1}{-n}\bar\psi_m^2\frac{\bar\psi_{-m}^1}{-m}|0\rangle z_2^{-n}z^n\bar z^{-m}\bar z_1^m + \frac{\kappa^{-3}}{4}\sum_{n\neq 0,m}\langle 0|\frac{\psi_n^2}{n}\psi_{-n}^1\frac{\bar\psi_m^2}{-m}\frac{\bar\psi_{-m}^1}{-m}|0\rangle z_2^{-n}z^n\bar z^{-m}\bar z_1^m$$

$$+\frac{\kappa^{-3}}{4}\sum_{n\neq 0,m}\langle 0|\frac{\bar\psi_{-n}^2}{-n}\frac{\bar\psi_n^1}{-n}\psi_{-m}^2\frac{\psi_m^1}{m}|0\rangle\bar z_2^n z^m\bar z^{-n}z_1^{-m} - \frac{\kappa^{-3}}{4}\sum_{n\neq 0,m}\langle 0|\frac{\bar\psi_{-n}^2}{-n}\bar\psi_n^1\frac{\psi_{-m}^2}{-m}\frac{\psi_m^1}{m}|0\rangle\bar z_2^n z^m\bar z^{-n}z_1^{-m}$$

$$+\frac{\kappa^{-3}}{4}\sum_{n\neq 0,m}\langle 0|\frac{\bar\psi_{-n}^2}{-n}\frac{\bar\psi_n^1}{-n}\bar\psi_m^2\frac{\bar\psi_{-m}^1}{-m}|0\rangle\bar z_2^n\bar z^{-n-m}\bar z_1^m + \frac{\kappa^{-3}}{4}\sum_{n\neq 0,m}\langle 0|\frac{\bar\psi_{-n}^2}{-n}\bar\psi_n^1\frac{\bar\psi_m^2}{-m}\frac{\bar\psi_{-m}^1}{-m}|0\rangle\bar z_2^n\bar z^{-n-m}\bar z_1^m$$

(3.90)

Evaluating each scalar product gives

$$G_\eta(z_2, z, z_1) =$$

$$\frac{\kappa^{-3}}{2}\log|z_2|^2 + \frac{\kappa^{-3}}{4}\log|z_2|^2\sum_{p>0}z^{-p}z_1^p + \frac{\kappa^{-3}}{4}\log|z_2|^2\sum_{p<0}\bar z^p\bar z_1^{-p}$$

$$-\frac{\kappa^{-3}}{4}\log|z|^2\sum_{p>0}z_2^{-p}z^p - \frac{\kappa^{-3}}{4}\log|z|^2\sum_{p<0}\bar z_2^p\bar z^{-p}$$

$$-\frac{\kappa^{-3}}{4}\sum_{n>0,m<0}\frac{z_2^{-n}z^{n+m}z_1^{-m}}{n} + \frac{z_2^{-n}z^{n+m}z_1^{-m}}{m} - \frac{\kappa^{-3}}{4}\sum_{n>0,m>0}\frac{z_2^{-n}z^n\bar z^{-m}\bar z_1^m}{n} - \frac{z_2^{-n}z^n\bar z^{-m}\bar z_1^m}{m} \quad (3.91)$$

$$+\frac{\kappa^{-3}}{4}\sum_{n<0,m<0}\frac{\bar z_2^n z^m\bar z^{-n}z_1^{-m}}{n} - \frac{\bar z_2^n z^m\bar z^{-n}z_1^{-m}}{m} + \frac{\kappa^{-3}}{4}\sum_{n<0,m>0}\frac{\bar z_2^n\bar z^{-n-m}\bar z_1^m}{n} + \frac{\bar z_2^n\bar z^{-n-m}\bar z_1^m}{m}$$

$$-\frac{\kappa^{-3}}{2}\sum_{n>0}\frac{z_2^{-n}z^n}{n} + \frac{\kappa^{-3}}{2}\sum_{n<0}\frac{\bar z_2^n\bar z^{-n}}{n}$$

65

or in a simpler form

$$G_\eta(z_2, z, z_1) = \frac{\kappa^{-3}}{4}\left(\frac{z}{z - z_2} + \frac{\bar{z}}{\bar{z} - \bar{z}_2}\right)\log|z - z_1|^2 + \frac{\kappa^{-3}}{4}\left(\frac{z}{z - z_1} + \frac{\bar{z}}{\bar{z} - \bar{z}_1}\right)\log|z - z_2|^2$$

$$\tag{3.92}$$

Formula (3.85) gives here, with $\langle \phi_0^1 | \phi_0^2 \rangle = (2\kappa)^{-1}$

$$\delta\hat{e} = -\kappa^2 \times 2\kappa \times \frac{\kappa^{-3}}{4} \times 2 = -1 \tag{3.93}$$

which is indeed the correction computed in (3.74).

2-point functions

If we were to compute the 3-point function $\langle 0|\partial\eta^2\eta^2\mathcal{V}\eta^1\partial\eta^1|0\rangle$ with the same method as in the previous example, one would have to take into account the term $:\mathcal{V}:$ and the computations would become quite cumbersome. Actually, such a computation can always be recast into a product of 2-point functions, like a Wick's theorem. Indeed, since the anticommutator of two modes is a complex number, to evaluate the 3-point function (3.84) one has to contract every mode of the middle field $\mathcal{V}$ with modes of the right and left fields, and then contract the remaining modes between them. The 2-point functions that appear in the result involve the following fields and their derivatives:

$$\eta^1(z) = \eta_0^1 + i\frac{\pi_0^2}{2\kappa}\log|z|^2 + i\sum_{n\neq 0}\frac{\psi_n^1 z^{-n} + \bar{\psi}_n^1\bar{z}^{-n}}{n\sqrt{2\kappa}}, \qquad \eta^2(z) = \eta_0^2 - i\frac{\pi_0^1}{2\kappa}\log|z|^2 + i\sum_{n\neq 0}\frac{\psi_n^2 z^{-n} + \bar{\psi}_n^2\bar{z}^{-n}}{n\sqrt{2\kappa}}$$

$$\partial_x\eta^1(z) = -\frac{1}{\sqrt{2\kappa}}\sum_{n\neq 0}\psi_n^1 z^{-n} - \bar{\psi}_n^1\bar{z}^{-n}, \qquad \partial_x\eta^2(z) = -\frac{1}{\sqrt{2\kappa}}\sum_{n\neq 0}\psi_n^2 z^{-n} - \bar{\psi}_n^2\bar{z}^{-n}$$

$$\pi^1(z) = \pi_0^1 + \sqrt{\frac{\kappa}{2}}\sum_{n\neq 0}\psi_n^2 z^{-n} + \bar{\psi}_n^2\bar{z}^{-n}, \qquad \pi^2(z) = \pi_0^2 - \sqrt{\frac{\kappa}{2}}\sum_{n\neq 0}\psi_n^1 z^{-n} + \bar{\psi}_n^1\bar{z}^{-n}$$

$$\tag{3.94}$$

The 2-point function between these fields are known or computed without problems [84]. For example

$$2\kappa\langle 0|\eta^2(z)\eta^1(w)|0\rangle = -i\log|z|^2\langle 0|\pi_0^1\eta_0^1|0\rangle - \sum_{n>0,m<0}\frac{z^{-n}w^{-m}}{nm}\langle 0|\psi_n^2\psi_m^1|0\rangle - \sum_{n>0,m<0}\frac{\bar{z}^{-n}\bar{w}^{-m}}{nm}\langle 0|\bar{\psi}_n^2\bar{\psi}_m^1|0\rangle$$

$$= \log|z|^2 - \sum_{n>0}\frac{z^{-n}w^n}{n} - \sum_{n>0}\frac{\bar{z}^{-n}\bar{w}^n}{n}$$

$$= \log|z|^2 + \log(1 - w/z) + \log(1 - \bar{w}/\bar{z})$$

$$\tag{3.95}$$

hence

$$\langle 0|\eta^2(z)\eta^1(w)|0\rangle = \frac{1}{2\kappa}\log|z - w|^2 \tag{3.96}$$

66

Similarly

$$\langle 0|\eta^2(z)\partial_x\eta^1(w)|0\rangle = -\langle 0|\eta^1(z)\partial_x\eta^2(w)|0\rangle = \frac{1}{2\kappa}\left(\frac{iw}{z-w} + \frac{-i\bar{w}}{\bar{z}-\bar{w}}\right)$$

$$\langle 0|\eta^1(z)\pi^1(w)|0\rangle = \langle 0|\eta^2(z)\pi^2(w)|0\rangle = \frac{i}{2}\left(\frac{w}{z-w} + \frac{\bar{w}}{\bar{z}-\bar{w}}\right)$$

(3.97)

For instance, these formulas enable us to reexpress the previous 3-point function as

$$G_\eta(z_2, z, z_1) = -\kappa^{-2}i(-\langle\eta^2(z_2)\pi^2(z)\rangle\langle\eta^2(z)\eta^1(z_1)\rangle + \langle\eta^2(z_2)\eta^1(z)\rangle\langle\pi^1(z)\eta^1(z_1)\rangle) \quad (3.98)$$

where we use the simplified notation $\langle X\rangle$ for $\langle 0|X|0\rangle$.

Because of the fields η that involve log there is no scale invariance and the 2-point function of the fields ϕ_m^1 is not as simply constrained as usual. In particular there are sub-leading corrections to the dominant terms. In the following we will denote by $\sim$ an equality up to sub-leading terms. The computation of the dominant behaviour of the 2-point functions of the fields ϕ_m^1 is classical. We have

$$\begin{aligned}
\langle 0|\phi_m^2(z_2)\phi_m^1(z_1)|0\rangle &= \langle 0|\partial^m\eta^2(z_2)...\partial\eta^2(z_2)\eta^2(z_2)\eta^1(z_1)\partial\eta^1(z_1)...\partial^m\eta^1(z_1)|0\rangle \\
&\sim \frac{1}{2\kappa}\log|z_2-z_1|^2\langle 0|\partial^m\eta^2(z_2)...\partial\eta^2(z_2)\partial\eta^1(z_1)...\partial^m\eta^1(z_1)|0\rangle \\
&\sim \frac{1}{2\kappa}\log|z_2-z_1|^2\sum_{\sigma\in\mathfrak{S}_m}(-1)^\sigma\prod_{k=1}^m\langle 0|\partial^k\eta^2(z_2)\partial^{\sigma(k)}\eta^1(z_1)|0\rangle \\
&\sim \frac{1}{2\kappa}\log|z_2-z_1|^2\sum_{\sigma\in\mathfrak{S}_m}(-1)^\sigma\prod_{k=1}^m\frac{(-1)^{k-1}(k+\sigma(k)-1)!}{(z_2-z_1)^{k+\sigma(k)}2\kappa} \\
&\sim \frac{\log|z_2-z_1|^2}{(z_2-z_1)^{m(m+1)}(2\kappa)^{m+1}}\det((-1)^{k-1}(k+p-1)!)_{k,p}
\end{aligned}$$

(3.99)

where in the second line the dominant term is given by contracting η^1 with η^2 (otherwise the power-law is the same but without log, thus sub-dominant). This gives the norm

$$\langle\phi_m^2|\phi_m^1\rangle = (2\kappa)^{-m-1}\det\left\{(-1)^{k-1}(k+p-1)!\right\}_{k,p=1}^m = (2\kappa)^{-m-1}(-1)^{\lfloor m/2\rfloor}m!\prod_{k=1}^{m-1}(k!)^2$$

(3.100)

Dominant behaviour of the 3-point functions $\langle \phi_m^2 \mathcal{V} \phi_m^1 \rangle$

Using the 2-point functions one can compute all the $\langle \phi_m^2 \mathcal{V} \phi_m^1 \rangle$. For example one has

$$\langle \partial \eta^2(z_2) \eta^2(z_2) \mathcal{V}(z) \eta^1(z_1) \partial \eta^1(z_1) \rangle =$$

$$\frac{\kappa^{-4}}{8} \log |z_2 - z|^2 \frac{|z|^2}{(z_2 - z)^2 |z_1 - z|^2} + \frac{\kappa^{-4}}{8} \log |z_2 - z_1|^2 \frac{z}{(z_2 - z)^2(z_1 - z)}$$

$$- \frac{\kappa^{-4}}{8} \log |z_2 - z|^2 \left(\frac{z}{(z_1 - z)(z_2 - z_1)^2} + \frac{\bar{z}}{(\bar{z}_1 - \bar{z})(z_2 - z_1)^2} + \frac{z}{(z_2 - z_1)(z_1 - z)^2} \right)$$

$$+ \frac{\kappa^{-4}}{4} \frac{|z|^2}{(z_2 - z)^2 |z_1 - z|^2} + \frac{\kappa^{-4}}{8} \frac{\bar{z}}{(\bar{z}_2 - \bar{z})(z_1 - z)(z_2 - z_1)} + \frac{\kappa^{-4}}{8} \frac{z}{(z_2 - z)(z_1 - z)(z_2 - z_1)}$$

$$+ (z_1 \to z_2, \quad z_2 \to z_1)$$
$$(3.101)$$

The dominant behaviour is given by

$$G_{\eta \partial \eta}(z_2, z, z_1) \sim \frac{\kappa^{-4}}{8} \log |z_2 - z|^2 \frac{|z|^2}{(z_2 - z)^2 |z_1 - z|^2} + \frac{\kappa^{-4}}{8} \log |z_1 - z|^2 \frac{|z|^2}{(z_1 - z)^2 |z_2 - z|^2} \quad (3.102)$$

Formula (3.85) gives for the full correlation function

$$\delta \hat{e} = -\kappa^2 \times (2\kappa)^2 \times \frac{\kappa^{-4}}{8} \times 3 = -3/2 \tag{3.103}$$

However formula (3.85) does not capture only the dominant term in (3.101), but also the sub-dominant term $- \log |z_2 - z|^2 \left(\frac{z}{(z_1 - z)(z_2 - z_1)^2} + \frac{\bar{z}}{(\bar{z}_1 - \bar{z})(z_2 - z_1)^2} \right)$. The dominant term comes from the normally ordered part of the potential $:\mathcal{V}:$ whereas the second term comes from the regularized part $\xi_0(\eta^2 \pi^2 + \eta^1 \pi^1)$. Both contribute to the displacement of energies, but only the first one is visible at leading order in the 3-point function. Note that this sub-dominant term is not even the next-to-leading order term.

Let us evaluate the dominant term in the 3-point function $G_{\phi_m}(z_2, z, z_1)$. Let us first remark that in $\mathcal{V}$ the regularized term will always contribute one power less than the normally ordered term, so that the dominant term is given by $:\mathcal{V}:$. We have thus

$$G_{\phi_m}(z_2, z, z_1) \sim \langle 0 | \partial^m \eta^2(z_2) ... \eta^2(z_2) :(\eta^2 \eta^1 \partial_x \eta^2 \partial_x \eta^1 + \kappa^{-2} \eta^2 \eta^1 \pi^1 \pi^2)(z): \eta^1(z_1) ... \partial^m \eta^1(z_1) | 0 \rangle \tag{3.104}$$

A priori, the dominant term will be given by contracting the four η together, yielding a $\log |z_1 - z|^2 \log |z_2 - z|^2$. However we have the relations, using the abbreviated notations $\partial \eta$ for $\partial_z \eta$:

$$\langle 0 | \pi^1(z) \partial^k \eta^1(w) | 0 \rangle = -\kappa \langle 0 | \partial_x \eta^2(z) \partial^k \eta^1(w) | 0 \rangle$$
$$\langle 0 | \pi^2(z) \partial^k \eta^2(w) | 0 \rangle = \kappa \langle 0 | \partial_x \eta^1(z) \partial^k \eta^2(w) | 0 \rangle$$
$$(3.105)$$

valid for all $k \geq 1$. Thus

$$\langle 0 | \partial^m \eta^2(z_2) ... \partial \eta^2(z_2) :(\partial_x \eta^2 \partial_x \eta^1 + \kappa^{-2} \pi^1 \pi^2)(z): \partial \eta^1(z_1) ... \partial^m \eta^1(z_1) | 0 \rangle = 0 \tag{3.106}$$

68

and the $\log^2$ term vanishes. Similarly, if one contracts only $\eta^2(z_2)$ with $\eta^1(z)$, then one has to contract $\partial_x\eta^2(z)$ with $\eta^1(z_1)$ and $\pi^1(z)$ with $\eta^1(z_1)$ since the relations (3.105) are verified for all k but $k = 0$ (otherwise the terms in $\partial_x\eta^2$ and π^1 will cancel out). Then:

$$G_{\phi_m}(z_2, z, z_1) \sim (2\kappa)^{-3}\log|z_2 - z|^2\frac{4i\bar{z}}{\bar{z} - \bar{z}_1}\langle 0|\partial^m\eta^2(z_2)...\partial\eta^2(z_2) :\eta^2\pi^2(z): \partial\eta^1(z_1)...\partial^m\eta^1(z_1)|0\rangle$$

$$+ (2\kappa)^{-3}\log|z_1 - z|^2\frac{4i\bar{z}}{\bar{z} - \bar{z}_2}\langle 0|\partial^m\eta^2(z_2)...\partial\eta^2(z_2) :\eta^1\pi^1(z): \partial\eta^1(z_1)...\partial^m\eta^1(z_1)|0\rangle$$

$$(3.107)$$

Contracting the remaining fields in the normal order, one gets

$$\langle 0|\partial^m\eta^2(z_2)...\partial\eta^2(z_2) :\eta^2\pi^2(z): \partial\eta^1(z_1)...\partial^m\eta^1(z_1)|0\rangle$$

$$= \sum_{k,p=1}^{m}(-1)^{k+p+1}\langle 0|\partial^k\eta^2(z_2)\pi^2(z)|0\rangle\langle 0|\eta^2(z)\partial^p\eta^1(z_1)|0\rangle\langle 0|\prod_{a=1,\neq k}^{m}\partial^a\eta^2(z_2)\prod_{b=1,\neq q}^{m}\partial^b\eta^1(z_1)|0\rangle$$

$$= -\sum_{k,p=1}^{m}\frac{iz}{2}\frac{k!(p-1)!(2\kappa)^{-m}}{(z_2 - z)^{k+1}(z_1 - z)^p(z_2 - z_1)^{m(m+1)-k-p}}\det((-1)^{a-1}(a+b-1)!)_{a\neq k,b\neq q}$$

$$(3.108)$$

Denote H_m the $m \times m$ matrix whose (a, b) coefficient is $(-1)^{a-1}(a+b-1)!$. Using the relation between the adjugate matrix $\mathrm{adj}H_m$ and its inverse, $\mathrm{adj}H_m = (H_m^{-1})^t\det H_m$, we have

$$G_{\phi_m}(z_2, z, z_1) \sim (2\kappa)^{-m-3}\frac{|z|^2\log|z_2 - z|^2}{|z - z_1|^2}2\det H_m\sum_{k,p=1}^{m}\frac{(-1)^{k+p}k!(p-1)!(H_m^{-1})_{p,k}}{(z_2 - z)^{k+1}(z_1 - z)^{p-1}(z_2 - z_1)^{m(m+1)-k-p}}$$

$$+ (z_1 \to z_2, \quad z_2 \to z_1)$$

$$(3.109)$$

This is the full dominant terms in the 3-point function. As already said, formula (3.85) also counts a sub-dominant term in the 3-point function that is obtained by taking the regularized part of the potential. This term is

$$\langle 0|\partial^m\eta^2(z_1)...\eta^2(z_2) :\eta^1\pi^1: (z)\eta^1(z_1)...\partial^m\eta^1(z_1)|0\rangle$$
$$\sim \log|z_2 - z|^2\langle 0|\partial^m\eta^2(z_1)...\eta^2(z_2)\pi^1(z)\eta^1(z_1)...\partial^m\eta^1(z_1)|0\rangle$$

$$(3.110)$$

If one contracts $\pi^1(z)$ with a $\partial^k\eta^1(z_1)$, the resulting power of z_2 will be $-m(m+1)+k$ when the power of z is zero and $z_1 = 0$, and will contribute to formula (3.85) only if $k = 0$. Thus the only term that counts is $(2\kappa)^{-m-3}\log|z - z_2|^2\langle\pi^1(z)\eta^1(z_1)\rangle\det H_m(z_2 - z_1)^{-m(m+1)}$. It contributes to -1 to $\delta\hat{e}$.

To apply now formula (3.85) to the 3-point function (3.109), let us expand

$$\frac{(-1)^{k+p}k!(p-1)!(H_m^{-1})_{p,k}}{(z_2 - z)^{k+1}(0 - z)^{p-1}(z_2 - 0)^{m(m+1)-k-p}}$$

$$= (-1)^{k-1}k!(p-1)!(H_m^{-1})_{p,k}z^{1-p}z_2^{-m(m+1)+p-1}\sum_{q\geq 0}\frac{(k+q)!}{k!q!}(z/z_2)^q$$

$$(3.111)$$

Only $q = p - 1$ contributes to $\delta\hat{e}$. This gives

$$
\begin{aligned}
\delta\hat{e} &= -1 - \frac{1}{2}\sum_{k,p=1}^{m}(-1)^{k-1}(k+p-1)!(H_m^{-1})_{p,k} \\
&= -1 - \frac{1}{2}\sum_{k,p=1}^{m}(H_m)_{k,p}(H_m^{-1})_{p,k} \\
&= -1 - \frac{1}{2}\operatorname{tr}H_m H_m^{-1}
\end{aligned}
\tag{3.112}
$$

hence

$$
\delta\hat{e} = -1 - \frac{m}{2}
\tag{3.113}
$$

recovering the previously derived correction (3.74).

Conclusion

We conclude that in case of non-quasi-primary fields the relation between the logarithmic corrections to the energy levels and the three-point function is more involved than in [92]. In particular the three-point function exhibits m^2 many equally dominant terms (i.e. with the same total divergence power, see (3.109)), that all contribute to the scaled gap. It moreover involves sub-dominant terms that contribute to the energy (although in a way independent from the magnetization).

3.3 $OSp(2|2)$

3.3.1   The spectrum from field theory

The action

For the $osp(2|2)$ case the constraint (3.11) can be satisfied by setting

$$
\phi_1 = (1 - \eta^2\eta^1)\cos\phi, \quad \phi_2 = (1 - \eta^2\eta^1)\sin\phi
\tag{3.114}
$$

so that the action reads

$$
S = \frac{\kappa}{2\pi g}\int dx dt \left(\frac{1}{2}\partial_\mu\phi\partial_\mu\phi + \partial_\mu\eta^2\partial_\mu\eta^1 - \eta^1\eta^2\partial_\mu\eta^1\partial_\mu\eta^2 - \partial_\mu\phi\partial_\mu\phi\eta^2\eta^1\right)
\tag{3.115}
$$

Rescaling all the fields $\phi \to \sqrt{g}\phi$, $\eta^{1,2} \to \sqrt{g}\eta^{1,2}$ yields

$$
S = \frac{\kappa}{2\pi}\int dx dt \left(\frac{1}{2}\partial_\mu\phi\partial_\mu\phi + \partial_\mu\eta^2\partial_\mu\eta^1 - g\eta^1\eta^2\partial_\mu\eta^1\partial_\mu\eta^2 - g\partial_\mu\phi\partial_\mu\phi\eta^2\eta^1\right)
\tag{3.116}
$$

with here

$$
g = \frac{\kappa}{2\log L}
\tag{3.117}
$$

Note that the boson ϕ with original radius 2π becomes a boson with radius $2\pi/\sqrt{g}$.

The normally ordered Hamiltonian

To find the Hamiltonian, we write the action as

$$S = \frac{\kappa}{2\pi} \int dx dt \left(-\partial_x \eta^2 \partial_x \eta^1 + \dot{\eta}^2 \dot{\eta}^1 - \frac{1}{2}(\partial_x \phi)^2 + \frac{1}{2}\dot{\phi}^2 + g\mathcal{V}(\eta^1, \eta^2, \phi) \right) \tag{3.118}$$

With the modes

$$\phi(x,t) = \sum_k \phi_k(t) e^{ikx} \tag{3.119}$$

it reads

$$S = \kappa \int dt \left(-k^2 \eta_k^2 \eta_{-k}^1 + \dot{\eta}_k^2 \dot{\eta}_{-k}^1 - \frac{1}{2}k^2 \phi_k \phi_{-k} + \frac{1}{2}\dot{\phi}_k \dot{\phi}_{-k} + gV \right) \tag{3.120}$$

The conjugate momentum to ϕ_k is

$$\pi_k^\phi = \kappa \dot{\phi}_{-k} + \kappa g \frac{dV}{d\dot{\phi}_k} \tag{3.121}$$

The quantization procedure imposes at equal times

$$[\phi_k, \pi_p^\phi] = i\delta_{k,p} \tag{3.122}$$

The Hamiltonian is then

$$H = \kappa k^2 \eta_k^2 \eta_{-k}^1 + \kappa^{-1} \pi_k^2 \pi_{-k}^1 + \frac{\kappa}{2}k^2 \phi_k \phi_{-k} + \frac{\kappa^{-1}}{2}\pi_k^\phi \pi_{-k}^\phi - \kappa g V \tag{3.123}$$

The $osp(2|2)$ charges are

$$J_z = \frac{\eta_k^1 \pi_k^1 - \eta_k^2 \pi_k^2}{2i}, \qquad J_+ = -i\eta_k^1 \pi_k^2, \qquad J_- = -i\eta_k^2 \pi_k^1$$
$$F_1 = \cos(\sqrt{g}\phi)_k(1 - g\eta_l^2 \eta_m^1)\pi_{-n}^2 - \sqrt{g}\eta_k^1 \sin(\sqrt{g}\phi)_l \pi_{-m}^\phi$$
$$F_2 = \sin(\sqrt{g}\phi)_k(1 - g\eta_l^2 \eta_m^1)\pi_{-n}^2 + \sqrt{g}\eta_k^1 \cos(\sqrt{g}\phi)_l \pi_{-m}^\phi$$
$$G_1 = \cos(\sqrt{g}\phi)_k(1 - g\eta_l^2 \eta_m^1)\pi_{-n}^1 + \sqrt{g}\eta_k^2 \sin(\sqrt{g}\phi)_l \pi_{-m}^\phi \tag{3.124}$$
$$G_2 = \sin(\sqrt{g}\phi)_k(1 - g\eta_l^2 \eta_m^1)\pi_{-n}^1 - \sqrt{g}\eta_k^2 \cos(\sqrt{g}\phi)_l \pi_{-m}^\phi$$
$$Q = \frac{1}{2}\pi_0^\phi$$

The temporal derivatives can be computed as in the $osp(1|2)$ case. For example at order g one has

$$\partial_t F_1 = \partial_t F_1^{osp(1|2)} + g\left(-\frac{\kappa}{2}\phi_k \phi_l \eta_m^1 m^2 - \kappa^{-1}\eta_k^1 \pi_{-l}^\phi \pi_{-m}^\phi + \kappa \eta_k^1 \phi_l \phi_m m^2 + \kappa \frac{dV_\phi}{d\eta_0^2} \right) \tag{3.125}$$

if one decomposes the potential V as $V = V^{osp(1|2)} + V_\phi$.

We now impose the following perturbation

$$\mathcal{V}(\eta^1, \eta^2, \phi) = (\partial_x \phi)^2 \eta^2 \eta^1 - (\partial_t \phi)^2 \eta^2 \eta^1 + \eta^2 \eta^1 \partial_x \eta^2 \partial_x \eta^1 - \eta^2 \eta^1 \partial_t \eta^2 \partial_t \eta^1 \qquad (3.126)$$

that gives

$$V = -kl\phi_k \phi_l \eta_m^2 \eta_n^1 - \kappa^{-2} \pi_{-k}^\phi \pi_{-l}^\phi \eta_m^2 \eta_n^1 - mn\eta_k^2 \eta_l^1 \eta_m^2 \eta_n^1 + \kappa^{-2} \eta_k^2 \eta_l^1 \pi_{-m}^1 \pi_{-n}^2 \qquad (3.127)$$

This ensures the conservation of the $osp(2|2)$ charges.

Define now the modes

$$a_k = \frac{-ik\phi_k \kappa^{1/2} + \pi_{-k}^\phi \kappa^{-1/2}}{\sqrt{2}}, \quad \bar{a}_k = \frac{-ik\phi_{-k}\kappa^{1/2} + \pi_k^\phi \kappa^{-1/2}}{\sqrt{2}} \qquad (3.128)$$

that satisfy

$$[a_k, a_{-k}] = k, \quad [\bar{a}_k, \bar{a}_{-k}] = k \qquad (3.129)$$

The former modes read

$$\phi_k = \frac{i}{k\sqrt{2\kappa}}(a_k - \bar{a}_{-k}), \quad \pi_k^\phi = \sqrt{\kappa/2}(a_k + \bar{a}_{-k}) \qquad (3.130)$$

and the potential can be rewritten

$$V = \frac{1}{2\kappa^2}\left(-i\sqrt{2\kappa}\eta_0^2 + \frac{\psi_k^2 - \bar{\psi}_{-k}^2}{k}\right)\left(-i\sqrt{2\kappa}\eta_0^1 + \frac{\psi_l^1 - \bar{\psi}_{-l}^1}{l}\right)(\psi_m^2 \bar{\psi}_{-n}^1 + \bar{\psi}_{-m}^2 \psi_n^1 + a_m \bar{a}_{-n} + \bar{a}_{-m} a_n) \qquad (3.131)$$

The bosonic part is already normally ordered, and the fermionic part is the same as in the $osp(1|2)$ case. Hence

$$V =:V: +i\kappa^{-2}(\eta_k^2 \pi_k^2 + \eta_k^1 \pi_k^1)\xi_0 \qquad (3.132)$$

The total Hamiltonian reads then

$$H = \frac{1}{2}\sum_{k<0}(a_k a_{-k} + \bar{a}_k \bar{a}_{-k}) + a_0^2 + \sum_{k<0}(\psi_k^2 \psi_{-k}^1 - \psi_{-k}^1 \psi_k^2 + \bar{\psi}_k^2 \bar{\psi}_{-k}^1 - \bar{\psi}_{-k}^1 \bar{\psi}_k^2) + 2\psi_0^2 \psi_0^1 - \frac{c}{12} - \kappa g :V:$$
$$- ig\kappa^{-1}(\eta_k^2 \pi_k^2 + \eta_k^1 \pi_k^1)\xi_0 \qquad (3.133)$$

Construction of the states

Once again derivatives $\partial_z \eta^1$ involve terms $(1 + g/2\eta_0^2 \eta_0^1)$, that vanish when a η^1 is already present in a state. The highest-weight state of J_z-charge $m + 1/2$ and Q_z-charge n is

$$|\cos(2n\sqrt{g}\phi)\eta^1 \partial \eta^1 ... \partial^m \eta^1 \bar{\partial} \eta^1 ... \bar{\partial}^m \eta^1\rangle = \cos(2n\sqrt{g}\phi_0)\eta_0^1 \psi_{-1}^1 ... \psi_{-m}^1 \bar{\psi}_{-1}^1 ... \bar{\psi}_{-m}^1 |0\rangle \qquad (3.134)$$

Regularization

As in the $osp(1|2)$ case, we need a regularization, i.e., fixing the value of ξ_0. In this case we did not write the $osp(2|2)$ charges in terms of their normally ordered version. They also would depend on the ξ's, and any value for the ξ's would give a Hamiltonian with the $osp(2|2)$ symmetry and with the classical non-linear sigma model as classical limit. In the $osp(1|2)$ case, the regularization that we chose corresponded to imposing that the charges are not modified by the normal order. Here we can impose a similar constraint by constraining $\eta_0^1|0\rangle$, $\eta_0^2|0\rangle$, $\cos(\sqrt{g}\phi_0)(1 - g\eta_0^2\eta_0^1)|0\rangle$ and $\sin(\sqrt{g}\phi_0)(1 - g\eta_0^2\eta_0^1)|0\rangle$ to belong to the same representation, and thus to have the same energy at order g. We have

$$H\eta_0^1|0\rangle = g\kappa^{-1}\xi_0\eta_0^1|0\rangle, \quad H\eta_0^2|0\rangle = g\kappa^{-1}\xi_0\eta_0^2|0\rangle \tag{3.135}$$

and

$$
\begin{aligned}
H\cos(\sqrt{g}\phi_0)(1 - g\eta_0^2\eta_0^1)|0\rangle &= \frac{1}{2\kappa}(g - 2g)\cos(\sqrt{g}\phi_0)(1 - g\eta_0^2\eta_0^1)|0\rangle \\
&= -\frac{\kappa^{-1}g}{2}\cos(\sqrt{g}\phi_0)(1 - g\eta_0^2\eta_0^1)|0\rangle
\end{aligned}
\tag{3.136}
$$

Thus we impose

$$\langle 0|\xi_0|0\rangle = -\frac{1}{2} \tag{3.137}$$

Corrections to the energy levels

As soon as the states involve bosons only through $\cos(2n\sqrt{g}\phi_0)$ the bosonic part of the potential (3.131) does not play any role at order g, and the fermionic part is the $osp(1|2)$ case. Only the unperturbed part of the Hamiltonian plays a role for the bosons at order g. Thus the bosonic and the fermionic part are actually decoupled at order g and the calculations for the fermionic part are identical to the $osp(1|2)$ case. With

$$a_0^2\cos(2n\sqrt{g}\phi_0)|0\rangle = 2\kappa^{-1}n^2g\cos(2n\sqrt{g}\phi_0)|0\rangle \tag{3.138}$$

we get

$$
\begin{aligned}
&H|\cos(2n\sqrt{g}\phi)\eta^1\partial\eta^1...\partial^m\eta^1\bar\partial\eta^1...\bar\partial^m\eta^1\rangle \\
&= (m(m+1) - (m(m+1) + \tfrac{1}{2} - 2n^2)\kappa^{-1}g)|\cos(2n\sqrt{g}\phi)\eta^1\partial\eta^1...\partial^m\eta^1\bar\partial\eta^1...\bar\partial^m\eta^1\rangle
\end{aligned}
\tag{3.139}
$$

hence

$$\boxed{\frac{L^2\Delta e_L}{2\pi v_F} = m(m+1) - (m(m+1) + \tfrac{1}{2} - 2n^2)\kappa^{-1}g} \tag{3.140}$$

Similarly for non-symmetric states $|\cos(2n\sqrt{g}\phi)\eta^1\partial\eta^1...\partial^m\eta^1\bar\partial\eta^1...\bar\partial^{\bar m}\eta^1\rangle$ one has

$$\frac{L^2\Delta e_L}{2\pi v_F} = \tfrac{m(m+1)}{2} + \tfrac{\bar m(\bar m+1)}{2} - (m\bar m + \tfrac{m+\bar m}{2} + \tfrac{1}{2} - 2n^2)\kappa^{-1}g \tag{3.141}$$

Density of critical exponents

The previous formula gives an infinite number of fields with the same conformal weight $h = m(m+1)$ when $L \to \infty$, thanks to the bosonic degree of freedom n. In finite size, the degenerescence is lifted with a $2\kappa^{-1}gn^2 = n^2/\log L$ and one actually sees a continuum of conformal weights starting from $m(m+1)$. The question is to find the number of states that are there between h and $h + dh$ in finite size L. Denote $C_L^m(h)$ the number of such states for magnetization m. This number is for large L

$$C_L^m(h) = \# \left\{ n \geq 0, h \leq \frac{n^2}{\log L} \leq h + dh \right\} \tag{3.142}$$

if we assume that the higher-order correction terms to the conformal dimensions behave as $n^k (\log L)^{-p}$ with $k < 2p$ (this is true in the XXX case for example, see [103]). $\#S$ denotes the number of elements in the set S. At first order in dh/h these n must satisfy

$$\sqrt{h \log L} \leq n \leq \sqrt{h \log L}(1 + \tfrac{dh}{2h}) \tag{3.143}$$

Hence:

$$C_L^m(h) = \frac{1}{2}\sqrt{\frac{\log L}{h}} dh + O(dh^2) \tag{3.144}$$

Introduce now the variable s by $h = s^2$. This gives the density of states $\rho^m(s)$ for the variable s for magnetization m

$$\rho^m(s) = 1 \tag{3.145}$$

in the sense that there are $\rho^m(s)\sqrt{\log L}ds$ states with magnetization m whose s is between s and $s + ds$ in size L. This is the dominant behaviour of the density as $L \to \infty$. The corrections in finite size may contain a more complicated behaviour such as the black hole CFT [104].

3.3.2 The spectrum from the spin chain

Bethe equations

In the $osp(2|2)$ case, typical irreducible representations are characterized by a pair of numbers q, j (and denoted $[q, j]$ in what follows) which are the eigenvalues of the generators Q_z and J_z on the highest-weight state. Here q can be any complex number, while $j = 0, 1/2, \ldots$. These representations have dimension $8j$ [105], and Casimir

$$\mathcal{C} = 2j^2 - 2q^2 \tag{3.146}$$

Note that in contrast with $osp(1|2)$, the tensor products of the $[0, 1/2]$ representations at each site of the chain involve not completely reducible representations. The simplest example of this is the tensor product of $[0, 1/2]$ with itself which is a direct sum of the eight-dimensional adjoint $[0, 1]$ and of an indecomposable mixing the atypical representations

$[\pm 1/2, 1/2]$ (both of dimension 3) and two copies of the identity $[0, 0]$. For example, the ground state in even sizes is 8 times degenerated, has a Bethe state with charges $Q_z = 1/2, J_z = 1/2$, and decomposes into $[1/2, 1/2]$, $[-1/2, 1/2]$ and two copies of the identity $[0, 0]$. The Bethe state with charges $Q_z = 3/2, J_z = 1/2$ belongs to a $8 \times \frac{1}{2} = 4$-dimensional irreducible representation $[3/2, 1/2] = (3/2, 1/2) \oplus (1, 0) \oplus (2, 0)$. Another Bethe state with charges $Q_z = -3/2, J_z = 1/2$ belongs to a similar 4-dimensional irreducible representation, making this energy level 8 times degenerated.

The $osp(2|2)$ spin chain is described by two families of roots λ_i and μ_i satisfying the Bethe equations [99, 106]

$$\left(\frac{\lambda_i + i/2}{\lambda_i - i/2}\right)^L = \prod_j \frac{\lambda_i - \mu_j + i}{\lambda_i - \mu_j - i}$$

$$\left(\frac{\mu_i + i/2}{\mu_i - i/2}\right)^L = \prod_j \frac{\mu_i - \lambda_j + i}{\mu_i - \lambda_j - i} \tag{3.147}$$

An eigenvalue of the Hamiltonian for one set of solutions $\lambda_1, ..., \lambda_{K_1}, \mu_1, ..., \mu_{K_2}$ to these equations is then

$$e_L = -\frac{1}{L} \sum_{i=1}^{K_1} \frac{1}{\lambda_i^2 + 1/4} - \frac{1}{L} \sum_{i=1}^{K_2} \frac{1}{\mu_i^2 + 1/4} \tag{3.148}$$

The spins j and q (ie, the eigenvalue of J_z and Q_z respectively) corresponding to a solution with $K_{1,2}$ roots λ_i, μ_i are given by

$$K_1 = L/2 - (j + q), \qquad K_2 = L/2 - (j - q) \tag{3.149}$$

Note that if another grading is chosen, i.e., another choice for the fermionic sign in (3.13), the Bethe equations would be different. As far as the eigenvalues are concerned, the two gradings are equivalent, see appendix A.1.

In the $osp(2|2)$ we observe that the Bethe states have same charges J_z and Q_z as the highest-weight state of the multiplet they belong to.

Root structure

On the lattice in even size L, the field $\cos(2n\sqrt{g}\phi_0)\eta^1\partial\eta^1...\partial^m\eta^1\bar{\partial}\eta^1...\partial^m\eta^1$ is obtained with $L/2 - (n+m+1/2)$ roots λ and $L/2 - (m-n+1/2)$ roots μ. They are real and symmetrically distributed. See Figure 3.3 for a plot of some root structures.

The gap computed previously for the ground state of the sector $Q_z = q$, $J_z = j$ reads, when $2j$ and q are integers with same parity:

$$\frac{L^2 \Delta e_L}{2\pi v_F} = j^2 - \frac{1}{4} - \left(j^2 - 2q^2 + \frac{1}{4}\right)\kappa^{-1}g \tag{3.150}$$

Like for $osp(1|2)$, we see that the vector representation is degenerate with the ground state in the limit $g \to 0$ since $j^2 - \frac{1}{4} = 0$ for $j = 1/2$. We also see that the order g corrections vanishes when $j = 1/2, q = \pm 1/2$: this is compatible with the fact that the corresponding
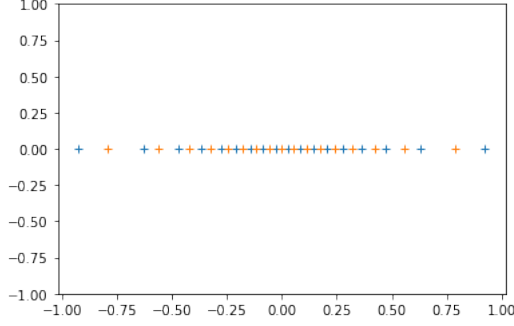
Figure 3.3: Bethe roots in the complex plane for the ground state (first family λ_i in blue, second family μ_i in orange), for $L = 36$.

representations are "mixed" with the identity in a bigger $osp(2|2)$ indecomposable representation.

Numerical results

We give numerical evidence in Figure 3.4 for the formula given in (3.139), with $Z_L^{q,j}$ denoting the measured $Z_L^{q,j} = (\frac{L^2}{2\pi v_F}(e_L - e_L^0) - (h + \bar{h})) \log L$ in finite size L for the state $[q, j]$. Here e_L^0 denotes the state $[-1/2, 1/2]$.

3.4 $OSp(3|2)$

3.4.1 The spectrum from the spin chain

The Bethe equations

Irreducible representations of $osp(3|2)$ are characterized by a pair of numbers q, j corresponding to the spin of the underlying $o(3)$ and $sp(2)$ bosonic sub-algebras. Here $q = 0, 1, \ldots$ is integer, and $j = 0, 1/2, \ldots$ is half-integer. The five-dimensional fundamental representation is $[0, 1/2]$ and the twelve-dimensional adjoint representation is $[0, 1]$. The (quadratic) Casimir eigenvalues are

$$\mathcal{C} = j(2j - 1) - \frac{1}{2}q(q + 1) \tag{3.151}$$

The $osp(3|2)$ spin chain is described by two families of roots ν_i and μ_i satisfying the

76

Figure 3.4: In reading direction: plots of $Z_L^{-3/2,3/2}$, $Z_L^{-5/2,5/2}$, $Z_L^{-1/2,5/2}$, $Z_L^{-3/2,7/2}$, $Z_L^{-5/2,1/2}$, $Z_L^{-9/2,1/2}$, as a function of $1/\log L$, together with their extrapolated curve with functions f_{12}, f_{12}, f_{10}, f_{10}, f_{12}, f_{10}. The theoretical results are, respectively, 1, 3, -3, -4, 6, 20.

Bethe equations [99, 91]

$$\left(\frac{\nu_i + i/2}{\nu_i - i/2}\right)^L = \prod_{j=1}^{K_2} \frac{\nu_i - \mu_j + i/2}{\nu_i - \mu_j - i/2}$$

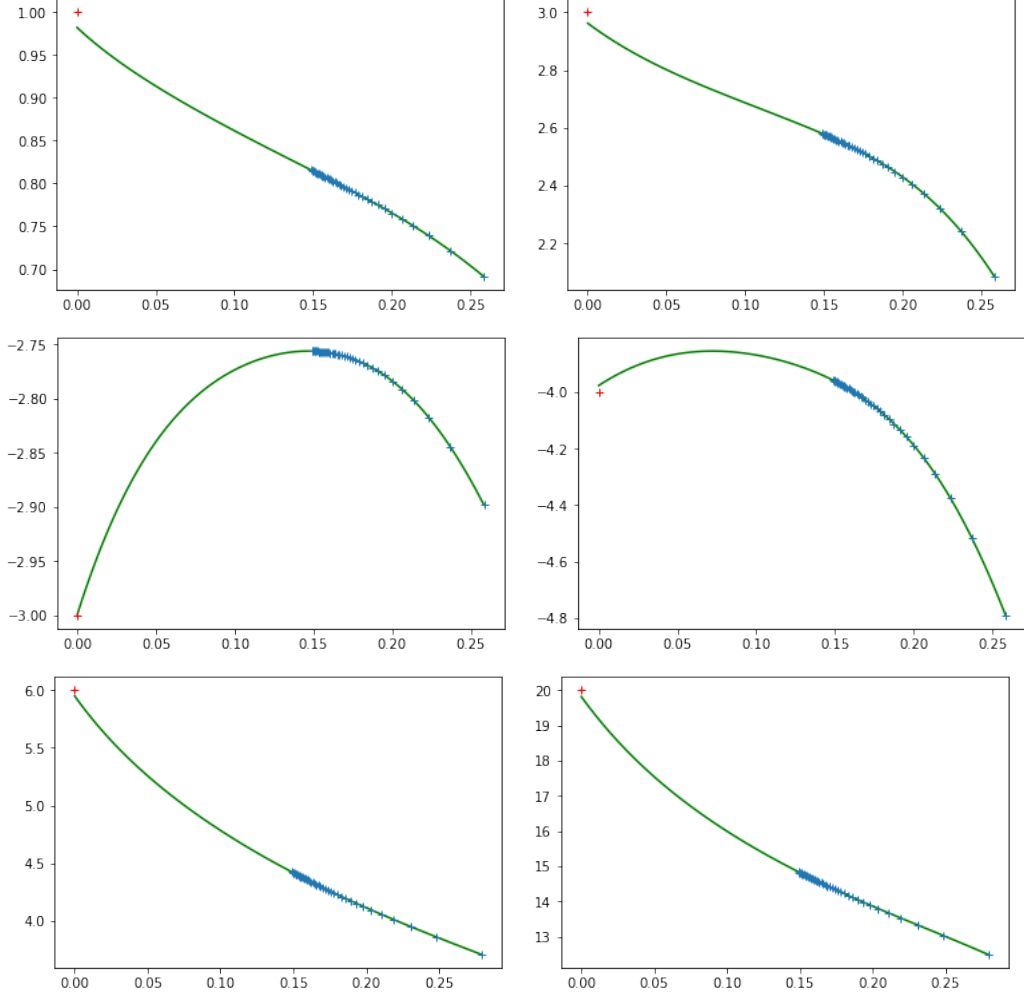$$1 = \prod_{j=1}^{K_1'} \frac{\mu_i - \nu_j + i/2}{\mu_i - \nu_j - i/2} \prod_{j \neq i} \frac{\mu_i - \mu_j - i/2}{\mu_i - \mu_j + i/2} \tag{3.152}$$

As already explained, the Bethe equations depend on the choice of the grading, see appendix A.1. It turns out that they are more convenient in another grading. We write λ_i and μ_i the roots of the Bethe equations in this second grading. They read

$$\left(\frac{\lambda_i + i/2}{\lambda_i - i/2}\right)^L = \prod_{j=1}^{K_2} \frac{\lambda_i - \mu_j + i/2}{\lambda_i - \mu_j - i/2}$$

$$1 = \prod_{j=1}^{K_1} \frac{\mu_i - \lambda_j + i/2}{\mu_i - \lambda_j - i/2} \prod_{j \neq i} \frac{\mu_i - \mu_j + i/2}{\mu_i - \mu_j - i/2} \cdot \frac{\mu_i - \mu_j - i}{\mu_i - \mu_j + i} \tag{3.153}$$

For each solution (ν_i, μ_i) of the equations in the first grading there exist a solution (λ_i, μ_i) of the equations in the second grading, and vice versa. The μ_i stay the same (as anticipated by the notation), and the roots λ_i and ν_i are related by the fact that together, they form all the roots of the following polynomial

$$P(X) = (X + i/2)^L \prod_{j=1}^{K_2} (X - \mu_j - i/2) - (X - i/2)^L \prod_{j=1}^{K_2} (X - \mu_j + i/2) \tag{3.154}$$

In the second grading an eigenvalue of the Hamiltonian is given by

$$e_L = \frac{1}{L} \sum_{i=1}^{K_1} \frac{1}{\lambda_i^2 + 1/4} \tag{3.155}$$

The spins j and q (ie, the eigenvalue of J_z and Q_z respectively) for a solution with K_1 roots λ_i and K_2 roots μ_i are related to M_1 and K_2 through

$$K_1 = L - q, \qquad K_2 = L - 2j - q \tag{3.156}$$

However an important remark has to be made. It is known that for the XXX spin chain, the Bethe vectors are highest-weight vectors with respect to J_z, meaning that they are annihilated by the total J_+. It turns out that it is not the case for $osp(3|2)$: some Bethe vectors are indeed annihilated by the raising operators of the $sp(2)$ and $o(3)$ subalgebras, but not by the raising operators of the full $osp(3|2)$ algebra. To see this, one can go to the q-deformed version where most of the $osp(3|2)$ degeneracies are lifted. In this case there are states with similar root structure as in the $q = 1$ undeformed case, but with additional roots

with imaginary part $i\pi/2$. When $q \to 1$, the energy of theses states converge to the same multiplet with the same energy in finite size, since the extra roots at $i\pi/2$ have no effect in this limit. For example there is one state at $q \neq 1$ that has one extra root $\lambda_1 = i\pi/2$ compared to the $q = 1$ case, that falls into the multiplet when $q \to 1$. In its multiplet at $q \neq 1$ there is the state that becomes annihilated by all the raising operators of $osp(3|2)$ when $q \to 1$, which is the highest-weight state. The important point is that the charges of this state with an extra root has a Q_z decreased by 1 and a J_z increased by $1/2$ compared to the state that can be built with the Bethe ansatz at $q = 1$. Therefore the charge of the multiplet of the Bethe vector has actually a Q_z decreased by 1 and a J_z increased by $1/2$. This is important for the bosonic part of logarithmic corrections to match the value of the Casimir, but it will also be important in section 3.5.4.

This created some confusion in [91]. To make contact with their[2] notations $(p_{\mathrm{FM}}, q_{\mathrm{FM}})$ for labelling the Bethe states (but not the multiplets), we have $p_{\mathrm{FM}} = 2j$ and $q_{\mathrm{FM}} = q/2$. As for the notations $(p_{\mathrm{VdJ}}, q_{\mathrm{VdJ}})$ in [107], we have $p_{\mathrm{VdJ}} = q$ and $q_{\mathrm{VdJ}} = j$.

For example the first excited state belongs to a 12-dimensional multiplet and the Bethe state has charges $(Q_z, J_z) = (2, 0)$. In [91] it was interpreted as the irreducible representation $q_{\mathrm{VdJ}} = 1, p_{\mathrm{VdJ}} = 0$ of dimension 12 in [107], whereas it is actually the irreducible representation $q_{\mathrm{VdJ}} = 1/2, p_{\mathrm{VdJ}} = 1$ of dimension 12 as well. It is a reducible representation for $o(3) \otimes sp(2)$ that reads $(1, 1/2) \oplus (0, 0) \oplus (2, 0)$ in terms of Q_z, J_z. Only the state with $(Q_z, J_z) = (1, 1/2)$ is annihilated by the raising operators of the whole $osp(3|2)$ algebra.

Root structure

A particular feature of this model is that the energy of the ground state e_L^0 is independent of L. In terms of Bethe roots it is given by L coinciding roots μ at zero, see [91]. Note that in the $O(1)$ model a similar phenomenon inspired the Razumov-Stroganov conjecture concerning the entries of the eigenvector associated to this particular eigenvalue [108, 109].

The first state whose Bethe state has charges j integer and q even is given on the lattice in the second grading by $L/2 - (q/2 + j)$ strings composed of 2 roots λ_i whose imaginary part is approximately $\pm 3/4$ and 2 roots μ_i whose imaginary part is approximately $\pm 1/4$, plus $2j$ real roots λ_i taking a large value, lying outside the strings. This is illustrated in Figure 3.5.

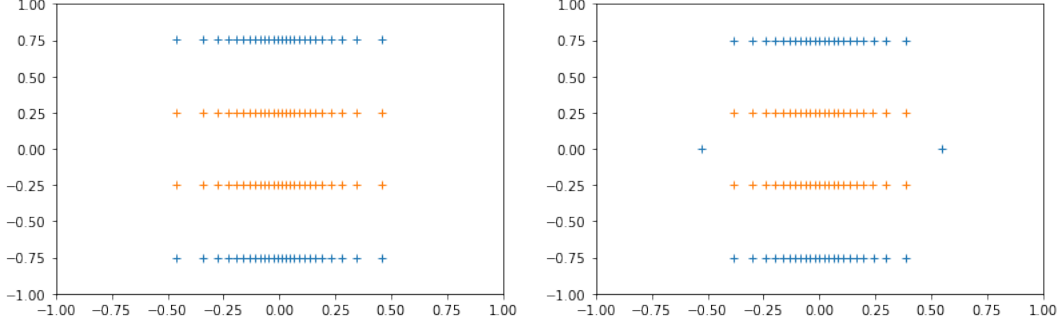
[2]The subscripts are the author's initials [91, 107].

Figure 3.5: Bethe roots in the complex plane for the states $j = 0, q = 2$ (left) and $j = 1, q = 2$ (right), for $L = 54$.

The presence of strings is a complication, both numerically and analytically. The typical deviation of their imaginary part from $\pm i/4$ or $\pm 3i/4$ is observed to behave as $\log L/L$ with the size of the system.

Numerical results

We observe numerically the following behaviour at large L, in terms of the charges j and q in (3.156) *of the Bethe states*

$$\frac{L^2 \Delta e_L}{2\pi v_F} = j(j+1) - \left(j(j+1) - \frac{1}{2}q(q-1) \right) \kappa^{-1} g \qquad (3.157)$$

In terms of the charges j and q *of the multiplet* it belongs to, it reads

$$\boxed{\frac{L^2 \Delta e_L}{2\pi v_F} = j^2 - \frac{1}{4} - \left(j^2 - \frac{1}{4} - \frac{1}{2}q(q+1) \right) \kappa^{-1} g} \qquad (3.158)$$

The bosonic part corresponds to the Casimir (3.151), but not the fermionic part.

Here we see the importance of considering the charges of the multiplet and not those of the Bethe state. To our knowledge it has not been noticed before for this model. It is observed only for $osp(3|2)$ and not $osp(1|2)$ nor $osp(2|2)$, and in some other spin chains with Lie superalgebra symmetry their highest-weight property has been proven [28], suggesting that it is peculiarity of this model rather than a common feature. However one can ask if this also happens in the higher-rank superalgebras studied numerically in [90]. From our experience it seems that studying the q-deformed version of the spin chain helps understanding these aspects: most of the $osp(3|2)$ degeneracies are then lifted and more Bethe states can be built that fall into a same multiplet as $q \to 1$; but with different charges, and in particular with higher J_z charge than that of the only Bethe state that can be built at $q = 1$.

In Figure 3.6 are shown the numerical verifications of formula (3.157), where $Z_L^{j;q}$ denotes the measured $Z_L^{j;q} = (\frac{L^2}{2\pi v_F}(e_L - e_L^0) - (h + \bar{h})) \log L$ in finite size L for the state whose Bethe state has $J_z = j$, $Q_z = q$, where e_L^0 is the reference state $j, q = 0, 0$.
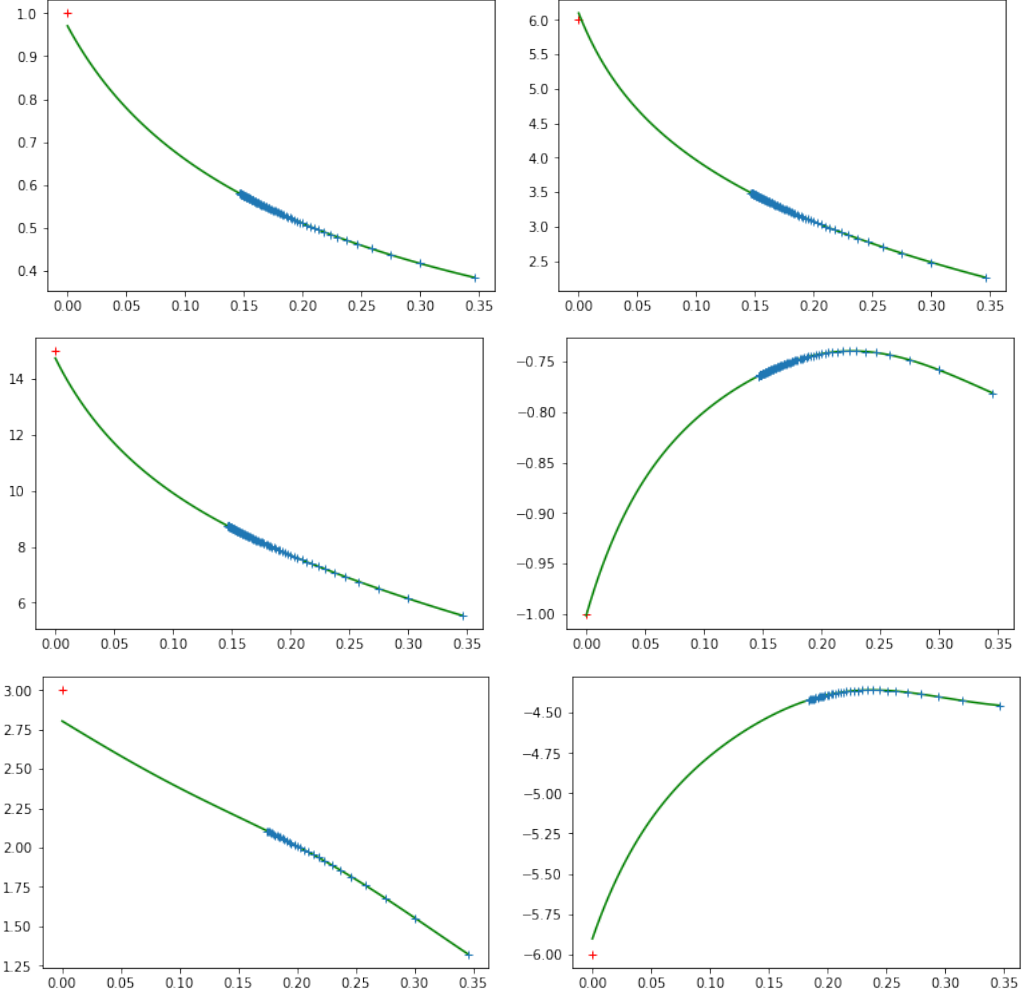
Figure 3.6: In reading direction: plots of $Z_L^{0,2}$, $Z_L^{0,4}$, $Z_L^{0,6}$, $Z_L^{1,2}$, $Z_L^{1,4} - Z_L^{0,2}$, $Z_L^{2,2} - Z_L^{0,2}$, as a function of $1/\log L$, together with their extrapolated curve with functions f_8, f_8, f_8, f_5, f_5, f_8. The theoretical results are, respectively, 1, 6, 15, -1, 3, -6.

3.5 Physical properties of fully packed trails

This section is devoted to the application of the previous energy calculations to 'watermelon' exponents in intersecting loops, also called fully packed trails.

We begin with some results on the $osp(r|2s)$ spin chains by showing that they describe intersecting loop soups with loop weight $N = r - 2s$ [85]. We then show for the first time that the spectrum of the $osp(r|2s)$ model is exactly included—in finite-size—in the spectrum of all the $osp(r+p|2s+p)$ models, as observed but not understood nor proved in [90]. We finally establish a correspondence between sectors of fixed charges and specific properties of loop configurations. This enables us to compute some watermelon 2-point functions that exhibits logarithmic behavior, which is the main new result of this section.

3.5.1 A model for loops with crossings

Let us first explain why the $osp(r|2s)$ vertex model can be reformulated as a model for intersecting loops with weight $N = r - 2s$. The mere observation that the R-matrix (3.17) is built from elements of the Brauer algebra [85, 110] is a bit unsatisfactory, since it does not explain how to treat the boundary conditions and the special weight that comes with them, and also because in this context the role of the graded tensor product is not clear.

In this section we prove the equivalence of the $osp(r|2s)$ model with a model of intersecting loops, starting directly from the expression of the transfer matrix (3.15), where from (3.17)

$$R(\lambda)_{ik}^{lj} = \lambda \delta_{ij}\delta_{kl} + (-1)^{p_i p_j}\delta_{il}\delta_{jk} + \frac{2\lambda}{2 - r + 2s - 2\lambda}(-1)^{i>r+s}(-1)^{j\leq s}\delta_{ik'}\delta_{jl'} \qquad (3.159)$$

We recall the definition of the conjugate index, $i' = D + 1 - i$, for any $i = 1, \ldots, D$ with $D = r + 2s$. We will work at constant spectral parameter λ and will sometimes omit the dependence on λ in order to simplify the notations. Define the partition function Z of this model on an $L \times M$ lattice as

$$Z = \operatorname{tr}(t(\lambda)^M) \qquad (3.160)$$

where $t(\lambda)$ is the transfer matrix given by (3.14)–(3.15). It is thus

$$Z = \sum_{c:,\alpha:=1}^{D} \prod_{m=1}^{M} R_{c_1^m \alpha_L^m}^{\alpha_L^{m+1}c_L^m} R_{c_L^m \alpha_{L-1}^m}^{\alpha_{L-1}^{m+1}c_{L-1}^m} \ldots R_{c_2^m \alpha_1^m}^{\alpha_1^{m+1}c_1^m} (-1)^{p_{c_1^m}} (-1)^{\sum_{j=2}^{L}(p_{\alpha_j^m}+p_{\alpha_j^{m+1}})\sum_{i=1}^{j-1} p_{\alpha_i^m}} \qquad (3.161)$$

with the identification $M + 1 \equiv 1$ due to periodic boundary conditions. We will use the same convention as in Figure 2.1 for the graphical depiction of each R term. The three terms in the R-matrix are generators of the Brauer algebra [85, 110] and can be represented diagrammatically as in Figure 3.7.
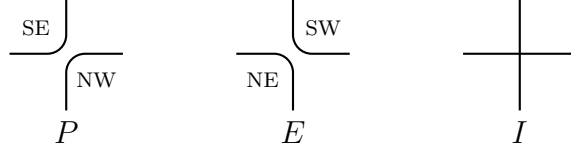
Figure 3.7: Graphical representation of the three possible ways to match the four indices, corresponding to the three generators of (3.17).

The graphical representation of Figure 3.7 naturally induces a representation of the partition function as a sum over dense intersecting loops, each vertical (resp. horizontal) edge carrying an index α (resp. c). In this representation L is the horizontal length, and M the vertical height of the $L \times M$ lattice.

There are three issues to be resolved in order to define a proper model of intersecting loops:

1. There are all the fermionic signs that seem to weigh each configuration with an arbitrary sign.

2. The loops are not all equivalent since they carry an index $i = 1, \ldots, D$ that must eventually be summed over. Moreover this index changes to its conjugate value along a loop at the SE and NW corners.

3. The weight of each fixed-index loop is one, but the proper weight after summation over the index will have to be worked out by taking carefully into account the boundary conditions.

All these issues are of course related, and analysing them properly will lead to the resolution of the problem. The crux resides in a proper understanding of the fermionic signs. This relies on the following lemma, the proof of which is relegated to Appendix A.2.

Lemma 4. *If the index a of a loop in a configuration is changed so that p_a changes, all other things being equal, then the weight of the configuration is multiplied by $(-1)^{b_v+1}$ where b_v is the number of times the loop crosses the top and bottom boundaries (i.e., those corresponding to the direction of length M).*

Proof. See Appendix A.2. □

One sees that the number of times a boundary is crossed in the vertical or horizontal directions plays a different role. We will say that a loop is *non-contractible* in the vertical direction (or simply non-contractible loop) if it crosses the whole lattice in the vertical direction, i.e. if it is possible to follow the loop from top to bottom without crossing the vertical boundary conditions. We say that a loop is contractible if it is not non-contractible. We will denote by *even/odd non-contractible* a non-contractible loop that crosses the top and bottom boundaries an even/odd number of times (without saying anything about the

right and left boundaries). In the subsequent subsections we will also represent by a diagram like ⊔⊔ or ⋊ the sum of all configurations of loops which possess a certain number of non-contractible loops linked from top to bottom as indicated by the diagram. We refer the reader to Figure 3.8 for illustrative examples on a 2×2 lattice with periodic boundary conditions.

From this lemma comes the theorem:

Theorem 2 (Intersecting loop soup model). $Z = tr(t^M)$ *is the partition function for a model of intersecting loops with loop weight $r - 2s$ for contractible loops and $r \pm 2s$ for odd/even non-contractible loops.*

Proof. If a configuration contains only loops with bosonic indices, all the $(-1)^{p_a}$ are $+1$ and the weight for a loop (with an index) is $+1$. But if a loop l is contractible, because of lemma 4 its weight is 1 if it is bosonic and -1 if it is fermionic, thus after summation over the indices the weight is $r - 2s$. If the loop is non-contractible the fermionic weight is ± 1 if it is odd/even, thus a weight $r \pm 2s$ after summation. $\square$

We note that if the transfer matrix were defined as the trace (and not the supertrace) of the monodromy matrix, i.e. if in (3.14) there were no $(-1)^{p_i}$, then one would have a weight $r + 2s$ for the odd non-contractible loops in the horizontal direction as well. On the contrary, to give the same weight $r - 2s$ to all the loops (contractible or not), one would need to modify the trace in (3.160) and define $Z = tr(K_L t^M)$ with K_L a matrix that will assign the desired weights according to the sector, as already explained in Section 2.3.1.
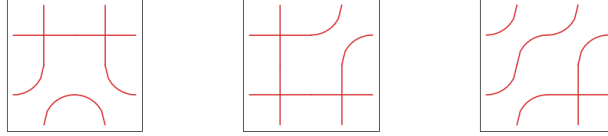
Figure 3.8: First figure: two contractible loops. Indeed, you cannot follow any of the two loops from top to bottom without crossing the vertical periodic boundary. Second figure: two odd non-contractible loops, and one contractible loop. Indeed, the horizontal line at the bottom is a contractible loop, and the two other loops are non-contractible and cross the vertical periodic boundary exactly once. Third figure: one even non-contractible loop. Indeed, there is only one loop that crosses the vertical periodic boundary twice.

If we now denote with a diagram like ⊔⊔ the connections between the four beginnings of strands ● at the top and the bottom of the lattice, then the strands in the first figure are connected like ⋮⋮ , in the second figure like ⊔⊔ , and in the last figure like ⋊ .

3.5.2 Inclusion of *osp* spectra

To prove the inclusion of the spectra for the *osp* chains, another lemma is needed:

Lemma 5. *If A and M are square matrices of size n and $n + m$ such that*

$$\forall k \in \mathbb{N}, \quad \forall i, j \in \{1, ..., n\}, \quad (M^k)_{i,j} = (A^k)_{i,j} \tag{3.162}$$

then the spectrum of A is included in the spectrum of M (with the degeneracies).

Proof. Writing M in block form

$$M = \begin{pmatrix} A & B \\ C & D \end{pmatrix} \tag{3.163}$$

the condition (3.162) implies

$$\forall k \in \mathbb{N}, \quad BD^kC = 0 \tag{3.164}$$

Let now $\lambda \in \mathbb{C}$ not in the spectrum of D. Since $D - \lambda I_m$ is invertible one can use Schur's complement to write

$$\det(M - \lambda I_{n+m}) = \det(A - \lambda I_n - B(D - \lambda I_m)^{-1}C) \det(D - \lambda I_m) \tag{3.165}$$

From Cayley-Hamilton theorem, $(D - \lambda I_m)^{-1}$ is a polynomial in $(D - \lambda I_m)$, thus in D, so that with (3.164) we have $B(D - \lambda I_m)^{-1}C = 0$. It follows that

$$\det(M - \lambda I_{n+m}) = \det(A - \lambda I_n) \det(D - \lambda I_m) \tag{3.166}$$

Since the function $\lambda \to \det(M - \lambda I_{n+m})$ is continuous in λ and since the spectrum of D is finite, the previous equation is true for all $\lambda \in \mathbb{C}$. Thus whenever λ is an eigenvalue of A, $\det(M - \lambda I_{n+m}) = 0$ and it is also an eigenvalue of M. Moreover since $\det(D - \lambda I_m)$ is a polynomial in λ there cannot be poles and the eigenvalues of A in the spectrum of M have at least the degeneracies they have in the spectrum of A. (However in general the eigenvectors of M corresponding to the eigenvalues of A cannot be expressed simply: in particular they may have non-zero i-th components for $i > n$.) $\qquad \square$

One can now prove the theorem:

Theorem 3 (Inclusion of spectra). *The spectrum of the $osp(r|2s)$ spin chain is included in finite size in the spectrum of the $osp(r + p|2s + p)$ spin chain for all even $p > 0$.*

Proof. Denote t the transfer matrix of the $osp(r|2s)$ spin chain, and T the one of the $osp(r + p|2s + p)$ spin chain. Let J be a subset of $2p$ indices among which p are bosonic and p are fermionic, and $I = \{1, ..., r + 2s + 2p\} \setminus J$. The indices of t are identified with I.
$(T^M)^{\alpha_1^{M+1}...\alpha_L^{M+1}}_{\alpha_1^1...\alpha_L^1}$ is the partition function of the model on a $L \times M$ lattice with fixed boundary conditions at the top and bottom boundaries. Inside the configuration, every loop whose index is in J has to be contractible, since at the up and down boundaries the indices must be in I. As J contains as many bosonic as fermionic indices, lemma 4 implies that these configurations add up to zero. Therefore all the loops can be considered having their indices in I, which is exactly $(t^M)^{\alpha_1^{M+1}...\alpha_L^{M+1}}_{\alpha_1^1...\alpha_L^1}$. Then lemma 5 applies and proves the theorem. $\qquad \square$

Note that taking the supertrace of the monodromy matrix is crucial to have this property. Otherwise the non-contractible loops in the horizontal direction would not cancel out. Notice also that integrability does not play any role here, so it is true for arbitrary weights in the R-matrix. Recall that such an inclusion is observed for $gl(r|s)$ models as well [111].

3.5.3 Charges and loop configurations

While most of our discussion about critical exponents has been based on studies of the integrable Hamiltonian, it is usually the case that the same universal properties would be obtained by focussing instead on the transfer matrix. Indeed, taking the Hamiltonian limit amounts to taking the continuum limit in the (imaginary) time direction, something that is not supposed to modify the continuum description of the lattice model. The transfer matrix language is on the other hand more natural to describe loops, especially when the spectral parameter $\lambda = 1$, corresponding to an *isotropic* loop soup on the square lattice. We have checked that the log of the largest eigenvalues of the transfer matrix have the same behaviour as those of the Hamiltonian, simply with the Fermi velocity v_F replaced by a sound velocity $\sin(\lambda v_F)$, that is 1 at the isotropic point.

This means that the finite-size corrections to the first excited states of the Hamiltonian, among which are the lowest eigenvalues in a sector imposing specific values of charges, correspond in the transfer matrix point of view to finite-size corrections to the largest eigenvalues of the transfer matrix t in a sub vector space with specific values of charges. We recall that the partition function in (3.160) is given by the trace of the M-th power of $t = t(\lambda)$ the transfer matrix, that is dominated when $M \to \infty$ by the largest eigenvalue of t. Similarly, the trace of the M-th power of t over a sub vector space where the charges take specific values, is dominated by the largest eigenvalue of t in this sub vector space.

The question is now to understand the kind of constraint that is imposed on the intersecting loop soup when this trace over a sub vector space where the charges take specific values is performed.

Let us treat the case of $osp(2|2)$, the simplest example with a 'fermionic charge' J_z and a 'bosonic charge' Q_z. In the grading given by (3.13), they are represented by

$$2J_z = \begin{pmatrix} 1 & 0 & 0 & 0 \\ 0 & 0 & 0 & 0 \\ 0 & 0 & 0 & 0 \\ 0 & 0 & 0 & -1 \end{pmatrix} , \quad 2Q_z = \begin{pmatrix} 0 & 0 & 0 & 0 \\ 0 & 1 & 0 & 0 \\ 0 & 0 & -1 & 0 \\ 0 & 0 & 0 & 0 \end{pmatrix} \tag{3.167}$$

When one traces over the vector space where Q_z is equal to q, one considers only the configurations where at the bottom (and at the top) of the lattice, there are $2q$ more strands with index 2 than strands with index 3. As already said, along a loop an index i is replaced by its conjugate i' (i.e., $1 \leftrightarrow 4$, $2 \leftrightarrow 3$) every time a NW or SE corner is encountered. It implies that a strand carrying a 2 at the bottom cannot directly (without crossing the vertical boundary) join another strand carrying a 2 at the bottom. Then the $2q$ extra 2's at the bottom and at the top of the lattice have to be connected between themselves by going through the whole lattice in the vertical direction. Since the loops with bosonic index (whether contractible or not) are always given the same weight equal to 1, it follows, after summing over the indices, that the boundary condition imposes to have (at least) $2q$ loops that propagate through the lattice in the vertical direction that are given weight 1. Note that an extra strand with index 2 at the bottom can be connected to any extra strand with index 2 at the top, with the same weight 1. For $2q = 2$ these configurations are $\text{⫼} + \text{⤬}$.

If one traces over the vector space where J_z is equal to j, the same reasoning shows that the configurations are constrained to have $2j$ more strands with index 1 than index 4 at the bottom, and that those at the top and the bottom of the lattice have to be connected between themselves. However since the index is fermionic, the weight of such a loop is 1 (resp. -1) if it crosses the top and bottom boundary an odd (resp. even) number of times, from lemma 4. The total weight given to these loops is then exactly the signature of the permutation that maps the bottom $2j$ extra 1's to the top $2j$ extra 1's they are connected to. For $2j = 2$ these configurations are $\text{II} - \text{X}$.

If one traces over the vector space where both J_z and Q_z are fixed as j and q respectively, then the configurations are constrained to possess $2j$ strands with index 1 and $2q$ strands with index 2 to propagate through the lattice from bottom to top. The total weight given to these loops is then the signature $\epsilon(\sigma_j)$ of the permutation σ_j that maps the bottom $2j$ extra 1's to the top $2j$ extra 1's they are connected to, without considering the $2q$ bosonic strands. Let us now denote $P_{L,M}(\sigma)$ the sum of all the configurations on a $L \times M$ lattice with $2j + 2q$ non-contractible strands, where the $2j$ 'fermionic' strands are at the left of the lattice at row 1, and where the $2j + 2q$ strands are permuted by σ at row M. Since a fermionic strand has to be connected to another fermionic strand through the periodic vertical boundary, this permutation has to be decomposable into $\sigma = \sigma_j \sigma_q$ where σ_j acts trivially on the bosonic strands and σ_q trivially on the fermionic strands. Then, denoting by $\text{tr}_{j,q}$ the trace over the sector $J_z = j, Q_z = q$, one can express the trace of the M-th power of the transfer matrix t as

$$\text{tr}_{j,q}(t^M) = \sum_{\sigma_j, \sigma_q} \epsilon(\sigma_j) Z_{L,M}(\sigma_j \sigma_q) \tag{3.168}$$

where the sum runs over the permutations σ_j and σ_q of $2j + 2q$ elements, that leave invariant the last $2q$ elements (respectively the first $2j$ elements). We recall that $\epsilon(\sigma_j)$ is the signature of the permutation σ_j. Here are some examples:

$$\text{tr}_{1,0}(t^M) = Z_{LM}((1\,2)) - Z_{LM}((2\,1))$$
$$\text{tr}_{0,1}(t^M) = Z_{LM}((1\,2)) + Z_{LM}((2\,1)) \tag{3.169}$$
$$\text{tr}_{1,1}(t^M) = Z_{LM}((1\,2\,3\,4)) - Z_{LM}((2\,1\,3\,4)) + Z_{LM}((1\,2\,4\,3)) - Z_{LM}((2\,1\,4\,3))$$

where we write $(i_1 \ldots i_n)$ the permutation that maps 1 onto i_1, etc, n onto i_n. The configuration of strands connections to which these three traces correspond are respectively $\text{II} - \text{X}$, $\text{II} + \text{X}$ and $\text{IIII} - \text{XII} + \text{IIX} - \text{XX}$.

Equation (3.168) is reminiscent of the Young symmetrizer for the Young tableau

$$
\begin{array}{c}
\boxed{1}\ldots\boxed{2q} \\
\boxed{1} \\
\ldots \\
\boxed{2j}
\end{array}
\tag{3.170}
$$

which here takes the form of a 'supertableau' applying independently a symmetrizer to the $2q$ bosonic strands and an antisymmetrizer to the $2j$ fermionic strands. Compared to the usual Young supertableux, e.g. in [112], there is an empty box at the top left merely because we shifted the first row, to make explicit the fact that each box must be counted either in the column or in the row.

An unpleasant aspect of formula (3.168) is that it depends on the position of the 'fermionic' strands, whereas we would like to have a geometrical meaning for strands without specifying their 'bosonic' or 'fermionic' nature. This important issue will be addressed in the next subsection.

These considerations can be generalized without difficulties to $osp(r|2s)$ for arbitrary r and s. There is only an additional important remark to make on the case r odd. Indeed in this case there is an index i which is not associated to any charge, for example for $osp(1|2)$ the index 2 does not affect the charge J_z. Then the number of extra strands associated to the charges can be odd (whereas in the case r even it is necessarily even): in this case for even L there will be one extra strand with this index i that acts as a bosonic strand with a weight 1. For odd L the same observation holds for an even number of strands associated to the charges.

3.5.4   Transfer matrix eigenvalues and loop configurations

On an $L \times M$ lattice with $M \to \infty$ the trace of the M-th power of the transfer matrix in size L over the vector space with given charges behaves as $\propto \lambda_1^M$ where λ_1 is the maximal eigenvalue of the transfer matrix in this sector. Denoting by λ_0 the maximal eigenvalue of the transfer matrix, the quantity $(\log \lambda_1 - \log \lambda_0)^{-1}$ gives the correlation length on an infinite cylinder of circumference L for the property of the configurations induced by the sector of λ_1.

In the limit $M \to \infty$ some remarks have to be made on (3.168). On an infinite cylinder there is no periodic boundary conditions to impose that a bosonic (resp. fermionic) strand falls back on a bosonic (resp. fermionic) strand, i.e. that bosonic and fermionic strands are permuted among themselves after a certain number of applications of the transfer matrix. In (3.168) for M large, imposing the decomposition $\sigma = \sigma_j \sigma_q$ instead of taking a generic permutation σ only changes a multiplicative factor that is independent of M, and thus does not affect the free energy that is in both cases $-\log \lambda_1$. Any permutation σ should be possible in (3.168) in this $M \to \infty$ limit, not only those that can be decomposed into $\sigma_j \sigma_q$. Thus on an infinite cylinder we have

$$e^{-MF_M(j,q)} = \sum_{\sigma \in \mathfrak{S}_{2j+2q}} \epsilon_{2j}(\sigma) \tilde{Z}_{L,M}(\sigma) \tag{3.171}$$

with $F_M(j,q) \to -\log \lambda_1$ when $M \to \infty$, and where $\tilde{Z}_{L,M}(\sigma)$ is the sum of all the configurations where $2j + 2q$ strands (with the $2j$ fermionic ones at the left at row 1) are permuted by σ after M rows, on a $L \times M$ lattice *without* periodic boundary condition in the M direction. $\epsilon_{2j}(\sigma)$ is the 'partial signature' of the first $2j$ elements of σ, i.e., attributes a factor -1 to

each (i_1, i_2) with $i_1 < i_2 \leq 2j$ such that $\sigma(i_1) > \sigma(i_2)$. The sum now runs over all the permutations σ of $2j + 2q$ elements.

For example, for $j = 1$, $q = 1/2$ there are three strands, with 2 'fermionic' strands at the left. It gives the configurations $|||$ $-$ $\rtimes|$ $+$ $|\ltimes$ $+$ $\bowtie$ $-$ $\bowtie$ $-$ $\bowtie$.

The advantage of (3.171) is that although the summands still depend on the initial position of the fermionic strands, it can be easily transformed into a version that does not distinguish between bosonic and fermionic strands, by summing over all $\binom{2j+2q}{2j}$ ways of attributing $2j$ fermionic and $2q$ bosonic labels to the $2j + 2q$ strands. The fermionic signs are then attributed as before. Thus one gets

$$e^{-M\tilde{F}_M(j,q)} = \sum_{\sigma \in \mathfrak{S}_{2j+2q}} \left(\binom{2j + 2q}{2j} - 2\iota_{2j}(\sigma) \right) \tilde{Z}_{L,M}(\sigma) \tag{3.172}$$

with $\tilde{F}_M(j, q) \to -\log \lambda_1$ when $M \to \infty$, and where $\iota_{2j}(\sigma)$ is the number of subsets of $2j$ strands among the $2j + 2q$ strands permuted by σ, that intersect between themselves an odd number of times. A formal mathematical definition of $\iota_{2j}(\sigma)$ is

$$\iota_{2j}(\sigma) = \#\left\{ I \subset \{1, ..., 2j + 2q\} \text{ such that } \#I = 2j \,, \text{and } \#\{(i,j) \in I^2 \,/\, i < j \,, \sigma(i) > \sigma(j)\} \text{ is odd} \right\} \tag{3.173}$$

Note that with this definition (3.172) no longer refers to bosonic/fermionic strands, but simply to a total number of $2j + 2q$ unspecified strands. Clearly, $\iota_0(\sigma) = \iota_1(\sigma) = 0$. Moreover, $\iota_2(\sigma)$ is exactly the total number of intersections between the strands (in a graphical representation where two strands intersect 0 or 1 time and do not wind around the horizontal periodic boundary). And $\iota_3(\sigma)$ is the total number of intersections between the strands, where each intersection between strands $i < j$ is weighted by $2j + 2q - |i - j| - |\sigma(i) - \sigma(j)|$.

For instance, one has the following correspondences on the *infinite* cylinder between the Young tableaux and the loop configurations:

$$\boxed{1\,2\,3} \longrightarrow |||\; +\; \rtimes|\; +\; |\ltimes\; +\; \bowtie\; +\; \bowtie\; +\; \bowtie \qquad (j = 0\,, q = 3/2)$$

$$\boxed{\begin{smallmatrix}1\\2\\3\end{smallmatrix}} \longrightarrow |||\; -\; \rtimes|\; -\; |\ltimes\; +\; \bowtie\; +\; \bowtie\; -\; \bowtie \qquad (j = 3/2\,, q = 0) \qquad (3.174)$$

$$\boxed{\begin{smallmatrix}1\\1\,\,\\2\end{smallmatrix}} \longrightarrow 3\,|||\; +\; \rtimes|\; +\; |\ltimes\; -\; \bowtie\; -\; \bowtie\; -\; 3\,\bowtie \qquad (j = 1\,, q = 1/2)$$

These combinations now refers to three generic strands, without the need to specify which ones are fermionic, contrarily to (3.171) where the different strands are either fermionic or bosonic.

Note that due to the horizontal periodic boundary, there can be a permutation between two strands without crossings. The fermionic signs also count these situations.

When the circumference of the cylinder itself becomes large, a conformal transformation onto the plane gives access to the critical exponents of the corresponding watermelon exponents on the plane. To use the Bethe ansatz to compute these corrections in large sizes L,

one needs to find which eigenvalue is maximal for each sector. A possible source of difficulty is that the sector associated to other conserved quantities in which this λ_1 lies may change with the size of the system. For example for $osp(1|2)$ the state with integer magnetization $j > 0$ with minimal energy in the thermodynamic limit does not have symmetric Bethe roots, but in small sizes nothing prevents the state with equal magnetization but with symmetric Bethe roots from having lower energy. The determination of the finite-size corrections to these states close to the thermodynamic limit nevertheless permits to determine which one is the lowest.

In the following, we explicitly check the correspondence between the constraint encoded by a tableau $\young(12\cdots2q,1,\vdots,2j)$ and the eigenvalue of the transfer matrix, with a numerical code for loops with crossings. That is, we start from an eigenvalue of the osp transfer matrix, find its Bethe roots, deduce the corresponding charges from them, and then compare to a numerical transfer matrix that implements (3.171) on an intersecting loop soup with fermionic/bosonic strands, and (3.172) on a generic intersecting loop soup, and verify that it gives exactly the same eigenvalue.

$osp(2|2)$ case

In Table 3.1 we give the explicit correspondence between some eigenvalues of the transfer matrix of the $osp(2|2)$ model in size $L = 6$, and the Bethe roots and the kind of constraints that it imposes on the loop configurations.

Eigenvalue	Bethe roots $\{\lambda\}, \{\mu\}$	J_z, Q_z	Constraint on the loops
167.295	$\{0.02897, -0.02897, 0\}, \{0.0180, -0.0180\}$	$1/2, 1/2$	no constraint, or (tableau)
95.732	$\{0.5992, -0.5992, 0.1471, -0.1471\}, \{0\}$	$1/2, 3/2$	(tableau)
63.761	$\{0.3281, -0.0286\}, \{0.3281, -0.0286\}$	$1, 0$	(tableau)
44.140	$\{-0.5774, -0.1355, 0.1584\}, \{-0.1182\}$	$1, 1$	(tableau)
29.63	$\{-0.147, 0.147\}, \{0\}$	$3/2, 1/2$	(tableau)
22.750	$\{0.8660, -0.8660, 0.2887, -0.2887, 0\}, \{\}$	$1/2, 5/2$	(tableau)
3.482	$\{-0.1340\}, \{-0.1340\}$	$2, 0$	(tableau)

Table 3.1: Correspondence between some transfer matrix eigenvalues, Bethe roots, charges, and loop configurations for the $osp(2|2)$ case in size $L = 6$ at the isotropic integrable point.

Note that the Bethe roots for integral charges are associated to non-symmetric states,

given in (3.141) with $\bar{m} = m - 1$. Note also that the equivalence between the absence of constraints and $\boxed{\begin{smallmatrix}&\boxed{1}\\\boxed{2}&\end{smallmatrix}}$ on the infinite cylinder is very specific to $osp(2|2)$ in even size where the weight of a loop is zero, since in both cases it amounts to forbidding the contraction between the two strands.

$osp(3|2)$ case

The same work can be done for $osp(3|2)$ where the weight for a (contractible) loop is 1. Here we notice the importance of the remark of section 3.4.1, that gives the true charges of the multiplet a Bethe vector belongs to, and that has direct consequences on the configurations of loops associated to it. The J_z and Q_z indicated in Table 3.2 are those of the highest-weight of the multiplet the Bethe vector belongs to (note that with the conventions of $osp(3|2)$, $Q_z = q$ imposes q bosonic strands and not $2q$).

Eigenvalue	Bethe roots $\{\lambda\}, \{\mu\}$	J_z, Q_z	Constraint on the loops
656.84	degenerate roots	0, 0	no constraint
584.97	$\{-0.14 \pm 0.75i, -0.14 \pm 0.75i, \pm 0.75i\},$ $\{-0.14 \pm 0.25i, -0.14 \pm 0.25i, \pm 0.25i\}$	1/2, 1	$\boxed{1}$ over $\boxed{1}$
323.40	$\{0.0645 \pm 0.7501i, -0.0645 \pm 0.7501i\},$ $\{0.0645 \pm 0.249i, -0.0645 \pm 0.249i\}$	1/2, 3	$\boxed{1}\boxed{2}\boxed{3}$ over $\boxed{1}$
175.96	$\{-0.555, -0.057 \pm 0.749i, 0.057 \pm 0.749i, 0.555\},$ $\{-0.057 \pm 0.249i, 0.057 \pm 0.249i\}$	3/2, 1	$\boxed{1}$; $\boxed{1}\boxed{2}\boxed{3}$ (column)
100.40	$\{\pm 0.7500i\},$ $\{\pm 0.2499i\}$	1/2, 5	$\boxed{1}\boxed{2}\boxed{3}\boxed{4}\boxed{5}$ over $\boxed{1}$
67.27	$\{-0.883, \pm 0.7500i, 0.883\},$ $\{\pm 0.2499i\}$	3/2, 3	$\boxed{1}\boxed{2}\boxed{3}$; $\boxed{1}\boxed{2}\boxed{3}$ (column)
19.39	$\{-0.883, -0.308, \pm 0.7500i, 0.308, 0.883\},$ $\{\pm 0.2499i\}$	5/2, 1	$\boxed{1}$; $\boxed{1}\boxed{2}\boxed{3}\boxed{4}\boxed{5}$ (column)

Table 3.2: Correspondence between some transfer matrix eigenvalues, Bethe roots, charges, and loop configurations for the $osp(3|2)$ case in size $L = 8$ at the isotropic integrable point.

$osp(1|2)$ case

The same exercise for $osp(1|2)$ is a bit formal since it gives a weight -1 to each contractible loop, that cannot be interpreted as a probability. However the correspondence between eigenvalues of the transfer matrix and specific configurations of loops still holds, see Table 3.3.

Eigenvalue	Bethe roots $\{\lambda\}$	J_z	Constraint on the loops
254.23	$\{-0.558, -0.227, 0, 0.227, 0.558\}$	$1/2$	☐^{1}(grey) / $\boxed{1}$
225.95	$\{-0.449, -0.126, 0.5i, -0.5i, 0.126, 0.449\}$	0	no constraint
95.23	$\{-0.616, -0.262, -0.028, 0.200\}$	1	$\boxed{1}$ $\boxed{2}$ (column)
44.54	$\{-0.233, 0, 0.233\}$	$3/2$	☐^{1}(grey) / $\boxed{1}$ $\boxed{2}$ $\boxed{3}$ (column)
7.59	$\{-0.265, -0.018\}$	2	$\boxed{1}$ $\boxed{2}$ $\boxed{3}$ $\boxed{4}$ (column)

Table 3.3: Correspondence between some transfer matrix eigenvalues, Bethe roots, charges, and loop configurations for the $osp(1|2)$ case in size $L = 6$ at the isotropic integrable point.

Tableaux with odd number of boxes would appear for odd sizes only. The fact that there is one 'bosonic' strand for half-integer spin (denoted by a grey box) is explained in the last paragraph of section 3.5.3.

Imposing a constraint can increase the 'partition function' only because some Boltzmann weights are negative in the $osp(1|2)$ case. Remark also that since there is only one fermionic charge in $osp(1|2)$, one cannot get configurations like $\boxed{1}\boxed{2}\boxed{3}\boxed{4}$ and we are almost restricted to purely determinant-like combinations of probabilities. This is reminiscent of the correlation functions for the spanning trees and forests model that also exhibits an $osp(1|2)$ symmetry [113, 36]. However these combinations should appear in the $osp(3|4)$ model.

3.5.5 Watermelon 2-point functions for loops with crossings

We here collect our results for the logarithmic scaling of two-point functions in fully-packed trails, or intersecting loop models.

In the geometry of the plane in the scaling limit, for a permutation $\sigma \in \mathfrak{S}_{n+m}$ of $n + m$ elements, we denote by $P_\sigma^{n+m}(x)$ the probability that $n + m$ strands emanate from some small neighborhood and come close together again in another small neighborhood, separated from the first one by a distance x, with their ordering having been permuted by σ in-between the two neighbourhoods, see Figure 3.9.
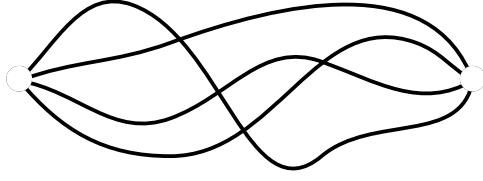
Figure 3.9: Example of a 4-legs watermelon 2 point function.

In this section we use all our previous results to determine the generalization of these power-law decays to the intersecting loop models. The same reasoning as in Section 2.4.4 of the first chapter can be used to translate an intersecting loops configurations on the plane such as Figure 3.9 to configurations of loops on the cylinder, where a certain number of strands propagate without forming loops, and undergoing a given permutation.

We saw that on the cylinder, the largest eigenvalue of the transfer matrix in a given sector is related to loop configurations through (3.172). Following this relation, we define the weight

$$W_\sigma^{n,m} = 1 - \frac{2\iota_m(\sigma)}{\binom{n+m}{m}} \tag{3.175}$$

which is merely the same weight as in (3.172) after a normalization. We recall that $\iota_m(\sigma)$ is the number of subsets of m strands among the $n + m$ strands that intersect between themselves an odd number of times (in a graphical representation where there is no winding around the two end points), defined in (3.173). We gave an example with the permutation $\sigma = (4\,1\,3\,2)$ in Figure 3.9. We have in this figure $\iota_0 = \iota_1 = 0$, $\iota_2 = 4$, $\iota_3 = 2$, $\iota_4 = 0$, so that $W_\sigma^{4,0} = 1, W_\sigma^{3,1} = 1, W_\sigma^{2,2} = -1/3, W_\sigma^{1,3} = 0, W_\sigma^{0,4} = 1$. Note that we always have $W_\sigma^{n,0} = W_\sigma^{n-1,1} = 1$.

Even number of legs

Equation (3.172) then directly translates into relations between the $P_\sigma^{n+m}(x)$. The cases of loop weights $N = 1, 0, -1$ are related to the $osp(r|2)$ models with $r = 3, 2, 1$ respectively. The results can be read off from eqs. (3.158), (3.150) and (3.73), by taking into account (2.122) and (2.123) that link the two terms in the expression to respectively the power law and logarithmic exponents. In the following, $\sim$ gives the asymptotic behaviour in x up to a constant multiplicative factor.

Loop weight 1 :

$$\boxed{\sum_{\sigma \in \mathfrak{S}_{n+m}} W_\sigma^{n,m} P_\sigma^{n+m}(x) \sim x^{-\frac{m^2-1}{2}} (\log x)^{\frac{m^2-1}{2} - n(n+1)} , \quad \text{for } n \text{ and } m \text{ odd}} \tag{3.176}$$

The case $m = 1$ where $W_\sigma^{n,1} = 1$ is consistent with Monte Carlo simulations in [93].

Loop weight 0 :

$$\sum_{\sigma \in \mathfrak{S}_{n+m}} W_\sigma^{n,m} P_\sigma^{n+m}(x) \sim \begin{cases} x^{-\frac{m^2}{2}} (\log x)^{\frac{m^2}{4} - \frac{n^2}{2}}, & \text{for } m \geq 2 \text{ even and } n \text{ even}, \\ x^{-\frac{m^2-1}{2}} (\log x)^{\frac{m^2}{4} - \frac{n^2}{2} + \frac{1}{4}}, & \text{for } n \text{ and } m \text{ odd} \end{cases}$$

$$(3.177)$$

Loop weight -1 :

One has access with $osp(1|2)$ to much less information. Keeping in mind that P is not a probability in this case but only a ratio of two partition functions, one can still write

$$\sum_{\sigma \in \mathfrak{S}_m} W_\sigma^{0,m} P_\sigma^m(x) \sim x^{-\frac{m(m+2)}{2}} (\log x)^{\frac{m(m-2)}{6}}, \quad \text{for } m \text{ even},$$

$$\sum_{\sigma \in \mathfrak{S}_{1+m}} W_\sigma^{1,m} P_\sigma^{1+m}(x) \sim x^{-\frac{m^2-1}{2}} (\log x)^{\frac{m^2+3}{6}}, \quad \text{for } m \text{ odd}$$

$$(3.178)$$

One leg

The information on the watermelon exponents for an odd number of legs is contained in the spin chains of odd size L. In particular the one-leg case corresponds to the order parameter. For a loop weight 0, it corresponds to the case $m = 0, n = 0$ in (3.140), and from (3.117) this gives a gap

$$\frac{L^2 \Delta e_L}{2\pi v_F} = -\frac{1}{4 \log L} \tag{3.179}$$

corresponding to the following behaviour of the order parameter

$$\langle \phi(x)\phi(0) \rangle \sim (\log x)^{\frac{1}{2}} \tag{3.180}$$

For a loop weight 1, the Bethe roots associated to the ground state of the $osp(3|2)$ model in odd size L are composed of $(L-1)/2$ strings, that happen to give exactly the same energy e_L in all odd sizes, as in the even size case. Thus the energy gap is exactly 0 and one gets

$$\langle \phi(x)\phi(0) \rangle \sim 1 \tag{3.181}$$

For a loop weight -1, the ground state in odd size corresponds to $m = 0$ in (3.73), that gives a gap

$$\frac{L^2 \Delta e_L}{2\pi v_F} = -\frac{1}{3 \log L} \tag{3.182}$$

hence

$$\langle \phi(x)\phi(0) \rangle \sim (\log x)^{\frac{2}{3}} \tag{3.183}$$

For these three cases we observe the behavior

$$\langle \phi(x)\phi(0) \rangle \sim (\log x)^{\frac{N-1}{N-2}} \tag{3.184}$$

3.5.6 Away from integrability

The integrable spin chains previously studied correspond to a crossing weight w equal to $(2 - N)/4$. For these values—and by using the Bethe-ansatz— we showed that the leading logarithmic corrections are indeed described by the supersphere sigma model. If there is universality, this correspondence has no particular reason to hold only at the integrable point: the supersphere sigma model should be relevant to describe the long distance physics of the dense loop soups for all finite crossing weights $w > 0$. Of course, away from the integrable point, this might be much more difficult to check, since then only direct numerical simulations are available. In Figure 3.10 we show as an example the measured logarithmic corrections corresponding to the 4-leg watermelon 2-point function, for different values of crossing weight w, for vanishing loop weight $N = 0$. The leading correction studied in this paper corresponds to the purple line. While the Bethe ansatz results show it does indeed give the correct results in the $L \to \infty$ limit, it is clear that for the sizes studied using direct transfer matrix diagonalization, next order corrections play an important role. It seems however that these corrections can be captured quite easily. The full solution to the RG equations for the sigma model coupling constant is

$$\frac{1}{g} = \frac{1}{g_0} + \frac{2 - N}{\kappa} \log(L/L_0) \tag{3.185}$$

Setting $L_0 = 1$ (i.e. measuring lengths in units of the lattice spacing) gives

$$g = \frac{\kappa}{2 - N} \frac{1}{\log L + \frac{\kappa}{(2-N)g_0}} \tag{3.186}$$

Meanwhile, we find that for $N = 0$ the numerical results can be collapsed approximately on (3.186) with $\frac{\kappa}{2g_0} \approx \pi w$. In other words, we have, to a very good approximation, $g_0 \approx \frac{\kappa}{2\pi w}$. Hence, we see that w plays the role of the inverse bare coupling constant

This observation suggests that at large w the corrections to the gap can be obtained with the same formulas we have derived earlier in this paper, but by using, instead of the running coupling constant $g \propto 1/\log L$, the bare constant $g_0 \propto 1/w$. Conversely, we can also imagine solving the problem at large w by elementary means, hence 're-deriving' the formulas for the corrections.

95
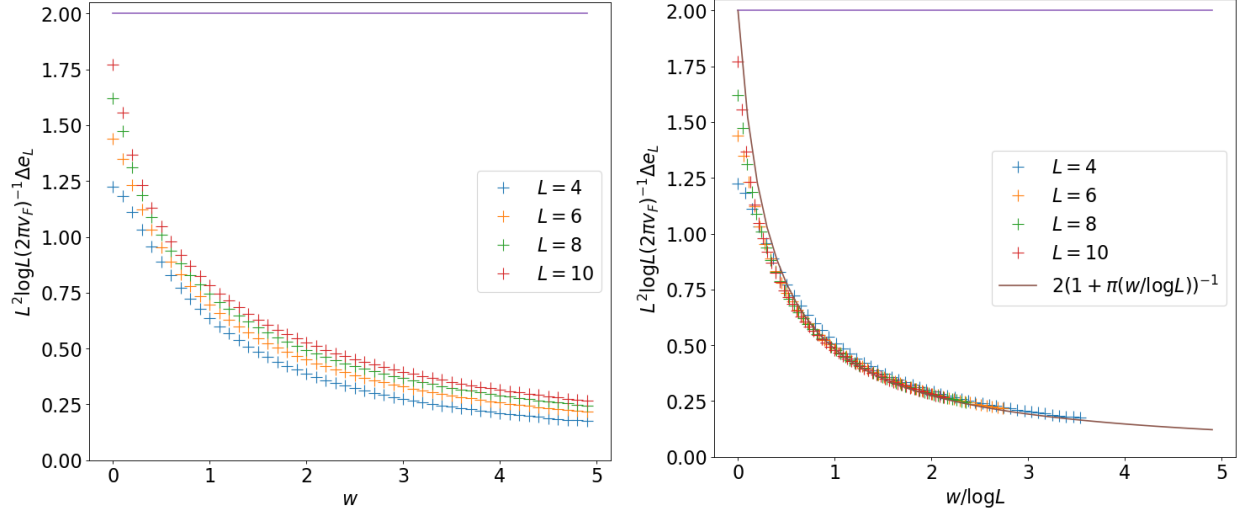
Figure 3.10: Left: measure of $\frac{L^2 \log L}{2\pi v_F} \Delta e_L$ for the 4-legs watermelon 2-point function with loop weight 0, as a function of w for different sizes. The limit value predicted by the supersphere sigma model is indicated in purple. The integrable point is $w = 0.5$. Right: the same data as a function of $w/\log L$.

To this end, we fix the weight for a loop to $N \geq 0$ and denote T the transfer matrix on a cylinder of size $L \times M$. This transfer matrix acts on L strands that are either connected to another strand, or are free, see Figure 3.11. The states are described by a vector space E which can be decomposed into a direct sum $E = \oplus_k E_k$, where E_k is the vector space generated by the states with k free strands among L strands, thus of dimension $\binom{L}{k}(L-k)!!$.

Figure 3.11: The 10 states in $E = E_4 \oplus E_2 \oplus E_0$ in size $L = 4$.

An important observation is that the transfer matrix, after building a row with L tiles chosen from the three possible tiles in Figure 3.7, cannot create new free strands, i.e. $TE_k \subset \oplus_{k' \leq k} E_{k'}$. Hence, the transfer matrix T is block-triangular and to find its eigenvalues one can work in a specific sector with a fixed number of free strands k. We will denote by T_k the restriction of the transfer matrix to E_k the sector with k free strands.

Let us now study the limit of large crossing weight $w \to \infty$. In this limit the transfer matrix T_k is dominated by choosing a crossing at each site, see Figure 3.12. It creates a loop in the horizontal direction and acts as the identity on the strands. Thus at leading order

$$T_k = Nw^L + O(w^{L-1}) \tag{3.188}$$

96

Figure 3.12: The only dominant term in T_k at order w^L: there are only tiles with crossings.

The next order is obtained by choosing a left or right corner among the L sites, see Figure 3.13. It does not create any loops and acts as the identity on the other strands. Then

$$T_k = Nw^L + 2Lw^{L-1} + O(w^{L-2}) \tag{3.189}$$

Figure 3.13: Two examples of terms at order w^{L-1} in T_k: there is only one tile without crossing.

Denote now $w^{L-2}R_k$ the transfer matrix that corresponds to the next order, i.e., that creates only two corners among the L sites, see Figure 3.14. Since it commutes with the dominant order, one simply has to compute its dominant eigenvalue. Whatever is the connection between the strands, there are $4 \cdot \binom{L}{2}$ possibilities of placing the corners, but $2 \cdot \binom{k}{2}$ of them (when the two corners are in opposite direction as in the two cases at the bottom in Figure 3.14) will connect 2 of the k free strands, which must not be counted; and among the other possibilities, $2 \cdot \frac{L-k}{2}$ will create a loop. Thus the sum of the entries of each column of R_k is always equal to $4 \cdot \binom{L}{2} - 2 \cdot \binom{k}{2} + (N-1)(L-k)$. Since the entries of R_k are nonnegative ($N \geq 0$ case), one can conclude that the dominant eigenvalue of R_k is exactly $4 \cdot \binom{L}{2} - 2 \cdot \binom{k}{2} + (N-1)(L-k)$. It follows that the dominant eigenvalue of T_k at order w^{L-2} is

$$\lambda_k = Nw^L + 2Lw^{L-1} + w^{L-2}\left(4 \cdot \binom{L}{2} - 2 \cdot \binom{k}{2} + (N-1)(L-k)\right) + O(w^{L-3}) \tag{3.190}$$
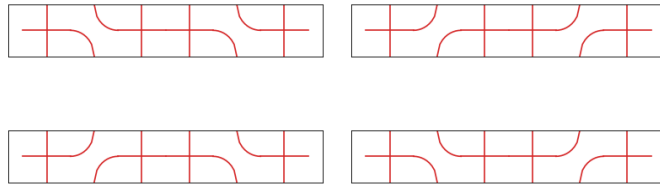
Figure 3.14: Four examples of terms at order w^{L-2} in T_k: there are two tiles without crossing among the L tiles.

This expansion has been checked numerically. It can also be continued at order w^{L-3}. At order w^{L-4} complications appear since at each transfer matrix step the number of possibilities depends on the state; and from order w^{L-5} on, the interaction between different orders counts and probably cannot be simply taken into account.

Assume now $N = 0$. We have

$$-\log(\lambda_k/\lambda_0) = \frac{k(k-2)}{2}\frac{1}{wL} + O(w^{-2}) \qquad (3.191)$$

corresponding to a gap

$$\frac{L^2\Delta e_L^k}{2\pi v_F} = \frac{k(k-2)}{2}\frac{1}{2\pi w} \qquad (3.192)$$

This matches the result equation (3.150) with $j = 1/2, q = (k-1)/2$ (that corresponds to 1 fermionic box and $k-1$ bosonic boxes in the Young tableau, equivalent to k free bosonic strands on the infinite cylinder), and the coupling constant must be put to $\kappa^{-1}g = \frac{1}{2\pi w}$, in agreement with our earlier discussion. We conclude that, remarkably, the weak-coupling sigma model provides a very accurate description of the loop soup at large w with the very simple correspondence $g \propto 1/w$. See Figure 3.15 for further numerical evidence with other sectors. For reasons we do not quite understand, this simple correspondence seems to be true only for $N = 0$.
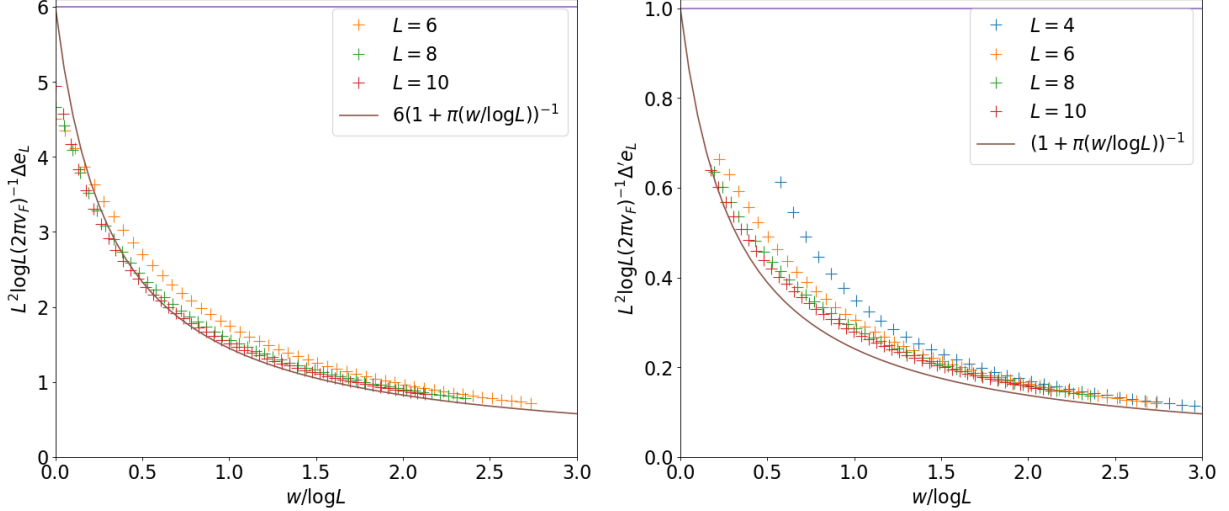
Figure 3.15: Left: measure of $\frac{L^2\log L}{2\pi v_F}\Delta e_L$ for the 6-legs watermelon 2-point function with loop weight 0, as a function of $w/\log L$ for different sizes. Right: measure of $\frac{L^2\log L}{2\pi v_F}\Delta' e_L$ with $\Delta' e_L$ the difference between the $(q, j) = (1, 1)$ sector and the $(q, j) = (0, 1)$ sector, with loop weight 0, as a function of $w/\log L$ for different sizes. The limit values predicted by the supersphere sigma model are indicated in purple.

Let us nevertheless give some comments on the $N \neq 0$ case. One can compute the large w regime of the eigenvalues as well:

$$- \log(\lambda_k/\lambda_0) = \frac{k(k+N-2)}{N} \frac{1}{w^2} + O(w^{-3}) \tag{3.193}$$

which corresponds to a gap

$$\frac{L^2 \Delta e_L^k}{2\pi v_F} = \frac{k(k+N-2)}{N} \frac{L}{2\pi w^2} + O(w^{-3}) \tag{3.194}$$

However the presence of the factor L and the behavior in w^{-2} suggest that the coupling constant g at $N \neq 0$ could behave as $\propto (\log L + ... + \mathrm{C} \times w^2/L)^{-1}$ where the dots indicate a term subdominant in w, and C a constant. When $w \to \infty$ the w^2/L part dominates and one observes the behavior (3.194). However it turns out that the finite-size corrections are not as easily captured as in the $N = 0$ case. Note finally that the expansion (3.194) for the energy gaps is valid for the singular case $N = 2$ as well.

Chapter 4

Excitation spectrum computation

4.1 Introduction

In this chapter we study the calculation of the excitation spectrum from the Bethe ansatz, and derive formulas (4.75) and (4.123) for the values of the finite-size corrections up to order $L^{-2}(\log L)^{-1}$ for any state[1] close to the ground state that can be recast into real roots plus a perturbation by a generic odd function. No such a systematic calculation has been carried out before, especially for the logarithmic corrections. Besides, we use a new approach that differs from the existing ones.

We will use the following convention for the Fourier transform of a function $f(x)$

$$\hat{f}(\omega) = \int_{-\infty}^{\infty} f(x)e^{i\omega x}dx \tag{4.1}$$

and for the convolution between two functions $f(x)$ and $g(x)$

$$(f \star g)(x) = \int_{-\infty}^{\infty} f(y)g(x - y)dy \tag{4.2}$$

4.1.1 Historical review

Root density approach and Wiener-Hopf equation

The first works on finite-size corrections in Bethe-ansatz solvable models date back to [114, 115, 116] where saddle-point approximations were used to obtain the corrections to the ground state of first gapped and then gapless systems. This approximation turned out to not work to compute the excitation spectrum, and the problem was then formulated in [23, 117, 118] in terms of root densities and *Wiener-Hopf equations*. The idea is the following. Denoting $S_L(\lambda) = \frac{1}{L}\sum_{k=1}^{K}\delta(\lambda - \lambda_k) - \sigma_L(\lambda)$ where λ_k are the Bethe roots and $\sigma_L(\lambda)$ the density in finite size L (i.e., the derivative of the counting function $z_L(\lambda)$ – see the subsequent

---

[1]Only symmetric states are considered for the logarithmic corrections.

sections for the definitions), one can use Euler-MacLaurin formula to write for a function $\phi(\lambda)$

$$\int_{-\infty}^{\infty} \phi(\lambda)S(\lambda)d\lambda \approx -\left(\int_{-\infty}^{-\Lambda} d\lambda + \int_{\Lambda}^{\infty} d\lambda\right)\phi(\lambda)\sigma_L(\lambda) + \frac{\phi(\Lambda) + \phi(-\Lambda)}{2L} + \frac{\phi'(\Lambda) - \phi'(-\Lambda)}{12L^2\sigma_L(\lambda)}$$
(4.3)

with Λ the largest Bethe root. The validity of this formula actually depends crucially on the way $\phi(\lambda)$ behaves at infinity. In particular, if one applies it directly to the definition of the root density in finite-size (that involves a sum over the Bethe roots) the correction terms are not negligible at order $O(L^{-2})$, and one has to manipulate the equation so that to involve the so-called *dressed* functions. However, even after this operation, it was argued by some authors [24] that the correction terms are still not negligible in some cases, and that one has to verify that the remaining terms do not impact the end result. This equation was anyway used to obtain in the asymptotic regime $\Lambda \to \infty$ a Wiener-Hopf equation for $f(x) = \sigma_L(x + \Lambda)$, i.e. an equation of the type

$$f(x) + \int_0^{\infty} f(y)K(x - y)dy = g(x)$$
(4.4)

where $g(x)$ is a source term, K a kernel, and $f(x)$ the unknown function. Here, $g(x)$ also depends on the unknown root density $\sigma_L(\lambda)$.

This equation has a long history, and techniques to solve it were first developed by Wiener and Hopf [119] to study the Sommerfeld diffraction problem [120], that is the amplitude of a wave diffracted by a half plane. Let us explain briefly how this method works [121, 122]. The difficulty in solving (4.4) is the lower limit of the integral, that makes it unsolvable by a mere Fourier transform that would suffice if it were $-\infty$. To go around the problem, one introduces functions $f_\pm(x)$ that are equal to $f(x)$ for x positive/negative, and vanish otherwise, so that the integral term is then a convolution between K and f_+, yielding

$$\hat{f}_+(\omega)(1 + \hat{K}(\omega)) + \hat{f}_-(\omega) = \hat{g}(\omega)$$
(4.5)

The Fourier transform $\hat{f}_\pm(\omega)$ of $f_\pm(x)$ is not particularly related to that of $f(x)$, but it has an important property: it is analytic on the upper/lower half-plane, since the integrand in the definition of the Fourier transform remains integrable in this region. Let us assume now that we have a decomposition of the kernel into a product of functions $K_\pm(\omega)$ analytic on the upper/lower half-plane:

$$1 + \hat{K}(\omega) = \frac{1}{K_+(\omega)K_-(\omega)}$$
(4.6)

If one decomposes

$$\hat{g}(\omega)K_-(\omega) = Q_+(\omega) + Q_-(\omega)$$
(4.7)

with $Q_\pm(\omega)$ analytic on the upper/lower half-plane, we obtain

$$\frac{\hat{f}_+(\omega)}{K_+(\omega)} - Q_+(\omega) = Q_-(\omega) - \hat{f}_-(\omega)K_-(\omega)$$
(4.8)

which implies that both sides have to be analytic on the whole plane. By studying the behaviour at infinity, one typically finds that they are a polynomial in ω, depending on additional constraints of the problem. Then one can deduce the value of $\hat{f}_\pm(\omega)$, and thus $f(x)$.

There are two decompositions to perform in this method, an additive one (4.7) and a multiplicative one (4.6). The additive decomposition can be done by merely separating the poles of the function; however, the multiplicative decomposition is a stronger assumption. When $f(x), g(x)$ are 1-component functions and K a 1×1 matrix, this decomposition can be generically written by taking the logarithm; but if they are n-component functions and K a $n \times n$ matrix for $n > 1$, because of non-commutativity, one cannot reduce the problem to an additive decomposition of the logarithm of $1 + \hat{K}(\omega)$ and no generic solution is known [121, 122].

Coming back to our problem, one finds then the value of $\sigma_L(\Lambda)$, and after several calculations the correction terms to the ground state energy. Adaptations to excited states are possible, but require a significant amount of additional work [24]. In case of approximate strings, although it was shown that the deviation of strings could be computed within this framework [123], no derivation of the finite-size effects to the ground state energy exists. As for higher-rank systems where (4.4) is now a vectorial equation, the difficulty of factorizing the kernel could prevent in principle the extension of the method.

Non-linear integral equation

Another method was then developed in [25, 124, 125, 126], where the problem is formulated in terms of *Non-Linear Integral Equations* (NLIE). The starting point is to identify domains in the complex plane where a set of functions (the eigenvalue $\Lambda(\lambda)$ in terms of the spectral parameter λ, the source term $\Phi(\lambda)$ in the Bethe equations, the polynomial $q(\lambda)$ whose roots are the Bethe roots) are analytic and non-zero. This property can be then extended to auxiliary function(s), and allows to compute Fourier transforms by different ways by deforming the integration path. For example for the XXZ chain, it leads to an equation on $a(x) = 1/p(x - i\gamma/2)$ where $p(x)$ is the Bethe ansatz function (equal to -1 on a Bethe root), that reads

$$\log a(x) = L \log \tanh \frac{\pi x}{2\gamma} + \int_{-\infty}^{\infty} (F(y) \log(1 + a(x-y)) - F(y + i\epsilon - i\gamma) \log(1 + \bar{a}(x-y))) dy \quad (4.9)$$

with $F(x)$ a known function. Remarkably, this equation holds for *all* finite size L: no asymptotic expansion has been carried out to obtain it. Since the system size L is merely a parameter in this equation, it can actually be solved numerically for a priori arbitrary sizes L (whereas the direct numerical solution of the Bethe equations can be done up to 10^3, 10^4 sites). We should also mention that a bit later [127, 128], the same non linear integral equations were shown to be obtained by observing that a sum over Bethe roots can be expressed as a contour integral

$$\sum_i \phi(\lambda_i) = \frac{1}{2i\pi} \oint \phi(x) \frac{d}{dx} \log(1 + e^{2i\pi L z_L(x)}) dx \quad (4.10)$$

with $z_L(\lambda)$ the counting function, when the Bethe numbers are half-integers, and where the integration contour must encircle the Bethe roots.

From (4.9) and another equation that expresses the energy in terms of $a(x)$, one can then perform an asymptotic analysis to find the leading corrections in finite-size, that result from dilogarithm identities. This permitted to settle the debate on the amplitudes of logarithmic corrections that cannot be suppressed by simply solving the Bethe equations [23, 129, 130, 131]. With some additional work, the non-linear integral equations can be adapted to excited states, for primaries or descendants, leading to the computation of the full spectrum of the six-vertex model [26]. Contrarily to the root density approach, it was also shown to be applicable to higher spin XXZ model with approximate strings [26, 132, 133, 134]. It is also widely used for finite-temperature studies, see e.g. [135], where the peculiar structure of Bethe roots prevents any use of root densities. For these reasons this approach is very efficient and powerful, and is now more considered to be the standard than the historical root density and Wiener-Hopf equation approach.

However, the method relies on analyticity properties of auxiliary functions that have to be constructed for every model, without general known construction method. For example, no non-linear integral equations are known for the $su(5)$ integrable spin chain, apart from some conjectures [136]. Moreover, every modification of the Bethe root configuration still requires an additional amount of work to derive the corresponding finite-size corrections, see e.g. [26] for the corrections to the descendant states.

Another approach

For these reasons I tried to understand if there could be another way to derive these corrections, that could be more easily adapted to different root configurations. The initial observation is that the finite-size corrections to sums over Bethe roots must be somehow directly visible in the counting function z_L, since it is itself expressed as a sum over Bethe roots; after identifying the general structure of the finite-size effects, one can sum the counting function over the Bethe roots (which is a known quantity since it is directly related to the Bethe numbers) to get a 'self-consistent' equation on the finite-size corrections [47].

The method is more easily adapted to special root configurations; in the following we derive the finite-size corrections with a generic additional source term that takes into account boundary condition effects or isolated Bethe roots. Its efficiency is also seen with the corrections to the descendant states, that require absolutely no more work than for the primaries. We show that the same technique can be extended to approximate strings case, up to now impossible to study with root densities. Moreover the same procedure is applicable to higher-rank systems whose Bethe roots are real.

Nevertheless, it still requires a certain number of technical steps. For this reason, I advice the reader to first understand the method in the case $t(\lambda) = 0$ and $\varphi = 0$, which lightens the notations without changing its spirit.

4.1.2 Euler-MacLaurin formula

The central tool to compute finite-size corrections is the *Euler-MacLaurin formula*, that gives the finite-size corrections to the Riemann sum of a function f, n times differentiable on $[0, 1]$

$$\frac{1}{L} \sum_{k=0}^{L-1} f(\tfrac{k+t}{L}) = \int_0^1 f(x)dx + \sum_{k=1}^{n} B_k(t) \frac{f^{(k-1)}(1) - f^{(k-1)}(0)}{k! L^k} + o(L^{-n}) \tag{4.11}$$

where t is a complex parameter, and $B_k(t)$ the Bernoulli polynomials with exponential generating function

$$\sum_{k=0}^{\infty} B_k(t) \frac{x^k}{k!} = \frac{xe^{xt}}{e^x - 1} \tag{4.12}$$

For instance, the first two polynomials are

$$B_1(t) = t - \tfrac{1}{2}, \qquad B_2(t) = t^2 - t + \tfrac{1}{6} \tag{4.13}$$

Note that (4.11) can be applied at order n to a sequence of functions f_L, if the sequence is *uniformly convergent* at order $o(L^{-n})$.

4.1.3 An introductory example: the free fermions

An important laboratory of quantum statistical physics is the XXZ spin chain at anisotropy parameter $\Delta = 0$, called *free fermions*, because the Hamiltonian can actually be reformulated in terms of fermionic variables through a Jordan-Wigner transformation. Under this form, it can be diagonalized explicitly. Not surprisingly, its Bethe ansatz formulation is equally simple. The Bethe equations decouple and read for K Bethe roots

$$\left(\frac{\sinh(\lambda_i + i\pi/4)}{\sinh(\lambda_i - i\pi/4)} \right)^L = (-1)^{K-1} \tag{4.14}$$

which is directly solved into

$$\lambda_i = \mathrm{argth} \tan \frac{I_i \pi}{L} \tag{4.15}$$

with I_i an integer (if K is odd) or a half-integer (if K is even) between $-L/2$ and $L/2$. An intensive energy level e_L of the Hamiltonian is then given by a set of distinct (half-)integers $\{I_1, ..., I_K\}$ between $-L/2$ and $L/2$, and reads

$$e_L = -\frac{1}{L} \sum_{i=1}^{K} \frac{1}{\cosh^2 \lambda_i - \frac{1}{2}} = -\frac{2}{L} \sum_{i=1}^{K} \cos \frac{2I_i \pi}{L} \tag{4.16}$$

where it is seen that the lowest energy level is obtained with $L/2$ roots whose Bethe numbers are between $-L/4 + 1/2$ and $L/4 - 1/2$. The momentum reads

$$p_L = \frac{2}{L} \sum_{i=1}^{K} \arctan \tanh \lambda_i \tag{4.17}$$

The direct application of Euler-MacLaurin formula with $f(x) = \cos(-\pi/2 + 2\pi x)$ and $t = 1/2$ gives for the ground state

$$e_L = -\frac{2}{\pi} - \frac{\pi}{3L^2} + O(L^{-3}) \tag{4.18}$$

In this case there are three types of excitations above the ground state, illustrated in Figure 4.1.

- the *magnetic* excitations, that correspond to changing the value of K by removing or adding a root in such a way that no internal vacancy (i.e., a vacancy between two Bethe integers) is created.

- the so-called *Umklapp* excitations, that correspond to removing one root with positive Bethe number and adding a new one with negative Bethe number (or the opposite), without creating internal vacancies.

- the *descendant* excitations, that correspond to shifting one root so that it creates an internal vacancy, without changing the number of positive or negative Bethe numbers.
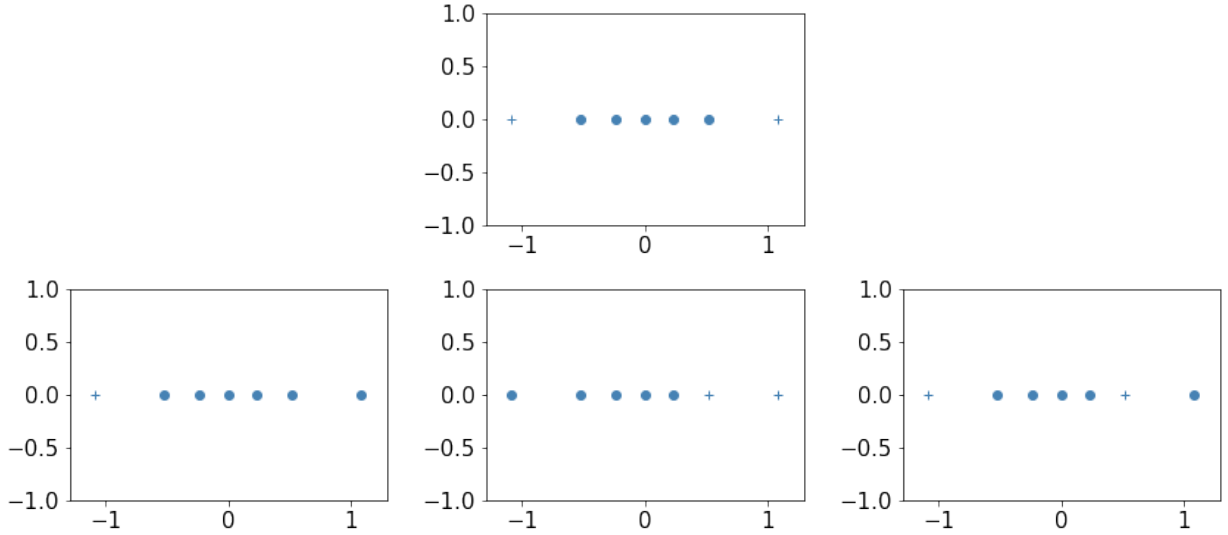
Figure 4.1: In reading direction: original root configuration; after a magnetic excitation; after an Umklapp excitation; after a descendant excitation. The dots indicate the position of the roots, and the crosses the vacancies.

Let us consider a state obtained from the ground state after a finite number of such elementary excitations, and denote by $n_\pm$ the number of roots with positive/negative Bethe numbers removed from the ground state, and $J_\pm$ the total number of times the roots with positive/negative Bethe numbers have been shifted one step away from the ground state

106

configuration. Then, directly from (4.16) and (4.18), expanding cos around $\pm\pi/2$:

$$e_L = -\frac{2}{\pi} - \frac{\pi}{3L^2} + \frac{4\pi}{L^2}\left(\sum_{k=1}^{n_+}(k-\tfrac{1}{2}) + \sum_{k=1}^{n_-}(k-\tfrac{1}{2}) + J_+ + J_-\right) \tag{4.19}$$

which gives

$$e_L = -\frac{2}{\pi} + \frac{4\pi}{L^2}\left(-\frac{1}{12} + \frac{1}{4}(n_+ + n_-)^2 + \frac{1}{4}(n_+ - n_-)^2 + J_+ + J_-\right) + O(L^{-3}) \tag{4.20}$$

As for the intensive momentum p_L, it reads

$$p_L = \frac{2\pi}{L^2}\sum_{i=1}^{K} I_i = -\pi\frac{n_+ - n_-}{2L} + \frac{2\pi}{L^2}\left(\frac{1}{2}(n_+ + n_-)(n_+ - n_-) + J_+ - J_-\right) \tag{4.21}$$

The *Fermi velocity* being defined as the proportionality constant between the energy and the momentum for a descendant excitation $\delta e_L = v_F \delta p_L$, we get $v_F = 2$, and equation (4.20) allows to identify the central charge $c = 1$ and conformal dimensions with formula (2.122).

The goal of the next sections is to generalize formula (4.20) to interacting theories solvable by the Bethe ansatz.

4.2 A glance at the interacting case: revisiting the free fermions

The free fermion case is particularly simple because the Bethe roots can be computed exactly, and the derivation of the finite-size corrections (4.20) were based on this property. In the general interacting case, no closed form expression for the roots can be obtained, and thus (4.20) should be obtained by rather different means. For this reason, we rederive here (4.20) without determining explicitly the Bethe roots, making the demonstration more easily adapted to the interacting case.

We first define the *counting function* $z_L(\lambda)$

$$z_L(\lambda) = s(\lambda) = \frac{1}{\pi}\arctan\tanh\lambda \tag{4.22}$$

such that $z_L(\lambda_i) = \frac{I_i}{L}$ for all the roots λ_i, that we will assume to be half-integers, re-using the notations in (2.20). The derivative of its limit function $z'_\infty(\lambda)$ gives the *density* of Bethe roots, namely the function such that an interval of length dx around x contains asymptotically $z'_\infty(x)dxL$ roots in the limit $L \to \infty$. We introduce the real number v_F such that this density behaves as

$$z'_\infty(x) \underset{|x|\to\infty}{\sim} e^{-v_F|x|} \tag{4.23}$$

The notation clearly anticipates the fact that v_F is indeed the Fermi velocity, as will be shown later.

A first simple observation is that the momentum p_L can be directly obtained by summing the counting function over the Bethe roots:

$$p_L = \frac{2\pi}{L} \sum_{i=1}^{K} s(\lambda_i) = \frac{2\pi}{L} \sum_{i=1}^{K} z_L(\lambda_i) = \frac{2\pi}{L} \sum_{i=1}^{K} \frac{I_i}{L} \qquad (4.24)$$

without a priori knowledge of the explicit form of the roots, because the counting function evaluates very simply at them; the expression then simplifies like in (4.21).

As for the energy e_L, it reads

$$e_L = -\frac{2\pi}{L} \sum_{i=1}^{K} s'(\lambda_i) \qquad (4.25)$$

However, the derivative of the counting function $z'_L(\lambda_i)$ does not evaluate simply at a root. The general idea to go around the problem is to observe that the excitations mainly modify the largest roots in absolute value, and for large λ, $s'(\lambda) = z'_L(\lambda)$ is close to $-v_F \,\mathrm{sgn}\,(\lambda)z_L(\lambda)$, so that the energy should be obtained by summing $v_F \,\mathrm{sgn}\,(\lambda)z_L(\lambda)$ over the Bethe roots. To formalize it, let us introduce the following *distribution* $\mathbb{S}$ that applies on *test functions* $\phi(x)$:

$$\mathbb{S}_x[\phi(x)] = \frac{1}{L} \sum_{i=1}^{K} \phi(\lambda_i) - \int_{-\infty}^{\infty} \phi(x)z'_{\infty}(x)dx \qquad (4.26)$$

The distribution $\mathbb{S}$ clearly depends on L, but we did not write an explicit dependance in order to simplify the notations. The dummy index x merely indicates the variable of the function on which it applies. Note that we subtracted the limit value of the Riemann sum in the definition, so that $\mathbb{S}_x[\phi(x)] \to 0$ when $L \to \infty$. We have

- If $\phi(x)$ is infinitely differentiable with compact support, then since z_L is a sequence of increasing functions it converges uniformly on any bounded segment (Dini's theorem), and so (4.11) can be applied to get

$$\mathbb{S}_x[\phi(x)] = \int_{-\infty}^{\infty} \phi(x)z'_L(x)dx - \int_{-\infty}^{\infty} \phi(x)z'_{\infty}(x)dx \qquad (4.27)$$

  up to an exponentially small correction in L (by 'exponentially small' we loosely mean negligible in front of any powers of L^{-1}). Indeed, since ϕ is infinitely differentiable with compact support, all the derivatives in the Euler-MacLaurin vanish at the boundaries. Using then (4.22), one gets $\mathbb{S}_x[\phi(x)] = 0$ up to exponentially small corrections.

- If $\phi(x)$ is infinitely differentiable and decays faster than any exponentials at infinity, then it can be approximated by a function with compact support on a segment $[\Lambda_-, \Lambda_+]$ where $\Lambda_{\pm}$ are the largest/smallest Bethe roots: since they grow as $\log L$ from (4.23), the approximation holds with exponentially small corrections, so that $\mathbb{S}_x[\phi(x)] = 0$ as well.

- If $\phi(x)$ is infinitely differentiable and decays exponentially fast $\phi(x) \sim a e^{-bx}$ when $x \to \infty$, then its Fourier transform $\hat{\phi}(\omega)$ has a pole at $\omega = -ib$ with residue ia. Introducing $f(x)$ a function such that $\hat{f}(\omega)$ has zeros at $-ib$ and similarly at the other poles of ϕ, one gets that the Fourier transform of $(\phi \star f)(x)$ has no poles, and thus this function decays faster than any exponential at infinity. It follows that $\mathbb{S}_x[(\phi \star f)(x)] = 0$, and so since this is valid for all test functions ϕ with this behaviour, one gets

$$\hat{\mathbb{S}} \cdot \hat{f} = 0 \tag{4.28}$$

which means that the support of the distribution $\hat{\mathbb{S}}$ lies within the zeros of $\hat{f}$, and so $\mathbb{S}_x[\phi(x)]$ can only depend on the residues of the poles of $\hat{\phi}$ (and so only on the behaviour at infinity of $\phi(x)$). It follows:

$$\mathbb{S}_x[\phi(x)] = \sum_\omega A_\omega \mathrm{Res}_\omega(\hat{\phi}) \tag{4.29}$$

where ω runs over the poles of ϕ. A_ω are numbers that depend on L, but not on ϕ. The dominant part of this sum is obtained for the poles with the smallest (in absolute value) imaginary part.

- If there are discontinuities in ϕ, then there are accordingly additional terms in (4.27) that come from the Euler-MacLaurin formula for $t = 1/2$ since the Bethe numbers are half-integers. In particular if there is a discontinuity in ϕ and in the derivative of ϕ at zero, then at leading order

$$\mathbb{S}_x[\phi(x)] = \frac{\phi'(0+) - \phi'(0-)}{24 z'_\infty(0) L^2} + \sum_\omega A_\omega \mathrm{Res}_\omega(\hat{\phi}) \tag{4.30}$$

- For very specific functions, the definition (4.26) enables to compute directly the value of $\mathbb{S}$ on them

$$\mathbb{S}_x[1_{x>0}] = -\frac{n_+}{L}, \qquad \mathbb{S}_x[1_{x<0}] = -\frac{n_-}{L} \tag{4.31}$$

Since the leading decay of $-s'(\lambda)/v_F$ and $\mathrm{sgn}\,(\lambda)s(\lambda)$ are the same, the part in (4.53) involving the residues is the same for both functions at leading order. However, there is an additional discontinuity of $2s'(0)$ in the derivative of this latter function at zero, and additional limit values $\pm s(\pm\infty)$ at infinity. Thus we get at leading order

$$\mathbb{S}_x[\,\mathrm{sgn}\,(x)s(x)] = -\frac{\mathbb{S}_x[s'(x)]}{v_F} + \mathbb{S}_x[1_{x>0}s(+\infty)] - \mathbb{S}_x[1_{x<0}s(-\infty)] + \frac{2s'(0)}{24 z'_\infty(0) L^2} \tag{4.32}$$

and so

$$\mathbb{S}_x[s'(x)] = -v_F \mathbb{S}_x[\,\mathrm{sgn}\,(x)s(x)] - v_F \frac{n_+ + n_-}{4L} + \frac{v_F}{12L^2} + o(L^{-2}) \tag{4.33}$$

Now, using (4.22)

$$\mathbb{S}_x[\,\mathrm{sgn}\,(x)s(x)] = \frac{1}{L} \sum_{i=1}^{K} |z_L(\lambda_i)| - \frac{1}{16} = \frac{1}{L^2} \sum_{i=1}^{K} |I_i| - \frac{1}{16} \tag{4.34}$$

so that

$$\mathbb{S}_x[s'(x)] = -\frac{v_F}{L^2}\left(-\frac{1}{12} + \frac{n_+^2 + n_-^2}{2} + J_+ + J_-\right) \tag{4.35}$$

recovering (4.20) with $e_L = e_\infty - 2\pi\mathbb{S}_x[s'(x)]$.

4.3 Finite-size corrections in the interacting case

4.3.1 Presentation

In a general interacting case, the excitations above the ground state involve the three types of excitations already encountered in the free fermion case, as well as other types of excitations such as exact or approximate strings, or isolated Bethe roots, see Figure 2.2. These can often be taken into account by introducing an additional source term in the Bethe equations. For example, in the XXZ spin chain, if there is an exact string $\pm i\gamma/2$ in the Bethe roots, then the other roots $\lambda_1, ..., \lambda_{K-2}$ exactly satisfy the following equations

$$\left(\frac{\sinh(\lambda_i + i\gamma/2)}{\sinh(\lambda_i - i\gamma/2)}\right)^L \frac{\sinh(\lambda_i - i\gamma/2)\sinh(\lambda_i - 3i\gamma/2)}{\sinh(\lambda_i + i\gamma/2)\sinh(\lambda_i + 3i\gamma/2)} = \prod_{j=1,\neq i}^{K-2} \frac{\sinh(\lambda_i - \lambda_j + i\gamma)}{\sinh(\lambda_i - \lambda_j - i\gamma)} \tag{4.36}$$

Modified boundary conditions often result in such an additional source term as well. Besides, certain physical applications require to use a *twisted* transfer matrix, or to introduce *twisted* boundary conditions in the Hamiltonian, that results in the presence of an additional source term in the Bethe equations. For these reasons, we will consider the following Bethe equations

$$s(\lambda_i) + \frac{t(\lambda_i)}{L} + \frac{\varphi}{L} = \frac{I_i}{L} + \frac{1}{L}\sum_{j=1}^{K} r(\lambda_i - \lambda_j) \tag{4.37}$$

where φ is a real parameter (the twist), and $t(x)$ a continuous function assumed to be odd (the additional source term). Similarly to the free fermion case, the Bethe numbers I_i are integers (if K is odd) or half-integers (if K is even). Upon introducing a twist $\varphi = 1/2$, one will actually always consider that the Bethe numbers are half-integers. We will denote $\alpha L - (n_+ + n_-)$ the total number of Bethe roots, $\frac{\alpha L}{2} - n_+$ the number of positive Bethe numbers and $\frac{\alpha L}{2} - n_-$ the number of negative Bethe numbers. We will assume that $\alpha = 1$ ($osp(1|2)$ case) or $\alpha = 1/2$ ($su(2)$ case)[2], and that the largest roots are not bounded and go to infinity when $L \to \infty$. We will moreover assume that the root density defined below as the derivative of (4.39) decays exponentially fast at infinity.

---

[2]If $\alpha = \frac{1}{4}$ for example, there could be different effects depending on L modulo 4.

The energy e_L and momentum p_L are defined as[3]

$$e_L = -\frac{2\pi}{L} \sum_{i=1}^{K} s'(\lambda_i), \qquad p_L = \frac{2\pi}{L} \sum_{i=1}^{K} s(\lambda_i) \tag{4.38}$$

As in the free fermion case, we introduce the counting function

$$z_L(\lambda) = s(\lambda) + \frac{t(\lambda)}{L} + \frac{\varphi}{L} - \frac{1}{L} \sum_{j=1}^{K} r(\lambda - \lambda_j) \tag{4.39}$$

such that $z_L(\lambda_i) = I_i/L$. Its derivative in the thermodynamic limit z'_∞ is the root density, that can be computed exactly with Fourier transform through a classical calculation [137, 138] whenever the support of the roots extends to $\pm\infty$ when $L \to \infty$, and that yields

$$\widehat{z'_\infty} = \frac{\hat{s'}}{1 + \hat{r'}}, \qquad z'_\infty(\lambda) = \frac{1}{2\gamma \cosh(\pi\lambda/\gamma)} \quad \text{in the XXZ case} \tag{4.40}$$

See Figure 4.2 for an illustration of this density. Again, we define v_F the number such that

$$z'_\infty(\lambda) \sim e^{-v_F|\lambda|} \tag{4.41}$$

that is π/γ in the XXZ case.
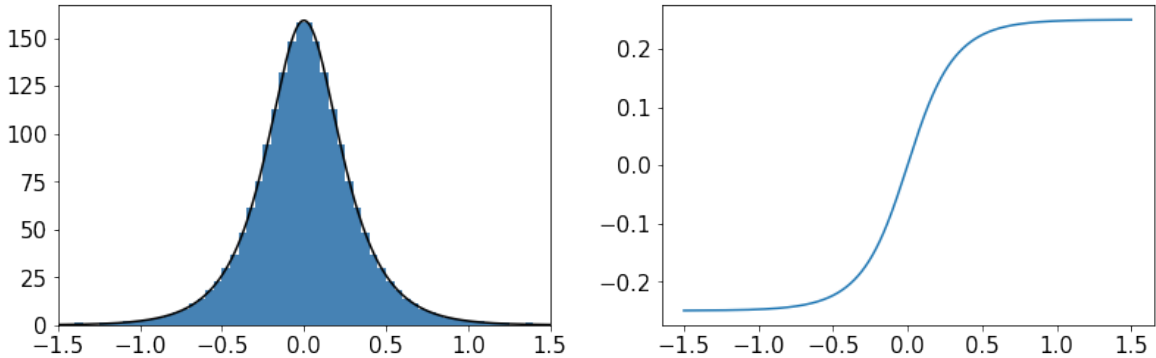
Figure 4.2: Left: histogram of the number of roots in slices of length $dx = 0.05$, in size $L = 4000$ for the XXZ spin chain at $\gamma = \pi/5$ (blue), together with the root density $z'_\infty(x)dxL$ (black). Right: counting function $z_L(x)$ for the ground state in size $L = 4000$ for $\gamma = \pi/5$.

---

[3]We decided to write the energy under this generic form, but some models such as the Lieb-Liniger model have their specific expression of the energy in terms of the Bethe roots. Moreover the energy of the XXZ spin chain is usually defined with a multiplicative $\sin\gamma$ factor, which has the only effect of multiplying the Fermi velocity by $\sin\gamma$.

4.3.2 Properties of the distribution $\mathbb{S}$

Following the free fermion case, we define the distribution $\mathbb{S}$ that applies on test functions $\phi(x)$ as

$$\mathbb{S}_x[\phi(x)] = \frac{1}{L} \sum_{i=1}^{K} \phi(\lambda_i) - \int_{-\infty}^{\infty} \phi(x) z'_{\infty}(x) dx \tag{4.42}$$

It has the following properties

- If $\phi(x)$ is infinitely differentiable with compact support, then since z_L is a sequence of increasing functions it is uniformly convergent on any bounded segment, so that the Euler-MacLaurin formula applies. The properties of ϕ imply that all the terms at the boundaries in (4.11) vanish, yielding

$$\mathbb{S}_x[\phi(x)] = \int_{-\infty}^{\infty} \phi(y) z'_L(y) dy - \int_{-\infty}^{\infty} \phi(y) z'_{\infty}(y) dy \tag{4.43}$$

with exponentially small corrections. Using (4.39) gives

$$\mathbb{S}_x[\phi(x)] = \frac{1}{L} \int_{-\infty}^{\infty} \phi(y) t'(y) dy - \int_{-\infty}^{\infty} \phi(y) \mathbb{S}_x[r'(y - x)] dy \tag{4.44}$$

that is, with δ the Dirac delta distribution

$$\mathbb{S}_x[(\phi \star (\delta + r'))(x)] = \frac{1}{L} \int_{-\infty}^{\infty} \phi(y) t'(y) dy \tag{4.45}$$

Since this is valid for any ϕ, it gives the equation between distributions

$$\mathbb{S} \star (\delta + r') = \frac{t'}{L} \tag{4.46}$$

that becomes, after Fourier transforming

$$\hat{\mathbb{S}} \cdot (1 + \hat{r}') = \frac{\hat{t}'}{L} \tag{4.47}$$

whose solutions are $\frac{1}{L} \hat{t}'/(1 + \hat{r}')$ plus Dirac deltas at points where $1 + \hat{r}'$ vanishes[4]. We define the *dressed* function ϕ_{dr} as

$$\widehat{\phi}_{\mathrm{dr}} = \frac{\hat{\phi}}{1 + \hat{r}'} \tag{4.48}$$

---

[4]There can also be derivatives of δ if the derivatives of $1 + \hat{r}'$ vanish as well. For the XXZ case when $e^{i\gamma}$ is not a root of unity this does not happen, which is dense in the possible values of γ. We still treated the case $e^{i\gamma}$ root of unity in [47].

Since ϕ has compact support, $\hat{\phi}$ has no poles and thus the zeros of $1 + \hat{r}'$ are exactly the poles of $\hat{\phi}_{\mathrm{dr}}$. It follows that these solutions are exactly

$$\mathbb{S}_x[\phi(x)] = \frac{1}{L} \int_{-\infty}^{\infty} \phi(x) t'_{\mathrm{dr}}(x) dx + \sum_\omega A_\omega \mathrm{Res}_\omega(\hat{\phi}_{\mathrm{dr}}) \tag{4.49}$$

where A_ω are numbers depending on L but not on ϕ, and where the sum over ω runs over the poles of $\hat{\phi}_{\mathrm{dr}}$.

- If $\phi(x)$ is infinitely differentiable and decays faster than any exponentials at infinity, then it can be approximated by a function with compact support on a segment $[\Lambda_-, \Lambda_+]$ where $\Lambda_\pm$ are the largest/smallest Bethe roots. Since they grow as $\log L$ from (4.40), the approximation holds with corrections smaller than any inverse power of L, so that (4.49) holds as well.

- If $\phi(x)$ is infinitely differentiable and decays exponentially fast $\phi(x) \sim ae^{-bx}$ when $x \to \infty$, then its Fourier transform $\hat{\phi}(\omega)$ has a pole at $\omega = -ib$ with residue ia. Introducing $f(x)$ a function such that $\hat{f}(\omega)$ has zeros at $-ib$, one gets that the Fourier transform of $(\phi \star f)(x)$ has no poles, and thus this function decays faster than any exponential at infinity. Following the same arguments as for the compact support case, one finds that the distribution $\mathbb{S}$ when applied on test functions with the same exponential decay as ϕ, must satisfy

$$\hat{\mathbb{S}} \cdot \hat{f} \cdot (1 + \hat{r}') = \frac{\hat{f}\hat{t}'}{L} \tag{4.50}$$

whose solutions are $\frac{1}{L}\hat{t}'/(1 + \hat{r}')$ plus Dirac deltas at points where $\hat{f} \cdot (1 + \hat{r}')$ vanishes. Since the zeros of $\hat{f}$ are the poles of $\hat{\phi}$, one gets exactly the same solutions as in equation (4.49) with the same dressing (4.48). Moreover, since the largest Bethe roots grow as $\frac{\log L}{v_F}$ from (4.41), an exponential decay $e^{-a|\lambda|}$ contributes to a correction of order $O(L^{-1-|\frac{a}{v_F}|})$.

It is seen that the previous properties generalize the free fermion case in a simple way: the test functions $\phi(x)$ are replaced by their dressed version $\phi_{\mathrm{dr}}(x)$. However, there is an important change in the interacting case: because of the dependence of the roots on the other roots, $z_L^{-1}(0)$ (i.e., the real λ such that $z_L(\lambda) = 0$) is not necessarily equal to 0, and this occurs in particular whenever $\varphi \neq 0$ or $n_+ \neq n_-$. To understand the consequence it has on the roots, let us consider λ_i a root that is $O(L^{-1})$, thus with a $O(1)$ Bethe integer I_i associated to it. We have

$$\begin{aligned}
\lambda_i = z_L^{-1}(\tfrac{I_i}{L}) &= z_L^{-1}(0) + \frac{I_i}{Lz'_L(\lambda_i)} + o(L^{-1}) \\
&= z_L^{-1}(0) + \frac{I_i}{Lz'_\infty(0)} + o(L^{-1}) \\
&= \frac{I_i - \delta I}{Lz'_\infty(0)} + o(L^{-1})
\end{aligned} \tag{4.51}$$

113

where we see that the Bethe numbers close to 0 are effectively shifted by δI (that is independent of i) defined by

$$z_L^{-1}(0) = -\frac{\delta I}{L z_\infty'(0)} + o(L^{-1}) \qquad (4.52)$$

Thus the two last properties of $\mathbb{S}$ in the free fermion case are modified as follows in the interacting case:

- If there are discontinuities in $\phi(x)$, then the corresponding terms in the Euler-MacLaurin formula must be added in (4.43). If these discontinuities occur at 0, because of our choice of considering half-integer Bethe numbers, and because of the shift δI, the t in (4.11) that must be used is $t = \frac{1}{2} - \delta I$. However, in the following the discontinuities will occur at a point between the roots with positive Bethe numbers and those with negative Bethe numbers, that is $z_L^{-1}(0) = -\frac{\delta I}{L z_\infty'(0)}$. Relatively to this point, the Bethe numbers are not shifted, and $t = 1/2$ must be used as in the free fermion case. Thus, in case of discontinuities at $z_L^{-1}(0)$:

$$\mathbb{S}_x[\phi(x)] = \frac{\phi'(z_L^{-1}(0)+) - \phi'(z_L^{-1}(0)-)}{24 z_\infty'(0) L^2} + \frac{1}{L} \int_{-\infty}^{\infty} \phi(x) t_{\mathrm{dr}}'(x) dx + \sum_\omega A_\omega \mathrm{Res}_\omega(\hat{\phi}_{\mathrm{dr}}) \quad (4.53)$$

- As in the free fermion case, the value of $\mathbb{S}$ on some specific functions can be computed directly with its definition (4.42):

$$
\begin{aligned}
\mathbb{S}_x[1_{x>z_L^{-1}(0)}] &= \frac{\frac{\alpha L}{2} - n_+}{L} - \int_{z_L^{-1}(0)}^{\infty} z_\infty'(x) dx \\
&= \frac{\alpha}{2} - \frac{n_+}{L} - \frac{\alpha}{2} + z_\infty(z_L^{-1}(0)) \qquad (4.54) \\
&= \frac{-n_+ - \delta I}{L} + o(L^{-1})
\end{aligned}
$$

Similarly:

$$\mathbb{S}_x[1_{x<z_L^{-1}(0)}] = \frac{-n_- + \delta I}{L} + o(L^{-1}) \qquad (4.55)$$

Summary

We can summarize the previous properties in the following equation, valid for a function $f(x)$ with limits $f(\pm\infty)$ at $\pm\infty$, such that its dressed function f_{dr} decays (to its limits $\frac{f(\pm\infty)}{1+2r(\infty)}$) exponentially fast as $a_\pm e^{-b|x|}$ at $\pm\infty$; and with a possible discontinuity of $\Delta f'$ in

the derivative of f at $z_L^{-1}(0)$:

$$\mathbb{S}_x[f(x)] = -f(\infty)\frac{n_+ + \delta I}{L} - f(-\infty)\frac{n_- - \delta I}{L} + \frac{a_+ A_b + a_- A_{-b}}{L^{1+|b/v_F|}}$$
$$+ \frac{1}{L}\int_{-\infty}^{\infty} f(x)t'_{\mathrm{dr}}(x)dx - \frac{t(\infty)(f(\infty) + f(-\infty))}{L(1 + 2r(\infty))} - \frac{\delta I t'_{\mathrm{dr}}(0)(f(\infty) - f(-\infty))}{L^2 z'_\infty(0)}$$
$$+ \frac{\Delta f'}{24 z'_\infty(0)L^2}$$
$$+ o(L^{-2})$$

$$(4.56)$$

with $A_{\pm b}$ numbers that are $O(L^0)$ and that depend only on b. It is obtained by decomposing $f(x) = (f(x) - f(+\infty)1_{x>z_L^{-1}(0)} - f(-\infty)1_{x<z_L^{-1}(0)}) + f(+\infty)1_{x>z_L^{-1}(0)} + f(-\infty)1_{x<z_L^{-1}(0)}$ and applying formulas (4.54) and (4.55) on the two last constant terms. This formula is not complicated: the first line gives the corrections coming from the behaviour of f at infinity (its limit value, and its exponential decay), the second line the corrections coming from the perturbation $t(\lambda)$, and the third line the Euler-MacLaurin term coming from a possible discontinuity in the derivative at zero.

Let us write this formula in two particular useful cases, where we assume now that the function $f(x)$ is odd. Denoting for convenience

$$\theta(x) = \mathrm{sgn}\,(x - z_L^{-1}(0)) \tag{4.57}$$

we have

$$\mathbb{S}_x[f(x)] = -f(\infty)\frac{n_+ - n_- + 2\delta I}{L} + o(L^{-1}) \tag{4.58}$$

and

$$\mathbb{S}_x[\theta(x)f(x)] = \frac{1}{L}\int_{-\infty}^{\infty}\theta(x)f(x)t'_{\mathrm{dr}}(x)dx - \frac{2t(\infty)f(\infty)}{L(1 + 2r(\infty))} - f(\infty)\frac{n_+ + n_-}{L} + \frac{f'(0)}{12 z'_\infty(0)L^2}$$
$$+ \frac{a_+(A_b + A_{-b})}{L^{1+|b/v_F|}} + o(L^{-2})$$

$$(4.59)$$

4.3.3   Computing the shift δI

Formula (4.56) depends on the shift δI. To determine it, we start by rewriting the counting function as

$$z_L(\lambda) = z_\infty(\lambda) + \frac{t(\lambda)}{L} + \frac{\varphi}{L} - \mathbb{S}_x[r(\lambda - x)] \tag{4.60}$$

by using the definition of $\mathbb{S}$. Then, we evaluate it at $\lambda = z_L^{-1}(0)$:

$$
\begin{aligned}
z_L(z_L^{-1}(0)) &= 0 \\
&= z_\infty(z_L^{-1}(0)) + \frac{t(z_L^{-1}(0))}{L} + \frac{\varphi}{L} - \mathbb{S}_x[r(z_L^{-1}(0) - x)] \\
&= -\frac{\delta I}{L} + \frac{\varphi}{L} + \mathbb{S}_x[r(x)] + o(L^{-1}) \\
&= -\frac{\delta I}{L} + \frac{\varphi + r(\infty)(n_- - n_+ - 2\delta I)}{L} + o(L^{-1})
\end{aligned}
\tag{4.61}
$$

where we used the oddness of r and t to get the third line, and used (4.58) to get the last line. This equation can be solved for δI

$$
\delta I = \frac{\varphi + (n_- - n_+)r(\infty)}{1 + 2r(\infty)}
\tag{4.62}
$$

See Figure 4.3 for a numerical verification of this value.

Figure 4.3: Left: measured δI in size L as a function of $L^{-1/2}$, for $\gamma = \pi/5$, $n_+ = 2$, $n_- = 0$, $J_+ = J_- = 0$, $\varphi = 0$ and $t(\lambda) = 0$. The exact value is -0.375 and is in the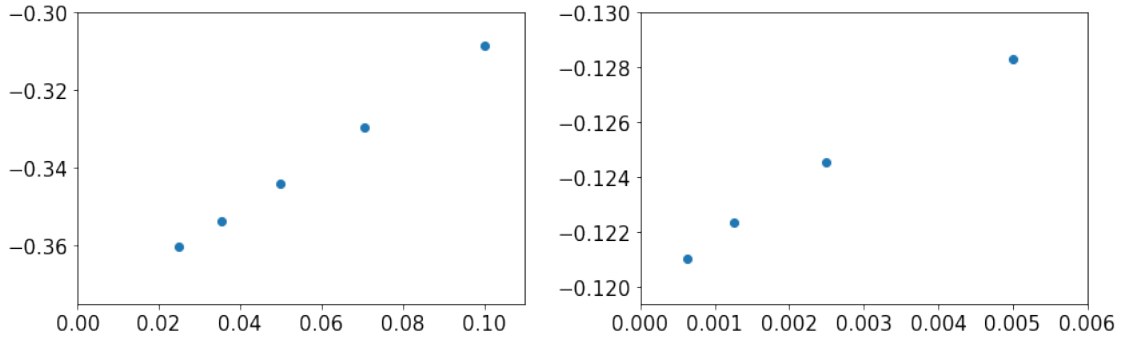 bottom-left corner; a linear fit on the last two points gives -0.376. Right: measured δI in size L as a function of L^{-1}, for $\gamma = \pi/3$, $n_+ = 1$, $n_- = 1$, $J_+ = 1$, $J_- = 0$, $\varphi = -1/(2\pi)$ and $t(\lambda) = 0$. The exact value is ≈ -0.1194 and is in the bottom-left corner; a linear fit on the last two points gives -0.1197.

4.3.4 The momentum

As in the free fermion case, the momentum is more easily computed than the energy. It is obtained by summing the counting function z_L over the Bethe roots:

$$\frac{p_L}{2\pi} = \frac{1}{L} \sum_{i=1}^{K} s(\lambda_i)$$

$$= \frac{1}{L} \sum_{i=1}^{K} z_L(\lambda_i) - \frac{1}{L^2} \sum_{i=1}^{K} t(\lambda_i) - \frac{\varphi}{L^2} \sum_{i=1}^{K} 1 + \frac{1}{L^2} \sum_{i,j} r(\lambda_i - \lambda_j)$$

$$= \frac{1}{L^2} \sum_{i=1}^{K} I_i - \frac{1}{L} \int_{-\infty}^{\infty} t(x) z'_\infty(x) dx - \frac{1}{L} \mathbb{S}_x[t(x)] - \frac{\varphi}{L^2}(\alpha L - n_+ - n_-)$$

$$= \alpha \frac{n_- - n_+}{2L} + \frac{1}{L^2}(\frac{n_+^2}{2} - \frac{n_-^2}{2} + J_+ - J_-) + \frac{1}{L^2} t(+\infty)(n_+ - n_- + 2\delta I) - \frac{\varphi}{L^2}(\alpha L - n_+ - n_-) + o(L^{-2})$$

$$(4.63)$$

where in the third line we used that $r(x)$ is odd to get $\sum_{i,j} r(\lambda_i - \lambda_j) = 0$ whatever the roots are, and in the fourth line that $t(x)$ is odd. Hence

$$\boxed{p_L = -\pi\alpha \frac{n_+ - n_- + 2\varphi}{L} + \frac{\pi}{L^2}(n_+ + n_-)(n_+ - n_- + 2\varphi) + \frac{2\pi}{L^2}(J_+ - J_-) + \frac{2\pi}{L^2} t(+\infty)(n_+ - n_- + 2\delta I)}$$

$$(4.64)$$

4.3.5 The energy

The computation of the energy e_L needs a bit more work. Similarly to the free fermion case, this quantity is obtained by summing the absolute value of the Bethe numbers $|I_i|$.

Computing $\sum_{i=1}^{K} |I_i|$

We have

$$\frac{1}{L^2} \sum_{i=1}^{K} |I_i| = \frac{1}{L} \sum_{i=1}^{K} |z_L(\lambda_i)|$$

$$= \frac{1}{L} \sum_{i=1}^{K} \theta(\lambda_i) z_L(\lambda_i)$$

$$= \frac{1}{L} \sum_{i=1}^{K} \theta(\lambda_i) z_\infty(\lambda_i) + \frac{1}{L^2} \sum_{i=1}^{K} \theta(\lambda_i) t(\lambda_i) + \frac{\varphi}{L^2} \sum_{i=1}^{K} \theta(\lambda_i) - \frac{1}{L} \sum_{i=1}^{K} \theta(\lambda_i) \mathbb{S}_x[r(\lambda_i - x)]$$

$$= \frac{1}{L} \sum_{i=1}^{K} \theta(\lambda_i) z_\infty(\lambda_i) + \frac{1}{L^2} \sum_{i=1}^{K} \theta(\lambda_i) t(\lambda_i) - \frac{1}{L} \sum_{i=1}^{K} \theta(\lambda_i) \mathbb{S}_x[r(\lambda_i - x)] + \varphi \frac{n_- - n_+}{L^2}$$

$$(4.65)$$

where we evaluated $\sum_{i=1}^{K} \theta(\lambda_i) = -n_+ + n_-$ the difference between the number of positive and negative Bethe numbers.

The first term in (4.65) is

$$\frac{1}{L}\sum_{i=1}^{K}\theta(\lambda_i)z_\infty(\lambda_i) = \int_{-\infty}^{\infty}\theta(x)z_\infty(x)z_\infty'(x)dx + \mathbb{S}_x[\theta(x)z_\infty(x)]$$

$$= \frac{\alpha^2}{4} - \frac{\delta I^2}{L^2} + \mathbb{S}_x[\theta(x)z_\infty(x)] \tag{4.66}$$

where we used the definition of $\mathbb{S}$ in (4.42) to write the first line; and then we integrated the first term to get the second line.

The second term in (4.65) is

$$\frac{1}{L^2}\sum_{i=1}^{K}\theta(\lambda_i)t(\lambda_i) = \frac{1}{L}\int_{-\infty}^{\infty}\theta(x)t(x)z_\infty'(x)dx + \frac{1}{L}\mathbb{S}_x[\theta(x)t(x)]$$

$$= \frac{1}{L}\int_{-\infty}^{\infty}\theta(x)t(x)z_\infty'(x)dx + \frac{1}{L^2}\int_{-\infty}^{\infty}\theta(x)t(x)t_{\mathrm{dr}}'(x) - \frac{1}{L^2}\frac{2t(\infty)^2}{1+2r(\infty)} - \frac{t(\infty)(n_+ + n_-)}{L^2} \tag{4.67}$$

where we used again the definition of $\mathbb{S}$ to write the first line; then we used formula (4.59) at order L^{-1} to get the second line at order L^{-2}.

The third term in (4.65) is

$$-\frac{1}{L}\sum_{i=1}^{K}\theta(\lambda_i)\mathbb{S}_x[r(\lambda_i - x)]$$

$$= -\int_{-\infty}^{\infty}\theta(y)\mathbb{S}_x[r(y-x)]z_\infty'(y)dy - \mathbb{S}_y[\theta(y)\mathbb{S}_x[r(y-x)]]$$

$$= \mathbb{S}_x\left[\int_{-\infty}^{\infty}\theta(y)r'(y-x)z_\infty(y)dy\right] - \mathbb{S}_x\left[r(\infty)\alpha - 2r(z_L^{-1}(0) - x)z_\infty(z_L^{-1}(0))\right]$$

$$- 2\mathbb{S}_y\left[1_{y>z_L^{-1}(0)}\mathbb{S}_x[1_{x<z_L^{-1}(0)}r(y-x)]\right]$$

$$= \mathbb{S}_x\left[\int_{-\infty}^{\infty}\theta(y)r'(y-x)z_\infty(y)dy\right] + \frac{r(\infty)\alpha}{L}(n_+ + n_-) + 2\frac{\delta I(\delta I - \varphi)}{L^2}$$

$$- 2\mathbb{S}_y\left[1_{y>z_L^{-1}(0)}\left(-r(\infty)\frac{n_- - \delta I}{L} + \frac{1}{L}\int_{-\infty}^{0}r(y-x)t_{\mathrm{dr}}'(x)dx - \frac{1}{L}\frac{t(\infty)r(\infty)}{1+2r(\infty)}\right)\right]$$

$$= \mathbb{S}_x\left[\int_{-\infty}^{\infty}\theta(y)r'(y-x)z_\infty(y)dy\right] + \frac{r(\infty)\alpha}{L}(n_+ + n_-) + 2\frac{\delta I(\delta I - \varphi)}{L^2}$$

$$- \frac{2r(\infty)}{L^2}(n_- - \delta I)(n_+ + \delta I) + \frac{2r(\infty)}{L^2}\left(\frac{t(\infty)}{1+2r(\infty)}\right)^2 - \frac{1}{L^2}\int_{-\infty}^{\infty}\theta(x)(r \star t_{\mathrm{dr}}')(x)t_{\mathrm{dr}}'(x)dx \tag{4.68}$$

where the first line is the definition of $\mathbb{S}$; in the second line the first two terms come from an integration by part on the first term in the first line, and the third term is a rewriting of the last term of the first line using the oddness of r [5]; to get the third line we evaluated

---

[5]This transformation avoids the undefined limit of $x - y$ when $x, y \to \infty$.

the second term of the second line at order L^{-2}, and evaluated the innermost $\mathbb{S}$ with (4.56) at order L^{-1} to get the last term; finally to get the last line we evaluated the outmost $\mathbb{S}$ in the last term with (4.56), and used again the oddness of r to rewrite the integral term as a convolution.

From these three pieces we have the combination:

$$\int_{-\infty}^{\infty} \theta(x)t(x)t'_{\mathrm{dr}}(x)dx - \int_{-\infty}^{\infty} \theta(x)(r \star t'_{\mathrm{dr}})(x)t'_{\mathrm{dr}}(x)dx = \int_{-\infty}^{\infty} \theta(x)t_{\mathrm{dr}}(x)t'_{\mathrm{dr}}(x)dx$$
$$= \left(\frac{t(\infty)}{1 + 2r(\infty)}\right)^2 + o(L^0) \tag{4.69}$$

using, by definition, $t(x) = t_{\mathrm{dr}}(x) + (r' \star t_{\mathrm{dr}})(x)$.

Evaluating now:

$$\frac{1}{L^2}\sum_{i=1}^{K}|I_i| = \frac{\alpha^2}{4} - \frac{\alpha}{2L}(n_+ + n_-) + \frac{1}{2L^2}(n_+^2 + n_-^2) + \frac{J_+ + J_-}{L^2} \tag{4.70}$$

equation (4.65) yields

$$\mathbb{S}_x[f(x)] = -\alpha(n_+ + n_-)\frac{1 + 2r(\infty)}{2L} - \frac{1}{L}\int \theta(x)t(x)z'_\infty(x)dx$$
$$+ \frac{1}{L^2}\left(\frac{n_+^2 + n_-^2}{2} + 2r(\infty)(n_+ + \delta I)(n_- - \delta I) - \delta I^2 + (2\delta I + n_+ - n_-)\varphi \right. \tag{4.71}$$
$$\left. + t(\infty)(n_+ + n_-) + \frac{t(\infty)^2}{1 + 2r(\infty)} + J_+ + J_-\right)$$

with

$$f(x) = ((\delta + r') \star (\theta z_\infty))(x) \tag{4.72}$$

that is such that $f_{\mathrm{dr}}(x) = \theta(x)z_\infty(x)$.

Recovering $\mathbb{S}_x[s'(x)]$

The function $f(x)$ has a discontinuity in its derivative of $2z'_\infty(0)$ at $z_L^{-1}(0)$, has limits $(1 + 2r(\infty))\alpha$ at $\pm\infty$, and its dressed function $f_{\mathrm{dr}}(x)$ is $f_{\mathrm{dr}}(x) = \theta(x)z_\infty(x) = \theta(x)s_{\mathrm{dr}}(x)$. Thus its dominant exponential decay at $\pm\infty$ is exactly $-\frac{1}{v_F}$ times that of $s'_{\mathrm{dr}}(x)$. It follows that at leading order

$$\mathbb{S}_x[f(x)] = -\frac{\mathbb{S}_x[s'(x)]}{v_F} + \frac{1}{12L^2} - \alpha\frac{1 + 2r(\infty)}{L}(n_+ + n_-) + \frac{1}{L}\int \left(f(x) + \frac{s'(x)}{v_F}\right)t'_{\mathrm{dr}}(x)dx - \frac{2t(\infty)f(\infty)}{L(1 + 2r(\infty))} \tag{4.73}$$

and so one can deduce $\mathbb{S}_x[s'(x)]$. Integrating by part the $f(x)$ part in the integral in (4.73), with $\int f(x)t_{\mathrm{dr}}(x)dx = \int f_{\mathrm{dr}}(x)t(x)dx$, and using the expression for δI in (4.62), after a bit

119

of rearrangement of the terms in (4.71), it yields

$$
\mathbb{S}_x[s'(x)] = \frac{1}{L} \int s'(x) t'_{\mathrm{dr}}(x) dx - \frac{v_F}{L^2} \left(-\frac{1}{12} + \frac{1 + 2r(\infty)}{4}(n_+ + n_-)^2 + \frac{(n_+ - n_- + 2\varphi)^2}{4(1 + 2r(\infty))} \right.
$$
$$
\left. + t(\infty)(n_+ + n_-) + \frac{t(\infty)^2}{1 + 2r(\infty)} + J_+ + J_- \right)
$$

(4.74)

Thus one concludes that $e_L = -\frac{2\pi}{L} \sum_{i=1}^{K} s'(\lambda_i)$ is

$$
\boxed{
\begin{aligned}
e_L &= -2\pi \int_{-\infty}^{\infty} s'(x) z'_\infty(x) dx - \frac{2\pi}{L} \int_{-\infty}^{\infty} t'(x) z'_\infty(x) dx \\
&\quad + \frac{2\pi v_F}{L^2} \left(-\frac{1}{12} + \frac{1 + 2r(\infty)}{4}(n_+ + n_-)^2 + \frac{(n_+ - n_- + 2\varphi)^2}{4(1 + 2r(\infty))} \right. \\
&\qquad\qquad \left. + t(\infty)(n_+ + n_-) + \frac{t(\infty)^2}{1 + 2r(\infty)} + J_+ + J_- \right) \\
&\quad + o(L^{-2})
\end{aligned}
}
$$

(4.75)

Comparing this formula with (4.64), one sees that v_F is indeed the Fermi velocity[6].

If there is no additional source term $t(\lambda)$, (4.75) shows that the finite-size corrections are those of a boson with Luttinger parameter $K = (1 + 2r(\infty))^{-1} = (2(1 - \gamma/\pi))^{-1}$ for the XXZ spin chain.

Let us illustrate the utility of the additional source term. If there are $L/2$ Bethe roots and no twist and no $t(\lambda)$, then it is seen from the expression of the counting function $z_L(\lambda)$ that the Bethe numbers cannot exceed $\pm L/4$. As a consequence, one cannot form the descendant and Umklapp excitations as usual, since it requires to increase one external Bethe number by 1, and these excitations must be obtained with another root configuration. For instance, the Umklapp state is obtained with $L/2$ roots with $L/2 - 1$ real roots symmetrically distributed, and one root $\lambda = i\pi/2$. This can be understood in the previous setup by setting $t(\lambda) = \frac{i}{2\pi} \log -\frac{\sinh(\lambda + i(\pi/2 - \gamma))}{\sinh(\lambda - i(\pi/2 - \gamma))}$ and having $n_+ + n_- = 1$ and $n_+ - n_- = 0$, and finally adding $-\frac{2\pi s'(i\pi/2)}{L}$ to e_L to form $\tilde{e}_L$ (since the root we removed must be counted in the energy separately). With $t(\infty) = \gamma/\pi$, one finds

$$
\tilde{e}_L = e_\infty + \frac{2\pi v_F}{L^2} \left(-\frac{1}{12} + \frac{1}{2(1 - \gamma/\pi)} \right)
$$

(4.76)

which indeed corresponds to the values $n_+ + n_- = 0$ and $n_+ - n_- = 2$ of an Umklapp state with a usual root configuration.

---

[6] As already mentioned, the most common definition of the energy comes with a multiplicative $\sin \gamma$ that results in multiplying v_F by $\sin \gamma$.

4.4 Strings

4.4.1 Definitions and notations

In the previous section we computed the conformal L^{-2} correction whenever the root configuration can be recast into real roots with continuous functions $s(\lambda)$ and $r(\lambda)$, perturbed by a twist φ/L and an additional odd source term $t(\lambda)/L$. This includes for example an exact (or exponentially approximate) isolated string.

However, there is one case that is regularly encountered in more exotic spin chains and that does not fulfill these conditions. It is the case of a ground state (and excited states) given by a *thermodynamic number* of approximate strings. The simplest example is the spin-$S > 1/2$ XXZ spin chain, that is given by $L/2$ strings composed of $2S$ roots, and whose thermodynamic limit is described by a level $2S$ $su(2)$ Wess-Zumino-Witten model. As explained in the introduction, the finite-size corrections have been calculated with non-linear integral equations [125, 132, 133, 134]; however no derivation without this formalism exists, and in particular it is not understood how to derive it with root densities.

The problematic point is not the fact that the roots are complex per se (the usual spin-1/2 chain with imaginary twist is described by the previous corrections although it has roots with non-zero imaginary part), but rather that they come close to a logarithmic singularity in $r(\lambda)$. Indeed, the Euler-MacLaurin formula (4.11) can be applied to functions with discontinuities (by slicing appropriately the domain of application), but clearly not to functions with divergent singularities, since the correction terms in (4.11) involve the value of the function at the boundaries of the interval where the function is regular.

To be concrete, we consider the Bethe equations for the spin-S XXZ spin chain

$$\left(\frac{\sinh(\lambda_i + i\gamma S)}{\sinh(\lambda_i - i\gamma S)}\right)^L = \prod_{j=1, j\neq i}^{K} \frac{\sinh(\lambda_i - \lambda_j + i\gamma)}{\sinh(\lambda_i - \lambda_j - i\gamma)} \tag{4.77}$$

Inside a string, the roots are separated by $\approx i\gamma$ and are symmetrically distributed with respect to the real axis, see Figure 4.4.
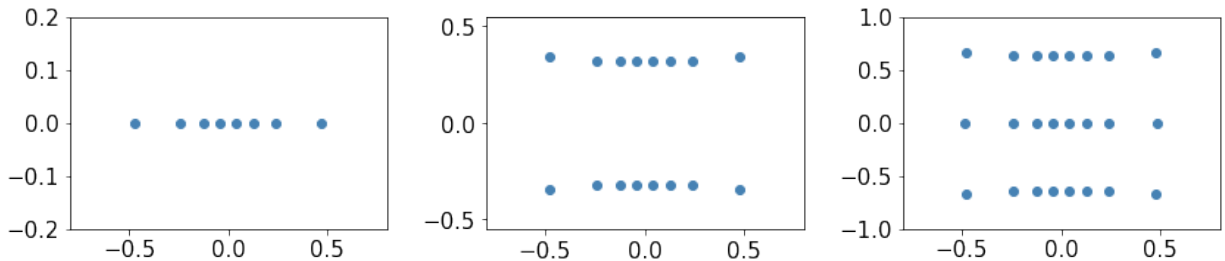

Figure 4.4: Configuration of roots for the ground state of the XXZ spin chain with $\gamma = \pi/5$ in size $L = 16$, for spin 1/2 (left), spin 1 (middle), and spin 3/2 (right).

We introduce the counting function

$$z_L(\lambda) = s(\lambda) - \frac{1}{L} \sum_{j=1}^{K} r(\lambda_i - \lambda_j) \tag{4.78}$$

with

$$s(\lambda) = \frac{i}{2\pi} \log - \frac{\sinh(\lambda + i\gamma S)}{\sinh(\lambda - i\gamma S)}$$

$$r(\lambda) = \begin{cases} \frac{i}{2\pi} \log - \frac{\sinh(\lambda + i\gamma)}{\sinh(\lambda - i\gamma)} & \text{if } |\Im\lambda| < \gamma/2 \\ \frac{i}{2\pi} \log \frac{\sinh(\lambda + i\gamma)}{\sinh(\lambda - i\gamma)} & \text{if } |\Im\lambda| > \gamma/2 \end{cases} \tag{4.79}$$

The function r is such that

$$r(i\gamma \pm \infty) = \mp\gamma/\pi, \qquad r(-i\gamma \pm \infty) = \mp\gamma/\pi \tag{4.80}$$

and is singular around $\pm i\gamma$:

$$r(\lambda \pm i\gamma) \underset{\lambda \to 0}{\sim} \mp \frac{i}{2\pi} \log \lambda \tag{4.81}$$

This way, the Bethe numbers I_i for the ground state (the only state that we will consider) range from $-L/4 + 1/2$ to $L/4 - 1/2$ and each of them is $2S$-fold degenerate: all the roots in a given string have the same Bethe number. The inverse of $z_L(\lambda)$ is thus a multivalued function; we will denote $z_{L,q}^{-1}(x)$ the branch that has values with imaginary part close to $iq\gamma$. As in the real root case, we define the shift δI_q by

$$z_{L,q}^{-1}(0) = -\frac{\delta I_q}{z_\infty'(iq\gamma)L} \tag{4.82}$$

In this case, we will see that the shifts are purely imaginary and are the deviations of the strings with zero real part from their imaginary part in the thermodynamic limit. This is illustrated in Figure 4.5 where we plotted the real and imaginary parts of z_L: the fact that the imaginary part is not constant means that there is a deviation and that it depends on the root. The thermodynamic densities can be computed from (4.78) assuming that the deviation of the strings vanishes in this limit. One gets that $z_\infty'(iq\gamma + x)$ is independent of q, and an explicit (non relevant) expression of its Fourier transform can be obtained.

We define as in the real root case the distribution $\mathbb{S}$ as

$$\mathbb{S}_x[\phi(x)] = \frac{1}{L} \sum_{i=1}^{K} \phi(\lambda_i) - \sum_{q=-S+1/2}^{S-1/2} \int_{-\infty}^{\infty} \phi(iq\gamma + y) z_\infty'(iq\gamma + y) dy \tag{4.83}$$

where we subtracted the limit value when $L \to \infty$ for the ground state.

It is shown that this functional $\mathbb{S}$ enjoys similar properties as in the real root case, but with some local changes due to the fact that there are multiple types of roots distinguished
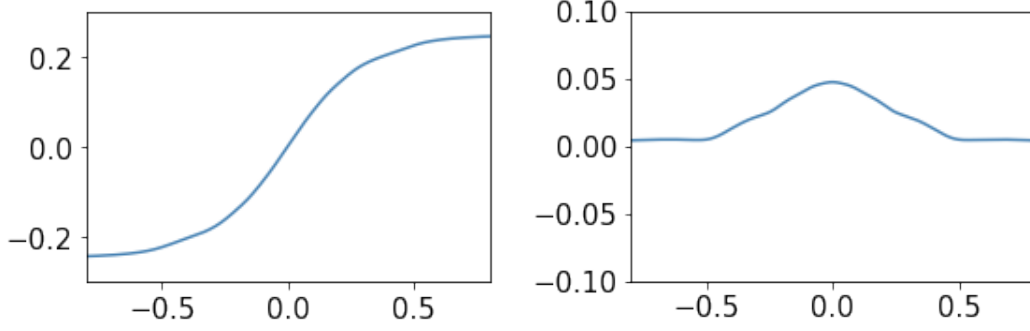
Figure 4.5: Counting function $z_L(x + i\gamma/2 - \delta I_{1/2}/L)$ in size $L = 16$ for the spin-1 XXZ spin chain at $\gamma = \pi/5$, real part (left) and imaginary part (right).

according to their imaginary part. For instance, the dressed function ϕ_{dr} associated to ϕ is defined as the solution of

$$\phi_{\mathrm{dr}}(x) + \sum_{q=-S+1/2}^{S-1/2} \int_{-\infty}^{\infty} \phi_{\mathrm{dr}}(x - y - iq\gamma) z'_\infty(iq\gamma + y) dy = \phi(x) \tag{4.84}$$

One has the analog of (4.58) for an odd function $f(x)$:

$$\mathbb{S}_x[f(x)] = -2 \sum_{q=-S+1/2}^{S-1/2} f(\infty + iq\gamma) \frac{\delta I_q}{L} + o(L^{-1}) \tag{4.85}$$

4.4.2 Riemann sums with logarithmic singularities

In the following lemma we show how the corrections terms to the Riemann sums of logarithms are modified:

Lemma 6. *Let $f(x)$ be a function such that $f(x) - \log x$ is regular (continuous and differentiable), t a purely imaginary complex number[7] and $\epsilon > 0$. The finite-size corrections to the Riemann sum*

$$\frac{1}{L} \sum_{k=-\epsilon L}^{\epsilon L - 1} f(\tfrac{k+t}{L}) \tag{4.86}$$

involve the usual Euler-MacLaurin terms for f, plus Δ_1/L given by

$$\frac{\Delta_1(t)}{L} = \frac{1}{L} \left(sgn\,(\Im t) i\pi\,(t - 1/2) + \log(2 \sin \pi t) \right) + o(L^{-1}) \tag{4.87}$$

---

[7]The formulas also hold for a generic complex t, but up to multiples of $2i\pi$ that come when using $\log(zz') = \log z + \log z' + 2i\pi n$ with $n \in \{-1, 0, 1\}$. However, this dependence does seem to be easily described and is anyway irrelevant for our purposes.

The finite-size corrections to the following double Riemann sum for $\Im t > 0$

$$\frac{1}{L^2} \sum_{k=-\epsilon L}^{\epsilon L - 1} \sum_{p=-\epsilon L}^{\epsilon L - 1} sgn\,(k + 1/2) f(\tfrac{k-p+t}{L}) \tag{4.88}$$

involve the Euler-MacLaurin terms for f, plus Δ_2/L^2 given by

$$\frac{\Delta_2(t)}{L^2} = \frac{1}{L^2} \left(i\frac{Li_2\left(e^{2i\pi t}\right)}{2\pi} - i\pi t^2 + \frac{i\pi t}{2} - t\log(2\sin \pi t) \right) + o(L^{-2}) \tag{4.89}$$

where Li_2 is the dilogarithm.

The proof of this lemma is relegated to appendix A.3.

Let us treat the following example to illustrate the lemma: the function $f(x) = \log \sinh(x)$, which is equivalent to $\log x$ for x close to zero. The Riemann sum of this function cannot be directly computed like the Riemann sum of log. However, the lemma gives the following finite-size correction to the Riemann sum if $\Im t > 0$:

$$\frac{1}{L} \sum_{k=-L}^{L-1} \log \sinh \frac{k+t}{L} = \int_{-1}^{1} \log \sinh x dx + \frac{t-1/2}{L}(\log \sinh 1 - \log \sinh(-1)) + \frac{\Delta_1(t)}{L} + o(L^{-1})$$

$$= \int_{-1}^{1} \log \sinh x dx + \frac{\log(2\sin \pi t)}{L} + o(L^{-1}) \tag{4.90}$$

which is composed of the usual Euler-MacLaurin term, plus the correction Δ_1 coming from the logarithmic singularity.

4.4.3 Computing the shifts δI_q

In this subsection are computed the deviation to the strings, using Lemma 6, yielding the same result as in [123] where they were computed with contour integrals.

As in the real root case, we start by writing

$$z_L(\lambda) = z_\infty(\lambda) - \mathbb{S}_x[r(\lambda - x)] \tag{4.91}$$

and then apply it to λ_i with Bethe number $I_i = 1/2$ and imaginary part $\approx iq\gamma$. We get

$$
\begin{aligned}
z_L(\lambda_i) &= \frac{1}{2L} \\
&= z_\infty(\lambda_i) - \mathbb{S}_x[r(\lambda_i - x)] \\
&= \frac{\frac{1}{2} - \delta I_q}{L} + \mathbb{S}_x[r(-iq\gamma + \tfrac{\delta I_q - \frac{1}{2}}{Lz'_\infty(iq\gamma)} + x)]
\end{aligned}
\tag{4.92}
$$

There are two pieces in $\mathbb{S}_x[r(-iq\gamma + \frac{\delta I_q - \frac{1}{2}}{Lz'_\infty(iq\gamma)} + x)]$: the one coming from the limits at $\pm\infty$, and the one coming from the logarithmic singularity at $i(q\pm 1)\gamma$ that is accounted by (4.87). Thus one has

$$\mathbb{S}_x[r(-iq\gamma + \frac{\delta I_q - \frac{1}{2}}{Lz'_\infty(iq\gamma)} + x)]$$
$$= \sum_{p=-S+1/2}^{S-1/2} \left(-r(i(p-q)\gamma + \infty)\frac{2\delta I_p}{L}\right) + \frac{i}{2\pi L}\Delta_1(\delta I_q - \delta I_{q-1}) - \frac{i}{2\pi L}\Delta_1(\delta I_q - \delta I_{q+1})$$

$$(4.93)$$

if $q \neq \pm(S - 1/2)$, and

$$\mathbb{S}_x[r(-iq\gamma + \frac{\delta I_q - \frac{1}{2}}{Lz'_\infty(iq\gamma)} + x)]$$

$$(4.94)$$

$$= \sum_{p=-S+1/2}^{S-1/2} \left(-r(i(p-q)\gamma + \infty)\frac{2\delta I_p}{L}\right) \mp \frac{i}{2\pi L}\Delta_1(\delta I_q - \delta I_{q\pm 1})$$

if $q = \mp(S - 1/2)$. We now look for a solution such that $\Im(\delta I_{q+1} - \delta I_q) < 0$. By symmetry, we have moreover $\delta I_q = -\delta I_{-q}$. Using $r(iq\gamma + \infty) = -\gamma/\pi$ if $q \neq 0$, and $r(\infty) = 1/2 - \gamma/\pi$, one finds

$$\frac{1}{4} = -\frac{3\delta I_{S-1/2} + \delta I_{S-3/2}}{2} + \frac{i}{2\pi}\log(2\sin\pi(\delta I_{S-1/2} - \delta I_{S-3/2}))$$
$$\frac{1}{2} = -\frac{\delta I_{q+1} + 2\delta I_q + \delta I_{q-1}}{2} + \frac{i}{2\pi}(\log(2\sin\pi(\delta I_q - \delta I_{q-1})) - \log(2\sin\pi(\delta I_q - \delta I_{q+1})))$$
$$\text{for } -S + 1/2 < q < S - 1/2$$
$$\frac{1}{4} = -\frac{3\delta I_{-S+1/2} + \delta I_{-S+3/2}}{2} - \frac{i}{2\pi}\log(2\sin\pi(\delta I_{-S+1/2} - \delta I_{-S+3/2}))$$

$$(4.95)$$

These equations were already solved in [123]. The solution reads

$$\delta I_q = \frac{i}{2\pi}\log\frac{\cos\frac{\pi}{2}\frac{q+1/2}{S+1}}{\cos\frac{\pi}{2}\frac{q-1/2}{S+1}} \tag{4.96}$$

This gives for example $\delta I_{1/2} = -i(\log 2)/(4\pi)$ for spin 1, and $\delta I_1 = -i\log(\frac{1+\sqrt{5}}{2})/(2\pi)$ for spin 3/2.

4.4.4 The energy

Computing $\sum_i |I_i|$

As in the previous cases, to evaluate the energy e_L we compute the sum of the absolute value of the Bethe integers. We are going to get an equation very similar to (4.71). The major difference with the real root case is that when computing $\frac{1}{L}\sum_i z_L(\lambda_i)$ expressed in

terms of r, we encounter double Riemann sums of the type (4.88) because of the logarithmic divergence in r, that will contribute with the terms (4.89). Indeed, defining

$$\theta(x) = \text{sgn}\left(\Re(x)\right) \tag{4.97}$$

if we write

$$\frac{1}{L^2} \sum_i |I_i| = \frac{1}{L} \sum_i |z_L(\lambda_i)|$$

$$= \frac{1}{L} \sum_i \theta(\lambda_i) z_L(\lambda_i) \tag{4.98}$$

$$= \frac{1}{L} \sum_i \theta(\lambda_i) s(\lambda_i) - \frac{1}{L^2} \sum_{i,j} \theta(\lambda_i) r(\lambda_i - \lambda_j)$$

then in the last term we encounter double Riemann sums with a singularity like $\frac{1}{L^2} \sum_{k,p} \text{sgn}\,(k + 1/2) \log \frac{k-p+t}{L}$ with $t = \delta I_q - \delta I_{q+1}$ for $q = -S + 1/2, ..., S - 3/2$ multiplied by $\frac{i}{2\pi}$, and with $t = \delta I_q - \delta I_{q-1}$ for $q = -S + 3/2, ..., S - 1/2$ multiplied by $-\frac{i}{2\pi}$. Using the oddness of r, there are globally Riemann sums with a singularity like $\frac{1}{L^2} \sum_{k,p} \text{sgn}\,(k + 1/2) \log \frac{k-p+t}{L}$ with $t = \delta I_q - \delta I_{q+1}$ for $q = -S + 1/2, ..., S - 3/2$ multiplied by $\frac{i}{\pi}$. Lemma 6 applies and gives

$$\frac{1}{L^2} \sum_i |I_i| = \frac{1}{L} \sum_i \theta(\lambda_i) s(\lambda_i) - \frac{1}{L^2} \sum_{i,j} \theta(\lambda_i) \tilde{r}(\lambda_i - \lambda_j) + \frac{i}{\pi} \sum_{q=-S+1/2}^{S-1/2-1} \Delta_2(\delta I_q - \delta I_{q+1})$$

$$= \frac{1}{L} \sum_i \theta(\lambda_i) z_\infty(\lambda_i) - \frac{1}{L} \sum_i \theta(\lambda_i) \mathbb{S}_x[\tilde{r}(\lambda_i - x)] + \frac{i}{\pi} \sum_{q=-S+1/2}^{S-1/2-1} \Delta_2(\delta I_q - \delta I_{q+1})$$

$$\tag{4.99}$$

where the tilde $\tilde{r}(x)$ indicates that logarithmic singularity at zero has already been taken into account in the finite-size corrections to the Riemann sums. In further appearance of $\tilde{r}(x)$ we shall thus ignore its logarithmic singularity at zero. Equivalently, we could add and subtract a tiny part of width ϵ around zero to $r(x)$ and keep track of all the ϵ terms that shall vanish in the end.

The end of the calculation is then rather similar to the real root case. The first term in (4.99) is

$$\frac{1}{L} \sum_i \theta(\lambda_i) z_\infty(\lambda_i) = \sum_{q=-S+1/2}^{S-1/2} \int_{-\infty}^\infty \theta(x + iq\gamma) z_\infty(x + iq\gamma) z'_\infty(x + iq\gamma) dx + \mathbb{S}_x[\theta(x) z_\infty(x)]$$

$$= \sum_{q=-S+1/2}^{S-1/2} (z_\infty(iq\gamma + \infty))^2 - (z_\infty(iq\gamma + z_{L,q}^{-1}(0)))^2 + \mathbb{S}_x[\theta(x) z_\infty(x)]$$

$$= \frac{S}{8} - \sum_{q=-S+1/2}^{S-1/2} \frac{(\delta I_q)^2}{L^2} + \mathbb{S}_x[\theta(x) z_\infty(x)]$$

$$\tag{4.100}$$

where we used the definition of $\mathbb{S}$ to write the first line, and integrated directly the first term to get the second line.

The second term in (4.99) is

$$- \frac{1}{L} \sum_i \theta(\lambda_i) \mathbb{S}_x[\tilde{r}(\lambda_i - x)]$$

$$= - \sum_{q=-S+1/2}^{S-1/2} \int_{-\infty}^{\infty} \theta(x+iq\gamma) z'_{\infty}(x+iq\gamma) \mathbb{S}_y[\tilde{r}(x+iq\gamma - y)] dx - \mathbb{S}_x[\theta(x)\mathbb{S}_y[\tilde{r}(x-y)]]$$

$$= \sum_{q=-S+1/2}^{S-1/2} \mathbb{S}_y \left[\int_{-\infty}^{\infty} \theta(x+iq\gamma) z_{\infty}(x+iq\gamma) \tilde{r}'(x+iq\gamma - y) dx \right]$$

$$- 2 \sum_{q=-S+1/2}^{S-1/2} \mathbb{S}_y[z_{\infty}(iq\gamma + \infty)\tilde{r}(iq\gamma + \infty) - \tilde{r}(z^{-1}_{L,q}(0) + iq\gamma - y) z_{\infty}(iq\gamma + z^{-1}_{L,q}(0))]$$

$$- \mathbb{S}_x[\theta(x)\mathbb{S}_y[\tilde{r}(x-y)]]$$

$$= \sum_{q=-S+1/2}^{S-1/2} \mathbb{S}_y \left[\int_{-\infty}^{\infty} \theta(x+iq\gamma) z_{\infty}(x+iq\gamma) \tilde{r}'(x+iq\gamma - y) dx \right] - 2 \sum_{q=-S+1/2}^{S-1/2} \frac{(\delta I_q)^2}{L^2}$$

$$- 2 \sum_{q,p=-S+1/2}^{S-1/2} r(i(q-p)\gamma + \infty) \frac{-\delta I_p}{L} \frac{\delta I_q}{L}$$

$$= \sum_{q=-S+1/2}^{S-1/2} \mathbb{S}_y \left[\int_{-\infty}^{\infty} \theta(x+iq\gamma) z_{\infty}(x+iq\gamma) \tilde{r}'(x+iq\gamma - y) dx \right] - \sum_{q=-S+1/2}^{S-1/2} \frac{(\delta I_q)^2}{L^2}$$

$$\tag{4.101}$$

where we used the definition of $\mathbb{S}$ to write the first line; then we performed an integration by part on the the first term of the first line to get the first and second terms of the second line; to get the third line we evaluated in the second line $\mathbb{S}_y[\tilde{r}(y - iq\gamma)] = -\sum_{q'=-S+1/2}^{S-1/2} 2r(\infty + i(q' - q)\gamma)\delta I_{q'} = -\delta I_q$; and then the last line follows from the values of $r(\infty + iq\gamma)$.

Besides, we have

$$\frac{1}{L} \sum_k \frac{|I_k|}{L} = \frac{2S}{L^2} \sum_{k=-L/4}^{L/4-1} |k + \tfrac{1}{2}| = \frac{S}{8} \tag{4.102}$$

From this we conclude

$$\mathbb{S}_x[f(x)] = \frac{2}{L^2} \sum_{q=-S+1/2}^{S-1/2} (\delta I_q)^2 - \frac{i}{\pi} \sum_{q=-S+1/2}^{S-1/2-1} \Delta_2(\delta I_q - \delta I_{q+1}) \tag{4.103}$$

with

$$f(x) = \theta(x) z_{\infty}(x) + \sum_{q=-S+1/2}^{S-1/2} \int_{-\infty}^{\infty} \theta(y+iq\gamma) z_{\infty}(y+iq\gamma) \tilde{r}'(y - x + iq\gamma) dy \tag{4.104}$$

127

that is such that $f_{\mathrm{dr}}(x) = \theta(x)z_\infty(x)$.

Recovering e_L

As in the real root case, we have $s'_{\mathrm{dr}}(x) = z'_\infty(x)$, so that the exponential decay of $f_{\mathrm{dr}}(x) = \theta(x)z_\infty(x)$ is exactly $-1/v_F$ times that of $s'_{\mathrm{dr}}(x)$. The function $f(x + iq\gamma)$ also has a discontinuity in its derivative $2z'_\infty(iq\gamma) = 2z'_\infty(0)$ for each of the $2S$ values of q, due to the part $\theta(x)z_\infty(x)$. There is no logarithmic singularity to evaluate since it was already taken into account in $\tilde{r}$. Thus

$$\mathbb{S}_x[f(x)] = -\frac{\mathbb{S}_x[s'(x)]}{v_F} + \frac{2S}{12L^2} \tag{4.105}$$

so that

$$e_L = e_\infty + \frac{2\pi v_F}{L^2} \left(-\frac{2S}{12} + 2\sum_{q=-S+1/2}^{S-1/2} (\delta I_q)^2 - \frac{i}{\pi} \sum_{q=-S+1/2}^{S-1/2-1} \Delta_2(\delta I_q - \delta I_{q+1}) \right) \tag{4.106}$$

We now use the following Lemma:

Lemma 7. *With $\Delta_2(t)$ given by (4.89) and δI_q given by (4.96), one has the equality:*

$$\frac{i}{\pi} \sum_{q=-S+1/2}^{S-1/2-1} \Delta_2(\delta I_q - \delta I_{q+1}) = -\frac{2S}{12} + \frac{1}{12}\frac{3S}{S+1} + 2\sum_{q=-S+1/2}^{S-1/2} (\delta I_q)^2 \tag{4.107}$$

the proof of which is relegated to appendix A.4. This permits to conclude

$$e_L = e_\infty - \frac{2\pi v_F}{L^2}\frac{3S}{12(S+1)} \tag{4.108}$$

and to identify the central charge

$$c = \frac{3S}{S+1} \tag{4.109}$$

which corresponds to that of a level $2S$ $su(2)$ Wess-Zumino-Witten model.

4.5 Logarithmic corrections

4.5.1 Presentation

Higher-order corrections to the excitation spectrum, for example in the XXZ spin chain, although remarkably predicted with field theory in [103], are not known from a Bethe ansatz approach. If they are admittedly of lesser importance than the L^{-2} corrections since they do not form part of the excitation spectrum in the thermodynamic limit, they are still proportional to the couplings of the irrelevant operators that perturb the theory in a continuum description [22] as explained in Chapter 2. Hence they are not universal in general, but

ratios between them should contain universal quantities such as the structure constants of the underlying CFT.

Among these higher-order corrections, logarithmic corrections [92] play a particularly important role for several reasons: e.g. they modify the correlation functions with a multiplicative logarithm as in (2.123), and they can also be universal corrections that reveal the presence of a continuous spectrum in the thermodynamic limit [139, 140, 141]. Although some of them were computed in particular cases such as the ground state and magnetic excitations of the XXX model [23, 142] with Wiener-Hopf equations, and sometimes corrected later with non-linear integral equations [80], no systematic study of their dependance on the Bethe equations has been carried out. This is the purpose of this section.

At a generic value of γ, the higher-order corrections to formula (4.75) come from subleading exponential decays of the functions we encounter in its derivation. As explained above, since the largest Bethe roots grow as $\frac{\log L}{v_F}$, an exponential decay $e^{-a|\lambda|}$ contribute to a correction of order $O(L^{-1-|\frac{a}{v_F}|})$, which are (generically non integer) powers of L^{-1}.

However, in the limit $\gamma \to 0$ the functions s and r, instead of decaying exponentially fast at infinity, decay *algebraically* as λ^{-1}. These algebraic decay contribute to *logarithmic* corrections of order $O(L^{-1}(\log L)^{-1})$. Such an algebraic decay at infinity for a function $\phi(x)$ translates in discontinuities (in the function or in its derivatives) of its Fourier transform $\hat{\phi}$. In the study of the properties of the distribution $\mathbb{S}$ in section 4.3.2 leading to equation (4.49), the distribution $\mathbb{S}$ should thus be understood in a generalized way where the test functions can have discontinuities (the usual distributions applying only on infinitely differentiable test functions). This generalization has been studied in [143] where one has to take into account a new distribution $\beta(\phi)$ which gives the discontinuity of ϕ at zero. Without entering a detailed exposition of it, it is seen that if a distribution T satisfies $T \cdot f = 0$ with f a function having a discontinuity at zero, i.e. $T(\phi(x)f(x)) = 0$ for all infinitely differentiable test functions $\phi(x)$, then $T(\psi(x))$ can contain a term that gives the discontinuity of $\psi(x)/f(x)$ at zero (since $\phi(x)/f(x) \cdot f(x)$ do not have discontinuities). Hence, the generalization of (4.49) when $\hat{r}$ may have discontinuities (i.e. when r has an algebraic decay at infinity) is

$$\mathbb{S}_x[\phi(x)] = \frac{1}{L}\int_{-\infty}^{\infty}\phi(x)t'_{\mathrm{dr}}(x)dx + \sum_\omega A_\omega \mathrm{Res}_\omega(\hat{\phi}_{\mathrm{dr}}) + \sum_{n\geq 1} B_n^+\{\phi_{\mathrm{dr}}\}_n^+ + B_n^-\{\phi_{\mathrm{dr}}\}_n^- \quad (4.110)$$

where $\{f\}_n^\pm$ denotes the term in λ^{-n} in the algebraic decay of $f(\lambda)$ at $\pm\infty$. $B_n^\pm$ are numbers that depend on L but not on ϕ, and are $O(L^{-1}(\log L)^{-n})$.

In the following, we will consider only symmetric states for which the number of holes in the positive/negative Bethe roots is the same and for which the twist $\varphi = 0$ vanishes, implying $B_n^+ = -B_n^- \equiv B_n$. Moreover, we will study only the first logarithmic correction B_1.

4.5.2 Computing B_1

To compute B_1, we should evaluate $\mathbb{S}$ on a function that has an algebraic decay and for which the value at a Bethe root is known. This is almost the case of $\frac{1}{\log(\alpha/2 - z_L(x))}$ (where we recall that $\pm\alpha/2$ is the limit value of $z_\infty(x)$ at $\pm\infty$): we know its value at a Bethe root, and in the limit $L \to \infty$ it decays as $(v_F x)^{-1}$ at infinity, since $z_\infty(x)$ converges to $\alpha/2$ as $e^{-v_F|x|}$. However, in finite-size there are $1/L$ corrections to the algebraic decay, because of the additional source term $\frac{t(\lambda)}{L}$ that prevent to approximate z_L by z_∞ at order $L^{-1}(\log L)^{-1}$. We thus use the following trick. We add an 'odd' twist ψ to the Bethe equations by defining the counting function $z_L(\lambda)$ as

$$z_L(\lambda) = s(\lambda) + \frac{t(\lambda)}{L} - \frac{1}{L}\sum_{j=1}^{K} r(\lambda - \lambda_j) - \text{sgn}\,(\lambda)\frac{\psi}{L} \tag{4.111}$$

and the Bethe numbers I_i (half-integers) by

$$z_L(\lambda_i) = \begin{cases} \frac{I_i - \psi}{L} & \text{if } I_i > 0 \\ \frac{I_i + \psi}{L} & \text{if } I_i < 0 \end{cases} \tag{4.112}$$

so that the roots λ_i are exactly the same as for the original counting function $z_L(\lambda)$ (the one without ψ) and the original definition of the Bethe numbers.

We can now choose ψ so that $1/L$ correction in terms of λ vanishes when $\lambda \to \infty$. At order $L^{-1}(\log L)^{-1}$ we have

$$z_L(\lambda) = z_\infty(\lambda) + \frac{t(\lambda)}{L} - \frac{1}{L}\int_{-\infty}^{\infty} r(\lambda - x)t_{\text{dr}}(x)dx - \text{sgn}\,(\lambda)\frac{\psi}{L} + o(L^{-1}(\log L)^{-1}) \tag{4.113}$$

because $B_1^+ = -B_1^-$ by assumption, and because r is odd. Thus if we set

$$\psi = \frac{t(\infty)}{1 + 2r(\infty)} \tag{4.114}$$

then we have $z_L(\lambda) = z_\infty(\lambda) + \frac{w(\lambda)}{L} + o(L^{-1}(\log L)^{-1})$, with $w(\lambda) \to 0$ when $\lambda \to \pm\infty$. Hence

$$\mathbb{S}_x\left[\frac{1_{x>0}}{\log(\frac{\alpha}{2} - z_L(x))}\right] = \mathbb{S}_x\left[\frac{1_{x>0}}{\log(\frac{\alpha}{2} - z_\infty(x))}\right] + o(L^{-1}(\log L)^{-1}) \tag{4.115}$$

We now use the following corrections to the singular Riemann sum

Lemma 8. *We have*

$$\frac{1}{L}\sum_{k=n}^{\alpha L/2} \frac{1}{\log(\frac{k+t}{L})} = \int_0^{\alpha/2} \frac{dx}{\log x} + \frac{t - \frac{1}{2}}{L\log(\alpha/2)} + \frac{n + t - \frac{1}{2}}{L\log L} + o(L^{-1}(\log L)^{-1}) \tag{4.116}$$

which is proved in appendix A.5. This yields

$$\mathbb{S}_x \left[\frac{1_{x>0}}{\log(\frac{\alpha}{2} - z_\infty(x))} \right] = \frac{\psi}{\log(\alpha/2)} \frac{1}{L} - \frac{B_1}{v_F(1 + 2r(\infty))} + o(L^{-1}(\log L)^{-1})$$
$$= \frac{\psi}{\log(\alpha/2)} \frac{1}{L} + \frac{n + \psi}{L \log L} + o(L^{-1}(\log L)^{-1}) \tag{4.117}$$

Hence

$$B_1 = -v_F(1 + 2r(\infty)) \frac{n + \psi}{L \log L} \tag{4.118}$$

We note that because of the shift ψ, in this symmetric case $n_+ = n_- = n$, formula (4.56) becomes

$$\mathbb{S}_x[f(x)] = -f(\infty) \frac{n + \psi}{L} - f(-\infty) \frac{n + \psi}{L} + \frac{a_+ A_b + a_- A_{-b}}{L^{1 + |b/v_F|}}$$
$$+ \frac{1}{L} \int_{-\infty}^{\infty} f(x) t'_{\mathrm{dr}}(x) dx - \frac{t(\infty)(f(\infty) + f(-\infty))}{L(1 + 2r(\infty))}$$
$$+ \frac{\Delta f'}{24 z'_\infty(0) L^2}$$
$$+ o(L^{-2}) \tag{4.119}$$

Note that in case of non-symmetric root configurations, the term $\frac{1}{L} \sum_{j=1}^{K} r(\lambda_i - \lambda_j)$ in (4.111) involves $L^{-1}(\log L)^{-1}$ corrections since $B_1^+ \neq -B_1^-$, that cannot be canceled out by introducing a twist and shifting the Bethe numbers because this trick works only at order L^{-1}. This term prevents from writing (4.115) and conclude. We were not able to find a way to go around the problem, but from the symmetric root case we guessed a likely formula in the non-symmetric case that matches the numerics reasonably well.

4.5.3   Logarithmic corrections to the energy

Let us now come back to the different steps in section 4.3.5 for the computation of the L^{-2} correction to the energy levels, and take into account the corrections coming from B_1. We introduce η and η_t the real numbers such that for $\lambda \to \infty$

$$r(\lambda) = r(\infty) - \frac{\eta}{\lambda} + o(\lambda^{-1}), \qquad t(\lambda) = t(\infty) - \frac{\eta_t}{\lambda} + o(\lambda^{-1}) \tag{4.120}$$

- In (4.66) there are no logarithmic correction since no evaluation of $\mathbb{S}$ is performed.

- In (4.67) there is a logarithmic correction to $\frac{1}{L} \mathbb{S}_x[\theta(x)t(x)]$. The function $\theta(x)t(x)$ decays as $\mp \frac{\eta_t}{x}$ when $x \to \pm\infty$, hence the dressed function $(\theta t)_{\mathrm{dr}}(x)$ decays as $\mp \frac{\eta_t}{(1+2r(\infty))x}$ when $x \to \pm\infty$. It follows that there is a logarithmic correction $-2 \frac{B_1 \eta_t}{(1+2r(\infty))L} = 2 v_F \eta_t \frac{n + \psi}{L^2 \log L}$.

131

- In (4.68) there are logarithmic corrections only to the term $\mathbb{S}_y[1_{y>0}\mathbb{S}_x[1_{x<0}r(y-x)]]$ in the symmetric case. This term requires particular care since the decay of the innermost function $x \mapsto 1_{x<0}r(y-x)$ depends on y. There are three types of corrections: the terms coming from $t(\lambda)$, which are bulk contributions, and those coming from the limit value of $r(x)$ and its $1/x$ decay, which are large Bethe roots contributions. Each of the $L^{-2}(\log L)^{-1}$ correction to $\mathbb{S}_y[1_{y>0}\mathbb{S}_x[1_{x<0}r(y-x)]]$ comes from one of these three terms for each $\mathbb{S}$. The correction coming from the $1/x$ decay of the innermost $\mathbb{S}$ and the limit value in large y in the outmost $\mathbb{S}$ both correspond to large Bethe roots of order $O(\log L)$, positive for y and negative for x; hence the decay in $1/x$ is effectively $\frac{\eta}{2x}$, and the total logarithmic correction is $\frac{\eta}{2(1+2r(\infty))}B_1(n+\psi)$. The correction coming from the $t(\lambda)$ term for the innermost $\mathbb{S}$, and the $1/y$ decay for the outmost $\mathbb{S}$ is $\frac{B_1}{L(1+2r(\infty))}\tilde{\eta}$ where $\tilde{\eta}$ is the $1/y$ decay of $\int_{-\infty}^{0} r(y-x)t'_{\mathrm{dr}}(x)dx$, equal to $-\frac{\eta t(\infty)}{1+2r(\infty)}$. The correction coming from the $1/x$ decay of the innermost $\mathbb{S}$ and the $t(\lambda)$ term for the outmost $\mathbb{S}$ is $-\frac{\eta}{1+2r(\infty)}B_1\frac{1}{L}\int_0^{\infty}t'_{\mathrm{dr}}(x)dx = -\frac{B_1\eta}{1+2r(\infty)}\frac{t(\infty)}{1+2r(\infty)}\frac{1}{L}$.

Hence the global logarithmic correction $L^{-2}(\log L)^{-1}$ to the right-hand side of (4.68) and then (4.71) is

$$v_F\eta(n+\psi)^2 + 2v_F(n+\psi)(\eta_t - \eta\frac{2t(\infty)}{1+2r(\infty)}) \tag{4.121}$$

Then, using the value of ψ in (4.114), we conclude that the asymptotic expansion of the energy e_L at order $L^{-2}(\log L)^{-1}$ is given by

$$e_L = -2\pi\int_{-\infty}^{\infty}s'(x)z'_{\infty}(x)dx - \frac{2\pi}{L}\int_{-\infty}^{\infty}t'(x)z'_{\infty}(x)dx + \frac{2\pi v_F}{L^2}\epsilon_L \tag{4.122}$$

where

$$\boxed{\begin{aligned}\epsilon_L = &-\frac{1}{12} + \frac{t_{\infty}^2}{1+2r_{\infty}} + n^2(1+2r_{\infty}) + 2nt_{\infty} \\ &-\frac{v_F}{\log L}\left(\eta n^2 + 2\left(\eta_t - \eta\frac{t_{\infty}}{1+2r_{\infty}}\right)n - 3\eta\left(\frac{t_{\infty}}{1+2r_{\infty}}\right)^2 + 2\eta_t\frac{t_{\infty}}{1+2r_{\infty}}\right)\end{aligned}} \tag{4.123}$$

which is with (4.75) one of the two main results of this chapter. We recall that this analytic derivation applies to symmetric cases $n_+ = n_- = n$ only.

For the generic case $n_+ \neq n_-$ and with a twist φ, together with the L^{-2} correction in (4.75), we conjecture the following plausible formula in reasonable agreement with the numerics:

$$\begin{aligned}\epsilon_L = &-\frac{1}{12} + \frac{t_{\infty}^2}{1+2r_{\infty}} + \frac{(n_+ + n_-)^2}{4}(1+2r_{\infty}) + \frac{(n_+ - n_- + 2\varphi)^2}{4}\frac{1}{1+2r_{\infty}} + t_{\infty}(n_+ + n_-) \\ &-\frac{v_F}{\log L}\left(\eta(n_+ + \varphi)(n_- - \varphi) + \left(\eta_t - \eta\frac{t_{\infty}}{1+2r_{\infty}}\right)(n_+ + n_-) - 3\eta\left(\frac{t_{\infty}}{1+2r_{\infty}}\right)^2 + 2\eta_t\frac{t_{\infty}}{1+2r_{\infty}}\right)\end{aligned}$$
$$\tag{4.124}$$

132

4.5.4 Examples and numerical checks

In this subsection are given numerical checks of formula (4.123). The Bethe equations are solved numerically for sizes up to ≈ 1500, and the results are extrapolated to the thermodynamic limit using a ratio of two polynomials in $\log L$. Many extrapolated results only slightly change with the degrees of the polynomials or with the sizes that are used in the extrapolation; however some cases with a wilder extrapolating curve such as the rightmost case in Figure 4.9 do vary more, although the global shape of the curve is often stable.

Periodic $su(2)$

The periodic $su(2)$ case is obtained with $r(\lambda) = \frac{1}{\pi}\arctan\lambda$ and $t(\lambda) = 0$, hence $v_F = \pi$, $1 + 2r(\infty) = 2$, $t(\infty) = 0$, $\eta = \frac{1}{\pi}$ and $\eta_t = 0$. It yields

$$\epsilon_L = -\frac{1}{12} + 2n^2 - \frac{n^2}{\log L} \tag{4.125}$$

Only this result was already known [23, 142].

Open $su(2)$

The open $su(2)$ case with trivial boundary matrix K has the following Bethe equations

$$\left(\frac{\lambda_i + i/2}{\lambda_i - i/2}\right)^L = \prod_{j\neq i} \frac{\lambda_i - \lambda_j + i}{\lambda_i - \lambda_j - i}\frac{\lambda_i + \lambda_j + i}{\lambda_i + \lambda_j - i} \tag{4.126}$$

where the roots λ_i are strictly positive. One can rewrite it with a usual root configuration μ_i by considering only symmetric root structures, i.e. set of roots that contains $-\mu_i$ if it contains μ_i, and adding the appropriate source term

$$\left(\frac{\mu_i + i/2}{\mu_i - i/2}\right)^L \frac{2\mu_i + i}{2\mu_i - i}\frac{\mu_i + i}{\mu_i - i} = \prod_{j\neq i}\frac{\mu_i - \mu_j + i}{\mu_i - \mu_j - i} \tag{4.127}$$

which is obtained with $r(\lambda) = \frac{1}{\pi}\arctan\lambda$ and $t(\lambda) = \frac{1}{\pi}\arctan 2\lambda + \frac{1}{\pi}\arctan\lambda$, hence $1 + 2r(\infty) = 2$, $t(\infty) = 1$, $\eta = \frac{1}{\pi}$ and $\eta_t = \frac{3}{2\pi}$. For $L/4 - n$ roots λ_i, there are $L/2 - 2n + 1$ roots μ_i, that yield

$$\epsilon_L = -\frac{1}{12} + 2n^2 - \frac{n(n+1)}{\log L} \tag{4.128}$$

133

Figure 4.6: Logarithmic correction to the open $su(2)$ states for $n = 0, 1, 2$ (from left to right). The measured limit value and the theoretical values are indicated above the plots.

Periodic $osp(1|2)$

For periodic $osp(1|2)$ with $L - 1 - 2n$ real roots, one has $v_F = \frac{2\pi}{3}$, $1 + 2r(\infty) = 1$, $t(\infty) = 0$, $\eta = \frac{1}{2\pi}$ and $\eta_t = 0$, that yield

$$\epsilon_L = -\frac{1}{12} + (n + \tfrac{1}{2})^2 - \frac{(n + \frac{1}{2})^2}{3 \log L} \tag{4.129}$$

Figure 4.7: Logarithmic correction to the periodic $osp(1|2)$ states for $n = 0, 1, 2$ (from left to right). The measured limit value and the theoretical values are indicated above the plots.

Periodic $osp(1|2)$ with strings

In case of an exact 2-string at 0 for periodic $osp(1|2)$ with $L - 2 - 2n$ other real roots, one has $1 + 2r(\infty) = 1$, $\eta = \frac{1}{2\pi}$, $t(\lambda) = \frac{1}{\pi} \arctan \lambda - \frac{1}{\pi} \arctan 2\lambda - \frac{1}{\pi} \arctan 2\lambda/3$, hence $t(\infty) = -\frac{1}{2}$, and $\eta_t = -\frac{1}{\pi}$, that yield

$$\epsilon_L = \frac{1}{6} + n(n + 1) - \frac{(n + 1)(n - 2) + \frac{5}{4}}{3 \log L} \tag{4.130}$$
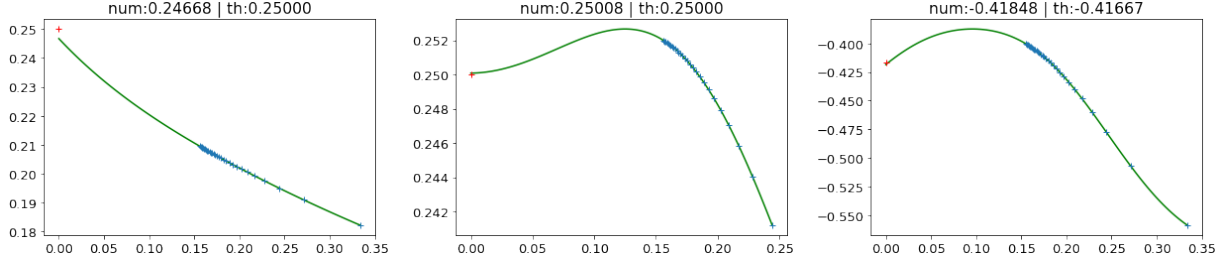
Figure 4.8: Logarithmic correction to the periodic $osp(1|2)$ states with an exact string at 0 for $n = 0, 1, 2$ (from left to right). The measured limit value and the theoretical values are indicated above the plots.

Open $osp(1|2)$

For open $osp(1|2)$ with $L/2 - n$ positive roots, hence $L - 2n + 1$ normal roots, one has $1 + 2r(\infty) = 1$, $\eta = \frac{1}{2\pi}$, $t(\lambda) = \frac{1}{\pi}\arctan\lambda - \frac{1}{\pi}\arctan 4\lambda$, hence $t(\infty) = 0$, and $\eta_t = \frac{3}{4\pi}$, that yield

$$\epsilon_L = -\frac{1}{12} + (n - \tfrac{1}{2})^2 - \frac{(n - \tfrac{1}{2})(n + \tfrac{5}{2})}{3\log L} \tag{4.131}$$
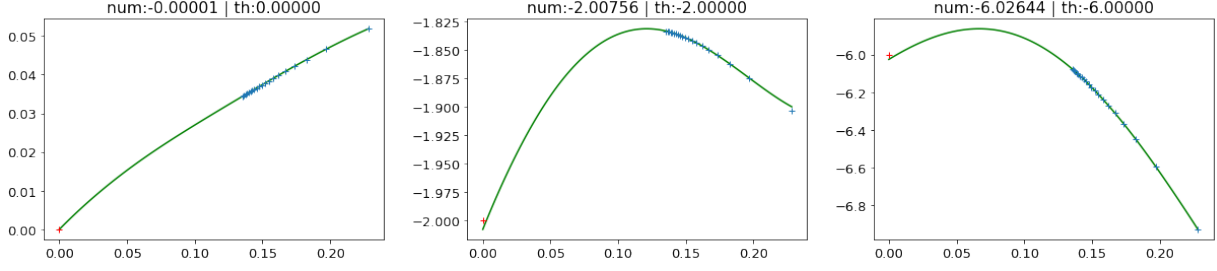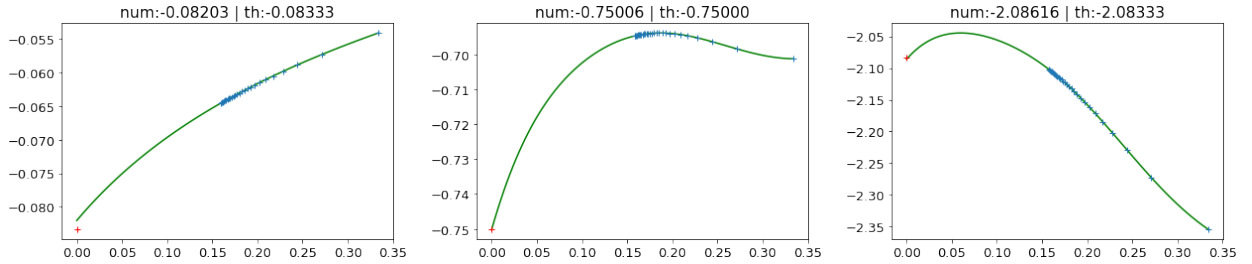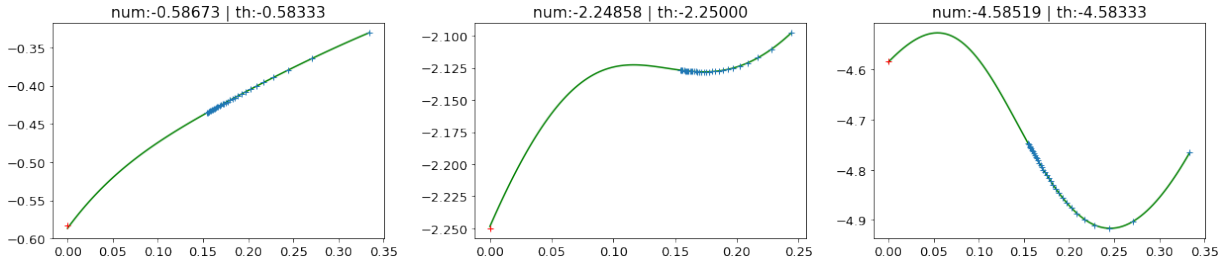

Figure 4.9: Logarithmic correction to the open $osp(1|2)$ for $n = 0, 1, 2$ (from left to right). The measured limit value and the theoretical values are indicated above the plots.

An asymmetric case

In order to give some numerical support to the conjectured general formula (4.124), we consider the $osp(1|2)$ case with $L/2 - n_\pm$ positive/negative roots, perturbed by $t(\lambda) = \frac{1}{\pi}\arctan\lambda$ with a twist φ. Formula (4.124) would give

$$\epsilon_L = -\frac{1}{12} + \frac{(n_+ + n_-)^2}{4} + \frac{(n_+ - n_- + 2\varphi)^2}{4} + \frac{n_+ + n_-}{2} - \frac{(n_+ + \varphi)(n_- - \varphi) + \frac{3}{2}(n_+ + n_-) + \frac{5}{4}}{3\log L} \tag{4.132}$$

135

Figure 4.10: Logarithmic correction for $osp(1|2)$ perturbed by $t(\lambda) = \frac{1}{\pi}\arctan\lambda$, for $(n_+ = \frac{1}{2}, n_- = \frac{1}{2}, \varphi = \frac{1}{2})$, $(n_+ = \frac{13}{2}, n_- = \frac{5}{2}, \varphi = 0)$, $(n_+ = \frac{13}{2}, n_- = \frac{5}{2}, \varphi = -1)$ (from left to right). The measured limit value and the theoretical values are indicated above the plots.

Chapter 5

Series expansions and magnetic field influence

5.1   Introduction

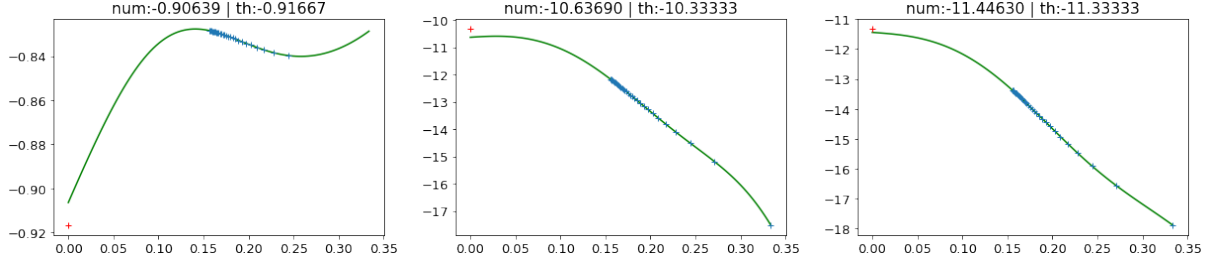This chapter is devoted to the study of magnetic field or anisotropy influence, and to the series expansions that we show permit to study it. The motivations are threefold.

Firstly, adding external sources is a way of probing the physical behavior of a system since it can either smoothly modify critical properties such as critical exponents, or drastically modify its continuum limit, by e.g. driving a non-critical system into a critical phase – this is for example the case of the XXZ chain with anisotropy $\Delta > 1$ that is driven out of a non-critical Néel phase into a paramagnetic critical phase. Although it is possible to write integral equations for root densities [144, 138, 28, 145] to compute physical quantities such as the acquired magnetization, the solution of these can be done only numerically and their numerical evaluation is rather indirect. In the first section of this chapter we show that for the XXZ spin chain in a magnetic field h, the acquired magnetization as well as the critical exponents can be written as a series in $\sqrt{h_c - h}$ where h_c is the smallest field for which the spin chain is fully polarized, whose coefficients are a rational function of π and Δ and can be computed exactly with a recurrence relation that involves only algebraic manipulations [48]. These series are new, and give to the old problem of the acquired magnetization of the Heisenberg spin chain [144] an answer that is the closest ever to an explicit analytic solution.

Secondly, on the statistical mechanics side, particular boundary conditions can naturally bring the system into a position-dependent anisotropy, which corresponds to a position and time-dependent magnetic field in the associated quantum system. This is the case of *limit shape* phenomena such as *arctic curves*, denoting a boundary-conditions-induced geographic separation of regions that lie in a different critical phase, although ruled by the same microscopic Boltzmann weights, and that occurs for example in the six-vertex model with domain wall boundary conditions [146, 147, 148]. The mean value of the magnetization within the arctic curve where the system is critical and not frozen is position-dependent, so that a coarse-grained approach naturally involves the free energy of the system at non-

zero magnetizations. This is the object of the third section of this chapter, where we study especially numerically the field theory description of the fluctuations inside the critical region of the six-vertex model with domain wall boundary conditions in the interacting case $\Delta \neq 0$. In the free fermion case it was proved to be given by a Gaussian Free Field [149, 150]; we yield evidence that in the interacting case that they are governed by an *inhomogeneous* Gaussian Free Field, i.e. a GFF with a position-dependent coupling constant [49]. This section is only weakly connected to the two other sections, and can be considered as a project on its own.

Thirdly, it is often observed in integrable systems that a non-zero magnetic field *regularizes* many quantities. This is probably best illustrated by the calculation of correlation functions in the XXZ spin chain from form factors formulas [151, 152, 12, 153, 154, 155, 156, 16, 157, 14], where both on the analytic and numerical sides the first results were obtained in a non-zero magnetic field, for example because the excitation structure above the ground state is much simpler in this case. From many points of view the non-zero magnetic field case is the *generic* case, much like considering inhomogeneities for the form factors computations, from which the limit of zero magnetic field can be taken. This principle is in a sense adopted in the second section, where we present some intermediate results on a still ongoing project about an integrable non-compact spin chain [158, 8, 159, 160]. The objective is to try another approach for the study of its large size behaviour, by taking the thermodynamic limit *before* analytically continuing certain parameters, whereas the standard approach is to perform an analytic continuation on the system in finite size. It brings us to the study of the analytic continuation of the free energy as a function of the magnetization, that we try to tackle with the series expansions previously derived.

5.2 The XXZ spin chain in a magnetic field

5.2.1 Historical review

We recall that the Hamiltonian of the XXZ spin chain reads

$$H = \sum_{i=1}^{N} \sigma_i^x \sigma_{i+1}^x + \sigma_i^y \sigma_{i+1}^y + \Delta(\sigma_i^z \sigma_{i+1}^z - \tfrac{1}{4}) - h\sigma_i^z \tag{5.1}$$

However widely studied this model is, the simple and physically relevant question of the magnetization acquired by the spin chain when put in an external magnetic field is still unsolved [144, 161]. It is equivalent to finding the free energy of the chain at any mean magnetization per site $-1/2 \leq \langle \sigma_i^z \rangle \leq 1/2$. Although a root density approach allows to find a closed form expression for the free energy at zero magnetization [137, 162], it does not permit to derive a magnetization-dependent expression. In this approach indeed, one needs to solve a so-called Wiener-Hopf equation on a finite interval [144, 138, 28, 145, 163]

$$\rho(x) + \int_{-\Lambda}^{\Lambda} \rho(t) r'(x-t) dt = s'(x) \tag{5.2}$$

where the unknown is ρ, while r and s are given, and $0 < \Lambda < +\infty$ is the largest Bethe root, related to the magnetization $\langle \sigma_i^z \rangle$ by $\int_{-\Lambda}^{\Lambda} \rho(t) dt = \frac{1}{2} - \langle \sigma_i^z \rangle$. The equation holds for all values of x and no periodicity of s and r is assumed (contrarily to the case $\Delta > 1$ where a similar equation holds at zero magnetic field, but with periodic s and r). This equation is equivalent to a two-dimensional classical Wiener-Hopf equation written in (4.4), for which no generic solution is known as we already explained [121, 122]. In the first paper where this problem was addressed [144], equation (5.2) was solved numerically for several values of the magnetization $\langle \sigma_i^z \rangle$ (i.e., several values of Λ), so that to know the free energy $F(\sigma)$ at generic magnetization σ with good precision; the magnetization curve $\sigma(h)$ is then computed numerically by taking the derivative of the Legendre transform of this function. Hence, even the numerical solution of the problem is rather indirect.

On the analytic side, only a first-order perturbation around zero magnetic field could be performed in this approach for various physical quantities [162, 164, 28, 165]. Since the first appearance of this approach in [144], apart from some works at finite temperature [166], no alternative method seems to have been tried.

In this section we present a different approach that expresses the free energy as a power series in $1/2 - \langle \sigma_i^z \rangle$, whose coefficients can be recursively computed in an explicit closed form with only algebraic manipulations. It leads to an expansion of the acquired magnetization of the chain in a magnetic field h, in terms of $\sqrt{h_c - h}$ where h_c is the smallest field for which the ground state is fully polarized. The calculation does not use root densities and is actually quite simple. The Bethe roots are written as a double power series in their corresponding Bethe number and in $1/2 - \langle \sigma_i^z \rangle$. The Bethe equations are then nothing but a recurrence relation on these coefficients. Surprisingly, this approach has not been tried before. Only the first coefficient in front of $\sqrt{h_c - h}$ was known [167, 168, 138], or the first two ones in similar models for other physical quantities [169].

The method presumably works for a large class of models. As an example we present another case where the Bethe roots lie on a curve in the complex plane, and derive similarly a power series for the free energy.

5.2.2 The Bethe equations as a recurrence relation

We consider Bethe equations written in logarithmic form for K roots λ_i (K even):

$$s(\lambda_i) = \frac{I_i}{L} + \frac{1}{L} \sum_{j=1}^{K} r(\lambda_i - \lambda_j) \tag{5.3}$$

with $I_i = -K/2 + 1/2, ..., K/2 - 1/2$ increasing half-integers. s and r are functions depending on the model, that are assumed to be odd and satisfy $s'(0) \neq 0$. Our goal is to compute the free energy

$$F = -\frac{2\pi}{L} \sum_{i=1}^{K} s'(\lambda_i) \tag{5.4}$$

in the limit $L \to \infty$, with K/L finite[1]. We set

$$\alpha_i = \frac{I_i}{L}, \qquad m = \frac{K}{L} = \frac{1}{2} - \langle \sigma_i^z \rangle \tag{5.5}$$

and first assume that all the λ_i and $\lambda_i - \lambda_j$ lie within the radius of convergence of s and r respectively as a power series around 0. The starting point is to write each λ_i as a power series in α_i and m:

$$\lambda_i = \sum_{a,b \geq 0} \alpha_i^a m^b c_{ab} \tag{5.6}$$

with c_{ab} some coefficients to determine. For convenience, we will use the notations for $n \geq 1$

$$\lambda_i^n = \sum_{a,b \geq 0} \alpha_i^a m^b c_{ab}^{[n]}, \qquad \text{where } c_{ab}^{[n]} = \sum_{\substack{a_1+\ldots+a_n=a \\ b_1+\ldots+b_n=b}} c_{a_1 b_1} \ldots c_{a_n b_n} \tag{5.7}$$

By definition we set $c_{00}^{[0]} = 1$, the other coefficients $c_{ab}^{[0]}$ being zero. Expanding $s(\lambda_i)$ yields

$$s(\lambda_i) = \sum_{a,b \geq 0} \alpha_i^a m^b \sum_{n \geq 0} \frac{s^{(n)}(0)}{n!} c_{ab}^{[n]} \tag{5.8}$$

Similarly for $r(\lambda_i - \lambda_j)$:

$$r(\lambda_i - \lambda_j) = \sum_{n \geq 0} \frac{r^{(n)}(0)}{n!} \sum_{q=0}^{n} (-1)^q \binom{n}{q} \sum_{a_1,a_2,b_1,b_2 \geq 0} \alpha_j^{a_1} m^{b_1} \alpha_i^{a_2} m^{b_2} c_{a_1 b_1}^{[q]} c_{a_2 b_2}^{[n-q]} \tag{5.9}$$

Now one has for even a

$$\frac{1}{L} \sum_{j=1}^{K} \alpha_j^a = \frac{2}{L^{a+1}} \sum_{j=1}^{K/2} (j - \tfrac{1}{2})^a = \frac{m^{a+1}}{2^a (a+1)} + O(L^{-1}) \tag{5.10}$$

while for a odd it is zero. This gives

$$\frac{1}{L} \sum_{j=1}^{K} r(\lambda_i - \lambda_j) = \sum_{a,b \geq 0} \alpha_i^a m^b \sum_{\substack{a_1+b_1+b_2+1=b \\ a_1 \text{ even}}} \sum_{n \geq 0} \frac{r^{(n)}(0)}{n!} \sum_{q=0}^{n} (-1)^q \binom{n}{q} \frac{c_{a_1 b_1}^{[q]} c_{ab_2}^{[n-q]}}{2^{a_1}(a_1+1)} \tag{5.11}$$

Since $c_{00} = 0$, each $c_{ab}^{[n]}$ depends on $c_{a'b'}^{[n-1]}$ with $a' \leq a$, $b' \leq b$, and at least $a' < a$ or $b' < b$. Thus one gets the following recurrence relation

$$c_{ab} = \frac{1}{s'(0)} \left(\sum_{\substack{a_1+b_1+b_2+1=b \\ a_1 \text{ even}}} \left(\sum_{n \geq 0} \frac{r^{(n)}(0)}{n!} \sum_{q=0}^{n} (-1)^q \binom{n}{q} \frac{c_{a_1 b_1}^{[q]} c_{ab_2}^{[n-q]}}{2^{a_1}(a_1+1)} \right) - \sum_{n \geq 2} \frac{c_{ab}^{[n]} s^{(n)}(0)}{n!} \right) \tag{5.12}$$

---

[1]The fact that the free energy is defined in terms of the same function s as in the Bethe equations is clearly not a constraint of the method, and it could be defined in terms of another function f as well.

with the initial conditions $c_{00} = 0$, $c_{10} = \frac{1}{s'(0)}$. Since $c_{ab}^{[n]} = 0$ for n large enough at fixed a, b, all the sums on the right-hand side are in fact finite sums. Note that c_{ab} depends on $c_{a'b'}$ with either (i) $a' \leq \max(b-1, a)$ and $b' \leq b-1$, and if $a' > a$ then $a' + b' \leq b-1$; or (ii) $b' = b$ and $a' < a$. In both cases one has $a' + b' < a + b$. Thus one can compute the c_{ab}'s by computing $c_{d-b,b}$ for increasing b's, and then increasing d's.

The free energy $F(m)$ is now

$$F(m) = -\frac{2\pi}{L} \sum_{i=1}^{K} \sum_{n \geq 0} \frac{s^{(n+1)}(0)}{n!} \sum_{a,b \geq 0} \alpha_i^a m^b c_{ab}^{[n]} \tag{5.13}$$

This gives the expansion

$$F(m) = \sum_{a \geq 0} m^a f_a$$

$$\text{with} \quad f_a = -\frac{\pi}{2^{a-1}} \sum_{\substack{b=0 \\ a-b \text{ odd}}}^{a} \frac{2^{b+1}}{a-b} \sum_{n \geq 0} \frac{s^{(n+1)}(0)}{n!} c_{a-b-1,b}^{[n]} \tag{5.14}$$

The calculation assumes that λ_i and $\lambda_i - \lambda_j$ lie within the radius of convergence of s and r; however it may happen that the resulting series $F(m)$ has a larger radius of convergence. If the free energy has the property of being expandable in a power series in all the physical range of m, then the two expressions must coincide for all m.

5.2.3   Example: the Heisenberg spin chain

The free energy

For the Heisenberg spin chain one has the functions

$$s(\lambda) = \frac{1}{\pi} \arctan 2\lambda, \qquad r(\lambda) = \frac{1}{\pi} \arctan \lambda \tag{5.15}$$

with

$$s^{(2n+1)}(0) = \frac{(-1)^n (2n)! 2^{2n+1}}{\pi}, \qquad r^{(2n+1)}(0) = \frac{(-1)^n (2n)!}{\pi} \tag{5.16}$$

Applying (5.12) and plugging the c's into (5.14), one directly finds the expansion

$$
\begin{aligned}
F(m) = {}&{-}4m + \frac{\pi^2}{3} m^3 + \frac{\pi^2}{3} m^4 + \left(-\frac{\pi^4}{60} + \frac{\pi^2}{4} \right) m^5 + \left(-\frac{\pi^4}{36} + \frac{\pi^2}{6} \right) m^6 \\
&+ \left(\frac{\pi^6}{2520} - \frac{\pi^4}{36} + \frac{5\pi^2}{48} \right) m^7 + \left(\frac{\pi^6}{1440} - \frac{\pi^4}{48} + \frac{\pi^2}{16} \right) m^8 \\
&+ \left(-\frac{\pi^8}{181440} + \frac{23\pi^6}{34560} - \frac{7\pi^4}{576} + \frac{7\pi^2}{192} \right) m^9 + O(m^{10})
\end{aligned}
\tag{5.17}
$$

and it can be readily continued from the recurrence relation. For example we computed the first 40 terms analytically with a computer (though we only present here the first few terms), and the first 100 terms numerically. We numerically observe that the radius of convergence of this series is $1/2$, i.e. it converges for all physical values of m. The expansion converges exponentially fast with the number of terms when $m < 1/2$, and quadratically (possibly with a multiplicative logarithmic correction) for $m = 1/2$. See Table 5.1 for a comparison with the direct numerical solution of the Bethe roots in finite size L (the extrapolation is linear in $1/L$ using sizes 3000 and 5000).

	$m = 0.05$	$m = 0.1$	$m = 0.2$	$m = 0.4$	$m = 0.5$
$L = 1000$	0.19956813	0.39637426	0.76823447	1.30357831	1.38629600
$L = 3000$	0.19956797	0.39637394	0.76823379	1.30357701	1.38629454
$L = 5000$	0.19956796	0.39637391	0.76823374	1.30357690	1.38629442
Extrapolation	0.19956794	0.39637388	0.76823366	1.30357675	1.38629425
20-term expansion	0.19956795	0.39637390	0.76823371	1.30357732	1.38641192

Table 5.1: The free energy $-F(m)$ of the Heisenberg model for different magnetizations.

For $m = 1/2$, we already know from the root density approach that $F(1/2) = -2\log 2$. It is a very non-trivial check of the validity of our approach that (5.17) converges to this value, see Figure 5.1. It is worth noting that although (5.12) assumes that the Bethe roots and their differences lie within the radius of convergence of s and r (which are $1/2$ and 1), the resulting series still converges at some values of m for which this property is not true anymore.
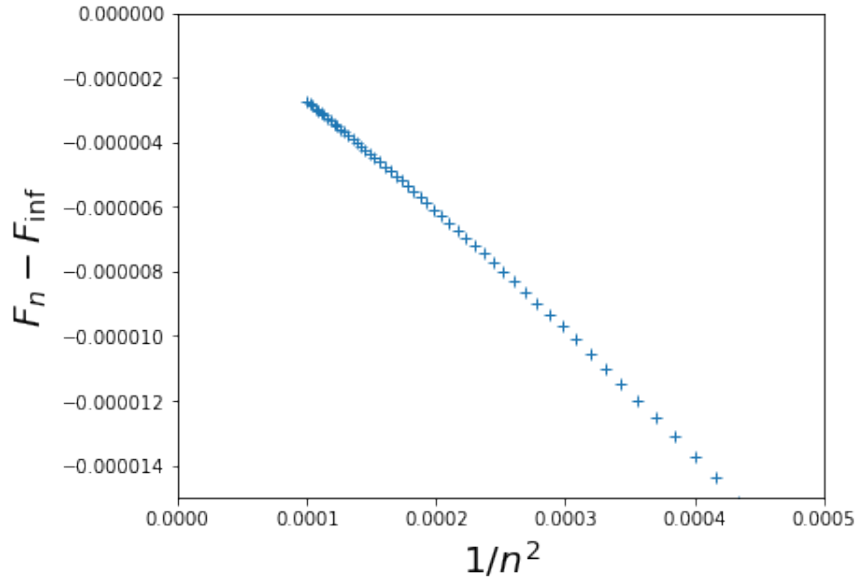

Figure 5.1: Difference between the series F_n truncated after the nth term and its known exact limit value $F_{\text{inf}} = F(1/2)$, as a function of $1/n^2$.

The acquired magnetization in a magnetic field

Let us denote now $-1/2 \leq \sigma \leq 1/2$ the mean magnetization per site of a state, i.e. the value of $\langle \sigma_i^z \rangle$ where σ_i^z is the spin operator in the z direction at site i, on a spin chain with L sites. As already mentioned, it is related to m through

$$\sigma = \frac{1}{2} - m \tag{5.18}$$

The energy e_m of the ground state of the sector with magnetization σ is

$$e_m = F(m) - (1/2 - m)h \tag{5.19}$$

If the minimum of e_m is obtained for $0 < m^* < 1/2$ then

$$m^* = (-F')^{-1}(h) \tag{5.20}$$

For $h = 4$ one sees that $m^* = 0$ and so for $h > h_c = 4$ the ground state is fully polarized $\sigma^* \equiv 1/2 - m^* = 1/2$. For $h < h_c$ one has the following expansion in $\sqrt{h_c - h}$ of the acquired magnetization σ^* of the chain[2]:

$$
\begin{aligned}
\sigma^* =& \frac{1}{2} - \frac{1}{\pi}(h_c - h)^{1/2} + \frac{2}{3\pi^2}(h_c - h) - \left(\frac{35}{72\pi^3} + \frac{1}{24\pi}\right)(h_c - h)^{3/2} + \left(\frac{10}{27\pi^4} + \frac{1}{12\pi^2}\right)(h_c - h)^2 \\
&- \left(\frac{1001}{3456\pi^5} + \frac{7}{64\pi^3} + \frac{3}{640\pi}\right)(h_c - h)^{5/2} + \left(\frac{56}{243\pi^6} + \frac{10}{81\pi^4} + \frac{1}{72\pi^2}\right)(h_c - h)^3 \\
&- \left(\frac{46189}{248832\pi^7} + \frac{3575}{27648\pi^5} + \frac{123}{5120\pi^3} + \frac{5}{7168\pi}\right)(h_c - h)^{7/2} \\
&+ \left(\frac{110}{729\pi^8} + \frac{7}{54\pi^6} + \frac{13}{384\pi^4} + \frac{103}{40320\pi^2}\right)(h_c - h)^4 + O((h_c - h)^{9/2})
\end{aligned}
\tag{5.21}
$$

The expansion can be continued as far as desired (we computed it exactly until order $(h_c - h)^{20}$). Only the first term $-\frac{1}{\pi}(h_c - h)^{1/2}$ was already known [167, 168, 138]. In the case of an integer-spin chain in a magnetic field, only the first two terms of a similar expansion for quantities such as the susceptibility were computed by different means [169].

5.2.4 Example: the XXZ spin chain

For the XXZ spin chain with anisotropy parameter $-1 < \Delta < 1$ one has

$$s(\lambda) = \frac{1}{\pi}\arctan\left(\sqrt{\frac{1+\Delta}{1-\Delta}}\tanh\lambda\right), \qquad r(\lambda) = \frac{1}{\pi}\arctan\left(\frac{\Delta}{\sqrt{1-\Delta^2}}\tanh\lambda\right) \tag{5.22}$$

---

[2]The star merely distinguishes the acquired magnetization σ^* from the generic variable σ.

and the free energy is defined with a multiplicative factor $\sqrt{1 - \Delta^2}$ in (5.4) to match usual conventions. Applying the same recipe as before one finds

$$F(m) = -2(1 + \Delta)m + \frac{\pi^2}{3}m^3 + \frac{2\pi^2\Delta}{3(1 + \Delta)}m^4 - \frac{4\pi^2}{(1 + \Delta)^2}\left(\frac{\pi^2}{240} + \frac{\pi^2\Delta}{120} + \Delta^2\left(\frac{\pi^2}{240} - \frac{1}{4}\right)\right)m^5$$
$$- \frac{8\pi^2\Delta}{(1 + \Delta)^3}\left(\frac{\pi^2}{90} + \frac{\pi^2\Delta}{120} + \Delta^2\left(\frac{\pi^2}{120} - \frac{1}{6}\right)\right)m^6 + O(m^7)$$

$$(5.23)$$

The application of the recurrence relation is not more costly than in the case $\Delta = 1$, so a 100-term expansion is reachable. As in the isotropic case, the radius of convergence of this series is observed to be $1/2$. The value $F(1/2)$ can be computed exactly with root densities, see e.g. [145]:

$$F(1/2) = -\sin\gamma \int_{-\infty}^{\infty} \frac{\sinh((\frac{\pi}{2} - \frac{\gamma}{2})x)^2}{\sinh(\frac{\pi x}{2})(\sinh(\frac{\pi x}{2}) + \sinh((\frac{\pi}{2} - \gamma)x))}dx, \quad \text{with } \Delta = \cos\gamma \quad (5.24)$$

See Table 5.2 and Figure 5.2 for the numerical verification of this expansion and of its radius of convergence, for $\Delta = \cos \pi/5$.

	$m = 0.05$	$m = 0.1$	$m = 0.2$	$m = 0.4$	$m = 0.5$
$L = 1000$	0.18406350	0.36172387	0.69569657	1.16699132	1.23606951
$L = 3000$	0.18166924	0.35938627	0.69361200	1.16608443	1.23606814
$L = 5000$	0.18119035	0.35891867	0.69319488	1.16590255	1.23606804
Extrapolation	0.18047201	0.35821726	0.69256920	1.16562972	1.23606787
18-term expansion	0.18047200	0.35821721	0.69256908	1.16562930	1.23605814

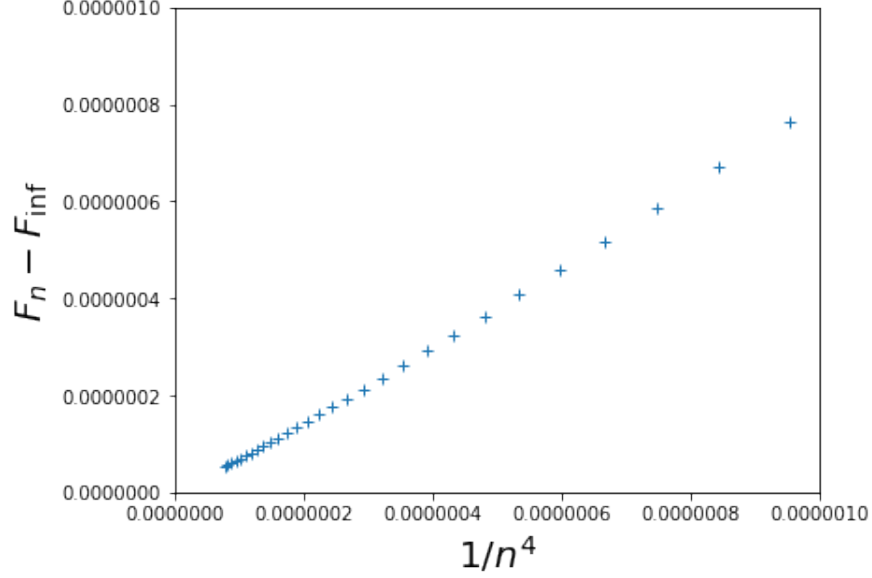Table 5.2: The free energy $-F(m)$ of the XXZ spin chain for different magnetizations, for $\Delta = \cos \pi/5$.

Figure 5.2: Difference between the series F_n truncated after the nth term and its known exact limit value $F_{\text{inf}} = F(1/2)$, as a function of $1/n^4$, for $\Delta = \cos \pi/5$.

Here the critical magnetic field is $h_c = 2(1 + \Delta)$ [138]. The expression for the acquired magnetization is

$$
\begin{aligned}
\sigma^* = {} & \frac{1}{2} - \frac{1}{\pi}(h_c - h)^{1/2} + \frac{4\Delta}{3\pi^2(1 + \Delta)}(h_c - h) \\
& - \frac{1}{72\pi^3(1 + \Delta)^2}\left(3\pi^2 + 6\pi^2\Delta + \left(140 + 3\pi^2\right)\Delta^2\right)(h_c - h)^{3/2} \\
& + \frac{\Delta}{135\pi^4(1 + \Delta)^3}\left(9\pi^2 + 63\pi^2\Delta + (400 + 18\pi^2)\Delta^2\right)(h_c - h)^2 + O((h_c - h)^{5/2})
\end{aligned}
\tag{5.25}
$$

Only the first term $-\frac{1}{\pi}(h_c - h)^{1/2}$ was already known [138, 170].

5.2.5 Radius of convergence of the series $\sigma^*(\sqrt{h_c - h})$

Although we have strong arguments in favour of the convergence of $F(m)$ as a series in m in the full physical range $0 \leq m \leq 1/2$, this does not ensure that the derivative of its Legendre transform $\sigma^*(\sqrt{h_c - h})$ has a similar property, i.e. that σ^* as a series in $\sqrt{h_c - h}$ converges in the range $0 \leq h \leq h_c$. Let us denote h_r (that depends on Δ) the smallest field for which this series converges in $h_r < h \leq h_c$.

Let us first look at the free fermion case $\Delta = 0$. In this case $r = 0$ in (5.22), so that the free energy $F(m)$ can be computed exactly

$$
F(m) = -2\pi \int_{-m/2}^{m/2} s'(s^{-1}(x))dx
\tag{5.26}
$$

145

From this one deduces $h_c = 2$ and

$$\sigma^*(\sqrt{h_c - h}) = \frac{1}{2} - \frac{2}{\pi} \arctan \sqrt{\frac{h_c - h}{h_c + h}} \tag{5.27}$$

which actually has a radius of convergence $\sqrt{2h_c}$, so that the expansion converges for $-h_c < h \le h_c$ and $h_r = -h_c$. For regularity reasons, it ensures that we must have $h_r < 0$ for Δ in a neighbourhood of 0. A strong check of $h_r < 0$ is to evaluate the series at $h = 0$, where one must have $\sigma^* = 0$. For values of Δ not close to 1, this is indeed observed, see Figure 5.3 for $\Delta = \cos 2\pi/5$ where the acquired magnetization is of order 10^{-7} at zero magnetic field, taking into account 60 terms in the expansion. At least for $\Delta \lesssim 0.6$ this convergence at $h = 0$ is observed to hold with precision better than 10^{-3}.
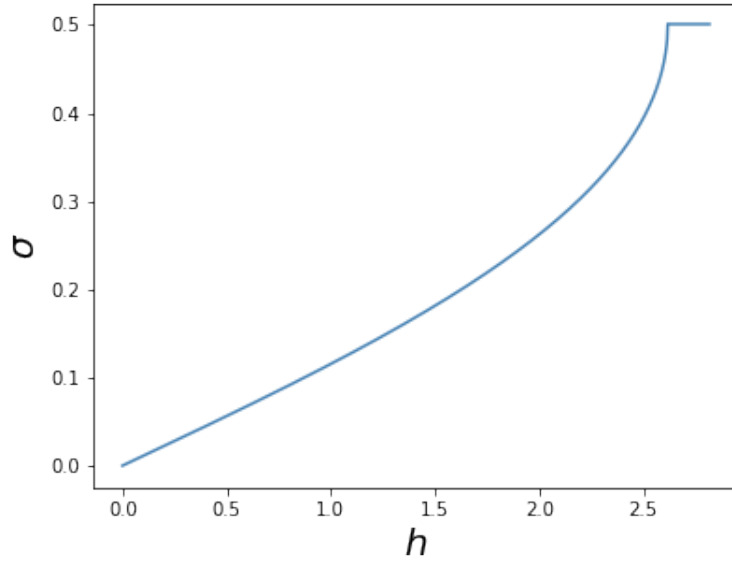
Figure 5.3: Acquired magnetization σ^* as a function of the magnetic field h, using an expansion with 60 terms, with $\Delta = \cos 2\pi/5$.

However, at larger values of Δ, in particular at $\Delta = 1$, the truncated series $\sigma^*(\sqrt{h_c - h})$ keeps oscillating for small magnetic fields with the order of the truncation. Although this is not uncommon in convergent series (the truncated series of $(1 + x)^{-1}$ keeps oscillating too near $x = 1$), it might also mean that $h_r > 0$. To investigate this question further, in Figure 5.4 we plotted $R_n = \exp{-\frac{\log |a_n|}{n}}$ where a_n is the nth term of σ^* as a series in $\sqrt{h_c - h}$, for $\Delta = \cos \pi/5$ and $\Delta = 1$. The series converges at $h = 0$ if there is only a finite number of points under the line $\sqrt{h_c}$. This suggests that it is not convergent at $h = 0$ for Δ close to 1, and that we would have $h_r > 0$ at $\Delta = 1$.
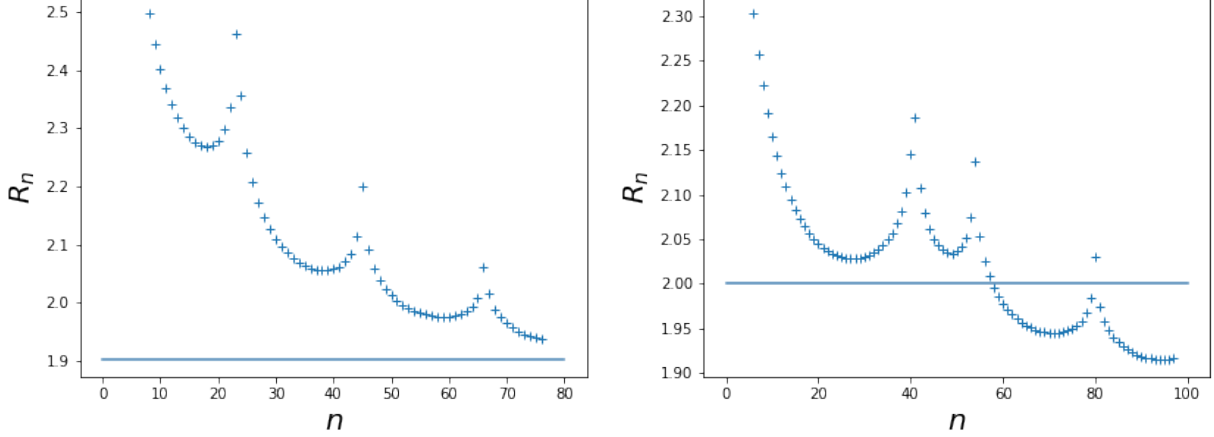
Figure 5.4: Measured radius of convergence R_n, as a function of the order of the truncation of the series n, for $\Delta = \cos \pi/5$ (left) and $\Delta = 1$ (right). The series converges at $h = 0$ if there is only a finite number of points below the line $\sqrt{h_c}$.

5.2.6 An example with complex roots

Our calculation does not assume that the roots λ_i are real. In this section we give the simple example of the Heisenberg spin chain with complex extensive twist $i\varphi$ (φ real), where the roots lie on a curve in the complex plane and show that our approach still applies. This variant is for example relevant for the six-vertex model (its free energy $F(m_x, m_y)$ is the Legendre transform of that of this spin chain with respect to φ, see Section 5.4.2 below) or for an inhomogeneous version of the Heisenberg spin chain [171, 172]:

$$H = \sum_{i=1}^{L} \frac{1}{2} \left(e^{-\varphi_i} \sigma_i^+ \sigma_{i+1}^- + e^{\varphi_i} \sigma_i^- \sigma_{i+1}^+ \right) + \sigma_i^z \sigma_{i+1}^z - \tfrac{1}{4} \tag{5.28}$$

where $\sum_{i=1}^{L} \varphi_i = L\varphi$ is real. The Bethe equations are

$$s(\lambda_p) = \frac{I_p}{L} + \frac{i\varphi}{\pi} + \frac{1}{L} \sum_{j=1}^{K} r(\lambda_p - \lambda_j) \tag{5.29}$$

with s and r the same functions as for the untwisted Heisenberg spin chain. As it is, the decomposition of λ_p has a non-vanishing c_{00}, which implies that there can be some non-vanishing $c_{ab}^{[n]}$ for arbitrary large n. To keep the sums over n finite in (5.12), we set $\lambda_p' = \lambda_p - s^{-1}(i\varphi/\pi)$ and define

$$\tilde{s}(\lambda) = s(s^{-1}(i\varphi/\pi) + \lambda) - \frac{i\varphi}{\pi} \tag{5.30}$$

147

so that $c_{00} = 0$ and a similar equation to (5.12) holds. One finds then the free energy with the normalization in (5.4)

$$F(m) = - 4\cosh^2(\varphi)m + \frac{\pi^2}{3}\cosh(2\varphi)m^3 + \frac{\pi^2}{3}(1 + \tanh^2\varphi)m^4 - \frac{\pi^2\cosh 2\varphi}{60\cosh^4\varphi}\left(\pi^2\cosh^4\varphi - 15\right)m^5$$

$$- \frac{\pi^2}{720\cosh^6\varphi}\left(5\pi^2 + (12\pi^2 - 120)\cosh 2\varphi + \pi^2\cosh 4\varphi + 2\pi^2\cosh 6\varphi\right)m^6$$

$$+ O(m^7) \tag{5.31}$$

We stress the fact that the Bethe roots are disposed on a curve in the complex plane that was up to now out of reach of analytic calculations. The agreement with the numerics is still excellent, see Table 5.3 for $\varphi = 0.1$ and Table 5.4 for $\varphi = 1$. In this case we do not know the value at $m = 1/2$, but we still think the series converges for all $m \leq 1/2$.

	$m = 0.05$	$m = 0.1$	$m = 0.2$	$m = 0.4$	$m = 0.5$
$L = 1000$	0.20557908	0.40424331	0.77921754	1.31659212	1.39756987
$L = 3000$	0.20290390	0.40162684	0.77686780	1.31553762	1.39756837
$L = 5000$	0.20236882	0.40110345	0.77639763	1.31532614	1.39756824
Extrapolation	0.20156621	0.40031838	0.77569238	1.31500891	1.39756806
18-term expansion	0.20156618	0.40031832	0.77569224	1.31500950	1.39758483

Table 5.3: The free energy $-F(m)$ of the twisted XXX spin chain for different magnetizations, for $\varphi = 0.1$.

	$m = 0.05$	$m = 0.1$	$m = 0.2$	$m = 0.4$	$m = 0.5$
$L = 1000$	0.47464203	0.93959272	1.79928056	2.95102536	3.10980581
$L = 3000$	0.47464147	0.93959159	1.79927833	2.95102151	3.10980172
$L = 5000$	0.47464143	0.93959150	1.79927815	2.95102120	3.10980140
Extrapolation	0.47464136	0.93959137	1.79927788	2.95102074	3.10980091
18-term expansion	0.47464140	0.93959145	1.79927805	2.95102056	3.10978951

Table 5.4: The free energy $-F(m)$ of the twisted XXX spin chain for different magnetizations, for $\varphi = 1$.

5.2.7 Finite-size corrections and critical exponents

Taking into account L^{-2} corrections

To derive the recurrence relation (5.12) the thermodynamic limit $L \to \infty$ was taken in (5.10) by keeping only the dominant term. Keeping some sub-dominant terms actually permits to get the finite-size corrections to the free energy. The finite-size corrections clearly depend on the precise distribution of roots of the state considered, and so the correction terms in

(5.10). For the ground state, i.e. Bethe numbers $-K/2 + 1/2, ..., K/2 - 1/2$, one has using Faulhaber's formula

$$\frac{1}{L} \sum_{j=1}^{K} \alpha_j^a = \begin{cases} \frac{m^{a+1}}{2^a(a+1)} - \frac{1}{L^2} \frac{am^{a-1}}{6 \cdot 2^a} + O(L^{-3}), & a \text{ even} \\ 0 + O(L^{-3}), & a \text{ odd} \end{cases} \tag{5.32}$$

For a state corresponding to a descendant, the Bethe numbers are identical to the ground state expect for $K/2 - 1/2$ that becomes $K/2 + 1/2$. Then one has

$$\frac{1}{L} \sum_{j=1}^{K} \alpha_j^a = \begin{cases} \frac{m^{a+1}}{2^a(a+1)} - \frac{1}{L^2} \frac{am^{a-1}}{6 \cdot 2^a} + \frac{1}{L^2} \frac{am^{a-1}}{2^{a-1}} + O(L^{-3}), & a \text{ even} \\ \frac{1}{L^2} \frac{am^{a-1}}{2^{a-1}} + O(L^{-3}), & a \text{ odd} \end{cases} \tag{5.33}$$

For a so-called 'Umklapp' state, $-K/2 + 1/2$ is replaced by $K/2 + 1/2$. Thus

$$\frac{1}{L} \sum_{j=1}^{K} \alpha_j^a = \begin{cases} \frac{m^{a+1}}{2^a(a+1)} - \frac{1}{L^2} \frac{am^{a-1}}{6 \cdot 2^a} + \frac{1}{L^2} \frac{am^{a-1}}{2^{a-1}} + O(L^{-3}), & a \text{ even} \\ \frac{1}{L} \frac{m^a}{2^{a-1}} + O(L^{-3}), & a \text{ odd} \end{cases} \tag{5.34}$$

With this, a recurrence relation analogous to (5.12) with L^{-1} and L^{-2} corrections can be derived. However, the sum $a_1 + b_1 + b_2 + 1 = b$ is replaced by $a_1 + b_1 + b_2 - 1 = b$ for L^{-2} corrections for example, and c_{ab} could appear in the right-hand side of the recurrence relation in the term proportional to L^{-2}. Even if it does, it does not prevent from computing recursively the expansion of c_{ab} to a desired order: one can just compute the c_{ab}'s order by order in L^{-1}. In fact, closer inspection indicates that it does not happen for the states discussed above.

The recurrence relation (5.12) with a L^{-2} term becomes e.g. for the ground state

$$c_{ab} = \frac{1}{s'(0)} \left(\sum_{\substack{a_1+b_1+b_2+1=b \\ a_1 \text{ even}}} \left(\sum_{n \geq 0} \frac{r^{(n)}(0)}{n!} \sum_{q=0}^{n} (-1)^q \binom{n}{q} \frac{c_{a_1 b_1}^{[q]} c_{ab_2}^{[n-q]}}{2^{a_1}(a_1+1)} \right) - \sum_{n \geq 1} \frac{c_{ab}^{[n]} s^{(n)}(0)}{n!} \right.$$

$$\left. - \frac{1}{6L^2} \sum_{\substack{a_1+b_1+b_2-1=b \\ a_1 \text{ even}}} \left(\sum_{n \geq 0} \frac{r^{(n)}(0)}{n!} \sum_{q=0}^{n} (-1)^q \binom{n}{q} a_1 \frac{c_{a_1 b_1}^{[q]} c_{ab_2}^{[n-q]}}{2^{a_1}} \right) \right) \tag{5.35}$$

See Table 5.5 for a numerical verification of these relations in size $L = 200$ for the XXX spin chain, for the ground state (GS), a descendant state (D) and the Umklapp state (U).

	$m = 0.05$	$m = 0.1$	$m = 0.2$	$m = 0.4$
GS(num.)	0.1995722665	0.3963828609	0.7682525850	1.303613450
GS (th.)	0.1995722664	0.3963828606	0.7682525844	1.303614161
D (num.)	0.1995206015	0.3962754120	0.7680261945	1.303174308
D (th.)	0.1995205738	0.3962753814	0.7680261588	1.303170391
U (num.)	0.1995231282	0.3962858646	0.7680691881	1.303332830
U (th.)	0.1995231262	0.3962858613	0.7680691846	1.303329318

Table 5.5: Some energy levels of the Heisenberg spin chain for different magnetizations, in finite size $L = 200$.

Spectrum of the model

Let us denote $\Delta_{\mathrm{GS}}, \Delta_{\mathrm{D}}, \Delta_{\mathrm{U}}$ the L^{-2} correction to the three states previously described. We define

$$v_F = \frac{\Delta_{\mathrm{D}} - \Delta_{\mathrm{GS}}}{2\pi}, \qquad c = -\frac{6\Delta_{\mathrm{GS}}}{\pi v_F},$$

$$\lambda = \frac{F''(m)}{\pi v_F}, \qquad \lambda^* = \frac{\Delta_{\mathrm{U}} - \Delta_{\mathrm{GS}}}{2\pi v_F} \tag{5.36}$$

and let us consider a state obtained from the ground state by removing n roots, changing the sign of $n^*/2$ negative roots (that become thus positive – a negative n^* means that the sign of $|n^*|/2$ positive roots is changed), and globally shifting the Bethe integers of the roots by $p_\pm$ for positive/negative roots (i.e., the sum of the positive Bethe integers is increased by p_+ and the sum of the negative Bethe integers by $-p_-$). We assume that the Bethe integer configuration is still a valid configuration, and that the modifications are done only at finite distance from the maximal and minimal roots of the ground state.

The n direction can actually be simply taken into account by changing m into $m - n/L$, so that one can assume in a first step $n = 0$. In this case one gets, with $\sum_{i=0}^{n^*-1}(1/2+i) = (n^*)^2/2$

$$\frac{1}{L}\sum_{j=1}^{K}\alpha_j^a = \begin{cases} \frac{m^{a+1}}{2^a(a+1)} - \frac{1}{L^2}\frac{am^{a-1}}{6\cdot2^a} + \frac{(n^*)^2}{L^2}\frac{am^{a-1}}{2^{a+1}} + \frac{p_++p_-}{L^2}\frac{am^{a-1}}{2^{a-1}} + O(L^{-3}), & a \text{ even} \\ \frac{1}{L}\frac{m^a}{2^a}n^* + \frac{p_+-p_-}{L^2}\frac{am^{a-1}}{2^{a-1}} + O(L^{-3}), & a \text{ odd} \end{cases} \tag{5.37}$$

Remark that the term with a odd can appear in the result only through its square, since it is multiplied by -1 if all the roots are multiplied by -1. It follows that there is no L^{-1} correction, that the n^*/L correction appears in the result through its square, and that the $p_\pm$ term for a odd does not contribute to the result. Thus the L^{-2} correction is $\Delta_{\mathrm{GS}} + (\Delta_{\mathrm{D}} - \Delta_{\mathrm{GS}})(p_+ + p_-) + (\Delta_{\mathrm{U}} - \Delta_{\mathrm{GS}})(n^*/2)^2$.

As for the n direction, it gives the correction to the free energy $F(m) - \frac{n}{L}F'(m) + \frac{n^2}{2L^2}F''(m)$. The L^{-1} term is compensated by the magnetic field part in the energy of the chain, so that remains only the L^{-2} part. It follows that the L^{-2} correction Δ_{Gen} of this generic state is

$$\Delta_{\mathrm{Gen}} = 2\pi v_F\left(-\frac{c}{12} + \frac{n^2}{4}\lambda + \frac{(n^*)^2}{4}\lambda^* + p_+ + p_-\right) \tag{5.38}$$

Note that $c = 1$ from (5.33) and (5.32). To fully recover the spectrum of a free compact boson, one needs

$$\lambda^* = \frac{1}{\lambda} \tag{5.39}$$

which is a very non-trivial statement on the recurrence relations for c_{ab}, that we could not prove at all orders, but checked order by order in m until m^{28}. The fact that λ and $1/\lambda^*$ give the same expansion is a very non-trivial check of validity of our approach.

For example one has for the XXZ spin chain

$$\lambda = 1 + \frac{2\Delta}{1+\Delta}m + \frac{3\Delta^2}{(1+\Delta)^2}m^2 + \frac{\Delta}{3(1+\Delta)^3}(-\pi^2 + \pi^2\Delta + 12\Delta^2)m^3$$
$$+ \frac{5\Delta^2}{6(1+\Delta)^4}(-2\pi^2 + 2\pi^2\Delta + 6\Delta^2)m^4$$
$$+ \frac{1}{60(1+\Delta)^5}\left(360\Delta^5 - 300\Delta^3\pi^2 + 300\Delta^4\pi^2 + \Delta\pi^4 - 11\Delta^2\pi^4 + 11\Delta^3\pi^4 - \Delta^4\pi^4\right)m^5$$
$$+ O(m^6)$$

(5.40)

and the Luttinger parameter $K = 1/\lambda$:

$$K = 1 - \frac{2\Delta}{1+\Delta}m + \frac{\Delta^2}{(1+\Delta)^2}m^2 - \frac{(\Delta-1)\Delta\pi^2}{3(1+\Delta)^3}m^3 - \frac{(\Delta-1)\Delta^2\pi^2}{3(1+\Delta)^4}m^4$$
$$+ \frac{(\Delta-1)\Delta\pi^2(\pi^2 - 10\Delta\pi^2 - 20\Delta^2 + \Delta^2\pi^2)}{60(1+\Delta)^5}m^5$$
$$+ \frac{1}{60(1+\Delta)^6}\left(20\Delta^4\pi^2 - 20\Delta^5\pi^2 - 2\Delta^2\pi^4 + 35\Delta^3\pi^4 - 38\Delta^4\pi^4 + 3\Delta^5\pi^4\right)m^6$$
$$+ O(m^7)$$

(5.41)

Critical exponent of the spin-spin two-point function

The spin-spin correlations decay with distance r as r^{-x} with $x = 2/\lambda$ for $0 \le \Delta \le 1$ [138]. This yields the critical exponent

$$x = 2 - \frac{4\Delta}{1+\Delta}m + \frac{2\Delta^2}{(1+\Delta)^2}m^2 - \frac{2(\Delta-1)\Delta\pi^2}{3(1+\Delta)^3}m^3 - \frac{2(\Delta-1)\Delta^2\pi^2}{3(1+\Delta)^4}m^4$$
$$+ \frac{(\Delta-1)\Delta\pi^2(\pi^2 - 10\Delta\pi^2 - 20\Delta^2 + \Delta^2\pi^2)}{30(1+\Delta)^5}m^5$$
$$+ \frac{1}{30(1+\Delta)^6}\left(20\Delta^4\pi^2 - 20\Delta^5\pi^2 - 2\Delta^2\pi^4 + 35\Delta^3\pi^4 - 38\Delta^4\pi^4 + 3\Delta^5\pi^4\right)m^6$$
$$+ O(m^7)$$

(5.42)

Again, only the first term of this expansion was known [164, 138]. In the case of a spin-1 chain in a magnetic field, the first two terms of a similar series were computed by different means [169]. See Figure 5.5 for a plot of this expansion for different values of Δ. At $\sigma^* = 0$ we know $x = (1 - \frac{1}{\pi}\arccos\Delta)^{-1}$ [114, 23, 24, 25, 26]. With a 28-term expansion, we find for $\Delta = \cos 2\pi/5$, $x = 1.66663$ (exact value 5/3), and $x = 1.204$ for $\Delta = \cos\pi/6$ (exact value 6/5). For $m \to 0$, i.e. close to the critical magnetic field h_c, the critical exponent goes to that of the free fermion case $\Delta = 0$, independently of Δ.
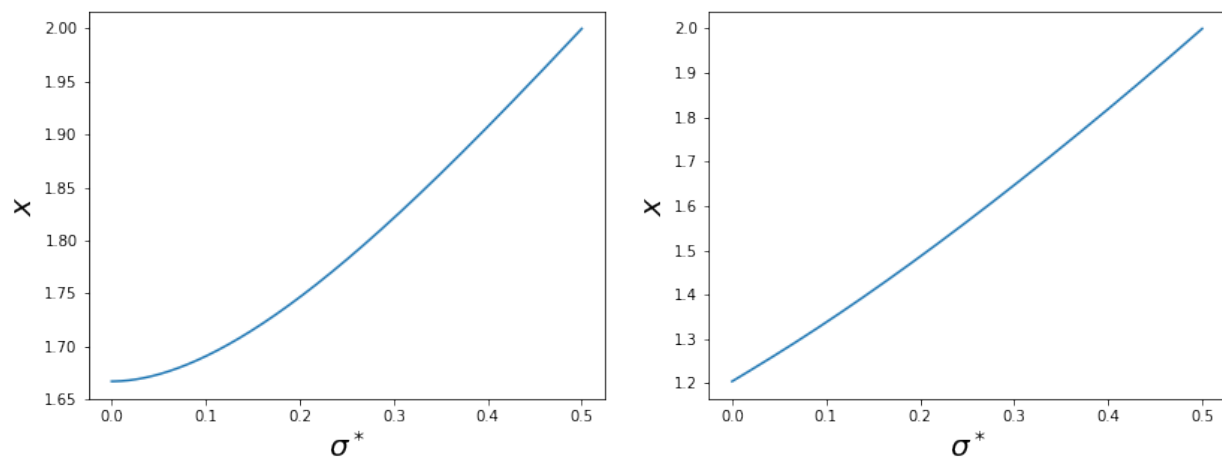
Figure 5.5: Critical exponent x as a function of the magnetization $\sigma^\star$, for $\Delta = \cos 2\pi/5$ (left) and $\Delta = \cos \pi/6$ (right), using a 28-term expansion in m.

5.3 Some intermediate results on a non-compact spin chain

5.3.1 Motivations

In this section, we present some intermediate results on a still ongoing project that could be an interesting application of the series expansions written above. It deals with the thermodynamic behaviour of a *non-compact* spin chain, i.e. a spin chain whose every site is described by an infinite dimensional vector space. As mentioned in the general introduction, among these exotic spin chains is the Chalker-Coddington model for the transition between plateaux in the IQHE. We will focus on another example, much more studied because of its integrability, that is the non-compact spin $s = 0$ Heisenberg spin chain [158, 8, 159, 160].

The Hamiltonian $\mathcal{H}$ of this spin chain on L sites, the i-th site being described by the vector space V of functions on the complex plane $\psi(z_i, \bar{z}_i)$, reads

$$\mathcal{H} = H + \bar{H} \tag{5.43}$$

with

$$H = \sum_{i=1}^{L} H_{i,i+1}, \qquad H_{i,i+1} = \sum_{k=0}^{\infty} \frac{2k+1}{k(k+1) + (z_i - z_{i+1})^2 \partial_{z_i} \partial_{z_{i+1}}} - \frac{2}{k+1} \tag{5.44}$$

and $\bar{H}$ defined similarly in terms of the conjugate variables $\bar{z}$. Since they commute, we will focus on H only for our arguments.

To each site are assigned the spin operators S_i^z, S_i^+, S_i^- as

$$S_i^+ = z_i^2 \partial_{z_i}, \qquad S_i^- = -\partial_{z_i}, \qquad S_i^z = z_i \partial_{z_i} \tag{5.45}$$

that satisfy the $su(2)$ commutation relations and that commute with H. The value h of the spin S_{tot}^z on an eigenstate of H is constrained to be of the form $h = \frac{1+n}{2} - i\nu$ with n an integer, and ν a real. That of $\bar{S}_{\text{tot}}^z$ on an eigenstate of $\bar{H}$ is then constrained as well to be $1 - h^*$, where h^* is the complex conjugate of h [160]. It has been shown [8, 159] that *only* for $h \geq L$ an integer, the Bethe ansatz can be used to derive the value of the (intensive) energy levels e_L of an eigenstate of H as

$$e_L = 2 + \frac{1}{L} \sum_{i=1}^{h-L} \frac{2}{\lambda_i^2 + 1} \tag{5.46}$$

where the roots λ_j satisfy the Bethe equations

$$\left(\frac{\lambda_i - i}{\lambda_i + i} \right)^L = \prod_{j=1,\neq i}^{h-L} \frac{\lambda_i - \lambda_j + i}{\lambda_j - \lambda_i - i} \tag{5.47}$$

153

We note that the condition $h \geq L$ cannot be satisfied simultaneously for H and $\bar{H}$, so that the Bethe ansatz cannot be directly used to compute any eigenvalue of the total Hamiltonian. Hence for the other values of h, one has to resort to Baxter's TQ relations where the function $Q(\lambda)$ is not anymore a polynomial, and where h that is now merely one of the $L - 1$ conserved quantities on which the state depends, is the variable upon which analytic continuation has to be performed [8, 159, 160]. This is of particular importance since the ground state of the total Hamiltonian is obtained for $h = \frac{1}{2}$. This procedure has been carried out in [160] for sizes up to $L = 8$, enabling to determine numerically the ground state as well as the energies of some excited states, with an analytic expression only at $L = 2$. In particular these results strongly suggest that in the thermodynamic limit $L \to \infty$ the energy of the ground state vanishes [45].

The basic idea we want to try is to take the thermodynamic limit *before* performing the analytic continuation. Indeed, from (5.46) and (5.47) one can get a series expansion for the energy levels of H in terms of $m \equiv \frac{h-L}{L}$ around $m = 0$ in the thermodynamic limit $L \to \infty$, for any state defined by their Bethe number structure. If one is able to analytically continue this energy down to $m = -1$, then one should directly capture the energy of these states in the thermodynamic limit at $h = \frac{1}{2}$. If such a procedure works, the finite-size corrections could be obtained similarly. As far as we understand, we do not seem to make any additional hypothesis compared to the method previously developed [8, 159, 160, 45]: in both cases the analytic continuation is done from the TQ relations that are equivalent to the Bethe equations for $h \geq L$ an integer.

The solutions to the Bethe equations (5.47) turn out to be very simple: there exist only solutions with real roots, whose Bethe numbers (integers if $h - L$ is odd, half-integers if $h - L$ is even) are strictly between $-\frac{h-1}{2}$ and $\frac{h-1}{2}$. From (5.46), it is clear that for $h \geq L$ integer the maximal energy state at this value of h is obtained by packing the Bethe roots around 0 as closely as possible, thus with Bethe numbers from $\frac{L-h+1}{2}$ to $\frac{h-L-1}{2}$. Hence for negative $m < 0$, at least for m close to 0, the analytic continuation of these states is expected to be minimal for this configuration of roots. Then, using the recurrence relation in section 5.2.2 with

$$s(\lambda) = -\frac{1}{\pi} \arctan \lambda, \qquad r(\lambda) = \frac{1}{\pi} \arctan \lambda \qquad (5.48)$$

one finds the following first terms of the series $F(m)$ for (5.46):

$$
\begin{aligned}
F(m) = {}& 2 + 2m - \frac{\pi^2}{6}m^3 + \frac{\pi^2}{3}m^4 + \frac{\pi^2(-60 + \pi^2)}{120}m^5 \\
& - \left(-\frac{2\pi^2}{3} + \frac{11\pi^4}{180} \right) m^6 - \left(\frac{5\pi^2}{6} - \frac{2\pi^4}{9} + \frac{\pi^6}{5040} \right) m^7 + O(m^8)
\end{aligned}
\qquad (5.49)
$$

whose radius of convergence is numerically observed to be $\approx \frac{1}{3}$. At this point, two questions arise:

1. Is it possible to analytically continue this function to obtain $F(-1)$?

2. Is $F(-1)$ still smaller than the analytic continuation of the energy levels of the other root configurations?

To tackle these questions, we are going to add an extensive imaginary twist in the Bethe equations as in Section 5.2.6 and study the free energy $F(m, \varphi)$ with this twist, that shall in the end be set to zero. In this situation, the answer to the first point is remarkably positive and $F(-1, \varphi)$ can be obtained. However, it is likely that the answer to the second point is negative, that a crossing of energy levels occur and that another function should be studied. Despite this fact, we will present in the following the analytic continuation of $F(m, \varphi)$ to $m = -1$, as it could be a good starting point to study other root configurations.

A word on numerical analytic continuation

In practice, in absence of an explicit expression for the generic term of the series, one can run the recurrence relation to get up to hundreds of terms for the energy (5.49). One could wonder if it is enough to perform a *numerical* analytic continuation to estimate the value of $F(-1)$. The basic principle of analytic continuation is the ability to re-expand a series around another point m_1 within the (supposedly non-zero) radius of convergence around $m_0 = 0$

$$F(m) = \sum_{a \geq 0} f_a^0 (m - m_0)^a = \sum_{a \geq 0} f_a^1 (m - m_1)^a \tag{5.50}$$

with f_a^1 coefficients that can be expressed in terms of the f_a^0's. The convergence disk of this new series may permit to reach new points outside the former convergence disk. Repeating the procedure enables in principle to reach any (non singular) point on the complex plane [173].

If the series is truncated at a given order in (5.50), the two expansions are clearly exactly equivalent, and one has effectively to truncate more the new series since the f_a^1's for larger a are built on too few f_a^0's. In practice, this process can actually be tremendously costly, especially if one gets close to singularities. For example, analytically continuing $\log z$ around the unit circle requires millions of terms in the starting expansion as explained in [173]. The case of our function (5.49) is essentially hopeless: some numerical analysis shows that are there two poles near $-0.1 \pm 0.3i$ and a very likely singularity at -0.5, blocking the way to $m = -1$.

There are of course plenty of other analytic continuation techniques, e.g. Padé approximants or Borel resummation. However, these methods have precise range of convergence and applicability conditions, and because of the unpleasant pole structure, none has actually given anything that comes close to a reliable result.

5.3.2 A dual recurrence relation

The Bethe equations with the twist φ read

$$s(\lambda_k) = \frac{I_k}{L} + i \frac{\varphi}{\pi} + \frac{1}{L} \sum_j r(\lambda_k - \lambda_j) \tag{5.51}$$

and an expansion in m with 'already resummed' φ-dependent coefficients (in the sense that no expansion in φ is performed, and their expression is valid for all φ) can be derived for the free energy $F(m, \varphi)$ as in Section 5.2.6. The starting point is to write its *dual* expansion, i.e. an *expansion in φ* with *already resummed m-dependent coefficients*, whose double expansion in m, φ coincides with the double expansion of the former φ-dependent series in m.

To that end, we assume that we can write

$$s(\lambda) = i\sigma \log(\lambda - \kappa) + \sum_{n \geq 0} s_n (\lambda - \kappa)^n \tag{5.52}$$

with κ, σ, s_n some complex numbers. Since the Bethe equations are written in logarithmic form, this expansion is quite natural; in our case (5.48), one has

$$\sigma = \frac{1}{2\pi}, \qquad s_0 = \frac{\log(-2i)}{2i\pi}, \qquad s_n = \frac{i}{2\pi n}\left(\frac{i}{2}\right)^n, \qquad \kappa = i \tag{5.53}$$

Then we look for λ_k in the form

$$\lambda_k = \kappa + \sum_{a,b \geq 0} \gamma_{ab} e^{-i\frac{I_k}{L\sigma}a} e^{\frac{\varphi}{\pi\sigma}b} \tag{5.54}$$

with γ_{ab} coefficients to determine, and with the notation $\gamma_{ab}^{[n]}$ such that

$$(\lambda_k - \kappa)^n = \sum_{a,b \geq 0} \gamma_{ab}^{[n]} e^{-i\frac{I_k}{L\sigma}a} e^{\frac{\varphi}{\pi\sigma}b} \tag{5.55}$$

By taking $\varphi \to \infty$ and $L \to \infty$, one sees that one must have $\gamma_{00} = \gamma_{01} = \gamma_{10} = 0$, since $\frac{I_k}{L} + i\frac{\varphi}{\pi}$ dominates in the right-hand side of (5.51), and

$$\gamma_{11} = e^{-\frac{s_0}{i\sigma}} \tag{5.56}$$

Then:

$$s(\lambda_k) = \frac{I_k}{L} + i\frac{\varphi}{\pi} - i\sigma \sum_{n \geq 1} \sum_{a,b \geq 0} (-1)^n \frac{\tilde{\gamma}_{ab}^{[n]}}{n} e^{-i\frac{I_k}{L\sigma}a} e^{\frac{\varphi}{\pi\sigma}b} + \sum_{n \geq 0} \sum_{a,b \geq 0} s_n \gamma_{ab}^{[n]} e^{-i\frac{I_k}{L\sigma}a} e^{\frac{\varphi}{\pi\sigma}b} \tag{5.57}$$

with

$$\tilde{\gamma}_{ab} = \begin{cases} \frac{\gamma_{a+1,b+1}}{\gamma_{11}} & \text{if } (a,b) \neq (0,0) \\ 0 & \text{if } (a,b) = (0,0) \end{cases} \tag{5.58}$$

Now, one has

$$r(\lambda_k - \lambda_j) = \sum_{n \geq 0} \sum_{k=0}^{n} \sum_{a_1,b_1,a_2,b_2 \geq 0} \frac{r^{(n)}(0)}{n!} \binom{n}{k} (-1)^k \gamma_{a_1 b_1}^{[k]} \gamma_{a_2 b_2}^{[n-k]} e^{\frac{\varphi}{\pi\sigma}(b_1+b_2)} e^{-i\frac{I_j}{L\sigma}a_1} e^{-i\frac{I_k}{L\sigma}a_2} \tag{5.59}$$

Using

$$\frac{1}{L}\sum_{j=1}^{K} e^{-i\frac{I_j}{L\sigma}a_1} = m \operatorname{sinc}\left(\frac{a_1 m}{2\sigma}\right) + O(L^{-1}) \tag{5.60}$$

for our root configuration, with $\operatorname{sinc} x = \frac{\sin x}{x}$, one gets

$$\frac{1}{L}\sum_{j=1}^{K} r(\lambda_k - \lambda_j) = m \sum_{n\geq 0}\sum_{k=0}^{n}\sum_{\substack{a,b\geq 0 \\ b_1+b_2=b \\ a_1\geq 0}} \frac{r^{(n)}(0)}{n!}\binom{n}{k}(-1)^k \gamma^{[k]}_{a_1 b_1}\gamma^{[n-k]}_{ab_2} \operatorname{sinc}\left(\frac{a_1 m}{2\sigma}\right) e^{-i\frac{I_k}{L\sigma}a}e^{\frac{\varphi}{\pi\sigma}b} \tag{5.61}$$

At order $e^{-i\frac{I_k}{L\sigma}a}e^{\frac{\varphi}{\pi\sigma}b}$ appears only once $\gamma_{a+1,b+1}$, all the other $\gamma_{a'b'}$ satisfying $b' \leq b$. Thus one finds the recurrence relation

$$\gamma_{a+1,b+1} = \frac{\gamma_{11}m}{i\sigma}\sum_{n\geq 0}\sum_{\substack{b_1+b_2=b \\ a_1\geq 0}} \frac{r^{(n)}(0)}{n!}\binom{n}{k}(-1)^k \gamma^{[k]}_{a_1 b_1}\gamma^{[n-k]}_{ab_2}\operatorname{sinc}\left(\frac{a_1 m}{2\sigma}\right) + \gamma_{11}\sum_{n\geq 2}(-1)^n\frac{\tilde{\gamma}^{[n]}_{ab}}{n} - \frac{\gamma_{11}}{i\sigma}\sum_{n\geq 0}s_n\gamma^{[n]}_{ab} \tag{5.62}$$

Defining now the free energy $\tilde{F}(m,\varphi)$ as[3]

$$\tilde{F}(m,\varphi) = -\frac{2\pi}{L}\sum_{k=1}^{K} s'(\lambda_k) \tag{5.63}$$

one gets

$$\tilde{F}(m,\varphi) = \sum_{b\geq -1} f_b(m)e^{\frac{\varphi b}{\pi\sigma}} \tag{5.64}$$

with

$$f_b(m) = \begin{cases} -\frac{4\pi i\sigma^2}{\gamma_{11}}\sin\left(\frac{m}{2\sigma}\right) & \text{if } b = -1 \\ -2\pi m\sum_{n,a\geq 0}\left(\frac{i\sigma}{\gamma_{11}}\tilde{\gamma}^{[n]}_{a,b+1}(-1)^n\operatorname{sinc}\left(\frac{(a-1)m}{2\sigma}\right) + (n+1)s_{n+1}\gamma^{[n]}_{ab}\operatorname{sinc}\left(\frac{am}{2\sigma}\right)\right) & \text{if } b \geq 0 \end{cases} \tag{5.65}$$

One can compare this expansion to the φ-dependent expansion in m, by performing an expansion in m of $f_b(m)$ and an expansion in $e^{\frac{\varphi}{\pi\sigma}}$ of the other series. We observe from the solution of the recurrence relation with a computer that the two double series coefficients are indeed exactly the same.

5.3.3   Analytic continuation at $m = -1$

Value of $F(-1,\varphi)$

The above expansion permits to analytically continue $\tilde{F}(m,\varphi)$ to any value of m; however, generically, the value will be expressed as a series in $e^{2\varphi}$. At $m = -1$ it is actually possible

---

[3]The tilde merely indicates that there is not the additive constant 2 compared to (5.46).

to resum this series and get a fully explicit expression. Indeed, since $\mathrm{sinc}\,(\pi a) = 0$ whenever $a \neq 0$, and since $\gamma_{ab} = 0$ for $a > b$ as is readily obtained recursively from (5.62), the recurrence relation (5.62) reduces at $m = -1$ to

$$\gamma_{a+1,b+1} = 2\pi i \gamma_{11} \sum_{n \geq 0} \frac{r^{(n)}(0)}{n!} \gamma_{ab}^{[n]} + \gamma_{11} \sum_{n \geq 2} \frac{(-1)^n}{n} \tilde{\gamma}_{ab}^{[n]} - \frac{\gamma_{11}}{i\sigma} \sum_{n \geq 0} s_n \gamma_{ab}^{[n]} \tag{5.66}$$

which means that λ_k defined in terms of γ_{ab}'s in (5.54) (it is no longer a Bethe root in the usual sense) satisfies

$$s(\lambda_k) = \frac{I_k}{L} + i\frac{\varphi}{\pi} - 2\pi\sigma r(\lambda_k - \kappa) \tag{5.67}$$

which implies that $\gamma_{ab} = 0$ if $a \neq b$ for these values of m, and that the generating function for γ_{aa} at $m = -1$ is

$$\gamma(x) \equiv \sum_{a \geq 0} \gamma_{aa} x^a = (s(\cdot + \kappa) + 2\pi\sigma r)^{-1}(i\sigma \log x) \tag{5.68}$$

where the inverse is the function inverse, and $s(\cdot + \kappa)$ denotes the function $\lambda \mapsto s(\lambda + \kappa)$. In case (5.48) with $m = -1$, this inverse can even be computed explicitly, yielding

$$\gamma(x) = -\frac{i}{2} + \frac{i}{2}\sqrt{1 - \frac{8x}{1-x}} \tag{5.69}$$

At $m = -1$, the expression of the energy simplifies as well. It reads

$$f_b(2\pi\sigma q) = 4\pi^2\sigma \sum_{n \geq 0} (n+1)s_{n+1}\gamma_{0b}^{[n]} + \frac{4i\pi^2\sigma^2}{\gamma_{11}} \sum_{n \geq 0} (-1)^n \tilde{\gamma}_{1,b+1}^{[n]} \tag{5.70}$$

for $b \geq 0$, and $f_{-1}(-1) = 0$. At $m = -1$, we have $\gamma_{0b}^{[n]} \neq 0$ if and only if $b = 0, n = 0$, and $\tilde{\gamma}_{1,b+1}^{[n]} \neq 0$, if and only if $b = 0, n = 1$. Using the expressions of these quantities at $m = -1$, it follows that only $f_0(m)$ is non zero, and then

$$\tilde{F}(-1, \varphi) = 8\pi^3\sigma^2 r'(0) + 8\pi^2\sigma s_1 \tag{5.71}$$

In case (5.48) it gives

$$\tilde{F}(-1, \varphi) = 1 \tag{5.72}$$

For this reason this Bethe root configuration very likely does not correspond to the ground state, since as far as we understand with the additive 2 in (5.46) it is expected to be 0 [45].

We note that the series in $e^{\frac{\varphi}{\pi\sigma}}$ of (5.64) has a certain radius of convergence that depends on m. For φ within this radius of convergence at $m = -1$, (5.72) has to hold. However, in absence of proof of analyticity of $F(m, \varphi)$ with φ (see [172] for peculiarities of the behaviour of energy levels with a complex φ) it does not necessarily hold outside this range.

Derivative

One can actually obtain more information on the function at $m = -1$, such as the value of $\partial_m \tilde{F}(-1, \varphi)$. Differentiating (5.65) at $m = -1$, we get

$$\partial_m \tilde{F}(-1, \varphi) = -2\pi s'(\gamma(-x) + \kappa) - (2\pi\sigma)^2 \frac{i}{\gamma_{11}} \left(\tilde{\gamma}'_1(x) - \frac{2\tilde{\gamma}_{11}}{\gamma_{11}} \gamma'_1(x) \right) \tag{5.73}$$

with $x = e^{\frac{\varphi}{\pi\sigma}}$ and the generating functions defined by

$$\tilde{\gamma}'_1(x) = \sum_{b \geq 0} \tilde{\gamma}'_{1,b+1} x^b, \qquad \gamma'_1(x) = \sum_{b \geq 0} \gamma'_{1,b+1} x^b \tag{5.74}$$

where all the γ_{ab}'s and $\tilde{\gamma}_{ab}$'s are evaluated at $m = -1$. Indeed, the first term in (5.73) is obtained from differentiating the terms in m in (5.65), and the second term from differentiating $\tilde{\gamma}_{1,b+1}$ and $\tilde{\gamma}^{[2]}_{1,b+1}$.

Now, differentiating (5.62) and setting $m = -1$, with $a = 0$ and $a = 1$, one gets

$$\gamma'_1(x) = \frac{\gamma_{11}}{i\sigma} r(-\gamma(-x))$$
$$\tilde{\gamma}'_1(x) = \frac{\gamma_{11}}{i\sigma} r'(-\gamma(-x)) + \left(\frac{\tilde{\gamma}_{11}}{\gamma_{11}} + 2i\pi r'(0) - \frac{s_1}{i\sigma} \right) \gamma'_1(x) \tag{5.75}$$

In case (5.48), using the explicit expression (5.69), one gets after some algebra

$$\partial_m \tilde{F}(-1, \varphi) = -(2\cosh^2 \varphi) \sqrt{5 + 4\tanh \varphi} \tag{5.76}$$

Again, in absence of proof of analyticity of $F(m, \varphi)$ with φ, this holds for φ within the radius of convergence of (5.64).

Finite-size correction to the ground state

The L^{-2} correction terms come from the corrections to (5.60). For the root structure studied one has

$$\frac{1}{L} \sum_{j=1}^{K} e^{-i\frac{I_j}{L\sigma} a} = m \operatorname{sinc}\left(\frac{am}{2\sigma} \right) \left(1 + \frac{a^2}{24\sigma^2 L^2} \right) + O(L^{-3}) \tag{5.77}$$

Hence, when evaluated at $m = -1$, the only non-zero term is for $a = 0$, for which there is no finite-size correction at order $O(L^{-2})$. Hence there is no finite-size correction at order $O(L^{-2})$ to the free energy value $F(-1, \varphi) = 1$.

Descendant excitation

The Fermi velocity is obtained from the L^{-2} correction to a descendant state given by a shifted Bethe number from the ground state configuration. One has in this situation (largest Bethe number shifted by 1)

$$\frac{1}{L} \sum_{j=1}^{K} e^{-i\frac{I_j}{L\sigma} a} = m \operatorname{sinc}\left(\frac{am}{2\sigma} \right) \left(1 + \frac{a^2}{24\sigma^2 L^2} \right) - \frac{iae^{-\frac{iam}{2\sigma}}}{\sigma L^2} + O(L^{-3}) \tag{5.78}$$

159

One can use these corrections to find the analog of (5.65) at $m = -1$ with L^{-2} corrections, and then obtain at order L^{-2}

$$\tilde{F}(2\pi\sigma q, \varphi) = \frac{2i\pi}{\sigma L^2} x \frac{d}{dx} \left[s'(\gamma(-x) + \kappa) \right] - (2\pi\sigma)^2 \frac{i}{\gamma_{11}} \left(\tilde{\gamma}_1(x) - \frac{2\tilde{\gamma}_{11}}{\gamma_{11}} (\gamma_1(x) - \gamma_{11}) - \frac{s_1}{\sigma} \right) \tag{5.79}$$

with $x = e^{\frac{\varphi}{\pi\sigma}}$ and the generating functions

$$\gamma_1(x) = \sum_{b \geq 0} \gamma_{1,b+1} x^b, \qquad \tilde{\gamma}_1(x) = \sum_{b \geq 0} \tilde{\gamma}_{1,b+1} x^b \tag{5.80}$$

Using (5.62) with the correction terms (5.78), for $a = 0$ and $a = 1$, one finds

$$\gamma_1(x) = \gamma_{11} - \frac{\gamma_{11}}{\sigma^2 L^2} x \frac{d}{dx} \left[r(-\gamma(-x)) \right]$$

$$\tilde{\gamma}_1(x) = \tilde{\gamma}_{11} - \frac{\gamma_{11}}{\sigma^2 L^2} x \frac{d}{dx} \left[r'(-\gamma(-x)) \right] + \frac{1}{L^2} (2i\pi r'(0) + \frac{\tilde{\gamma}_{11}}{\gamma_{11}} - \frac{s_1}{i\sigma}) \gamma_1(x) \tag{5.81}$$

In case (5.48), using the explicit expression for $\gamma(x)$ in (5.69), one finds the correction term in finite-size $\delta_{\text{desc}} \tilde{F}(-1, \varphi)$ for the descendant

$$\delta_{\text{desc}} \tilde{F}(-1, \varphi) = \frac{2i\pi}{L^2} \frac{4\cosh(2\varphi) + 5\sinh(2\varphi) - 2}{\sqrt{5 + 4\tanh\varphi}} \tag{5.82}$$

5.3.4   Perspectives

We have shown that the previously derived series expansions can indeed be used to analytically continue the free energy with a twist $F(m, \varphi)$ to the value $m = -1$ corresponding to the ground state that is at $h = \frac{1}{2}$. However, it turns out that the obtained value is not the expected value of the ground state, so that another root configuration should be tried. The simplifications that permitted to perform this analytic continuation do not necessarily occur for other root configurations and the task should be more difficult. Besides, while we have not found the right ground state root configuration we cannot be certain that the method works. But the previous calculations suggest at least another way to study these non-compact spin chains directly in the thermodynamic limit, and are still under study.

5.4 Fluctuations inside the arctic curve in the interacting six-vertex model

In this section, we present a concrete example of a statistical physics system with particular boundary conditions that impose an inhomogeneous magnetization profile in the bulk. This is the six-vertex model with domain-wall boundary conditions, that exhibits a so-called *arctic curve*, as will be explained. The purpose of the study is to understand the field theory that describes the fluctuations in the liquid region within the arctic curve.

Globally, it is only weakly related to the result of the other sections of this chapter, and can be considered as a project on its own. However, a link between the two results can be done with section 5.2.6, where the series expansion for the free energy of XXZ with a complex twist can in principle be used to compute the free energy $F(m_x, m_y)$ of the six-vertex model.

5.4.1 Presentation

The six-vertex model is one of the most famous statistical mechanics system in 2 dimensions, and consists in paving a region of the plane with the six possibles vertices depicted in Figure 5.6, with the constraint that an arrow cannot change direction along a line. The number $\Delta = 1 - \frac{c^2}{2}$ with c being the weight of the two last vertices is a parameter of the system [4], which becomes critical for $-1 \leq \Delta < 1$.
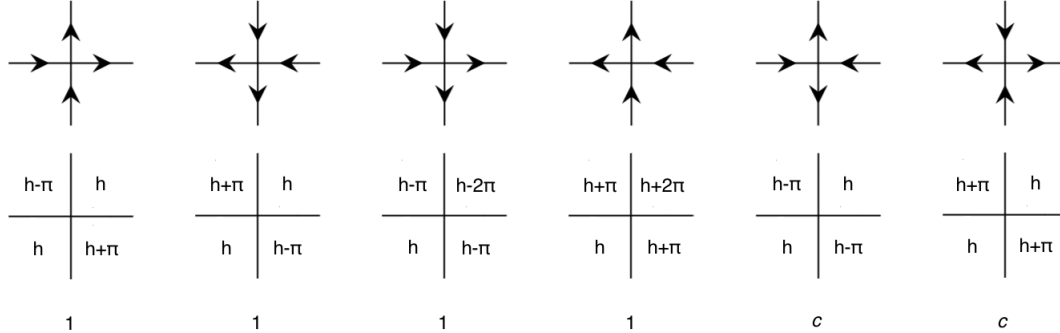
Figure 5.6: The six vertices of the six-vertex model. The top row shows the arrow configurations, while the bottom row shows the corresponding height field configurations. For simplicity, we work with the *isotropic six-vertex model*, which has the same Boltzmann weight 1 for the four first vertices, and another weight c for the last two vertices. This isotropic model is obviously symmetric under exchange of the x and y directions.

---

[4]We warn the reader of a different convention for the sign of Δ in this section compared to the rest of the manuscript. Indeed, we followed the common usage in the six-vertex model literature, according to which the sign of Δ is chosen so that it is -1 in the antiferromagnetic critical point, whereas it is 1 in the quantum spin chain literature.

In a square with free or periodic boundary conditions, a typical configuration of the six-vertex model in the thermodynamic limit is homogeneous in space, i.e. the density of each tile is constant in space. This is in agreement with the common idea that a change of boundary condition in the thermodynamic limit should not have a dramatic influence on the bulk behaviour, since it affects a negligible number of tiles.

However, if *domain-wall* boundary conditions are imposed on a square, i.e. if the arrows are imposed to go out of the square in the horizontal direction and go into the square in the vertical direction, see Figure 5.7 – such boundary conditions were first introduced to compute the norm of Bethe wave functions [174] – then in the limit of infinite number of sites, the free energy per site differs from that of free boundary conditions [175, 176, 177], and a limit-shape phenomenon appears [146, 147] similar to that of random domino tilings on an Aztec diamond observed earlier [148]. Near the boundaries, the vertices are statistically 'frozen' into only one possible vertex (by 'statistically', we mean not exactly frozen in finite size, but frozen with probability one in the continuum limit), while fluctuations still occur in the bulk of the system. The curve that separates the two domains is called arctic curve. It is a circle in the case $\Delta = 0$, and a union of portions of ellipses in the generic case, as determined in [178] with the so-called tangent method.
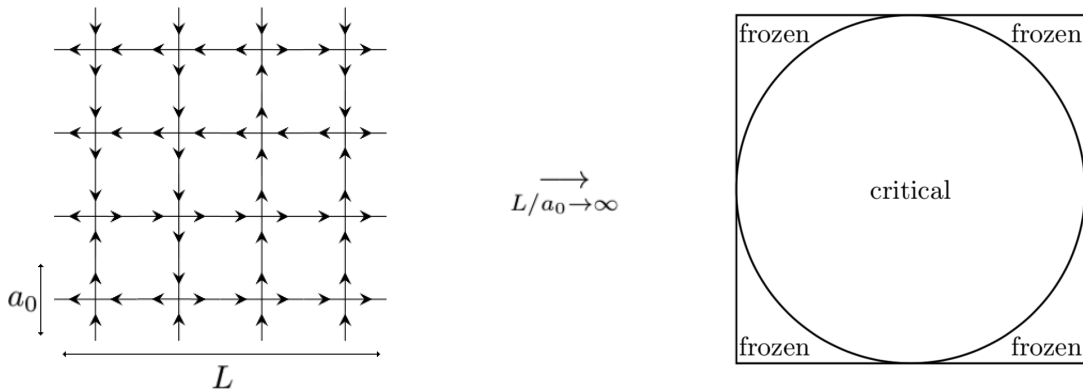
Figure 5.7: Left: example of a valid configuration of the six-vertex model with domain wall boundary conditions. Right: cartoon of the arctic circle phenomenon. The critical region is a disc only at the free fermion point $\Delta = 0$; in general it has a more complicated shape [178].

The fluctuations in the central liquid region in the case $\Delta = 0$ or in random domino tilings were shown to be described by a Gaussian Free Field [149, 150] after an appropriate change of coordinates. The objective of this section is to describe these fluctuations in the interacting case $\Delta \neq 0$, and to give evidence that they are described by a Gaussian Free Field as well, but with a space-dependent coupling constant, that cannot be made uniform by a change of coordinate.

162

To that end, we describe a $L \times L$ lattice configuration by a *height* function h at each site, defined in Figure 5.6 for each vertex. It is defined only up to a global additive constant, so that one can impose that it is zero in the left-bottom corner. In the continuum limit $L \to \infty$, the configuration is thus described by a continuous function $h(x,y)$ for $0 \leq x, y \leq 1$ that satisfies $|\partial_x h| \leq \pi$ and $|\partial_y h| \leq \pi$. The domain-wall boundary conditions translate into

$$\begin{cases} h(x,0) & = & \pi x \\ h(x,1) & = & \pi(1-x) \\ h(0,y) & = & \pi y \\ h(1,y) & = & \pi(1-y) \end{cases} \tag{5.83}$$

We define the magnetizations σ_x and σ_y by[5]

$$\sigma_x = \frac{1}{2\pi}\partial_x h \,, \qquad \sigma_y = -\frac{1}{2\pi}\partial_y h \tag{5.84}$$

and $F(\sigma_x, \sigma_y)$ the free energy (also called *surface tension*) of the configurations with magnetizations σ_x, σ_y, with free boundary conditions. The magnetizations are defined so that they belong to $[-1/2, 1/2]$. Following a coarse-grained approach, with the domain-wall boundary conditions the average height field h is obtained by minimizing

$$\min_h \int_{[0,1]^2} dxdy \, F\left(\frac{1}{2\pi}\partial_x h, -\frac{1}{2\pi}\partial_y h\right) \tag{5.85}$$

under the constraint $|\partial_{x,y} h| \leq \pi$ and (5.83). This is the approach that was used to study the model in the case $\Delta = 0$ [179, 149].

Our starting point is to consider a fluctuation $\delta h(x,y)$ around the optimal height function $h_0(x,y)$ and to write that it comes with an excess of free energy

$$\frac{1}{2} \int_\Omega dxdy \left(\begin{array}{cc} \partial_x \delta h & \partial_y \delta h \end{array} \right) (\text{Hess } F) \left(\begin{array}{c} \partial_x \delta h \\ \partial_y \delta h \end{array} \right) + \dots \tag{5.86}$$

Hess F is the hessian of the free energy $F(\sigma_x, \sigma_y)$, which we define as follows

$$\text{Hess } F = \left(\begin{array}{cc} \frac{\partial^2 F}{\partial(\partial_x h)^2} & \frac{\partial^2 F}{\partial(\partial_x h)\partial(\partial_y h)} \\ \frac{\partial^2 F}{\partial(\partial_y h)\partial(\partial_x h)} & \frac{\partial^2 F}{\partial(\partial_y h)^2} \end{array} \right) = \frac{1}{(2\pi)^2} \left(\begin{array}{cc} \frac{\partial^2 F}{\partial \sigma_x^2} & -\frac{\partial^2 F}{\partial \sigma_x \partial \sigma_y} \\ -\frac{\partial^2 F}{\partial \sigma_y \partial \sigma_x} & \frac{\partial^2 F}{\partial \sigma_y^2} \end{array} \right) \tag{5.87}$$

The action for this fluctuation is then given by

$$S[\delta h] = \int \frac{\sqrt{\det g} \, d^2 \text{x}}{8\pi K} g^{ab}(\partial_a \delta h)(\partial_b \delta h) \tag{5.88}$$

with g a certain metric that can be express in terms of F, and K the coupling constant

$$K = \left(4\pi\sqrt{\det(\text{Hess } F)}\right)^{-1} \tag{5.89}$$

Hence, all the physical information is contained in the free energy $F(\sigma_x, \sigma_y)$.

---

[5]In the paper we published on this subject [49], the magnetizations belong to $[-1, 1]$ - we changed the convention so that they belong to $[-1/2, 1/2]$ like in the rest of the manuscript.

5.4.2 The free energy $F(\sigma_x, \sigma_y)$

In this sub-section we explain why the free energy $F(\sigma_x, \sigma_y)$ is the Legendre transform with respect to φ of the free energy $f(\sigma_x, \varphi)$ of the XXZ spin chain with extensive imaginary twist φ in magnetization σ_x.

Denote $Z_{N_x N_y}(\sigma_x, \sigma_y)$ the partition function of the six-vertex model on an $N_x \times N_y$ square lattice with periodic boundary conditions, imposing mean value magnetizations $\langle \sigma_x \rangle = \sigma_x \in [-1/2, 1/2]$ and $\langle \sigma_y \rangle = \sigma_y \in [-1/2, 1/2]$. (5.84) on the lattice gives the following expression for the mean value of the magnetizations:

$$\langle \sigma_x \rangle = \frac{\text{card \{up arrows\}} - \text{card \{down arrows\}}}{2 N_x N_y}$$
$$\langle \sigma_y \rangle = \frac{\text{card \{right arrows\}} - \text{card \{left arrows\}}}{2 N_x N_y} \tag{5.90}$$

so that both belong to $[-1/2, 1/2]$. The free energy $F(\sigma_x, \sigma_y)$ is defined as

$$F(\sigma_x, \sigma_y) = \lim_{N_x, N_y \to \infty} \left(-\frac{1}{N_x N_y} \log Z_{N_x N_y}(\sigma_x, \sigma_y) \right) \tag{5.91}$$

The operators A, B, C, D in the monodromy matrix of the XXZ spin chain correspond to imposing particular boundary conditions in the horizontal direction. Specifically, one has right arrows at edges 0 and N_x for A, left arrows at edges 0 and N_x for D, a right arrow at edge 0 and a left arrow at edge N_x for B, a left arrow at edge 0 and a right arrow at edge N_x for C. The usual transfer matrix with periodic boundary conditions is defined as the trace of the monodromy matrix. The transfer matrix conserves the total magnetization σ_x, so one can work in a fixed magnetization sector, and then take the trace over the N_y-th power of the transfer matrix in that sector.

However, the magnetization σ_y cannot be imposed that way, since it is not associated to a conserved charge of the row-to-row transfer matrix. We need to resort to the following trick. Since each A contributes positively to $\langle \sigma_y \rangle$ and D negatively, we introduce an additional parameter φ and define the transfer matrix t_{N_x} as

$$t_{N_x} = e^{-N_x \varphi} A + e^{N_x \varphi} D \tag{5.92}$$

Denote $Z_{N_x N_y}(\sigma_x, \varphi)$ the partition function of this model with imposed magnetization $\langle \sigma_x \rangle = \sigma_x$. We have

$$Z_{N_x N_y}(\sigma_x, \varphi) = \sum_{i_1, \ldots, i_{N_y} \in \{-1, 1\}^{N_y}} e^{-(i_1 + \ldots + i_{N_y}) N_x \varphi} \, \text{tr}_{\sigma_x} X_{i_{N_y}} \ldots X_{i_1} \tag{5.93}$$

where $X_1 = A$, $X_{-1} = D$, and where tr_{σ_x} is the trace on the states with magnetization σ_x. Denote its free energy $f(\sigma_x, \varphi)$, where

$$f(\sigma_x, \varphi) = \lim_{N_x, N_y \to \infty} \left(-\frac{1}{N_x N_y} \log Z_{N_x N_y}(\sigma_x, \varphi) \right) \tag{5.94}$$

In terms of this transfer matrix, the mean value $\langle \sigma_y \rangle$ is given by

$$\langle \sigma_y \rangle = \frac{1}{Z_{N_x N_y}} \sum_{i_1,\ldots,i_{N_y} \in \{-1,1\}^{N_y}} \frac{i_1 + \ldots + i_{N_y}}{2N_y} e^{-(i_1 + \ldots + i_{N_y})N_x \varphi} \operatorname{tr}_{\sigma_x} X_{i_{N_y}} \ldots X_{i_1} \tag{5.95}$$

which is exactly

$$\langle \sigma_y \rangle = -\frac{1}{2} \partial_\varphi \frac{1}{N_x N_y} \log Z_{N_x N_y}(\sigma_x, \varphi) \tag{5.96}$$

Thus, in the thermodynamic limit, to impose a magnetization σ_y one has to fix φ to the value where the corresponding derivative $\partial_\varphi f$ gives $2\sigma_y$. In this sense, φ and σ_y are conjugate variables. Moreover it implies that, in Eq. (5.93), the terms with magnetization $\sigma_y = \frac{1}{2} \partial_\varphi f$ dominate in the sum. Then

$$Z_{N_x N_y}(\sigma_x, \varphi) \sim e^{-2N_x N_y \sigma_y \varphi} Z_{N_x N_y}(\sigma_x, \sigma_y) \tag{5.97}$$

which gives, in the thermodynamic limit,

$$F(\sigma_x, \sigma_y) = f(\sigma_x, \varphi) - 2\varphi\sigma_y \quad \text{where } \varphi \text{ satisfies} \quad \sigma_y = \tfrac{1}{2}\partial_\varphi f(\sigma_x, \varphi) \tag{5.98}$$

Thus the free energy $F(\sigma_x, \sigma_y)$ is the Legendre transform of $f(\sigma_x, \varphi)$ in terms of the conjugate variables σ_y and φ. We note that it should be symmetric in σ_x, σ_y, whereas it is not at all seen directly from its definition.

5.4.3 The free fermion case $\Delta = 0$

In this subsection we consider the simplest case $\Delta = 0$, derive an analytic expression for $F(\sigma_x, \sigma_y)$ that is manifestly symmetric, and show that $K(\sigma_x, \sigma_y)$ is identically equal to 1.

The free energy $f(\sigma_x, \varphi)$

To compute the free energy $F(\sigma_x, \sigma_y)$ we need the free energy $f(\sigma_x, \varphi)$, imposing σ_x but not σ_y, and with the parameter φ. The free fermion case corresponds to $\gamma = \pi/2$, or equivalently $c = \sqrt{2}$ or $\Delta = 0$. In this case the Bethe equations for K roots are

$$\left(\frac{\sinh(\lambda_i + i\pi/4)}{\sinh(\lambda_i - i\pi/4)} \right)^{N_x} = e^{2N_x \varphi} (-1)^{K-1} \tag{5.99}$$

whose solutions are

$$\lambda_k = \operatorname{argth} \tan(k\pi/N_x + i\varphi) \tag{5.100}$$

where k is an integer (if K is odd) or a half-integer (if K is even) between $-N_x/2$ and $N_x/2$. Imposing a magnetization σ_x corresponds to considering only $K = \sigma_x N_x$ of these roots. The maximal eigenvalue with this constraint is obtained by taking k between $-K/2$ and $K/2$.

The log of the modulus of this eigenvalue, determined by (2.15) with a twist, becomes in the thermodynamic limit

$$f(\sigma_x, \varphi) = -|\varphi| - \Re \int_{-(1-2\sigma_x)/4}^{(1-2\sigma_x)/4} \log \frac{\sinh(\operatorname{argth} \tan(\pi x + i\varphi) + i\pi/2)}{\sinh \operatorname{argth} \tan(\pi x + i\varphi)} dx \tag{5.101}$$

which simplifies to

$$f(\sigma_x, \varphi) = -|\varphi| + \Re \int_{-(1-2\sigma_x)/4}^{(1-2\sigma_x)/4} \log \tan(\pi x + i\varphi) dx \tag{5.102}$$

Differentiating with respect to φ, we get

$$\begin{aligned}
\partial_\varphi f &= -\operatorname{sign}\varphi + \Re \int_{-(1-2\sigma_x)/4}^{(1-2\sigma_x)/4} \partial_\varphi \log \tan(\pi x + i\varphi) dx \\
&= -\operatorname{sign}\varphi + \Re \frac{i}{\pi} \int_{-(1-2\sigma_x)/4}^{(1-2\sigma_x)/4} \partial_x \log \tan(\pi x + i\varphi) dx \\
&= -\operatorname{sign}\varphi - \frac{1}{\pi} \Im \log \frac{\tan(\frac{\pi}{4}(1 - 2\sigma_x) + i\varphi)}{\tan(-\frac{\pi}{4}(1 - 2\sigma_x) + i\varphi)}
\end{aligned} \tag{5.103}$$

Using the fact that the imaginary part of $\log(a + ib)$ is $\arctan b/a$ when $a > 0$, and using standard trigonometric identities, one gets after some algebra

$$\partial_\varphi f = -\frac{2}{\pi} \arctan \frac{\sinh 2\varphi}{\cos \pi \sigma_x} \tag{5.104}$$

Using now

$$\partial_\varphi f = 2\sigma_y \tag{5.105}$$

we get the following relation between the parameter φ and the magnetizations

$$\sinh 2\varphi = -\cos \pi \sigma_x \tan \pi \sigma_y \tag{5.106}$$

The free energy $F(\sigma_x, \sigma_y)$ is then, in terms of $f(\sigma_x, \varphi)$,

$$F(\sigma_x, \sigma_y) = f(\sigma_x, \varphi(\sigma_x, \sigma_y)) - 2\varphi(\sigma_x, \sigma_y)\sigma_y \tag{5.107}$$

where the function $\varphi(\sigma_x, \sigma_y)$ is given by (5.106).

Symmetry of the free energy $F(\sigma_x, \sigma_y)$ in the isotropic six-vertex model

Let us now rewrite $F(\sigma_x, \sigma_y)$ in a form that is manifestly symmetric under exchange of σ_x and σ_y. First we observe that because of the relation (5.105) we have

$$\partial_{\sigma_y} F(\sigma_x, \sigma_y) = -2\varphi(\sigma_x, \sigma_y) \tag{5.108}$$

166

so that in the following variables:

$$\alpha = \sin \pi \sigma_x, \quad \beta = \sin \pi \sigma_y \tag{5.109}$$

the cross derivative of F reads

$$\partial_{\sigma_x} \partial_{\sigma_y} F(\sigma_x, \sigma_y) = -\frac{\pi \alpha \beta}{\sqrt{1 - \alpha^2 \beta^2}} \tag{5.110}$$

which is clearly symmetric in σ_x, σ_y. A first integration gives

$$\partial_{\sigma_y} F(\sigma_x, \sigma_y) = -\pi \int_0^{\sigma_x} \frac{\alpha(u) \beta(\sigma_y)}{\sqrt{1 - \alpha^2(u) \beta^2(\sigma_y)}} du + \text{argsh} \tan \pi \sigma_y \tag{5.111}$$

and a second one

$$F(\sigma_x, \sigma_y) = -\pi \int_0^{\sigma_y} \int_0^{\sigma_x} \frac{\alpha(u) \beta(v)}{\sqrt{1 - \alpha^2(u) \beta^2(v)}} du dv + \int_0^{\sigma_y} \text{argsh} \tan(\pi v) dv + F(\sigma_x, 0) \tag{5.112}$$

Note now that $F(\sigma_x, 0) = f(\sigma_x, 0)$ given in (5.102). After a change of variable $x = (1 - 2u)/4$ and some manipulations, one gets

$$F(\sigma_x, 0) = F(0, 0) + 2 \int_0^{\sigma_x} \text{argth} \tan \pi \frac{u}{2} du \tag{5.113}$$

We now make use of the following relations, readily obtained by computing their derivatives

$$\begin{aligned} \text{argth} \tan \tfrac{x}{2} &= \tfrac{1}{2} \text{argsh} \tan x \\ \text{argsh} \tan &= \text{argth} \sin \end{aligned} \tag{5.114}$$

to get

$$\begin{aligned} F(\sigma_x, \sigma_y) = & -\frac{1}{\pi} \int_0^{\alpha} \int_0^{\beta} \frac{xy}{\sqrt{(1 - x^2 y^2)(1 - x^2)(1 - y^2)}} dx dy \\ & + \frac{1}{\pi} \left(\int_0^{\alpha} \frac{\text{argth} \, x}{\sqrt{1 - x^2}} dx + \int_0^{\beta} \frac{\text{argth} \, y}{\sqrt{1 - y^2}} dy \right) + F(0, 0) \end{aligned} \tag{5.115}$$

where $\alpha(\sigma_x)$ and $\beta(\sigma_y)$ are given by Eq. (5.109), which shows that $F(\sigma_x, \sigma_y)$ is indeed symmetric. We note that the dimer model on an Aztec diamond can be mapped onto the six-vertex model at $\Delta = 0$ (after a sum over certain configurations, see e.g. [180]), and the surface tension for a certain height function was calculated in [181]. However the height functions of the two models are defined differently, and do not seem to be easily related (the height function of the dimers does not satisfy $|h(i) - h(j)| = 1$ for neighbours i and j for example). In that sense our result for the surface tension of the isotropic six vertex model at $\Delta = 0$ is new to our knowledge.

Value of K

We now compute the value of $K(\sigma_x, \sigma_y)$ in the free fermion case. Since F was shown to be symmetric in its arguments, from the definition of F in (5.107) we have:

$$\partial_{\sigma_y}^2 F = -2(\partial_{\sigma_y}\varphi)(\sigma_x, \sigma_y), \quad \partial_{\sigma_x}^2 F = -2(\partial_{\sigma_y}\varphi)(\sigma_y, \sigma_x), \quad \partial_{\sigma_x}\partial_{\sigma_y} F = -2(\partial_{\sigma_x}\varphi)(\sigma_x, \sigma_y)$$
$$(5.116)$$

where we note the flipped arguments in the second expression. In terms of the variables α and β introduced in Sec. 5.4.3, the derivatives are

$$\partial_{\sigma_x}\varphi = \frac{\pi}{2}\frac{\alpha\beta}{\sqrt{1-\alpha^2\beta^2}}\,,$$

$$\partial_{\sigma_y}\varphi = -\frac{\pi}{2}\sqrt{\frac{1-\alpha^2}{1-\beta^2}}\frac{1}{\sqrt{1-\alpha^2\beta^2}}$$
$$(5.117)$$

This yields

$$K(\sigma_x, \sigma_y) = 1 \tag{5.118}$$

Thus, at the free-fermion point, the coupling constant of the GFF is constant (it does not depend on position, contrary to the interacting case), and we thus recover the fact that the fluctuations inside the arctic circle are governed by a standard (i.e. homogeneous) GFF. The fact that $K = 1$ is required in order to be able to fermionize the bosonic degrees of freedom is well-known.

5.4.4 Value of $K(m_x, m_y)$ in the interacting case

Numerical plots

In this section we present a numerical calculation of $K(\sigma_x, \sigma_y)$ obtained with the numerical Bethe ansatz method explained in Section 5.4.2. Figure 5.8 shows the function $K(\sigma_x, \sigma_y)$ for four different values of Δ, computed with a size $N_x = 156$ (except for $K(\sigma_x, \pm 1/2)$ and $K(\pm 1/2, \sigma_y)$ where N_x is several times larger, depending on the values of σ_x, σ_y).
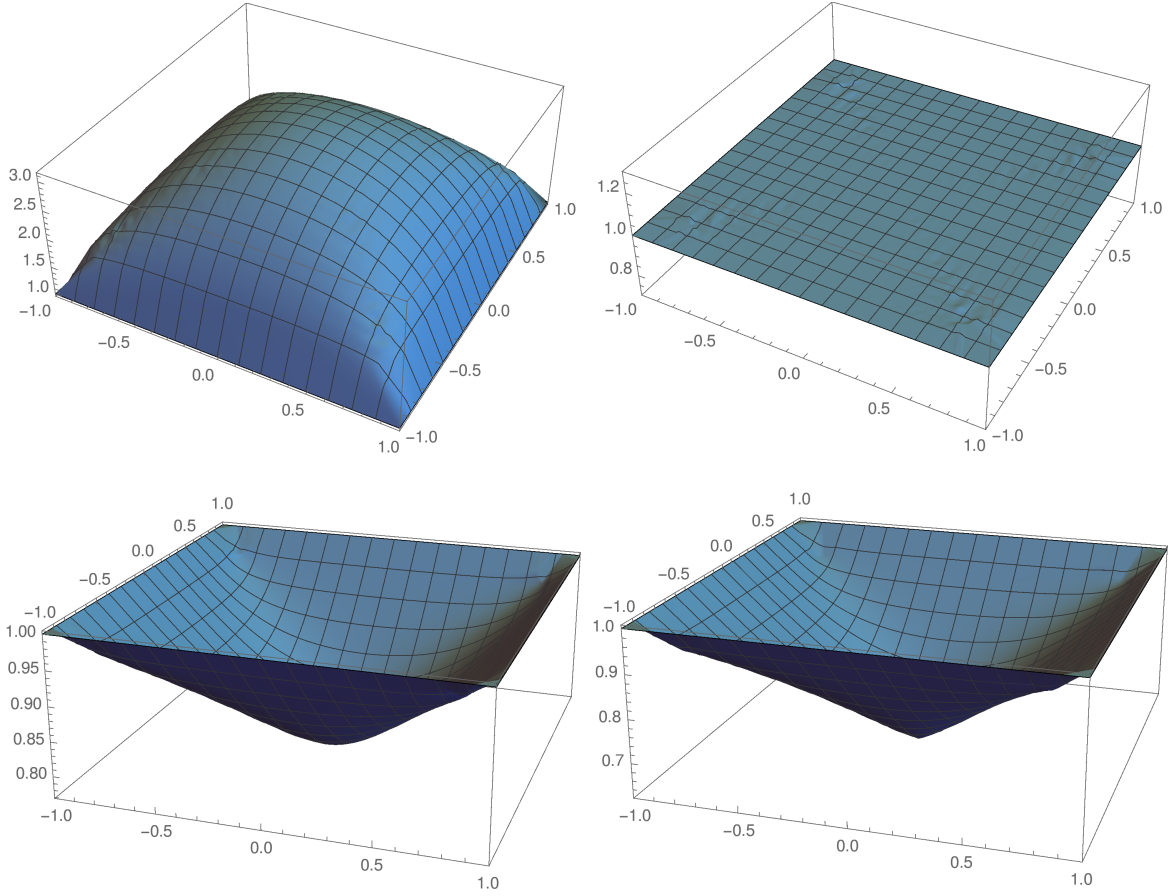
Figure 5.8: K as a function of $2\sigma_x$ and $2\sigma_y$ for $\Delta = 0.875$ (top left), $\Delta = 0$ (top right), $\Delta = -0.445$ (bottom left) and $\Delta \approx -0.8$ (bottom right).

Four qualitatively different cases are plotted: $\Delta > 0$ (top left), $\Delta = 0$ (top right), $-1/2 < \Delta < 0$ (bottom left) and $\Delta \leq -1/2$ (bottom right). It is seen that K is concave if $\Delta > 0$ and convex if $\Delta < 0$. These numerical results very clearly demonstrate the non-constant nature of $K(\sigma_x, \sigma_y)$.

Angular point at $(0,0)$

The plots presented in Figure 5.8 suggest that for $\Delta > -1/2$ the function is smooth (at least twice differentiable), and that for $\Delta \leq -1/2$ the point $(0,0)$ becomes a singular point. Namely, the second derivative of K at zero diverges for all $\Delta \leq -1/2$. For $\Delta < -1/2$, the slope of the singular point at the origin (observed in Fig. 5.8) seems to go to 0 as $\Delta \to -1/2$, and somehow hides the transition.

To give further evidence for this property, in Fig. 5.9 we show a more precise plot of $K(\sigma_x, 0) - K(0,0)$ for values of Δ around $-1/2$. On the first plot the blue and orange curve

appear to be singular at zero: the right and left derivatives seem to remain finite at zero, but are smaller as $\Delta \to -1/2$. This latter fact makes it difficult to identify the singular point without ambiguity. For this reason we plotted as well the quantity $\frac{K(\sigma_x,0)-K(0,0)}{|1/2+\Delta|}$, that reveals a change of regime around $\Delta = -1/2$. For $\Delta > -1/2$ the curves are parabolas whereas for $\Delta < -1/2$ all the curves superimpose and show a singular point. This also gives evidence for the fact that the slope behaves as $|1/2 + \Delta|$ for Δ close to $-1/2$.
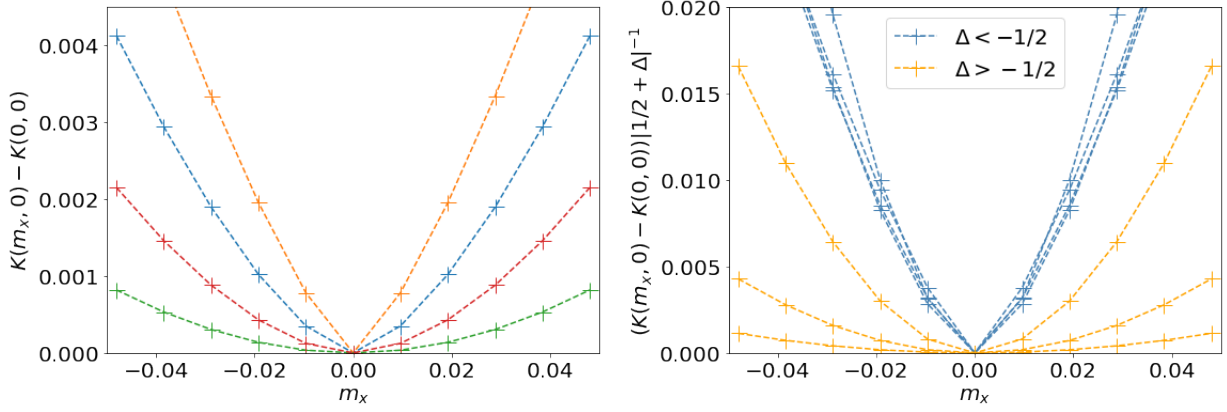

Figure 5.9: Left: $K(m_x,0)-K(0,0)$ as a function of $m_x \equiv 2\sigma_x$, for $\gamma = \pi/4, \pi/3.5, \pi/3, \pi/2.5$, ie $\Delta \approx -0.7, -0.62, -0.5, -0.3$ (orange, blue, red, green). Right: $\frac{K(m_x,0)-K(0,0)}{|1/2+\Delta|}$ as a function of $m_x = 2\sigma_x$, for $\gamma = \pi/4, \pi/3.75, \pi/3.5, \pi/3.25, \ \pi/2.75, \pi/2.5, \pi/2.25$, ie $\Delta \approx -0.7, -0.67, -0.6, -0.57, \ -0.42, -0.3, -0.17$.

5.4.5 Numerical checks

We now report a number of numerical checks that the fluctuations inside the arctic curve are Gaussian and are captured by the action (5.86). To give numerical evidence for the action (5.86) we use the procedure for calculating the free energy $F(\sigma_x, \sigma_y)$ presented in section 5.4.2, that we compare to a numerically exact transfer matrix evaluation of the connected correlations $\langle h(\mathrm{x})h(\mathrm{x}')\rangle$ on a 20×20 lattice. However, the way we check the gaussianity of fluctuations does not rely on the free energy calculations of section 5.4.2.

Check of Wick's theorem on a 20×20 lattice

We study the correlations of the height field h on a finite $N \times N$ lattice with domain-wall boundary conditions. We define the mean value of h on the lattice,

$$h_N(\mathrm{x}) = \langle h(\mathrm{x})\rangle \tag{5.119}$$

Our goal is to provide evidence that the action (5.86) is correct, and we start by checking that the fluctuations of the height field $h(\mathrm{x})$ around its mean value $h_N(\mathrm{x})$ become Gaussian in the thermodynamic limit.

To do so, we check that the four-point function of $\delta h(\mathrm{x}) = h(\mathrm{x}) - h_N(\mathrm{x})$ satisfies Wick's theorem,

$$
\begin{aligned}
\langle \delta h(\mathrm{x}_1)\delta h(\mathrm{x}_2)\delta h(\mathrm{x}_3)\delta h(\mathrm{x}_4)\rangle \quad = \quad & \langle \delta h(\mathrm{x}_1)\delta h(\mathrm{x}_2)\rangle\langle \delta h(\mathrm{x}_3)\delta h(\mathrm{x}_4)\rangle \\
+ \quad & \langle \delta h(\mathrm{x}_1)\delta h(\mathrm{x}_3)\rangle\langle \delta h(\mathrm{x}_2)\delta h(\mathrm{x}_4)\rangle + \langle \delta h(\mathrm{x}_1)\delta h(\mathrm{x}_4)\rangle\langle \delta h(\mathrm{x}_2)\delta h(\mathrm{x}_3)\rangle
\end{aligned} \tag{5.120}
$$

Numerically, we evaluate the following ratio,

$$
\delta W = \frac{\langle\phi_1\phi_2\phi_3\phi_4\rangle - \langle\phi_1\phi_2\rangle\langle\phi_3\phi_4\rangle - \langle\phi_1\phi_3\rangle\langle\phi_2\phi_4\rangle - \langle\phi_1\phi_4\rangle\langle\phi_2\phi_3\rangle}{\langle\phi_1\phi_2\phi_3\phi_4\rangle} \tag{5.121}
$$

with $\phi_j = \delta h(\mathrm{x}_j)$, which should be zero if Wick's theorem is satisfied. We work on an $N \times N$ lattice, with the maximal value $N = 20$. The correlation functions are calculated with a transfer matrix method which is numerically exact. There are N^8 four-point functions in total, and obtaining all of them is beyond reach for a system size $N = 20$, so we restrict ourselves to points x_i located in one of the four central squares of size $N/4$ (i.e., those defined by $N/2 \le x \le 3N/4$, $N/2 \le y \le 3N/4$ for the first one, $N/2 \le x \le 3N/4$, $N/4 \le y \le N/2$ for the second one, etc). Fig. 5.10 shows normalized histograms of the numerical calculation of these δW's.

Figure 5.10: Top: histograms of δW's for $\phi = \delta h$ for $c = 1/2$, i.e. $\Delta = 0.875$ (left) and $c = 19/10$, i.e. $\Delta \approx -0.8$ (right) in sizes $N = 12$ (red), $N = 16$ (blue), $N = 20$ (green). Inset: mean value (blue) an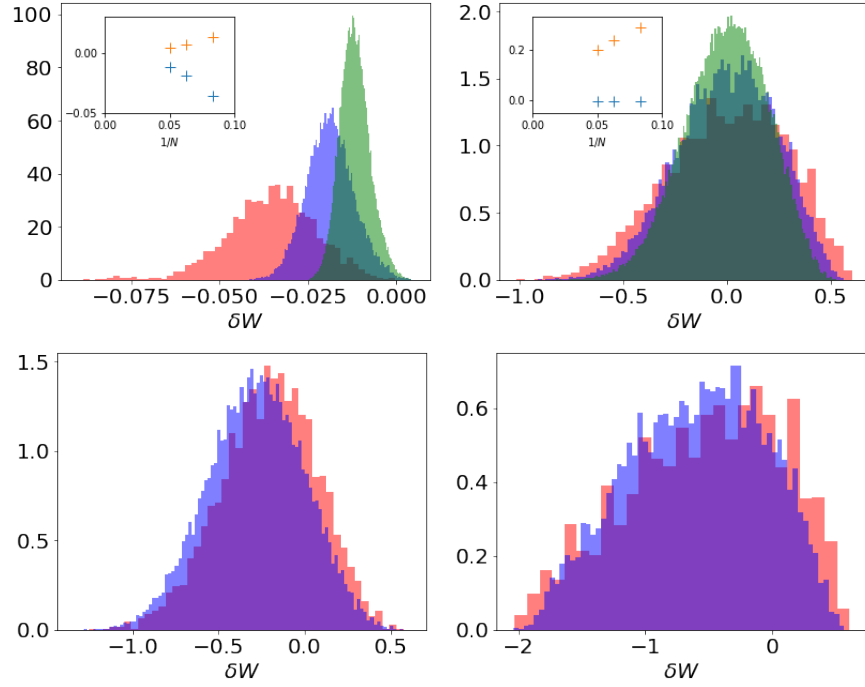d standard deviation (orange) of δW, as a function of $1/N$. Bottom: histograms of δW's for $\phi = (\delta h)^2$ for $c = 1/2$, i.e. $\Delta = 0.875$ (left) and $c = 19/10$, i.e. $\Delta \approx -0.8$ (right) in sizes $N = 12$ (red), $N = 16$ (blue).

In Fig. 5.10, the height of a narrow rectangle above the abscissa x is proportional to the number of measured four-point functions whose δW is between x and $x + dx$. They are normalized so that the integral is one. Thus, if Wick's theorem is perfectly satisfied, this plot should be a Dirac delta at 0. We see on the left that as N increases, the curve becomes narrower and closer to 0, indicating a convergence toward this distribution as $N \to \infty$. The convergence is much faster for $\Delta > 0$ than for $\Delta < 0$. As a control, to have an idea of the order of magnitude of δW for a generic quantity ϕ, we also plotted the same histograms for $\phi_j = (\delta h(\mathrm{x}_j))^2$. The δW's are much larger, as it should be since the square of a gaussian random variable is not gaussian and should not satisfy Wick's theorem.

From these numerical results we conclude that the theory describing the fluctuations inside the arctic curve is Gaussian.

Check of the action (5.86) on a 20×20 lattice

Next, we want to check that the two-point function of the height field is the one predicted by the action (5.86) in the thermodynamic limit. On the lattice, we define the connected correlation matrix, which is an $N^2 \times N^2$ matrix, as

$$G_N(\mathrm{x}, \mathrm{x}') = \langle h_N(\mathrm{x})h_N(\mathrm{x}')\rangle - \langle h_N(\mathrm{x})\rangle\langle h_N(\mathrm{x}')\rangle \qquad (5.122)$$

and its corresponding continuous function in the thermodynamic limit

$$G(\mathrm{x}, \mathrm{x}') = \langle h(\mathrm{x})h(\mathrm{x}')\rangle - \langle h(\mathrm{x})\rangle\langle h(\mathrm{x}')\rangle \qquad (5.123)$$

Then we make the following observation. If the fluctuations of h are described by the action (5.86), then $h(\mathrm{x})$ and $G(\mathrm{x}, \mathrm{x}')$ should satisfy the differential equation

$$-\nabla(\mathrm{Hess}\ F(h(\mathrm{x}))\nabla) \cdot G(\mathrm{x}, \mathrm{x}') = \delta(x - x') \qquad (5.124)$$

Denote $\mathcal{H}$ the differential operator $\mathcal{H}(h) = -\nabla(\mathrm{Hess}\ F(h(\mathrm{x}))\nabla)$. In finite size, the matrix G_N should satisfy a similar but discretized version of this differential equation. Denoting $\mathcal{H}_N$ the discretized version of $\mathcal{H}$ in size N (it acts on vectors with N^2 variables, so it is also an $N^2 \times N^2$ matrix), we have

$$\mathcal{H}_N(h_N)G_N = I_{N^2} \qquad (5.125)$$

As $N \to \infty$, $\mathcal{H}_N$ should be close to $-\nabla_N(\mathrm{Hess}\ F(h_N(\mathrm{x}))\nabla_N)$ where ∇_N stands now for discrete derivatives with respect to the two components of $\mathrm{x} = (x, y)$. This is what we intend to check numerically. Notice that Eq. (5.124) and Eq. (5.125) relate the two finite-size observables $h_N(.)$ and $G_N(.,.)$ to the thermodynamic free energy $F(.,.)$ studied in the previous section, so it really is a non-trivial check of the validity of the action (5.86).

To show that relation (5.124) holds, we rely on the following strategy. First, we evaluate the matrix G_N by a numerically exact transfer matrix method, and we invert it. Second, we analyze the matrix G_N^{-1}, and provide evidence that, at large N, it can be decomposed as a sum of discrete differential operators, the leading one being precisely a discretized version of $-\nabla(\mathrm{Hess}\ F(h(\mathrm{x}))\nabla)$, as expected from Eq. (5.124).

Expansion of $\mathcal{H}_N$ as a sum of discrete differential operators

Once the matrix G_N and thus $G_N^{-1} = \mathcal{H}_N$ is known numerically, our goal is to expand it as a sum of discrete differential operators, starting from the lowest-order ones,

$$\mathcal{H}_N = H_1 I_{N^2} + H_x \partial_x + H_y \partial_y + H_{xx} \partial_x^2 + 2 H_{xy} \partial_x \partial_y + H_{yy} \partial_y^2 + \ldots \qquad (5.126)$$

Here I_{N^2} is the identity, and ∂_x, ∂_y, ∂_x^2, $\partial_x \partial_y$, ∂_y^2 are discrete differential operators that are all represented as $N^2 \times N^2$ matrices. The corresponding matrices H_1, H_x, H_y, H_{xx}, H_{xy}, H_{yy} are all *diagonal* $N^2 \times N^2$ matrices, with N^2 diagonal coefficients associated with the lattice sites.

In principle, there exist different ways to discretize the operators ∂_x and ∂_y by using different finite-difference formulae, so the matrices $H_1, H_x, \ldots$ cannot be read off directly from the coefficients of the matrix $\mathcal{H}_N$. To circumvent that problem, we define 1 as the vector of size N^2 whose components are all 1, x as the vector of size N^2 with components $x_{i,j} = i$ for each $i, j = 1, \ldots, N$, and similarly $y_{i,j} = j$, $(x^2)_{i,j} = i^2$, $(y^2)_{i,j} = j^2$ and $(xy)_{i,j} = ij$. In the limit $N \to \infty$ these vectors become the corresponding functions, and regardless of the precise choice of the discretizations for the operators ∂_x and ∂_y, we should have $\partial_x \cdot 1 \to 0$ as $N \to \infty$, $\partial_x \cdot x \to 1$, etc. Thus the coefficients of $\mathcal{H}_N$ (now seen as vectors of size N^2) can estimated in finite-size by applying the matrix G_N^{-1} on these vectors $1, x, \ldots$:

$$
\begin{aligned}
H_1 &= G_N^{-1} \cdot 1 \\
H_x &= (G_N^{-1} - H_1 \delta_{1,N}) \cdot x \\
H_y &= (G_N^{-1} - H_1 \delta_{1,N}) \cdot y \\
H_{xx} &= \frac{1}{2}(G_N^{-1} - H_1 \delta_{1,N} - H_x \delta_{x,N}) \cdot x^2 \\
H_{yy} &= \frac{1}{2}(G_N^{-1} - H_1 \delta_{1,N} - H_y \delta_{y,N}) \cdot y^2 \\
H_{xy} &= \frac{1}{2}(G_N^{-1} - H_1 \delta_{1,N} - H_x \delta_{x,N} - H_y \delta_{y,N}) \cdot xy
\end{aligned}
\qquad (5.127)
$$

where $\delta_{1,N}$, $\delta_{x,N}$ and $\delta_{y,N}$ are $N^2 \times N^2$ matrices that are discretized versions of the operators 1, ∂_x and ∂_y without error term of order 2. We used $\delta_{x,N} f(x) \approx (f(x + \epsilon) - f(x - \epsilon))/(2\epsilon)$.

Results

In order to be compatible with the action (5.86), this procedure must lead to $H_1 = 0$, $H_x = \partial_x F \circ h_N$, $H_y = \partial_y F \circ h_N$, $H_{xx} = \partial_x^2 F \circ h_N$, $H_{yy} = \partial_y^2 F \circ h_N$ and $H_{xy} = \partial_x \partial_y F \circ h_N$ in the limit $N \to \infty$. In Fig. 5.11 we present a direct comparison between the coefficients of the diagonal matrices H_{xx} and H_{xy} obtained from G_N^{-1} with the above procedure, and a numerical evaluation of the discrete derivatives $\partial_x^2 F \circ h_N$ and $\partial_x \partial_y F \circ h_N$. The results are displayed for $c = 1/2$ and a lattice of size 20×20 in Figs. 5.11, 5.12 and 5.13.
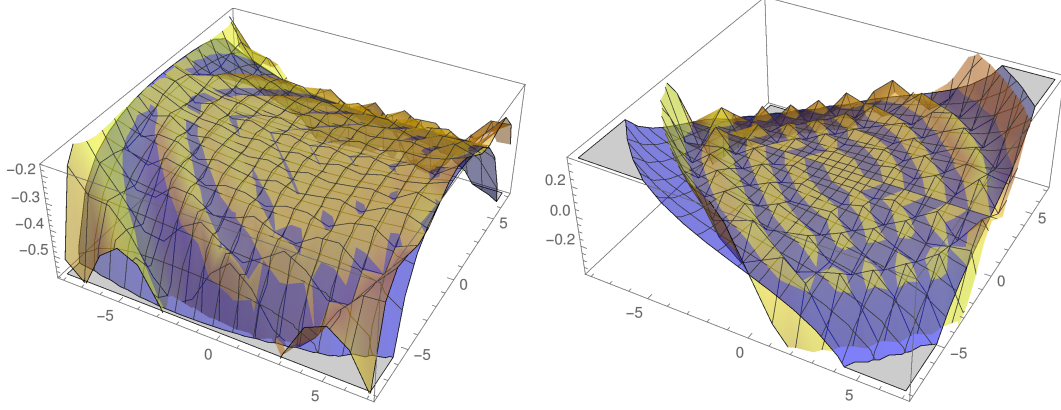
Figure 5.11: Coefficients of the differential operator H as a function of the position in the 20×20 lattice, with $(0,0)$ being the center (left: H_{xx} ; right: $2H_{xy}$). The transfer matrix measures (in yellow) are compared to the discrete derivatives $\partial_x^2 F \circ h_N$ and $2\partial_x\partial_y F \circ h_N$ with the thermodynamic free energy F calculated from the Bethe ansatz (in blue).

Figs. 5.11 and 5.12 show the general shape of the coefficients H_{xx} and H_{xy}, and illustrate that those computed with the Bethe ansatz are in good agreement with those extracted with the transfer matrix. There are strong parity effects that make the measured curve (in yellow in Fig. 5.11) oscillate around the theoretical curve (in blue). This is why, in Fig. 5.12, we show the same data, but where each point is averaged with its four neighbours according to the following scheme: $\frac{1}{2}(x,y) + \frac{1}{8}((x+1,y) + (x-1,y) + (x,y+1) + (x,y-1))$.
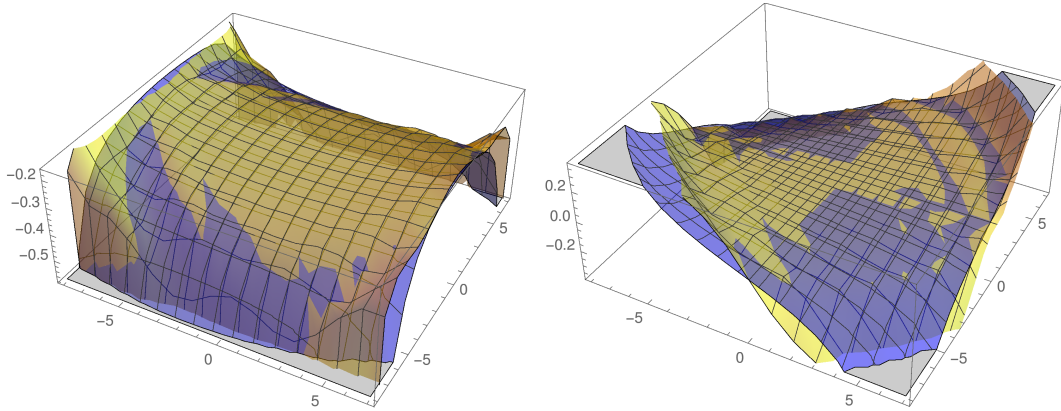
Figure 5.12: Averaged coefficients of the differential operator H as a function of the position in the 20×20 lattice, with $(0,0)$ being the centre (left: H_{xx} ; right: $2H_{xy}$). The transfer matrix measures (in yellow) are compared to the discrete derivatives of the free energy F calculated from the Bethe ansatz (in blue).

The coefficient H_{yy} is equal to H_{xx} because of the symmetry of the isotropic six-vertex

174

model. The coefficient H_1 is measured to be of order 10^{-3}, which is in good agreement with the fact that it should be zero in our description. The coefficients H_x and H_y are small both in the Bethe ansatz and the transfer matrix study (of order 10^{-2} – and should not be zero or particularly decrease with the system size N), but we do not have an agreement as satisfactory as for H_{xx} and H_{xy}. The fact that they are of order ten times smaller than the dominant coefficients H_{xx}, H_{yy}, H_{xy} certainly plays a role, being possibly scrambled by the oscillations or the averaging.

We study finite-size effects in Fig. 5.13. We show evidence for the convergence of the coefficients as N increases, by looking at the values on the diagonal of the lattice. In particular the ratio of the measured coefficient over the Bethe ansatz one clearly approaches 1 quite fast for $c = 1/2$ (top right). The value of H_{xx} at the center of the lattice also fits well with the Bethe ansatz calculation. As c increases (or as Δ decreases) the finite-size effects become stronger and a parity effect becomes visible (bottom right), but the ratio is still close to 1. This has to do with the fact that the first irrelevant operator becomes less and less irrelevant as Δ decreases, up to becoming marginal when $\Delta = -1$. In Fig. 5.11 the oscillations happen as well to increase when Δ decreases, and similar figures would be unreadable.
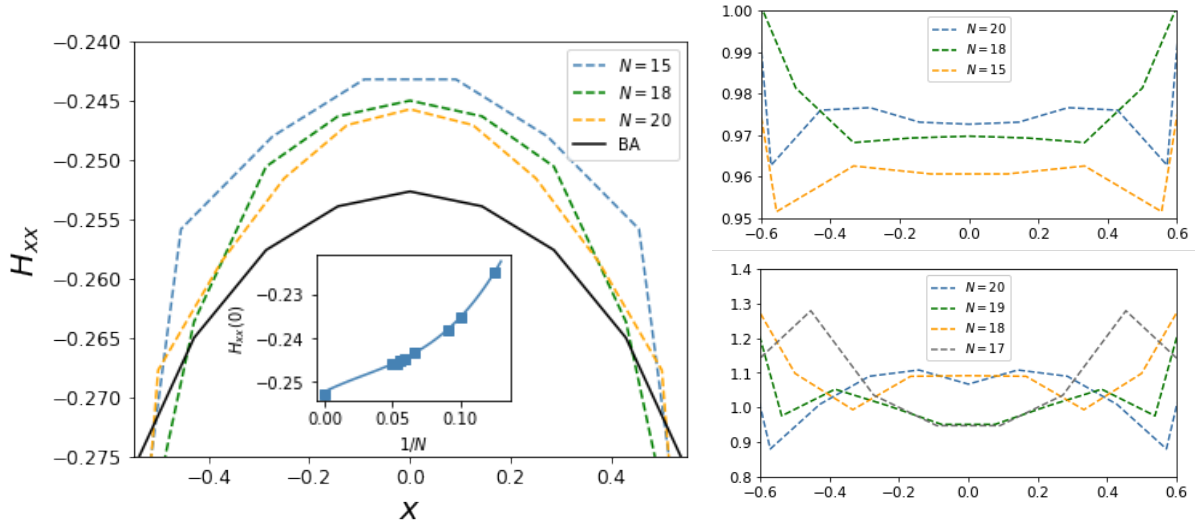
Figure 5.13: Left: averaged measured coefficient H_{xx} on the diagonal of the square lattice $(xN/2, xN/2)$ as a function of the normalized position x, for different sizes at $c = 1/2$. The black curve is computed with the Bethe ansatz, evaluated at the height function of the 20×20 square lattice. Inset: value of H_{xx} at the centre of the lattice $(0, 0)$ as a function of $1/N$, together with a polynomial extrapolation and its limit value computed with the Bethe ansatz. Right: same averaged measured coefficient H_{xx} as a function of x, but divided by the Bethe ansatz computation using the height function of the same lattice size, for $c = 1/2$, i.e. $\Delta = 0.875$ (top) and $c = 19/10$, i.e. $\Delta \approx -0.8$ (bottom).

To conclude this section, we have provided direct numerical evidence, from finite-size lattice calculations, that correlation functions of the height field are indeed captured by the action (5.86) in the the thermodynamic limit.

Conclusion

In this thesis we have studied exotic and less exotic quantum spin chains with the Bethe ansatz, and developed different analytic techniques to study their continuum limit.

We started with a thorough study of a family of integrable spin chains with orthosymplectic symmetry, that discretize the supersphere sigma models, generalizing the $O(N)$ model to any positive or negative integer $N < 2$. We established this correspondence by comparing a good part of the spectrum of the Hamiltonian in the field theory to the spectrum of the spin chain in finite size L, both numerically and analytically with the Bethe ansatz, up to (and including) order $L^{-2}(\log L)^{-1}$. Their continuum limit being a marginal perturbation of LCFT's, they offered a good opportunity to investigate for the first time the extent to which some properties of perturbed CFT's generalize to the logarithmic case. Besides, on the 2D statistical mechanics side, these spin chains describe fully packed trails which are possible descriptions of polymers. We established that their spectrum corresponds to critical exponents of algebraic and logarithmic decays of particular combinations of watermelon correlation functions, giving a previously unknown geometrical interpretation to the full spectrum. An interesting and natural direction would be to study their q-deformed version – their continuum limit and the geometrical meaning in terms of loops or Potts model – that seem to exhibit different non-compact directions in their spectrum.

The computation of logarithmic corrections to special states with isolated Bethe roots motivated a systematic study of the dependence of these finite-size effects on the Bethe equations. We developed a different setup in which the corrections are obtained through summation tricks from the Bethe equations, and in which the effects of e.g. descendant excitations are fairly simple to take into account, and facilitate the understanding of the effects of an additional source term that can encompass several root configurations.

We also showed that in presence of a magnetic field, several physical quantities of a spin chain such as the acquired magnetization or the critical exponents can be written as convergent series, whose terms can all be recursively computed in closed form. In the XXZ spin chain case these coefficients are rational functions of π and Δ, and can be said to solve the old problem of the acquired magnetization and continuum limit of the Heisenberg spin chain in a magnetic field. An important aspect of these series is that they permit to analytically continue certain parameters to domains where the Bethe ansatz does not directly apply. We

illustrate this point with the study of the free energy of a non-compact spin chain, for which we derive some intermediate results part of a still ongoing project. These series provide interesting directions of research, for their potential use in non-compact spin chains or their generalization to e.g. non-zero temperature.

Finally, we also worked on some other projects such as a mainly numerical study of the fluctuations inside the arctic curve of the interacting six-vertex model with domain-wall boundary conditions, for which we give evidence that they are described by an inhomogeneous Gaussian Free Field, and on the understanding of a priori unrelated criteria to identify admissible solutions in the Bethe ansatz.

Appendix A

A.1 Change of grading

In the algebraic Bethe Ansatz with fermionic degrees of freedom, a choice has to be made on the grading used, i.e., to chose which index of the R-matrix is bosonic or fermionic. Different gradings lead to different Bethe equations and different expressions for the eigenvalues and eigenvectors. But it turns out that in all the models considered one can pass from a grading to another by applying a transformation on the Bethe equations and Bethe eigenvalues. It shows that *for the eigenvalues*, all the gradings are equivalent, in the sense that if there is a set of Bethe roots in one grading that gives a precise eigenvalue, then there has to exist Bethe roots in all the other gradings (possibly degenerate) that give exactly the same eigenvalue. Nevertheless, nothing guarantees that the corresponding eigenvector in another grading will be non-zero. In other words, there may be some eigenvectors that we can build with the Bethe Ansatz only in particular gradings. All the gradings are equivalent for the eigenvalues, but not for the eigenvectors.

We present in the following the transformation in a rather general way. It is a generalization of what is presented in [97]. We assume that we have r distinct families of K_n Bethe roots λ_i^n, n being the index of the family and i the index of the root inside the family, and a set of reals $\alpha_{m,s}^n$, n and m indexing the families, and s being an aditionnal index varying from 1 to $u_{n,m}$ (that is needed for the Bethe equations to keep the same shape in another grading). We assume that the Bethe equations read for all $n = 1, ..., r$ and $i = 1, ..., K_n$:

$$\left(\prod_{s=1}^{u_{n,0}} \frac{\sinh(\lambda_i^n + i\gamma\alpha_{0,s}^n)}{\sinh(\lambda_i^n - i\gamma\alpha_{0,s}^n)} \right)^L = \prod_{m=1}^{r} \prod_{j=1}^{K_m} \prod_{s=1}^{u_{n,m}} \frac{\sinh(\lambda_i^n - \lambda_j^m + i\gamma\alpha_{m,s}^n)}{\sinh(\lambda_i^n - \lambda_j^m - i\gamma\alpha_{m,s}^n)} \tag{A.1}$$

for $\gamma > 0$ a parameter. Note that the case of non-q deformed Bethe equations can be recovered by taking $\gamma \to 0$ and rescale λ_i^n by $\gamma\lambda_i^n$. We impose without making it explicit that if $n = m$ in the product then the condition $i \neq j$ has to be taken. Two important assumptions have to be made in order to do be able to do the transformation:

- symmetry of the Bethe equations: $\alpha_{m,s}^n = \alpha_{n,s}^m$ and $u_{n,m} = u_{m,n}$.

- existence of a non-self-coupling family: there exists n such that $\alpha_{n,s}^n = 0$

These assumptions are stable under the transformation, as it will be shown. They are satisfied for the models studied in this paper.

Let n be such that $\alpha_{n,s}^n = 0$. The first step is to rewrite the equation for the n-th family as being the root of the polynomial $P(X)$ that reads:

$$P(X) = \left(\prod_{s=1}^{u_{n,0}}(Xq^{\alpha_{0,s}^n} - q^{-\alpha_{0,s}^n})\right)^L \prod_{m=1,\neq n}^r \prod_{j=1}^{K_m} \prod_{s=1}^{u_{n,m}}(Xq^{-\alpha_{m,s}^n} - t_j^m q^{\alpha_{m,s}^n})$$
$$- \left(\prod_{s=1}^{u_{n,0}}(Xq^{-\alpha_{0,s}^n} - q^{\alpha_{0,s}^n})\right)^L \prod_{m=1,\neq n}^r \prod_{j=1}^{K_m} \prod_{s=1}^{u_{n,m}}(Xq^{\alpha_{m,s}^n} - t_j^m q^{-\alpha_{m,s}^n})$$

(A.2)

where we set $t_j^m = \exp 2\lambda_j^m$ and $q = e^{i\gamma}$. The Bethe equation for the n-th family is thus $P(t_i^n) = 0$. But P is a polynomial of degree $Lu_{n,0} + \sum_{m=1,\neq n}^r u_{n,m}K_m$ which is not necessarily equal to K_n the number of Bethe roots in family n. Set $Lu_{n,0} + \sum_{m=1,\neq n}^r u_{n,m}K_m = K_n + K'_n$ and define $s_i^n = \exp 2\mu_i^n$ as the K'_n other roots of P. These will be the Bethe roots of family n in the other grading. They satisfy exactly the same Bethe equation as the former roots, but the equations for the other family are changed. All the λ_j^n must be changed for the μ_j^n. Consider first an $\alpha_{n,s}^m \neq 0$ that leads to a factor A of the type:

$$A = \log \prod_{j=1}^{K_n} \frac{\sinh(\lambda_i^m - \lambda_j^n + i\gamma\alpha_{n,s}^m)}{\sinh(\lambda_i^m - \lambda_j^n - i\gamma\alpha_{n,s}^m)} = -2K_n\alpha_{n,s}^m \log q + \sum_{j=1}^{K_n} \log \frac{t_i^m q^{2\alpha_{n,s}^m} - t_j^n}{t_i^m q^{-2\alpha_{n,s}^m} - t_j^n}$$

(A.3)

Define then the function $f(z)$ as:

$$f(z) = \log \frac{t_i^m q^{2\alpha_{n,s}^m} - z}{t_i^m q^{-2\alpha_{n,s}^m} - z}$$

(A.4)

In the complex plane, $(\log P)'(z)$ has $K_n + K'_n$ poles at t_j^n and s_j^n, and $f(z)$ has a branch cut where the argument of the log is real negative, which is a segment from $t_i^m q^{2\alpha_{n,s}^m}$ to $t_i^m q^{-2\alpha_{n,s}^m}$. Consider a contour $\mathcal{C}$ encircling the roots t_j^n and not the roots s_j^n, neither the branch cut. The residue theorem gives:

$$A = -2K_n\alpha_{n,s}^m \log q + \frac{1}{2i\pi} \oint_{\mathcal{C}} f(z)(\log P)'(z)dz$$

(A.5)

We now would like to deform the contour so that it encircles (in the other direction) the other poles. But then the branch cut enters in the integral, which becomes $2\pi i$ times the integral of $(\log P)'$ over the segment. It gives:

$$A = -2(K_n + K'_n)\alpha_{n,s}^m \log q - \sum_{j=1}^{K'_n} \log \frac{t_i^m q^{\alpha_{n,s}^m} - s_j^n q^{-\alpha_{n,s}^m}}{t_i^m q^{-\alpha_{n,s}^m} - s_j^n q^{\alpha_{n,s}^m}} + \log \frac{P(t_i^m q^{2\alpha_{n,s}^m})}{P(t_i^m q^{-2\alpha_{n,s}^m})}$$

(A.6)

But using the symmetry $\alpha_{n,s}^m = \alpha_{m,s}^n$, one of the two terms in P is zero when evaluated at these points, so that we get:

$$\frac{P(t_i^m q^{2\alpha_{n,s}^m})}{P(t_i^m q^{-2\alpha_{n,s}^m})} = -q^{2\alpha_{n,s}^m(Lu_{n,0}+\sum_{m'=1,\neq n}^r u_{n,m'})} \left(\prod_{s'=1}^{u_{n,0}} \frac{t_i^m q^{-\alpha_{0,s'}^n+\alpha_{n,s}^m} - q^{\alpha_{0,s'}^n-\alpha_{n,s}^m}}{t_i^m q^{\alpha_{0,s'}^n-\alpha_{n,s}^m} - q^{-\alpha_{0,s'}^n+\alpha_{n,s}^m}} \right)^L$$

$$\times \prod_{m'=1,\neq n}^r \prod_{j=1}^{K_{m'}} \prod_{s'=1}^{u_{n,m'}} \frac{t_i^m q^{\alpha_{n,s}^m+\alpha_{m',s'}^n} - t_j^{m'} q^{-\alpha_{n,s}^m-\alpha_{m',s'}^n}}{t_i^m q^{-\alpha_{n,s}^m-\alpha_{m',s'}^n} - t_j^{m'} q^{\alpha_{n,s}^m+\alpha_{m',s'}^n}}$$
(A.7)

Avoiding the term $i = j$ for $m' = m$ for every s' (which is present by symmetry of the α's, since $\alpha_{n,s}^m \neq 0$), the $-$ factor becomes $(-1)^{u_{n,m}-1}$. Since there are $u_{n,m}$ such multiplicative factors, they contribute to 1. The equations can be transformed back into sinh form, so that we get the Bethe equations for all $k = 1, ..., r$ and $i = 1, ..., K_k$:

$$\left(\prod_{s=1}^{u_{k,0}} \frac{\sinh(\lambda_i^k + i\gamma\kappa_{0,s}^k)}{\sinh(\lambda_i^k - i\gamma\kappa_{0,s}^k)} \right)^L = \prod_{m=1}^r \prod_{j=1}^{K_m} \prod_{s=1}^{u_{k,m}} \frac{\sinh(\lambda_i^k - \lambda_j^m + i\gamma\kappa_{m,s}^k)}{\sinh(\lambda_i^k - \lambda_j^m - i\gamma\kappa_{m,s}^k)}$$
(A.8)

with for $m, m' \neq n$:

$$\{\kappa_{0,s}^m\}_s = \{\alpha_{n,s}^m - \alpha_{0,s'}^n\}_{s',s} \cup \{-\alpha_{0,s'}^m\}_{s'}$$
$$\{\kappa_{n,s}^m\}_s = \{\alpha_{n,s}^m\}_s$$
$$\{\kappa_{m',s}^m\}_s = \{-\alpha_{m',s}^m\}_s \cup \{-\alpha_{n,s}^m - \alpha_{m',s'}^n\}_{s,s'}$$
(A.9)

and for all m:

$$\kappa_{m,s}^n = \alpha_{m,s}^n$$
(A.10)

We recall that in these new Bethe equations, the new K_n is the former K_n', and the new λ_i^n are the former μ_i^n. The two assumptions are still satisfied in this new grading, since the α's are symmetric and since the family n is still non-self-coupling (it is the only whose Bethe roots changed, but whose Bethe equations did not). We stress the fact that in the formulas (A.9), according to our conventions, a κ equal to zero must not be counted, a κ cancels a $-\kappa$, and importance must be given to the range of the s and s' (in particular in $\{...\}_{s,s'}$ if one of them sums over the empty set then the whole set is empty).

For example, for $osp(2|2)$ one has $\alpha_0^1 = \alpha_0^2 = 1/2$, $\alpha_1^1 = \alpha_2^2 = 0$, $\alpha_2^1 = \alpha_1^2 = 1$. After the transformation it gives no source term for the second family, and $\kappa_1^2 = 1$, $\kappa_2^2 = -2$.

A.2 Proof of Lemma 4

We give in this appendix a proof of Lemma 4.

Proof. First note that the absolute value of the weight of the configuration is independent of the indices of the loops that compose it, so that only the sign can change. This will precisely occur because of fermionic signs and the fact that $(-1)^{p_b} = -(-1)^{p_f}$ if b is bosonic ($p_b = 0$) and f fermionic ($p_f = 1$).

Let us choose a loop l in the configuration (see Figure A.1) and assume first that it does not cross the boundaries and does not intersect itself (but it can intersect other loops). After the change of index, all the $(-1)^{p_a}$ with a lying on the loop are multiplied by -1.
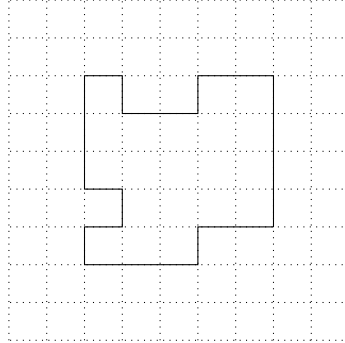

Figure A.1: The loop l. The other loops are not drawn.

Let us first consider the term $(-1)^{p_i p_j}$ in the I term in (3.159), that is present at each NW or SE corner. After the change of index, each NW and each SE corner thus contributes to a -1. In Figure A.2 we drew a red cross at an edge around each such corners to indicate this additional sign term.
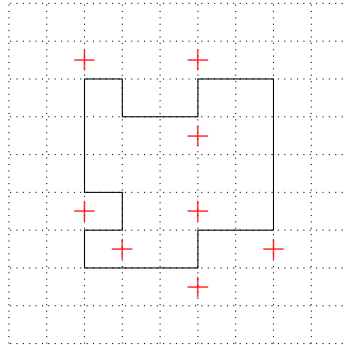

Figure A.2: The red crosses indicate an edge around each corner for which a $(-1)^{p_a}$ appears after changing the index of the loop, taking into account the term $(-1)^{p_i p_j}$ in (3.159).

Let us study now the term $(-1)^{\sum_{m=1}^{M} \sum_{j=2}^{L} (p_{\alpha_j^m} + p_{\alpha_j^{m+1}}) \sum_{i=1}^{j-1} p_{\alpha_i^m}}$. This one 'links' α_i^m and α_j^n whenever $m = n \pm 1$ and $i \gtrless j$, or $m = n$ and $i \neq j$. In the left panel of Figure A.3 the straight blue lines cross all the vertical edges that this sign term 'link' to the vertical edge indicated by a black cross. Notice that a straight line that begins inside the loop and that goes out intersects it an odd number of times; a straight line that begins outside the loop and that goes inside it and comes out intersects it an even number of times.

Consider an α_i^m (a vertical edge) that does not belong to the loop l. The parity of the number of α's linked to it by this sign term depends thus on the position of the points

$(m + 1/2, i + 1/2)$ and $(m − 3/2, i − 1/2)$ (the blue bullets in Figure A.3): if they both lie *inside* the loop or *outside* the loop, it is even; if one is inside and the other one outside it is odd. There is thus a $(−1)^{p_a}$ for each vertical edge with index a for which this number is odd, as shown in the middle panel of Figure A.3. Now the vertices that correspond to an intersection gives a possibility of simplification: every couple of $(−1)^{p_a}$ that are on each side of an edge that belongs to the loop l simplifies (since their index is primed and $p_a = p_{a'}$). One recovers signs only around SE or NW corners, see the right panel of Figure A.3. All these signs then exactly compensate with the signs of the first sign term.
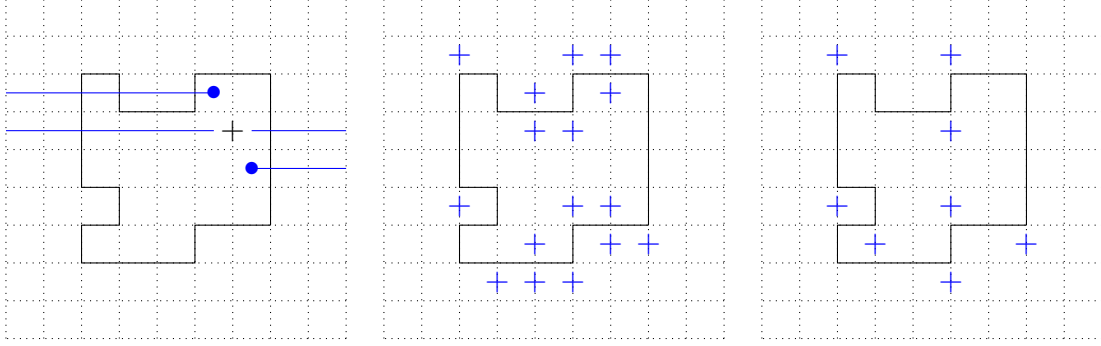

Figure A.3: The blue line intersects the vertical edges that are linked to the black cross in $(−1)^{\sum_{m=1}^{M} \sum_{j=2}^{L} (p_{\alpha_j^m} + p_{\alpha_j^{m+1}}) \sum_{i=1}^{j-1} p_{\alpha_i^m}}$. Then the blue crosses indicate the edges for which a $(−1)^{p_a}$ appears, and then after simplification.

Consider now an α_i^m (vertical edges) that is on the loop l. To avoid counting twice a change of sign, only the left-going straight blue lines in the left panel of Figure A.3 must be taken into account. There is a change of sign if and only if α_i^m belongs to a NE corner. This gives a $−1$ for each NE corner.

There is now the sign term that comes from the third term in (3.159) corresponding to E in (3.7). This one contributes to $−1$ or 1 for each SW and NE corner (the 'or' refers to whether the index of the loop, at say a SW corner, is smaller or larger than $D/2$, by inspection of (3.159) – but the sign is the same for both types of corners) in the loop l. Together with the $−1$ for each NE corner, it follows that there is finally a $−1$ for each SW *or* NE corner (again, according to the index of the loop at say a SW corner). But the number of NE corners (or of SW corners) is always odd for a loop that can be contracted into a point, which is the case for a non-self intersecting loop that does not cross the boundaries. Therefore the total contribution after the change of index of the loop l is $−1$.

If the loop l crosses only the left and right boundaries, then the previous arguments are still valid (because an horizontal line will always cross the loop an even number of times), but the number of SW or NE corners has now opposite parity as the number of times the left and right boundaries are crossed. Because of the sign term $(−1)^{\sum_{m=1}^{M} p_{c_1^m}}$ it cancels out and the total sign factor is still $−1$. Note the importance of taking the supertrace of the monodromy matrix to have this extra sign term.

If the loop l crosses the top and bottom boundaries, then the previous arguments are slightly modified (because an horizontal line will always cross the loop a number of times that has same parity as the number of times the up and down boundaries are crossed) but still hold. The only important difference is that there is no equivalent term to $(-1)^{\sum_{m=1}^{M} p_{c_1^m}}$ for the up and down boundaries, so that the resulting sign factor is $(-1)^{b_v+1}$ where b_v is the number of times the loop crosses the up and down boundaries.
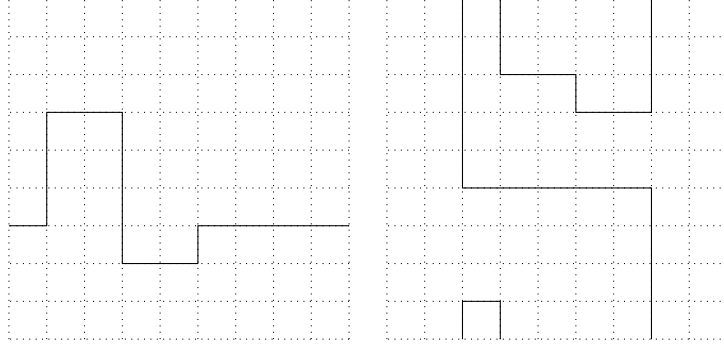

Figure A.4: Examples of non-contractible loops in both directions.

Finally, the intersections of the loop l with itself can be equally considered as a NW-SE couple of corners (if the indices of the two strands that intersect are the same) or a NE-SW couple of corners (if the indices of the two strands that intersect are primed) multiplied by a $(-1)^{p_\alpha}$ in both cases with α the index at the crossing. Indeed the fermionic signs stay the same during this transformation after the change of index, by inspection of (3.159). This transforms a loop with n self-intersections into a collection of $n+1$ independent non-self-intersecting loops, but whose indices have to be collectively changed at the same time when the index of the original loop l is changed. This gives an additional $(-1)^n$ that is compensated by the $(-1)^{p_\alpha}$ that comes with each transformation of a self-intersection into a corner, and that also contribute to $(-1)^n$ after the change of index.

$\square$

A.3 Proof of Lemma 6

Proof. To prove the lemma, we start by proving the following expansions:

$$\frac{1}{L} \sum_{k=-\epsilon L}^{\epsilon L-1} \log \frac{k+t}{L} = 2(\epsilon \log \epsilon - \epsilon) + \epsilon \operatorname{sgn}(\Im t) i\pi + \frac{\log(2 \sin \pi t)}{L} + o(L^{-1}) \qquad \text{(A.11)}$$

and

$$\frac{1}{L^2} \sum_{k=-\epsilon L}^{\epsilon L-1} \sum_{p=-\epsilon L}^{\epsilon L-1} \text{sgn}\,(k+1/2) \log \tfrac{k-p+t}{L}$$

$$= -\frac{1}{2} \text{sgn}\,(\Im t) i\pi \epsilon^2 + \frac{\epsilon}{L}(-\log \epsilon + 2t - \tfrac{1}{2} \text{sgn}\,(\Im t) i\pi) - \frac{1}{L^2}\left(\frac{\text{Cl}_2\,(2\pi t)}{2\pi} + t\log(2\sin\pi t)\right)$$

$$+ \frac{\epsilon}{L} \sum_{u=0}^{\epsilon L-1} \log(\epsilon + \tfrac{u+t}{L}) - \frac{1}{L}\sum_{u=0}^{\epsilon L-1}\frac{u}{L}(\log(\epsilon + \tfrac{u+t}{L}) + \log(-2\epsilon + \tfrac{u+t}{L})) + o(L^{-2})$$

$$\tag{A.12}$$

where Cl_2 is the Clausen function given by

$$\frac{\text{Cl}_2\,(2\pi t)}{2\pi} = t\log(\Gamma(t)\Gamma(1-t)) + \log\frac{G(1-t)}{G(1+t)} \tag{A.13}$$

with $G(z)$ the Barnes function.

To that end, we write

$$\frac{1}{L}\sum_{k=-\epsilon L}^{\epsilon L-1} \log \tfrac{k+t}{L} = -2\epsilon\log L + \frac{1}{L}\sum_{k=0}^{\epsilon L-1}\log(k+t) + \frac{1}{L}\sum_{k=0}^{\epsilon L-1}\log(k+1-t) + \frac{1}{L}L\epsilon\,\text{sgn}\,(\Im t)i\pi$$

$$= -2\epsilon\log L + \epsilon\,\text{sgn}\,(\Im t)i\pi + \frac{1}{L}\log\frac{\Gamma(\epsilon L+t)}{\Gamma(t)} + \frac{1}{L}\log\frac{\Gamma(\epsilon L+1-t)}{\Gamma(1-t)}$$

$$\tag{A.14}$$

and using Stirling's formula for the asymptotic expansion of $\log\Gamma(z)$, together with $\Gamma(t)\Gamma(1-t) = \pi/\sin(\pi t)$, one finds the formula (A.11).

To compute the second formula (A.12), one starts by performing the change of variable $u = k-p$. We have $-2\epsilon L+1 \le u \le 2\epsilon L-1$, $-\epsilon L \le p \le \epsilon L-1$, $-\epsilon L \le k \le \epsilon L-1$, hence for each positive or zero value of k there are $\max(\epsilon L + \min(-u,0) + \min(u,\epsilon L),0)$ possible values of p's, and for each strictly negative value of k there are $\max(\epsilon L + \min(u,0) + \min(-u,\epsilon L),0)$ possible values of p's. Thus

$$\frac{1}{L^2} \sum_{k=-\epsilon L}^{\epsilon L-1} \sum_{p=-\epsilon L}^{\epsilon L-1} \text{sgn}\,(k+1/2) \log \tfrac{k-p+t}{L}$$

$$= \frac{1}{L^2}\sum_{u=-\epsilon L}^{\epsilon L-1} u\log\tfrac{u+t}{L} + \frac{1}{L^2}\sum_{u=\epsilon L}^{2\epsilon L-1}(2\epsilon L-u)\log\tfrac{u+t}{L} - \frac{1}{L^2}\sum_{u=-2\epsilon L+1}^{-\epsilon L-1}(2\epsilon L+u)\log\tfrac{u+t}{L}$$

$$\tag{A.15}$$

$$= \frac{1}{L}\sum_{u=-\epsilon L}^{\epsilon L-1}\frac{u+t}{L}\log\tfrac{u+t}{L} - \frac{t}{L^2}\sum_{u=-\epsilon L}^{\epsilon L-1}\log\tfrac{u+t}{L} + \frac{\epsilon}{L}\sum_{u=0}^{\epsilon L-1}\log(\epsilon + \tfrac{u+t}{L})$$

$$- \frac{1}{L}\sum_{u=0}^{\epsilon L-1}\frac{u}{L}(\log(\epsilon + \tfrac{u+t}{L}) + \log(-2\epsilon + \tfrac{u+t}{L}))$$

Then

$$\frac{1}{L}\sum_{k=-\epsilon L}^{\epsilon L-1} \tfrac{k+t}{L}\log\tfrac{k+t}{L} = \epsilon(1-2t)\frac{\log L}{L} + \operatorname{sgn}(\Im t)\frac{i\pi\epsilon}{L}(-\tfrac{1}{2}+t) - \operatorname{sgn}(\Im t)\frac{i\pi\epsilon^2}{2} +$$

$$+ \frac{1}{L^2}\sum_{k=0}^{\epsilon L-1}(k+t)\log(k+t) - \frac{1}{L^2}\sum_{k=0}^{\epsilon L-1}(k+1-t)\log(k+1-t)$$

$$(A.16)$$

and

$$\sum_{k=0}^{\epsilon L-1}(k+t)\log(k+t) = (\epsilon L+t)\sum_{k=0}^{\epsilon L-1}\log(k+t) - \log\prod_{k=0}^{\epsilon L-1}(k+t) - \log\prod_{k=0}^{\epsilon L-2}(k+t)... - \log t$$

$$= (\epsilon L+t)\log\frac{\Gamma(\epsilon L+t)}{\Gamma(t)} - \log\frac{G(\epsilon L+1+t)}{G(1+t)} + \epsilon L\log\Gamma(t)$$

$$(A.17)$$

where we used the property $G(1+z) = \Gamma(z)G(z)$. Then, using an asymptotic expansion of $\log G(z)$ one finds

$$\frac{1}{L}\sum_{k=-\epsilon L}^{\epsilon L-1}\tfrac{k+t}{L}\log\tfrac{k+t}{L} = -\operatorname{sgn}(\Im t)\frac{i\pi\epsilon^2}{2} + \frac{\epsilon}{L}\left((2t-1)\log\epsilon + i\pi\operatorname{sgn}(\Im t)(-\tfrac{1}{2}+t)\right) - \frac{1}{L^2}\frac{\operatorname{Cl}_2(2\pi t)}{2\pi} + o(L^{-2})$$

$$(A.18)$$

hence formula (A.12), using (A.11).

Then the general technique to handle Riemann sums of a function $f(x)$ with a logarithmic singularity at $x=0$ is to add and subtract another function $\propto (\log x)1_{|x|<\epsilon}$ with the same singularity at $x=0$, but with a support of size ϵ. The function $f(x)-g_\epsilon(x)$ is not singular at $x=0$ so that its Riemann sum can be computed with Euler-MacLaurin formula; on the other hand the Riemann sum of $g_\epsilon(x)$ for ϵ small enough might be simple enough to be computed directly. One finds then that the corrections to the Riemann sums are the normal Euler-MacLaurin terms of $f(x)$, plus the corrections to the Riemann sum of $g_\epsilon(x)$, minus the normal Euler-MacLaurin terms of $g_\epsilon(x)$. From equation (A.11) one simply has to substract the Euler-MacLaurin terms of $\log x$ on the segment $[-\epsilon,\epsilon]$ to get the stated formula (4.87). To obtain (4.89), one subtracts as well the Euler-MacLaurin terms of $x\log x$ and $\log x$ from (A.12) (the remaining Riemann sums of the last line in (A.12) are not singular, so they are directly cancelled at order $O(L^{-2})$ by their Euler-MacLaurin terms) and then uses the following relation between the Clausen function and the dilogarithm for $\Im\theta \geq 0$ [182]

$$\operatorname{Li}_2(e^{i\theta}) = \frac{\pi^2}{6} - \frac{1}{4}\theta(2\pi-\theta) + i\operatorname{Cl}_2(\theta) \tag{A.19}$$

$\square$

This is illustrated in Figure A.5 for the function $r(\lambda)$. After removing the logarithmic singularity, there are additional discontinuities in the imaginary part, but the two compensate

exactly at order $1/L$. In the real part, there is still a discontinuity: thus the $1/L$ correction in the Riemann sum of $r(\lambda - i\gamma)$ involves the $1/L$ term correction in the Euler-MacLaurin formula to account for this discontinuity, and the additional term $1/L$ term in (4.87). The terms in (A.11) involving ϵ exactly simplify with the integral of $g_\epsilon(\lambda)$.
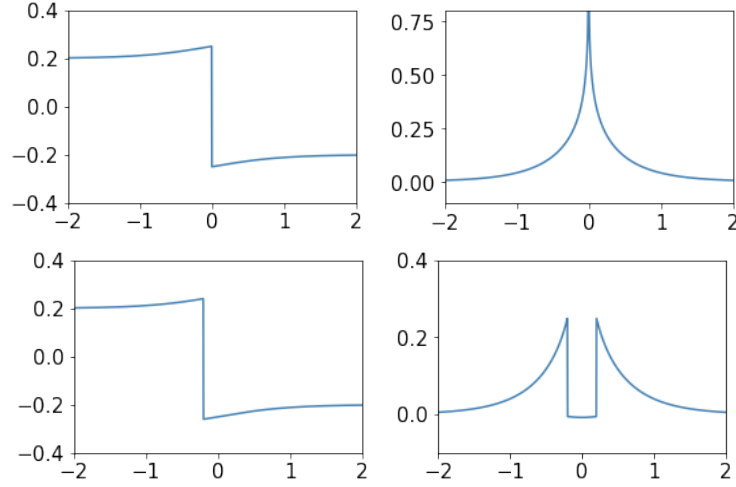
Figure A.5: Real and imaginary parts of $r(\lambda - i\gamma)$ as a function of λ (top), real and imaginary parts of $r(\lambda - i\gamma) - \frac{i}{2\pi}(\log x)1_{|x|<0.2}$ as a function of λ (bottom).

A.4   Proof of Lemma 7

Proof. Let us denote

$$X = \frac{i}{\pi} \sum_{q=-S+1/2}^{S-1/2-1} \Delta_2(\delta I_q - \delta I_{q+1}) \tag{A.20}$$

Using the expressions for Δ_2, one has

$$
\begin{aligned}
X = \sum_{q=-S+1/2}^{S-1/2-1} & -\frac{\mathrm{Li}_2\, e^{2i\pi(\delta I_q - \delta I_{q+1})}}{2\pi^2} + (\delta I_q - \delta I_{q+1})^2 \\
& -\frac{\delta I_q - \delta I_{q+1}}{2} - \frac{i(\delta I_q - \delta I_{q+1})}{\pi} \log 2\sin\pi(\delta I_q - \delta I_{q+1})
\end{aligned}
\tag{A.21}
$$

Let us evaluate the quantity Σ defined by

$$\Sigma = \sum_{q=-S+1/2}^{S-1/2-1} \frac{i(\delta I_q - \delta I_{q+1})}{\pi} \log(2\sin\pi(\delta I_q - \delta I_{q+1})) \tag{A.22}$$

187

To simplify it, we introduce the following notations: $a_q = i\dfrac{\log(2\sin\pi(\delta I_q - \delta I_{q+1}))}{2\pi}$, $b_q = -\dfrac{\delta I_{q-1} + 2\delta I_q + \delta I_{q+1}}{2}$ with $\delta I_{S+1/2} \equiv \delta I_{S-1/2}$ and $\delta I_{-S-1/2} \equiv \delta I_{-S+1/2}$, $c_q = \delta I_q - \delta I_{q+1}$ and M the $(2S-1)\times(2S-1)$ square matrix

$$M = \begin{pmatrix} 1 & 0 & \ldots & & & 0 \\ -1 & 1 & 0 & \ldots & & 0 \\ 0 & -1 & 1 & 0 & \ldots & 0 \\ \ldots & & & & & \\ 0 & & \ldots & & -1 & 1 \end{pmatrix} \tag{A.23}$$

System (4.95) translates into $b = Ma + x$ with $x = (1/4, 0, ..., 0)$, so that we have $\Sigma = 2c^t \cdot M^{-1}(b-x)$. Besides,

$$M^{-1} = \begin{pmatrix} 1 & 0 & \ldots & & & 0 \\ 1 & 1 & 0 & \ldots & & 0 \\ 1 & 1 & 1 & 0 & \ldots & 0 \\ \ldots & & & & & \\ 1 & 1 & \ldots & & & 1 \end{pmatrix} \tag{A.24}$$

that yields

$$\Sigma = -\sum_{q=-S+1/2}^{S-1/2} (\delta I_q - \delta I_{S+1/2})(\delta I_{q+1} + 2\delta I_q + \delta I_{q-1}) - \sum_{q=-S+1/2}^{S-1/2-1} \frac{\delta I_q - \delta I_{q+1}}{2} \tag{A.25}$$

which becomes after some rearrangement using $\delta I_{S-1/2} = -\delta I_{-S+1/2}$, with the convention $\delta I_{S+1/2} = \delta I_{S-1/2}$

$$\Sigma = -\sum_{q=-S+1/2}^{S-1/2} (\delta I_q + \delta I_{q+1})^2 - \sum_{q=-S+1/2}^{S-1/2-1} \frac{\delta I_q - \delta I_{q+1}}{2} \tag{A.26}$$

so that X becomes

$$X = \sum_{q=-S+1/2}^{S-1/2-1} -\frac{\mathrm{Li}_2\, e^{2i\pi(\delta I_q - \delta I_{q+1})}}{2\pi^2} + 4\sum_{q=-S+1/2}^{S-1/2} (\delta I_q)^2 \tag{A.27}$$

Let us focus now on the dilogarithm term. We rewrite it with the following function (the Rogers dilogarithm)

$$\mathrm{L}(x) = \mathrm{Li}_2(x) + \frac{1}{2}\log x \log(1-x) \tag{A.28}$$

giving

$$X = -\sum_{q=-S+1/2}^{S-1/2-1} \frac{\mathrm{L}\left(e^{2i\pi(\delta I_q - \delta I_{q+1})}\right)}{2\pi^2} + \Sigma' + 4\sum_{q=-S+1/2}^{S-1/2} (\delta I_q)^2 \tag{A.29}$$

where the following quantity Σ' appears

$$\Sigma' = \frac{i}{2\pi} \sum_{q=-S+1/2}^{S-1/2-1} (\delta I_q - \delta I_{q+1}) \log(1 - e^{2i\pi(\delta I_q - \delta I_{q+1})}) \tag{A.30}$$

From equation (4.96) we have

$$1 - e^{2i\pi(\delta I_q - \delta I_{q+1})} = \frac{\sin^2 \frac{\pi}{2} \frac{1}{S+1}}{\cos^2 \frac{\pi}{2} \frac{q+1/2}{S+1}} \tag{A.31}$$

so that we can write

$$\prod_{q'=-S+1/2}^{q} e^{4i\pi\delta I_{q'}} = \frac{\cos^2 \frac{\pi}{2} \frac{-S}{S+1}}{\cos^2 \frac{\pi}{2} \frac{q+1/2}{S+1}} = 1 - e^{2i\pi(\delta I_q - \delta I_{q+1})} \tag{A.32}$$

and Σ' becomes

$$\Sigma' = -2 \sum_{q=-S+1/2}^{S-1/2-1} (\delta I_q - \delta I_{q+1})(\delta I_{-S+1/2} + ... + \delta I_q) \tag{A.33}$$

which partially telescopes into

$$\Sigma' = -2 \sum_{q=-S+1/2}^{S-1/2} (\delta I_q)^2 \tag{A.34}$$

Now we use these two relations in [182] (equations 1.3 and 1.16), following [133, 134]

$$\mathrm{L}\,(x) + \mathrm{L}\,(1-x) = \frac{\pi^2}{6}, \quad 0 < x < 1$$
$$\sum_{q=0}^{2S-1} \mathrm{L}\,\left(\frac{\sin^2 \frac{\pi}{2} \frac{1}{S+1}}{\sin^2 \frac{\pi}{2} \frac{q+1}{S+1}} \right) = \frac{\pi^2}{6} \frac{3S}{S+1} \tag{A.35}$$

to get

$$X = -\frac{2S}{12} + \frac{1}{12} \frac{3S}{S+1} + 2 \sum_{q=-S+1/2}^{S-1/2} (\delta I_q)^2 \tag{A.36}$$

which is the claimed relation. $\qquad\square$

A.5 Proof of Lemma 8

Proof. For $0 < \nu < 1$ we have the following Riemann sum

$$\frac{1}{L} \sum_{k=0}^{\alpha L/2-1} \left(\frac{k+t}{L} \right)^{\nu} = \frac{(\alpha/2)^{\nu+1}}{\nu+1} + \frac{(\alpha/2)^{\nu}(t-\frac{1}{2})}{L} + \frac{\zeta(-\nu,t)}{L^{1+\nu}} + o(L^{-1-\nu}) \tag{A.37}$$

with $\zeta(-\nu, t)$ the Hurwitz zeta function, see [183] for the case $t = 1$. Integrating over ν between 0 and 1:

$$\frac{1}{L} \sum_{k=0}^{\alpha L/2-1} \left(\frac{\frac{k+t}{L}}{\log \frac{k+t}{L}} - \frac{1}{\log \frac{k+t}{L}} \right) = \int_0^1 \frac{(\alpha/2)^{\nu+1}}{\nu+1} d\nu + \frac{\alpha/2 - 1}{\log(\alpha/2)} \frac{t - \frac{1}{2}}{L} + \frac{\zeta(0,t)}{L \log L} + o(L^{-1}(\log L)^{-1})$$

(A.38)

which gives

$$\frac{1}{L} \sum_{k=0}^{\alpha L/2-1} \frac{1}{\log \frac{k+t}{L}} = \int_0^{\alpha/2} \frac{dx}{\log x} + \frac{1}{\log(\alpha/2)} \frac{t - \frac{1}{2}}{L} + \frac{t - \frac{1}{2}}{L \log L} + o(L^{-1}(\log L)^{-1}) \qquad (A.39)$$

and then, removing the first n terms of the sum

$$\frac{1}{L} \sum_{k=n}^{\alpha L/2-1} \frac{1}{\log \frac{k+t}{L}} = \int_0^{\alpha/2} \frac{dx}{\log x} + \frac{1}{\log(\alpha/2)} \frac{t - \frac{1}{2}}{L} + \frac{t - \frac{1}{2} + n}{L \log L} + o(L^{-1}(\log L)^{-1}) \qquad (A.40)$$

$\square$

Résumé français

Les modèles exactement solubles sont inestimables en physique, car ils fournissent des points de repère importants sur lesquels de nouvelles idées et théories peuvent être testées, ou autour desquels des perturbations peuvent être effectuées pour décrire des systèmes réels. Parfois, ces modèles capturent même une caractéristique essentielle d'un mécanisme physique qui est observé de façon similaire dans d'autres situations. Un des paradigmes en physique quantique et statistique est celui de la chaîne de spin de Heisenberg, introduite pour expliquer le magnétisme comme un ordre à longue portée émergeant d'interactions à courte portée entre une multitude d'atomes. Bethe effectua une avancée majeure en montrant que la chaîne unidimensionnelle peut être diagonalisée exactement avec un ansatz particulier. En raison de son adaptabilité à de nombreux autres modèles, cet ansatz a depuis fait l'objet de nombreuses recherches pour ses applications en physique quantique, statistique et de la matière condensée.

Cependant, une idée importante qui va souvent de pair avec l'intégrabilité est celle de l'universalité, à savoir que les détails des interactions à courte portée d'un système de physique quantique ou statistique n'influencent pas les corrélations critiques à longue portée, qui dépendent alors seulement de quelques caractéristiques essentielles des interactions qui les définissent telles que leur symétrie. L'une des pierres angulaires de la physique quantique et statistique moderne est donc d'établir une correspondance entre les symétries des poids de Boltzmann et la limite continue du modèle. Dans cette perspective, un système intégrable est considéré comme un simple représentant d'une classe d'universalité contenant possiblement des systèmes physiquement intéressants mais non intégrables, sur lesquels des calculs analytiques exacts peuvent être effectués.

Une propriété cruciale qui facilite l'identification de la limite continue d'un modèle est son invariance conforme, qui doit alors être une théorie conforme des champs. Dans cette hypothèse, la limite continue est caractérisée par un ensemble de nombres tels que la charge centrale, les dimensions d'échelle des champs et les constantes de structure ; et l'invariance conforme implique en fait qu'une bonne partie de ceux-ci est présente et visible dans le comportement asymptotique du spectre de basse énergie de la chaîne de spin dans la limite de volume infini.
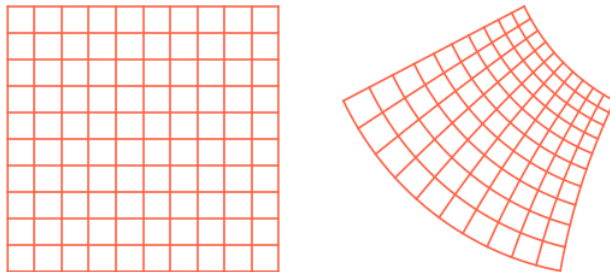
Figure A.6: Une grille et son image par une transformation conforme.

Bien que la limite continue des chaînes de spin intégrables avec une symétrie de groupe compact soit comprise, celles avec symétrie de supergroupe sont beaucoup moins bien comprises. La présence de supersymétrie s'explique par la nécessité parfois d'avoir recours à des variables anticommutantes comme dans le modèle Hubbard, ou parce qu'elles permettent d'étendre la gamme de certains paramètres à zéro ou à des entiers négatifs. Il s'agit donc d'une alternative à l'approche des répliques $n \to 0$ dans les systèmes désordonnés pour calculer la moyenne sur le désordre. La mauvaise compréhension de la limite continue des chaînes de spin supersymétriques provient d'un certain nombre de difficultés supplémentaires. Ces modèles sont en effet souvent non-hermitiens, présentent souvent des degrés de liberté non-compacts dans leur limite continue, à savoir qu'il y a des champs avec une dimension conforme réelle arbitraire. Ils sont également régulièrement des perturbations marginales de théories conformes des champs logarithmiques.

Ce manuscript présente à la fois des études détaillées de la limite continue de modèles intégrables sur réseau supersymétriques, et développe de nouvelles techniques pour étudier cette correspondance. Le manuscrit est organisé comme suit :

1. Le premier chapitre présente les notations et les résultats classiques sur l'ansatz de Bethe et la correspondance entre les modèles de boucles et CFT, que nous utiliserons tout au long du manuscrit. Il comprend un nouveau critère pour distinguer les solutions admissibles des solutions non admissibles aux équations de Bethe.

2. Le deuxième chapitre est une étude approfondie des chaînes de spin non unitaires à symétrie orthosymplectique *osp*, de leur limite continue qui sont des perturbations marginales de LCFT, de leurs réalisations en physique statistique 2D en tant que chemins et des corrections logarithmiques que cela implique sur leurs fonctions de corrélation.

3. Le troisième chapitre présente une nouvelle approche du calcul du spectre d'excitation des chaînes de spin critiques, qui évite l'utilisation des équations intégrales de Wiener-Hopf ou non linéaires. Il comprend une étude détaillée de la dépendance du spectre et de ses corrections logarithmiques par rapport aux fonctions de l'ansatz de Bethe.

4. Le quatrième chapitre est une étude de l'influence du champ magnétique, motivée par l'effet de régularisation qu'il peut avoir sur ces chaînes de spin exotiques. Il montre comment dériver des développements en série pour des chaînes de spin dans un champ magnétique externe par des relations de récurrence, et explique comment cela pourrait être utilisé pour étudier des modèles non compacts, qui est encore un projet en cours. Nous étudions également la théorie des champs qui décrit les fluctuations à l'intérieur de la courbe arctique du modèle à six vertex avec des conditions aux limites en mur.
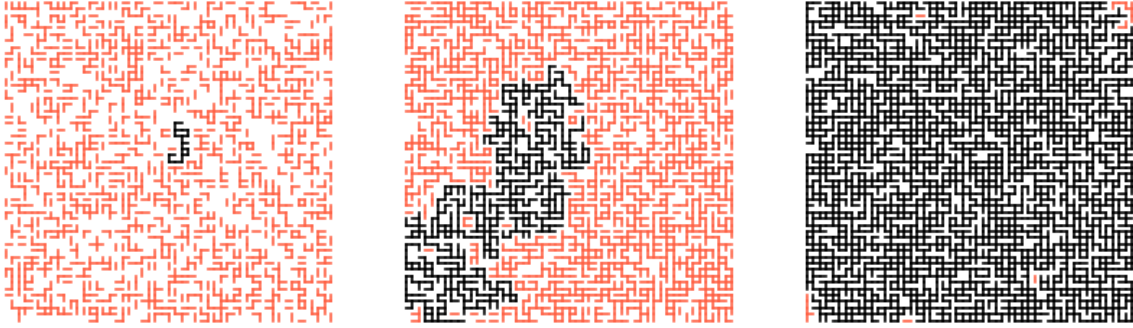

Figure A.7: Illustration du concept de limite continue avec l'exemple de la percolation. Chaque arête d'un réseau carré est coloriée avec une probabilité p (de gauche à droite, $p = 0.3, 0.5, 0.7$). Les arêtes connectées à l'arête centrale sont coloriées en noir. C'est uniquement à $p = 1/2$ que la probabilité que deux sommets soient connectés dépend de façon non triviale de la distance qui les sépare.

Dans le troisième chapitre nous étudions en détail la limite continue de chaînes de superspins non-unitaires (et parfois non-compactes) qui ont une symétrie orthosymplectique. Nous montrons qu'il s'agit de modèles sigma sur supersphère en calculant leur spectre avec la théorie des champs, avec l'ansatz de Bethe, et numériquement. Leur non-unitarité autorise une brisure spontanée de symétrie habituellement interdite par le théorème de Mermin-Wagner, et dans le cas $osp(2|2)$ et $osp(3|2)$ ils présentent un spectre non-compact d'exposants critiques. Leur caractère de perturbation marginale d'une théorie conforme des champs logarithmique est particulièrement étudié, et nous montrons que certains aspects des fonctions de corrélations des perturbations de théories conformes ordinaires ne sont plus vérifiés dans le cas logarithmique. Nous établissons également une correspondance précise entre le spectre et des configurations de boucles avec intersections, et obtenons de nouveaux exposants critiques pour les chemins non-recouvrants compacts ainsi que leurs corrections logarithmiques multiplicatives. Nous étudions finalement numériquement le comportement du modèle lorsqu'un paramètre est amené en dehors du point intégrable.
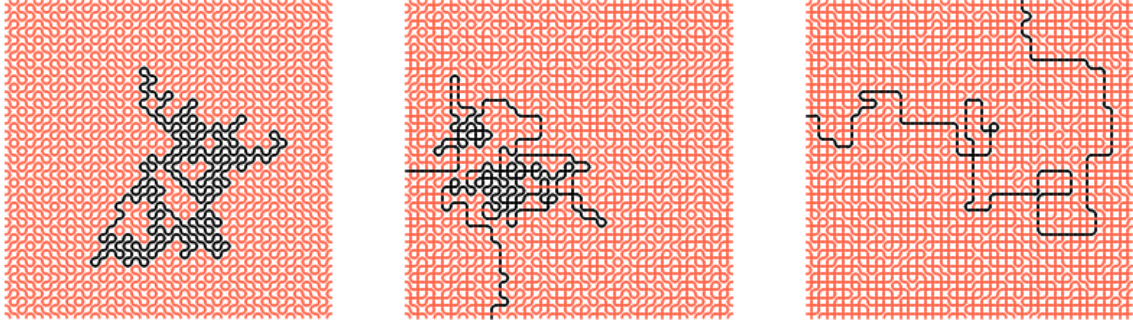
Figure A.8: Configurations du modèle des boucles intersectantes avec poids de boucle 1 et poids d'intersection $w = 0, 1, 4$ dans le sens de la lecture. Les arêtes reliées à l'arête centrale sont coloriées en noir.

Dans le quatrième chapitre nous calculons le spectre d'excitation d'une chaîne de spin quantique critique à partir de l'ansatz de Bethe avec une nouvelle méthode. Celle-ci évite les méthodes de Wiener-Hopf et les équations intégrales non-linéaires, et repose sur l'étude de la fonctionnelle qui évalue la somme d'une fonction test sur les racines de Bethe. Nous calculons en particulier la dépendance des corrections de taille finie correspondant aux exposants critiques et corrections logarithmiques, en fonction d'un terme source additionnel qui permet de prendre en compte des racines isolées ou un changement de conditions aux bords. Nous montrons que la méthode est également applicable au cas des strings de la chaîne XXZ avec spin $S \geq 1$.

Dans le cinquième chapitre nous abordons l'influence d'un champ magnétique sur une chaîne de spin quantique et montrons que des séries convergentes peuvent être obtenues pour plusieurs quantités physiques telles que l'aimantation acquise ou les exposants critiques, dont les coefficients peuvent être calculés efficacement par récurrence. La structure de ces relations de récurrence permet d'étudier génériquement le spectre d'excitation, et elles sont applicables y compris dans certains cas où les racines de Bethe sont sur une courbe dans le plan complexe. Nous espérons que l'étude de la continuation analytique de ces séries puisse être utile pour les chaînes non-compactes, en montrant que certaines quantités peuvent être effectivement continuées analytiquement. Par ailleurs, nous montrons que les fluctuations à l'intérieur de la courbe arctique du modèle à six vertex avec conditions aux bords de type mur sont décrites par un champ Gaussien libre avec une constante de couplage dépendant de la position, qui peut être calculée à partir de l'énergie libre de la chaîne XXZ avec une torsion imaginaire dans un champ magnétique.
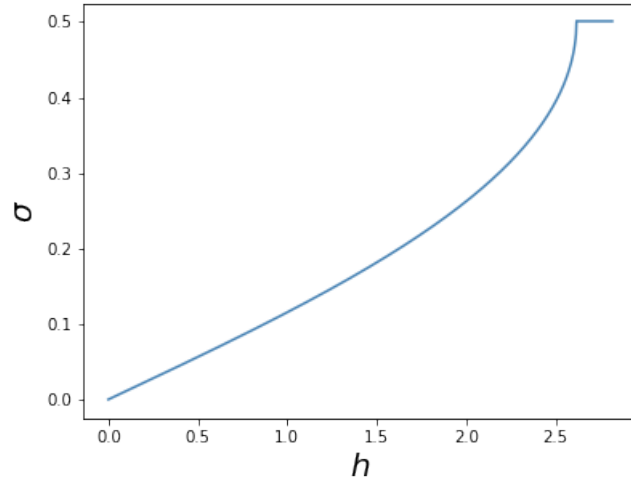
194

Figure A.9: Magnétisation de l'état fondamental de XXZ à $\Delta = \cos 2\pi/5$ en fonction du champ magnétique h, exprimée comme une série en $\sqrt{h_c - h}$.

Bibliography

[1] H. Bethe, "Zur Theorie der Metalle," *Z. Physik*, vol. 71, p. 205, 1931.

[2] L. Onsager, "Crystal statistics. I. A two-dimensional model with an order-disorder transition.," *Phys. Rev.*, vol. 65, p. 117, 1944.

[3] R. J. Baxter, *Exactly solved models in statistical mechanics.* Academic Press, 1982.

[4] L. D. Faddeev, E. K. Sklyanin, and L. A. Takhtajan, "Quantum inverse problem. I," *Theor. Math. Phys.*, vol. 40, p. 688, 1979.

[5] L. D. Faddeev and L. A. Takhtajan, "The quantum method of the inverse problem and the Heisenberg XYZ model," *Russian Math. Surveys*, vol. 34:5, p. 11, 1979.

[6] E. K. Sklyanin, "Quantum version of the method of inverse scattering problem," *J. Sov. Math.*, vol. 19:5, p. 1546, 1982.

[7] M. Jimbo, "Yang-Baxter equation in integrable systems," *Advanced series in mathematical physics*, vol. 10, 1990.

[8] L. D. Fadeev and G. P. Korchemsky, "High energy QCD as a completely integrable model," *Phys. Lett. B*, vol. 342, p. 311, 1995.

[9] E. K. Sklyanin, "Quantum inverse scattering method. Selected topics," *Nankai lectures*, p. 63, 1992.

[10] J. M. Maillet and G. Niccoli, "On quantum separation of variables," *Journal of Mathematical Physics*, vol. 59, p. 091417, 2018.

[11] N. A. Slavnov, "Calculation of scalar products of wave functions and form factors in the framework of the algebraic Bethe ansatz," *Theor. Math. Phys.*, vol. 79, 1989.

[12] N. Kitanine, J.-M. Maillet, N. Slavnov, and V. Terras, "Spin-spin correlation functions of the XXZ-1/2 Heisenberg chain in a magnetic field," *Nucl. Phys. B*, vol. 641, 2002.

[13] N. Kitanine, K. K. Kozlowski, J. M. Maillet, N. A. Slavnov, and V. Terras, "Algebraic Bethe ansatz approach to the asymptotic behavior of correlation functions," *J. Stat. Mech.*, vol. 4, p. 2009, 2009.

[14] J.-S. Caux, "Correlation functions of integrable models: a description of the ABACUS algorithm," *J. Math. Phys.*, vol. 50, 2009.

[15] D. A. Tennant, R. A. Cowley, S. E. Nagler, and A. M. Tsvelik, "Measurement of the spin-excitation continuum in one-dimensional KCuF3 using neutron scattering," *Phys. Rev. B*, vol. 52, p. 13368, 1995.

[16] J.-S. Caux, R. Hagemans, and J.-M. Maillet, "Computation of dynamical correlation functions of Heisenberg chains: the gapless anisotropic regime," *J. Stat. Mech.*, p. P09003, 2005.

[17] V. G. Drinfeld, "Hopf algebras and the quantum Yang-Baxter equation," *Dokl. Acad. Nauk SSSR*, vol. 283, p. 1060, 1985.

[18] I. Affleck, "Critical behavior of two-dimensional systems with continuous symmetries," *Phys. Rev. Lett.*, vol. 55, p. 1355, 1985.

[19] A. A. Belavin, A. M. Polyakov, and A. B. Zamolodchikov, "Infinite conformal symmetry in two-dimensional quantum field theory," *Nucl. Phys. B*, vol. 241, p. 333, 1984.

[20] H. W. Blöte, J. L. Cardy, and M. P. Nightingale, "Conformal invariance, the central charge, and universal finite-size amplitudes at criticality," *Phys. Rev. Lett.*, vol. 56, 1986.

[21] I. Affleck, "Universal term in the free energy at a critical point and the conformal anomaly," *Phys. Rev. Lett.*, vol. 56, 1986.

[22] J. L. Cardy, "Operator content of two-dimensional conformally invariant theories," *Nucl. Phys. B*, vol. 270, 1986.

[23] F. Woynarovich and H.-P. Eckle, "Finite-size corrections and numerical calculations for long spin 1/2 Heisenberg chains in the critical region," *J. Phys. A: Math. Gen.*, vol. 20, p. L97, 1987.

[24] M. Karowski, "Finite-size corrections for integrable systems and conformal properties of six-vertex models," *Nucl. Phys. B*, vol. 200, p. 473, 1988.

[25] A. Klümper and M. T. Batchelor, "Finite-size corrections and scaling dimensions of solvable lattice models: An analytic method," *J. Phys. A*, vol. 23, p. L189, 1990.

[26] A. Klümper, T. Wehner, and J. Zittartz, "Conformal spectrum of the six-vertex model," *J. Phys. A: Math. Gen.*, vol. 26, p. 2815, 1993.

[27] H. Saleur, "The continuum limit of $sl(N|K)$ integrable super spin chains," *Nucl. Phys. B*, vol. 578, p. 552, 2000.

[28] F. H. L. Essler, H. Frahm, F. Göhmann, A. Klümper, and V. E. Korepin, *The one-dimensional Hubbard model*. Cambridge University Press, 2003.

[29] F. H. L. Essler, V. E. Korepin, and K. Schoutens, "Complete solution of the one-dimensional Hubbard model," *Phys. Rev. Lett.*, vol. 67, p. 3848, 1991.

[30] F. H. L. Essler and V. E. Korepin, "Higher conservation laws and algebraic Bethe ansatz for the supersymmetric $t - j$ model," *Phys. Rev. B*, vol. 46, p. 9147, 1992.

[31] K. B. Efetov, "Supersymmetry and theory of disordered metals," *Adv. Phys.*, vol. 32, p. 53, 1983.

[32] D. Bernard, "(perturbed) conformal field theory applied to 2D disordered systems: an introduction," *arXiv:hep-th/9509137*, 1995.

[33] F. Wegner, *Supermathematics and its applications in statistical physics*. Springer, 2016.

[34] H. Saleur, "Polymers and percolation in two dimensions and twisted $N = 2$ supersymmetry," *Nucl. Phys. B*, vol. 382, p. 486, 1992.

[35] V. B. Priezzhev, "The dimer problem and the Kirchhoff theorem," *Sov. Phys. Usp.*, vol. 28, p. 1125, 1985.

[36] S. Caracciolo, J. L. Jacobsen, H. Saleur, A. D. Sokal, and A. Sportiello, "Fermionic field theory for trees and forests," *Phys. Rev. Lett.*, vol. 93, p. 080601, 2004.

[37] J. L. Jacobsen and H. Saleur, "The arboreal gas and the supersphere sigma model," *Nucl. Phys. B*, vol. 716, p. 439, 2005.

[38] V. Gurarie, "Logarithmic operators in conformal field theory," *Nucl. Phys. B*, vol. 410, p. 535, 1993.

[39] K. v. Klitzing, G. Dorda, and M. Pepper, "New method for high-accuracy determination of the fine-structure constant based on quantized Hall resistance," *Phys. Rev. Lett.*, vol. 45, p. 494, 1980.

[40] J. T. Chalker and P. D. Coddington, "Percolation, quantum tunnelling and the integer Hall effect," *J. Phys. C*, vol. 21, p. 2665, 1988.

[41] B. Huckestein, "Scaling theory of the integer quantum Hall effect," *Rev. Mod. Phys.*, vol. 67, p. 357, 1995.

[42] A. M. M. Pruisken, "On localization in the theory of the quantized Hall effect: a two-dimensional realization of the θ-vacuum," *Nucl. Phys. B*, vol. 235, p. 277, 1984.

[43] H. A. Weidenmüller, "Single electron in a random potential and a strong magnetic field," *Nucl. Phys. B*, vol. 290, p. 87, 1987.

[44] Y. Ikhlef, J. L. Jacobsen, and H. Saleur, "A staggered six-vertex model with non-compact continuum limit," *Nucl. Phys. B*, vol. 789, p. 483, 2008.

[45] S. E. Derkachov, G. P. Korchemsky, J. Kotanski, and A. N. Manashov, "Noncompact Heisenberg spin magnets from high-energy QCD: II. Quantization conditions and energy spectrum," *Nucl. Phys. B*, vol. 645, p. 237, 2002.

[46] E. Granet, J. L. Jacobsen, and H. Saleur, "Spontaneous symmetry breaking in 2D supersphere sigma models and applications to intersecting loop soups," *J. Phys. A*, vol. 52, p. 345001, 2019.

[47] E. Granet, J. L. Jacobsen, and H. Saleur, "A distribution approach to finite-size corrections in Bethe ansatz solvable models," *Nucl. Phys. B.*, vol. 934, p. 96, 2018.

[48] E. Granet, J. L. Jacobsen, and H. Saleur, "Analytical results on the Heisenberg spin chain in a magnetic field," *J. Phys. A*, vol. 52, p. 255302, 2019.

[49] E. Granet, L. Budzynski, J. Dubail, and J. L. Jacobsen, "Inhomogeneous Gaussian Free Field inside the interacting arctic curve," *J. Stat. Mech.*, 2019.

[50] R. Orbach, "Linear antiferromagnetic chain with anisotropic coupling," *Phys. Rev.*, vol. 112, p. 309, 1958.

[51] J.-S. Caux and J. Mossel, "Remarks on the notion of quantum integrability," *J. Stat. Mech.*, p. P02023, 2011.

[52] F. H. L. Essler, V. E. Korepin, and K. Schoutens, "Fine structure of the Bethe ansatz for the spin-1/2 Heisenberg XXX model," *J. Phys. A: Math. Gen.*, vol. 23, p. 4115, 1992.

[53] K. Fabricius and B. M. MacCoy, "Bethe's equation is incomplete for the XXZ model at roots of unity," *J. Stat. Phys.*, vol. 103, p. 516, 2001.

[54] R. I. Nepomechie and C. Wang, "Algebraic Bethe ansatz for singular solutions," *J. Phys. A*, vol. 46, p. 325002, 2013.

[55] L. Avdveev and A. Vladimirov, "Exceptional solutions of the Bethe ansatz equations," *Theor. Math. Phys.*, vol. 69, p. 1071, 1987.

[56] R. I. Nepomechie and C. Wang, "Twisting singular solutions of Bethe's equations," *J. Phys. A*, vol. 47, p. 505004, 2014.

[57] C. Marboe and D. Volin, "Fast analytic solver of rational Bethe equations," *J. Phys. A: Math. Theor.*, vol. 50, p. 204002, 2017.

[58] G. P. Pronko and Y. G. Stroganov, "Bethe equations 'on the wrong side of the equator'," *J. Phys. A: Math. Gen.*, vol. 32, p. 2333, 1999.

[59] R. Kenyon, "Dominos and the Gaussian Free Field," *The Annals of Probability*, vol. 29, 2001.

[60] S. Smirnov, "Critical percolation in the plane: conformal invariance, Cardy's formula, scaling limit," *Comptes Rendus de l'Académie des Sciences, Paris, Série I : Mathématiques*, vol. 333, p. 239, 2001.

[61] M. Henkel, *Conformal invariance and critical phenomena*. Springer, 2013.

[62] I. Affleck, D. Gepner, H. J. Schulz, and T. Ziman, "Critical behaviour of spin-s Heisenberg antiferromagnetic chains: analytic and numerical results," *J. Phys. A: Math. Gen.*, vol. 22, 1989.

[63] S. Eggert, "Numerical evidence for multiplicative logarithmic corrections from marginal operators," *Phys. Rev. B*, vol. 54, p. R9612, 1996.

[64] B. Nienhuis, "Coulomb gas formulations of two-dimensional phase transitions," *Phase transitions and critical phenomena*, vol. 11, 1987.

[65] B. Duplantier and H. Saleur, "Exact critical properties of two-dimensional dense self-avoiding walks," *Nucl. Phys. B*, vol. 290, p. 291, 1987.

[66] T. T. Wu, "Theory of Toeplitz determinants and the spin correlations of the two-dimensional Ising model. I.," *Phys. Rev.*, vol. 149, 1966.

[67] H. Cheng and T. T. Wu, "Theory of Toeplitz determinants and the spin correlations of the two-dimensional Ising model. III.," *Phys. Rev.*, vol. 164, 1967.

[68] A. Ludwig, "Infinite hierarchies of exponents in a diluted ferromagnet and their interpretation," *Nucl. Phys. B*, vol. 330, 1990.

[69] R. Shankar, "Exact critical behavior of a random-bond two-dimensional Ising model," *Phys. Rev. Lett.*, vol. 58, 1987.

[70] B. Berche and L. N. Shchur, "Numerical investigation of logarithmic corrections in two-dimensional spin models," *JETP Letters*, vol. 5, 2004.

[71] J. C. Lessa and S. L. A. de Queiroz, "Logarithmic corrections to correlation decay in two-dimensional random-bond Ising systems," *Phys. Rev. E*, vol. 74, 2006.

[72] M. R. Gaberdiel and H. G. Kausch, "A local logarithmic conformal field theory," *Nucl. Phys. B*, vol. 538, p. 631, 1999.

[73] H. G. Kausch, "Symplectic fermions," *Nucl. Phys. B*, vol. 583, p. 513, 2000.

[74] R. Vasseur, J. L. Jacobsen, and H. Saleur, "Logarithmic observables in critical percolation," *J. Stat. Mech.*, 2012.

[75] S. M. Flores, J. J. H. Simmons, and P. Kleban, "Multiple-SLE connectivity weights for rectangles, hexagons, and octagons," *arXiv:1505.07756*, 2015.

[76] G. Gori and J. Viti, "Exact logarithmic four-point functions in the critical two-dimensional Ising model," *Phys. Rev. Lett.*, vol. 119, 2017.

[77] R. Vasseur and J. L. Jacobsen, "Operator content of the critical Potts model in d dimensions and logarithmic correlations," *Nucl. Phys. B*, vol. 880, 2014.

[78] J. Cardy, "Logarithmic conformal field theories as limits of ordinary CFTs and some physical applications," *J. Phys. A: Math. Theor.*, vol. 46, 2013.

[79] Z. Maassarani and D. Serban, "Non-unitary Conformal Field Theory and logarithmic operators for disordered systems," *Nucl. Phys. B*, vol. 603, p. 489, 1997.

[80] A. Klümper, "The spin-1/2 Heisenberg chain: thermodynamics, quantum criticality and spin-Peierls exponents," *Eur. Phys. J. B.*, vol. 5, 1998.

[81] J. M. Kosterlitz and D. J. Thouless, "Ordering, metastability and phase transitions in two-dimensional systems," *J. Phys. C: Solid State Phys.*, vol. 6, p. 1181, 1973.

[82] L. Rozansky and H. Saleur, "Quantum field theory for the multi-variable Alexander-Conway polynomial," *Nucl. Phys. B*, vol. 376, p. 461, 1992.

[83] J.-S. Caux, I. I. Kogan, and A. M. Tsvelik, "Logarithmic operators and hidden continuous symmetry in critical disordered systems," *Nucl. Phys. B*, vol. 466, p. 444, 1996.

[84] H. G. Kausch, "Curiosities at $c = -2$," *ArXiv:hep-th/9510149*, 1995.

[85] M. J. Martins, B. Nienhuis, and R. Rietman, "An intersecting loop model as a solvable super spin chain," *Phys. Rev. Lett.*, vol. 81, p. 504, 1998.

[86] J. L. Jacobsen, N. Read, and H. Saleur, "Dense loops, supersymmetry, and Goldstone phases in two dimensions," *Phys. Rev. Lett.*, vol. 90, p. 090601, 2003.

[87] A. L. Owczarek and T. Prellberg, "The collapse point of interacting trails in two dimensions from kinetic growth simulations," *J. Stat. Phys.*, vol. 79, p. 951, 1995.

[88] R. M. Ziff, "Lorentz lattice-gas and kinetic-walk model," *Phys. Rev. A*, vol. 44, p. 2410, 1991.

[89] D. P. Foster, "Universality of collapsing two-dimensional self-avoiding trails," *J. Phys. A: Math. Theor.*, vol. 42, p. 372002, 2009.

[90] H. Frahm and M. J. Martins, "The fine structure of the finite-size effects for the spectrum of the $Osp(n|2m)$ spin chain," *Nucl. Phys. B*, vol. 930, p. 545, 2018.

[91] H. Frahm and M. J. Martins, "Finite-size effects in the spectrum of the $Osp(3|2)$ superspin chain," *Nucl. Phys. B.*, vol. 894, p. 665, 2015.

[92] J. L. Cardy, "Logarithmic corrections to finite-size scaling in strips," *J. Phys. A: Math. Gen.*, vol. 19, p. L1093, 1986.

[93] A. Nahum, P. Serna, A. M. Somoza, and M. Ortuño, "Loop models with crossings," *Phys. Rev. B*, vol. 87, p. 184204, 2013.

[94] M. Scheunert, *The theory of Lie superalgebras.* Springer, 1979.

[95] F. Wegner, "Four-loop order β-function of nonlinear σ-models in symmetric spaces," *Nucl. Phys. B*, vol. 316, p. 663, 1988.

[96] E. G. Floratos and D. Petcher, "A two-loop calculation of the mass gap for the $O(N)$ model in finite volume," *Nucl. Phys. B*, vol. 252, p. 689, 1985.

[97] F. H. L. Essler, V. E. Korepin, and K. Schoutens, "Exact solution of an electronic model of superconductivity in $1+1$ dimensions," *Int. J. Mod. Phys. B*, vol. 8, p. 3205, 1994.

[98] D. Arnaudon, J. Avan, N. Crampé, A. Doiku, L. Frappat, and E. Ragoucy, "R-matrix presentation for (super)-Yangians $Y(g)$," *J. Math. Phys.*, vol. 44, p. 302, 2003.

[99] W. Galleas and M. J. Martins, "R-matrices and spectrum of vertex models based on superalgebras," *Nucl. Phys. B*, vol. 699, p. 455, 2004.

[100] D. Arnaudon, J. Avan, N. Crampé, A. Doiku, L. Frappat, and E. Ragoucy, "Bethe ansatz equations and exact S matrices for the $osp(m|2n)$ open super spin chain," *Nucl. Phys. B*, vol. 687, p. 257, 2004.

[101] F. A. Berezin and V. N. Tolstoy, "The group with Grassmann structure $UOSp(1|2)$," *Commun. Math. Phys.*, vol. 78, 1981.

[102] M. J. Martins, "The exact solution and the finite-size behaviour of the $Osp(1|2)$-invariant spin chain," *Nucl. Phys. B*, vol. 450, p. 768, 1995.

[103] S. Lukyanov, "Low energy effective Hamiltonian for the XXZ spin chain," *Nucl. Phys. B*, vol. 552, p. 533, 1998.

[104] Y. Ikhlef, J. L. Jacobsen, and H. Saleur, "An integrable spin chain for the $SL(2, R)/U(1)$ black hole sigma model," *Phys. Rev. Lett.*, vol. 108, p. 081601, 2012.

[105] D. Lu, "On the classification of irreducible $osp(2|2)$ representations," *Kyushu J. Math.*, vol. 66, 2012.

[106] W. Galleas and M. J. Martins, "Exact solution and finite size properties of the $U_q(osp(2|2m))$ vertex model," *Nucl. Phys. B*, vol. 768, p. 219, 2007.

[107] J. V. der Jeugt, "Finite and infinite dimensional representations of the orthosymplectic superalgebra $osp(3|2)$," *J. Math. Phys.*, vol. 25, p. 3334, 1984.

[108] A. V. Razumov and Y. G. Stroganov, "Combinatorial nature of ground state vector of $O(1)$ loop model," *Theor. Math. Phys.*, vol. 138, 2004.

[109] A. Knutson and P. Zinn-Justin, "A scheme related to the Brauer loop model," *Advances in Mathematics*, vol. 214, 2007.

[110] B. Nienhuis and R. Rietman, "A solvable model for intersecting loops," *ITFA 92-35*, 1993.

[111] C. Candu, "Continuum limit of $gl(M|N)$," *JHEP*, vol. 1107, 2011.

[112] M. Gourdin, "Relation between the supertableaux of the supergroups $OSp(2|2)$ and $SU(1|2)$," *J. Math. Phys.*, vol. 27, 1986.

[113] E. V. Ivashkevich, "Correlation functions of dense polymers and $c = -2$ Conformal Field Theory," *J. Phys. A*, vol. 32, p. 1691, 1999.

[114] H. J. de Vega and F. Woynarovich, "Method for calculating finite size corrections in Bethe ansatz systems: Heisenberg chain and six-vertex model," *Nucl. Phys. B*, vol. 251, p. 439, 1985.

[115] L. V. Adveev and B.-D. Dorfel, "Finite-size corrections for the XXX antiferromagnet," *J. Phys. A: Math. Gen.*, vol. 19, p. L13, 1986.

[116] C. J. Hamer, "Finite-size corrections for ground states of the XXZ Heisenberg chain in the critical region," *J. Phys. A: Math. Gen.*, vol. 18, p. L1133, 1985.

[117] F. Woynarovich, "Excitation spectrum of the spin-1/2 Heisenberg chain and conformal invariance," *Phys. Rev. Lett.*, vol. 59, p. 259, 1987.

[118] C. J. Hamer, G. R. W. Quispel, and M. T. Batchelor, "Conformal anomaly and surface energy for Potts and Ashkin-Teller quantum chains," *J. Phys. A: Math. Gen.*, vol. 20, 1987.

[119] R. E. A. C. Paley and N. Wiener, *Fourier transforms in the complex domain.* American mathematical society, 1934.

[120] A. Sommerfeld, *Optics.* 1964.

[121] B. Noble, *Methods based on the Wiener-Hopf techniques for the solution of partial differential equations.* Chelsea Publication, 1959.

[122] V. G. Daniele and R. S. Zich, *The Wiener-Hopf method in electromagnetics.* Scitech publishing, 2014.

[123] H. J. de Vega and F. Woynarovich, "Solution of the Bethe Ansatz equations with complex roots for finite size: the spin $s \geq 1$ isotropic and anisotropic chains," *J. Phys. A:Math. Gen*, vol. 23, p. 1613, 1990.

[124] P. A. Pearce and A. Klümper, "Finite-size corrections and scaling dimensions of solvable lattice models: an analytic method," *Phys. Rev. Lett.*, vol. 66, 1991.

[125] A. Klümper, M. T. Batchelor, and P. A. Pearce, "Central charges of the 6- and 19-vertex models with twisted boundary conditions," *J. Phys. A: Math. Gen.*, vol. 24, 1991.

[126] A. Klümper and P. A. Pearce, "Conformal weights of RSOS lattice models and their fusion hierarchies," *Physica A*, vol. 183, 1992.

[127] C. Destri and H. J. de Vega, "New thermodynamic Bethe ansatz equations without strings," *Phys. Rev. Lett.*, vol. 69, 1992.

[128] C. Destri and H. J. de Vega, "Unified approach to thermodynamic Bethe Ansatz and finite size corrections for lattice models and field theories," *Nucl. Phys. B*, vol. 438, p. 413, 1994.

[129] K. Kawano and M. Takahashi, "Logarithmic correction terms of the magnetic susceptibility in highly correlated electron systems," *J. Phys. Soc. Jpn.*, vol. 64, 1995.

[130] M. Karbach and K.-H. Mutter, "The antiferromagnetic spin-1/2-XXZ model on rings with an odd number of sites," *J. Phys. A: Math. Gen.*, vol. 28, 1995.

[131] A. Klümper, "The spin-1/2 Heisenberg chain: thermodynamics, quantum criticality and spin-Peierls exponents," *Eur. Phys. B*, vol. 5, 1998.

[132] A. Klumper and M. T. Batchelor, "An analytic treatment of finite-size corrections in the spin-1 antiferromagnetic XXZ chain," *J. Phys. A: Math. Gen.*, vol. 23, p. L189, 1990.

[133] H. M. Babujian and A. M. Tsvelick, "Heisenberg magnet with an arbitrary spin and anisotropic chiral field," *Nucl. Phys. B*, vol. 265, p. 24, 1986.

[134] J. Suzuki, "Spinons in magnetic chains of arbitrary spins at finite temperatures," *J. Phys. A:Math. Gen*, vol. 32, p. 2341, 1999.

[135] A. Klümper, "Integrability of quantum chains: theory and applications to the spin-1/2 XXZ chain," *Lect. Notes Phys.*, vol. 645, p. 349, 2004.

[136] J. Damerau, "Nonlinear integral equations for the thermodynamics of integrable quantum chains," *Thesis, Wuppertal University*, 2008.

[137] L. Hulthén, "Über das Austauschproblem eines Kristalles," *Arkiv Mat. Astron. Fysik*, vol. 26A, no. 11, 1938.

[138] V. E. Korepin, N. M. Bogoliubov, and A. G. Izergin, *Quantum inverse scattering method and correlation functions.* Cambridge University Press, 1993.

[139] Y. Ikhlef, J. L. Jacobsen, and H. Saleur, "A staggered six-vertex model with non-compact continuum limit," *Nucl. Phys. B*, vol. 789, 2008.

[140] C. Candu and Y. Ikhlef, "Non-linear integral equations for the $SL(2, R)/U(1)$ black hole sigma model," *J. Phys. A: Gen.*, vol. 46, 2013.

[141] E. Vernier, J. L. Jacobsen, and H. Saleur, "Non compact conformal field theory and the $a_2^{(2)}$ (Izergin-Korepin) model in regime III," *J. Phys. A: Math. Theor*, vol. 47, 2014.

[142] C. J. Hamer, M. T. Batchelor, and M. N. Barber, "Logarithmic corrections to finite-size scaling in the four-state Potts model," *J. Stat. Phys.*, vol. 52, 1988.

[143] P. Kurasov, "Distribution theory for discontinuous test functions and differential operators with generalized coefficients," *Journal of Mathematical Analysis and Applications*, p. 201, 1966.

[144] R. B. Griffiths, "Magnetization curve at zero temperature for the antiferromagnetic Heisenberg linear chain," *Phys. Rev.*, vol. 133, p. A768, 1964.

[145] M. Gaudin, *La fonction d'onde de Bethe.* Masson, 1983.

[146] O. F. Syljuåsen and M. B. Zvonarev, "Directed-loop Monte Carlo simulations of vertex models," *Phys. Rev. E*, vol. 70, 2004.

[147] D. Allison and N. Reshetikhin, "Numerical study of the 6-vertex model with domain wall boundary conditions," *Ann. Inst. Fourier*, vol. 55, 2005.

[148] W. Jockusch, J. Propp, and P. Shor, "Random domino tilings and the arctic circle theorem," *ArXiv:math/9801068*, 1995.

[149] R. Kenyon, "Conformal invariance of domino tilings," *The Annals of Probability*, vol. 29, p. 1128, 2001.

[150] L. Petrov, "Asymptotics of uniformly random lozenge tilings of polygons. Gaussian Free Field," *Annals of Probability*, vol. 43, 2015.

[151] N. Kitanine, K. K. Kozlowski, J. M. Maillet, N. A. Slavnov, and V. Terras, "Algebraic Bethe ansatz approach to the asymptotic behavior of correlation functions," *J. Stat. Mech.*, vol. 04, p. P04003, 2008.

[152] N. Kitanine, J.-M. Maillet, and V. Terras, "Correlation functions of the XXZ Heisenberg spin-1/2 chain in a magnetic field," *Nucl. Phys. B*, vol. 567, 2000.

[153] N. Kitanine, J.-M. Maillet, N. Slavnov, and V. Terras, "Dynamical correlation functions of the XXZ spin-1/2 chain," *Nucl. Phys. B*, vol. 729, 2005.

[154] N. Kitanine, J.-M. Maillet, N. Slavnov, and V. Terras, "Master equation for spin-spin correlation functions of the XXZ chain," *Nucl. Phys. B*, vol. 712, 2005.

[155] D. Biegel, M. Karbach, and G. Müller, "Transition rates via Bethe ansatz for the spin-1/2 Heisenberg chain," *Europhys. Lett.*, vol. 59, p. 882, 2002.

[156] J. Sato, M. Shirosihi, and M. Takahashi, "Evaluation of dynamic spin structure factor for the spin-1/2 XXZ chain in a magnetic field," *J. Phys. Soc. Jpn.*, vol. 73, p. 3008, 2004.

[157] J.-S. Caux and J.-M. Maillet, "Computation of dynamical correlation functions of Heisenberg chains in a field," *Phys. Rev. Lett.*, vol. 95, p. 077301, 2005.

[158] L. N. Lipatov, "High energy asymptotics of multi-colour QCD and exactly solvable lattice models," *JETP Lett.*, vol. 59, p. 596, 1994.

[159] G. P. Korchemsky, "Bethe ansatz for QCD Pomeron," *Nucl. Phys. B*, vol. 443, p. 255, 1995.

[160] S. E. Derkachov, G. P. Korchemsky, J. Kotanski, and A. N. Manashov, "Noncompact Heisenberg spin magnets from high-energy QCD: I. Baxter Q-operator and separation of variables," *Nucl. Phys. B*, vol. 645, p. 237, 2002.

[161] C. N. Yang and C. P. Yang, "One-dimensional chain of anisotropic spin-spin interactions. III. Applications.," *Phys. Rev.*, vol. 151, p. 258, 1966.

[162] C. N. Yang and C. P. Yang, "One-dimensional chain of anisotropic spin-spin interactions. II Properties of the ground-state energy per lattice site for an infinite system," *Phys. Rev.*, vol. 150, p. 327, 1966.

[163] D. C. Cabra, A. Honecker, and P. Pujol, "Magnetization plateaux in N-leg spin ladders," *Phys. Rev. B*, vol. 58, p. 6241, 1998.

[164] N. M. Bogoliubov, A. G. Izergin, and V. E. Korepin, "Critical exponents for integrable models," *Nucl. Phys. B*, vol. 275, p. 687, 1986.

[165] G. I. Japaridze and A. A. Nersesyan, "Low-temperature thermodynamics of a one-dimensional interacting Fermi system," *Journal of Low Temperature Physics*, vol. 47, p. 91, 1982.

[166] M. Takahashi, "Correlation length and free energy of the $s = 1/2$ XXZ chain in a magnetic field," *Phys. Rev. B*, vol. 44, p. 12382, 1991.

[167] J. C. Bonner and M. E. Fisher, "Linear magnetic chains with anisotropic coupling," *Phys. Rev.*, vol. 135, p. A640, 1964.

[168] R. P. Hodgson and J. B. Parkinson, "Bethe ansatz for two-deviation states in quantum spin chains of arbitrary S with anisotropic Heisenberg exchange," *J. Phys. C: Solid State Phys.*, vol. 18, p. 6385, 1985.

[169] R. M. Konik and P. Fendley, "Haldane-gapped spin chains as Luttinger liquids: Correlation functions at finite field," *Phys. Rev. B*, vol. 66, p. 144416, 2002.

[170] S. Katsura, "Statistical mechanics of the anisotropic linear Heisenberg model," *Phys. Rev.*, vol. 127, p. 1508, 1962.

[171] C. M. Yung and M. T. Batchelor, "Exact solution for the spin-s XXZ quantum chain with non-diagonal twists," *Nucl. Phys. B*, vol. 446, p. 461, 1995.

[172] T. Fukui and N. Kawakami, "Spectral flow of non-hermitian Heisenberg spin chain with complex twist," *Nucl. Phys. B*, vol. 519, p. 715, 1998.

[173] P. Henrici, "An algorithm for analytic continuation," *J. SIAM Numer. Anal.*, vol. 3, p. 67, 1966.

[174] V. E. Korepin, "Calculation of norms of Bethe wave functions," *Commun. Math. Phys.*, vol. 86, 1982.

[175] A. G. Izergin, "Partition function of the six-vertex model in the finite volume," *Sov. Phys. Dokl.*, vol. 32, 1987.

[176] A. G. Izergin, D. A. Coker, and V. E. Korepin, "Determinant formula for the six-vertex model," *J. Phys. A: Math. Gen.*, vol. 25, 1992.

[177] V. Korepin and P. Zinn-Justin, "Thermodynamic limit of the six-vertex model with domain wall boundary conditions," *J. Phys. A*, vol. 33, 2000.

[178] F. Colomo and A. Pronko, "The arctic curve of the domain-wall six-vertex model," *J. Stat. Phys.*, vol. 138, 2010.

[179] L. P. et al, "Asymptotics of uniformly random lozenge tilings of polygons. Gaussian free field," *The Annals of Probability*, vol. 43, p. 1, 2015.

[180] P. Zinn-Justin, "Six-vertex, loop and tiling models: integrability and combinatorics," *arXiv preprint cond-mat/0901.0665*, 2009.

[181] H. Cohn, R. Kenyon, and J. Propp, "A variational principle for domino tilings," *Journal of the AMS*, vol. 14, p. 297, 2001.

[182] A. N. Kirillov, "Dilogarithm identities," *Prog. Theor. Phys. Suppl.*, vol. 118, p. 61, 1995.

[183] K. J. McGown and H. R. Parks, "The generalization of Faulhaber's formula to sums of non-integral powers," *Journal of Mathematical Analysis and Applications*, vol. 330, p. 571, 2007.

Titre : Analyse et techniques avancés d'intégrabilité pour l'étude de chaînes quantiques de spins

Mots clés : Intégrabilité, chaîne quantique de spins, ansatz de Bethe, théorie conforme des champs

Résumé : Dans cette thèse sont principalement étudiés des systèmes quantiques intégrables critiques avec l'ansatz de Bethe qui ont la propriété particulière d'être *non-unitaires* ou *non-compacts*. Ceci concerne des modèles de physique statistique non-locaux tels que la percolation, mais aussi par exemple les systèmes désordonnés. Ce manuscrit présente à la fois des études détaillées de la limite continue de modèles intégrables sur réseau, et développe de nouvelles techniques pour étudier cette correspondance.

Dans une première partie nous étudions en détail la limite continue de chaînes de superspins non-unitaires (et parfois non-compactes) qui ont une symétrie orthosymplectique. Nous montrons qu'il s'agit de modèles sigma sur supersphère en calculant leur spectre avec la théorie des champs, avec l'ansatz de Bethe, et numériquement. Leur non-unitarité autorise une brisure spontanée de symétrie habituellement interdite par le théorème de Mermin-Wagner. Leur caractère de perturbation marginale d'une théorie conforme des champs logarithmique est particulièrement étudié. Nous établissons également une correspondance précise entre le spectre et des configurations de boucles avec intersections, et obtenons de nouveaux exposants critiques pour les chemins non-recouvrants compacts ainsi que leurs corrections logarithmiques multiplicatives. Cette étude fut par ailleurs l'occasion de développer

une nouvelle méthode pour calculer le spectre d'excitation d'une chaîne de spin quantique critique à partir de l'ansatz de Bethe, incluant les corrections logarithmiques, également en présence de racines de Bethe dites 'en chaînes', et qui évite les méthodes de Wiener-Hopf et les équations intégrales non-linéaires.

Dans une deuxième partie nous abordons l'influence d'un champ magnétique sur une chaîne de spin quantique et montrons que des séries convergentes peuvent être obtenues pour plusieurs quantités physiques telles que l'aimantation acquise ou les exposants critiques, dont les coefficients peuvent être calculés efficacement par récurrence. La structure de ces relations de récurrence permet d'étudier génériquement le spectre d'excitation, et elles sont applicables y compris dans certains cas où les racines de Bethe sont sur une courbe dans le plan complexe. Nous espérons que l'étude de la continuation analytique de ces séries puisse être utile pour les chaînes non-compactes. Par ailleurs, nous montrons que les fluctuations à l'intérieur de la courbe arctique du modèle à six vertex avec conditions aux bords de type mur sont décrites par un champ Gaussien libre avec une constante de couplage dépendant de la position, qui peut être calculée à partir de l'énergie libre de la chaîne XXZ avec une torsion imaginaire dans un champ magnétique.

Title : Advanced integrable techniques and analysis for quantum spin chains

Keywords : Integrability, quantum spin chain, Bethe ansatz, conformal field theory

Abstract : This thesis mainly deals with integrable quantum critical systems that exhibit peculiar features such as non-unitarity or non-compactness, through the technology of Bethe ansatz. These features arise in non-local statistical physics models such as percolation, but also in disordered systems for example. The manuscript both presents detailed studies of the continuum limit of finite-size lattice integrable models, and develops new techniques to study this correspondance.

In a first part we study in great detail the continuum limit of non-unitary (and sometimes non-compact) super spin chains with orthosymplectic symmetry which is shown to be supersphere sigma models, by computing their spectrum from field theory, from the Bethe ansatz, and numerically. The non-unitarity allows for a spontenous symmetry breaking usually forbidden by the Mermin-Wagner theorem. The fact that they are marginal perturbations of a Logarithmic Conformal Field Theory is particularly investigated. We also establish a precise correspondance between the spectrum and intersecting loops configurations, and derive new critical exponents for fully-packed trails, as well as their multiplicative logarithmic corrections. During this study we developed a new method to compute the excitation spectrum of a

critical quantum spin chain from the Bethe ansatz, together with their logarithmic corrections, that is also applicable in presence of so-called 'strings', and that avoids Wiener-Hopf and Non-Linear Integral Equations.

In a second part we address the problem of the behaviour of a spin chain in a magnetic field, and show that one can derive convergent series for several physical quantities such as the acquired magnetization or the critical exponents, whose coefficients can be efficiently and explicitely computed recursively using only algebraic manipulations. The structure of the recurrence relations permits to study generically the excitation spectrum content - moreover they are applicable even to some cases where the Bethe roots lie on a curve in the complex plane. It is our hope that the analytic continuation of such series might be helpful the study non-compact spin chains, for which we give some flavour. Besides, we show that the fluctuations within the arctic curve of the six-vertex model with domain-wall boundary conditions are captured by a Gaussian free field with space-dependent coupling constant that can be computed from the free energy of the periodic XXZ spin chain with an imaginary twist and in a magnetic field.